FACULTY OF PHARMACY AND MEDICINE

New Prospectives on the Benzo[*b*]thiophene-3-ole Scaffold: Design, Synthesis, and Biological Evaluation of Novel Monoamine Oxidase Inhibitors

&

Photocatalytic Functionalization of Dehydroalanine-Derived   Peptides in Batch and Flow.

Ph.D. Thesis in Molecular Design and Characterization

for the Promotion of Health and Well-Being from Drug

to Food

XXXVII cycle

<table>
<tr><td>Ph.D. candidate</td><td>Supervisor</td></tr>
<tr><td>Dr. Francesca Arrighi</td><td>Prof. Daniela Secci</td></tr>
</table>

Summary

Abstract

Human monoamine oxidases (MAOs) are flavin-containing enzymes located on the outer mitochondrial membrane, which catalyse the oxidative degradation of amines. There are two different isoforms in human organism: hMAO-A and hMAO-B. The two MAO enzymes share similar affinity for dopamine, epinephrine, norepinephrine, and tyramine; serotonin is the preferred substrate for hMAO-A, while hMAO-B has high affinity for benzylamine. The activity of these enzymes significantly impacts the concentration and functional levels of catecholamines in the central nervous system (CNS). As a result, hMAO inhibitors that operate within the CNS are vital for decreasing the degradation of these neurotransmitters, which is essential for treating neurodegenerative conditions such as depression, Alzheimer's disease, and Parkinson's disease. Starting from this evidence, the focus of this project has been the design, synthesis, and biological evaluation of novel monoamine oxidase (MAO) inhibitors based on the open form of benzothiophene-3-ol scaffolds and benzo[*b*]thiophene-3-ole-2-phenylcarboxamide derivatives, with the aim of developing new effective neuroprotective agents. Initial studies conducted in 2019 by Professor Daniela Secci's research group identified the benzo[*b*]thiophene-3-ol core as a promising scaffold for neuroprotection, demonstrating impressive efficacy in inhibiting monoamine oxidases. [1] To further enhance the potential of the 2-aroyl-benzo[*b*]thiophen-3-ol scaffold, we explored chemical modifications inspired by previous structure-activity relationship (SAR) studies, showing that chromone-based compounds featuring an amide spacer at position 3 demonstrated the highest potency and selectivity for MAO inhibition. Building on this finding, we developed a series of carboxamide analogues of the 2-aroyl-benzo[b]thiophen-3-ols by substituting the carbonyl spacer with an amide. [2] All the derivatives were synthesized through a multi-step process (yields ranging from 33% to 45%) characterized using NMR spectroscopy (^{1}H and ^{13}C) and tested for inhibition of human MAO-A and MAO-B isoforms at a concentration of 10 μM. Most of the compounds demonstrated selectivity for MAO-B, with compound 5 (bearing a 2-methoxy group) achieving complete (100%) inhibition. Structural modifications, such as positional changes of substituents, significantly influenced the activity, with para-methyl (compound 4) showing 65.31% inhibition of MAO-B, while other substitutions were less effective. Additionally, halogenated derivatives showed promising inhibition patterns.

In the second part of the project, we developed novel open-structure analogues of benzo[*b*]thiophen-3-ols based on the methyl 2-(benzylthio)benzoate scaffold. The new derivatives were obtained through multi-step synthetic procedures, ensuring the reproducibility of the method and reaction yields ranging from 62% to 78%. Each compound was characterized using NMR spectroscopy (^{1}H and ^{13}C) and subsequently evaluated for its inhibitory activity against the A and B isoforms of the monoamine oxidase enzyme through preliminary assays at a fixed concentration of 10 μM. The results from the enzyme inhibition assays revealed that some derivatives, particularly 16B and 20A (methyl 2-((2-(4-bromophenyl)-2-oxoethyl) sulfonyl) benzoate and 2-((2-oxo-2-(p-tolyl) ethyl) sulfinyl) benzoic acid, respectively), exhibited inhibition percentages greater than 50% against the B isoform. Additionally, for derivatives 16, 16A, and 16B (methyl 2-((2-(4-bromophenyl)-2-oxoethyl)sulfonyl)benzoate, methyl 2-((2-(4-bromophenyl)-2-oxoethyl)sulfinyl)benzoate, methyl 2-((2-(4-bromophenyl)-2-oxoethyl)sulfonyl)benzoate), which showed more than 70% inhibition against the A isoform, further studies were conducted to determine their IC$_{50}$ values, yielding 3.01 μM, 3.16 μM, and 1.20 μM, respectively. Another promising result was observed for derivative 18A (methyl 2-((2-(4-nitrophenyl)-2-oxoethyl)sulfinyl)benzoate), which demonstrated an inhibition percentage of over 90% against the A isoform, with an IC$_{50}$ value of 2.86 μM. This research underscores the potential of these compounds as a monoamine oxidase inhibitor, paving the way for further investigation, including the determination of IC$_{50}$ values for the most promising derivatives and the inhibition essays toward the hMAO-B isoform. It also establishes a solid foundation for the continued development of neuroprotective agents aimed at treating neurodegenerative diseases.

The last part of the project has been focused on the Photocatalytic Functionalization of Dehydroalanine-Derived Peptides in Batch and Flow. Unnatural amino acids, and their synthesis via the late- stage functionalization (LSF) of peptides, play a crucial role in areas such as drug design and discovery. Historically, the LSF of biomolecules has predominantly utilized traditional synthetic methodologies that exploit nucleophilic residues, such as cysteine, lysine or tyrosine. In this study, we present a photocatalytic hydroarylation process targeting the electrophilic residue dehydroalanine (Dha). This residue possesses an α,β-unsaturated moiety and can be combined with various arylthianthrenium salts, both in batch and flow reactors. Notably, the flow setup proved instrumental for efficient scale-up, paving the way for the synthesis of unnatural amino acids and peptides in substantial quantities. Our photocatalytic approach, being inherently mild, permits the diversification of peptides even when they contain

sensitive functional groups. The readily available arylthianthrenium salts facilitate the seamless integration of Dha-infused peptides with a wide range of arenes, drug blueprints, and natural products, culminating in the creation of unconventional phenylalanine derivatives. The synergistic effect of the high functional group tolerance and the modular characteristic of the aryl electrophile enables efficient peptide conjugation and ligation in both batch and flow conditions.[3]

1. Guglielmi, P., Secci, D., Petzer, A., Bagetta, D., Chimenti, P., Rotondi, G., ... & Carradori, S. (2019). Benzo [b] tiophen-3-ol derivatives as effective inhibitors of human monoamine oxidase: design, synthesis, and biological activity. Journal of Enzyme Inhibition and Medicinal Chemistry, 34(1), 1511-1525.

2. Reis J, Cagide F, Chavarria D, Silva T, Fernandes C, Gaspar A, Uriarte E, Remião F, Alcaro S, Ortuso F, Borges F. Discovery of New Chemical Entities for Old Targets: Insights on the Lead Optimization of Chromone-Based Monoamine Oxidase B (MAO-B) Inhibitors. J Med Chem. 2016 Jun 23;59(12):5879-93. doi: 10.1021/acs.jmedchem.6b00527.

3. Kaplaneris N, Akdeniz M, Fillols M, Arrighi F, Raymenants F, Sanil G, Gryko DT, Noël T. Photocatalytic Functionalization of Dehydroalanine-Derived Peptides in Batch and Flow. Angew Chem Int Ed Engl. 2024 May 6;63(19):e202403271. doi: 10.1002/anie.202403271. Epub 2024 Apr 8. PMID: 38497510.

Chapter 1

Human monoamine oxidases (hMAOs)

1.1 Introduction

Monoamine oxidases (MAOs; EC 1.4.3.4) are flavoenzymes bound to the outer mitochondrial membrane which catalyse the oxidative degradation of amines. In human have been observed two different isoforms called A and B (hMAO-A / hMAO-B), respectively [1]. The first insight about mammalian MAOs date back to 1928 when Hare observed a tyramine oxidase activity in rabbit liver, not explainable with tyrosinase function [2]. The presence of these enzymes in the main organ addicted to the chemical inactivation of xenobiotics, prompted Hare to postulate that they were mainly involved in the metabolism of potentially toxic exogenous amines. Follow-up studies showed that these enzymes catalyse the oxidative deamination of various biogenic amines, which is an essential process in different physiological functions including the regulation of neurotransmitter levels. As matter of fact, this enzyme family is known to act on small-molecule monoamines, such as neurotransmitters including dopamine, norepinephrine, epinephrine and serotonin, the neurologically important amine phenethylamine as well as polyamines like putrescine, spermidine, and spermine] [3]. The two isoforms of monoamine oxidase exhibit similar overall structures, with highly conserved flavin adenine dinucleotide (FAD) binding domains that resemble the folding pattern observed in *p*-hydroxybenzoate hydroxylase. However, these enzymes possess diverse substrate-binding sites. As flavoprotein oxidases, they catalyse substrate oxidation through a two-step process. In the reductive half-reaction, the flavin cofactor accepts a hydride equivalent from the substrate, becoming reduced. This is followed by the oxidative step, where the reduced flavin is oxidized by molecular oxygen (**Figure** 1.1.1) [4,5,6]

Flavin-dependent enzymes play a crucial role in various biological processes, and the understanding of the underlying electron transfer mechanisms is essential for elucidating their catalytic activity. Several mechanisms have been proposed to explain the transfer of electrons from the substrate to the flavin cofactor.
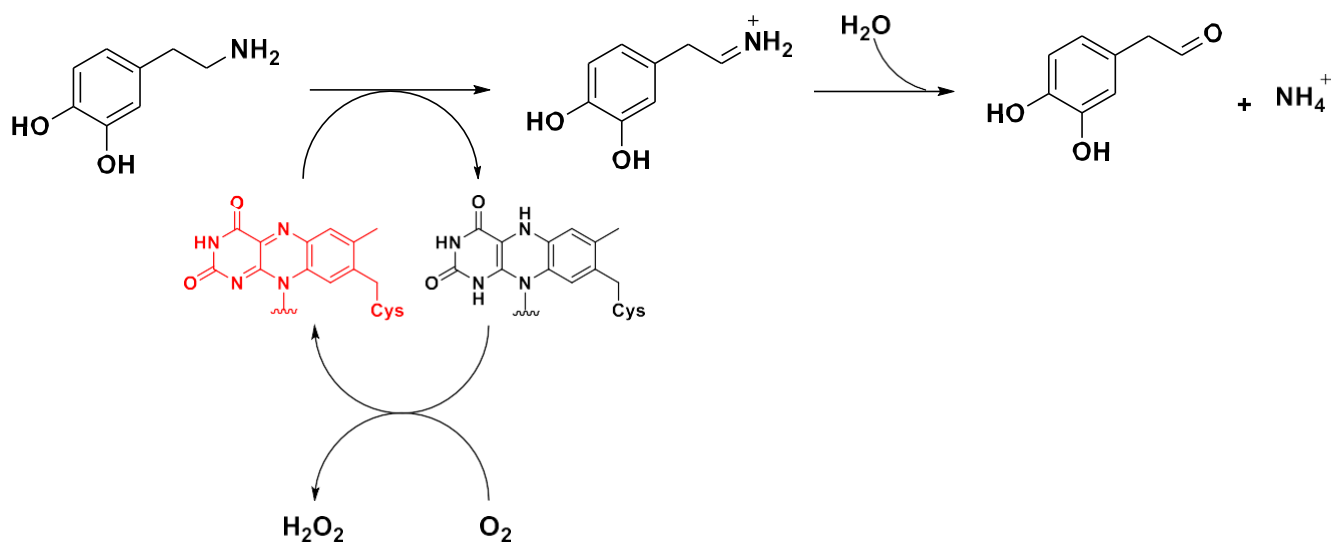
Figure 1.1.1. Chemical reaction catalysed by hMAOs using dopamine as an example of neurotransmitter substrate. The flavin cofactor is reported in yellow and undergoes a two-electron reduction substrate oxidation. Regeneration to its functional form is accomplished by molecular oxygen, leading to hydrogen peroxide production [7,8].

1.2 Catalytic mechanism of amine oxidation

The FAD cofactor is covalently bound via a thioether linkage to a Cys residue of the enzyme (Cys 406 for hMAO-A; Cys 397 for hMAO-B) at the 8a-methylene position of the isoalloxazine ring, playing a crucial role in oxidative deamination. Over the years, two main proposals have been suggested to explain the mechanism of electron transfer from the amine to the flavin ring. The first proposal is the single electron transfer (SET) mechanism proposed by Silverman (**Figure** 2) [9,10,11]However, experimental attempts to support the SET mechanism failed, reinforcing the conclusion that this pathway is both kinetically and thermodynamically improbable.
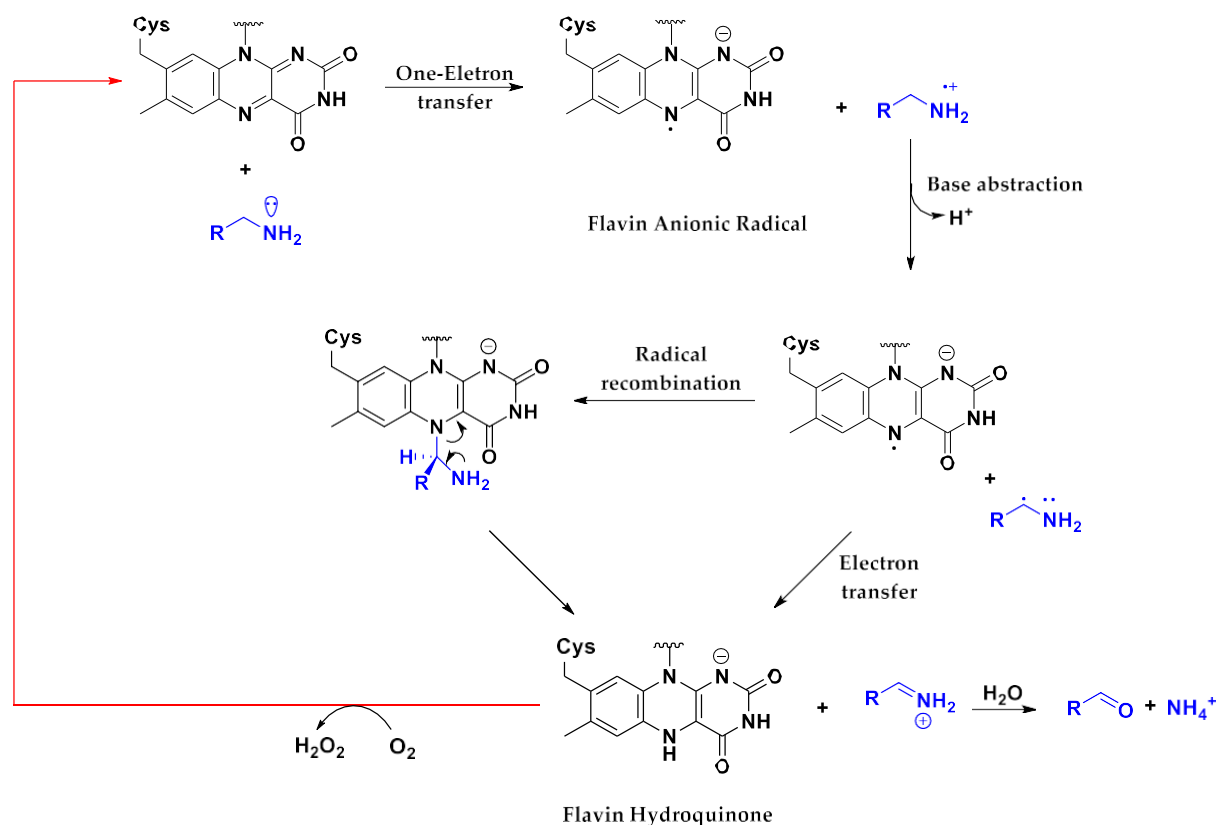
Figure 1.2.1. Single electron transfer (SET) mechanism of action of monoamine oxidases [8]

In 1999, Edmondson proposed the polar nucleophilic mechanism (Scheme), which aligns more closely with experimental evidence. This mechanism does not involve a radical process. Instead, the nucleophilic attack of the amine nitrogen on the C(4a) position of the isoalloxazine ring produces an adduct with a positively charged nitrogen derived from the amine substrate and a negatively charged nitrogen at N(5) of the FAD. This increases the pKa of the α-carbon protons, which can be easily abstracted due to the proximity to the negatively charged N(5) of the isoalloxazine, producing the iminium ion (**Figure** 3). [8]
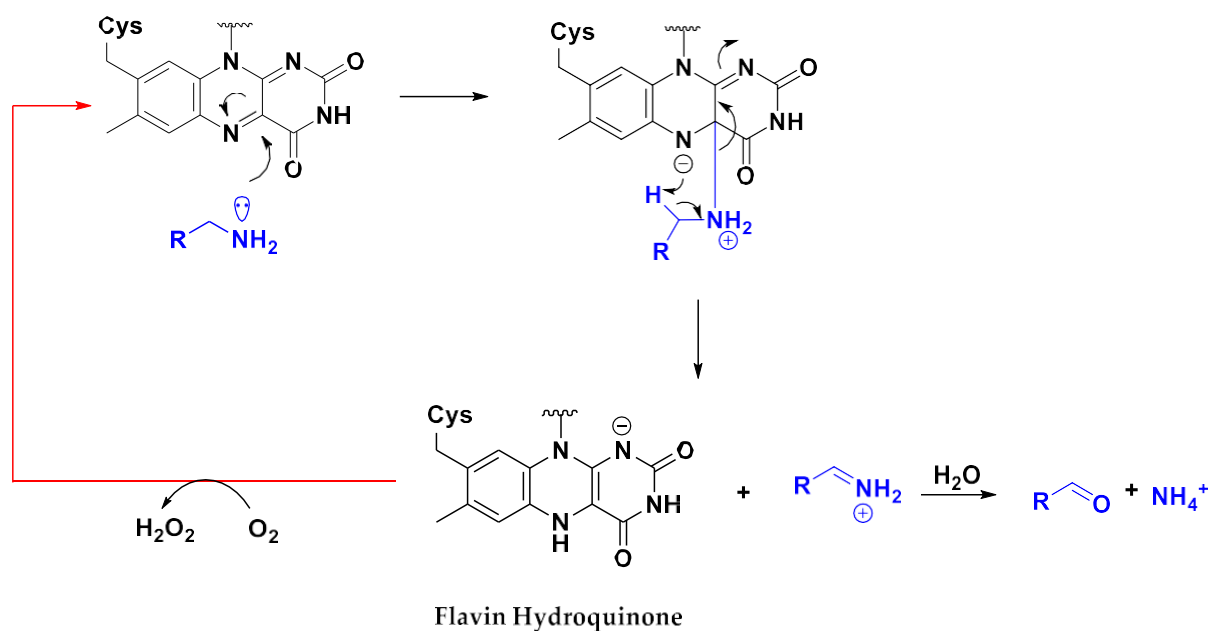
Figure 1.2.2. Polar nucleophilic mechanism of action of monoamine oxidases [12]

The main by-product of this metabolic pathway is hydrogen peroxide, which is typically deactivated by glutathione peroxidase (GDO). However, if glutathione (GSH) levels in the brain are low, hydrogen peroxide can be converted by Fe^{2+} ions (via the Fenton reaction) into highly reactive oxygen species (ROS), which have been implicated in the neurotoxicity observed in some neurodegenerative disorders. [12]

1.3 Structural properties of hMAOs

Human monoamine oxidases A and B share approximately 70% sequence identity and are found in most mammalian tissues [13,14]. These were originally distinguished by their sensitivities to the inhibitors clorgyline and l-deprenyl, as well as their substrate preferences. Generally, hMAO-A is inhibited by low concentrations of clorgyline and catalyses the oxidation of 5-hydroxytryptamine (i.e., serotonine, 5-HT), while MAO-B is inhibited by low concentrations of l-deprenyl and is active towards benzylamine and 2-phenylethylamine. Both isoforms of the enzyme can oxidize dopamine, noradrenaline, adrenaline, tryptamine, and tyramine. There is some evidence of heterogeneity in the behaviour of hMAO isoforms. For

instance, only about 10% of liver hMAO-B can bind imidazolines, and human platelet MAO-B binds imidazolines weakly [15,16]. It is unclear whether this reflects tissue-specific differences in enzyme processing or the effects of an endogenous ligand. Additionally, there are reports that hMAO-A, or a tightly bound component, can modify the substrate specificity of hMAO-B. When platelet hMAO-B was incubated with purified human placental MAO-A, its activity was altered to have both hMAO-A and hMAO-B substrate and inhibitor affinities while retaining hMAO-B immunospecificity. [17]

Reliable expression systems for hMAO-A and hMAO-B have been developed, enabling structural studies of these isoenzymes) [18] The structures of hMAO-B and hMAO-A provide crucial information for the development of effective and selective inhibitors. Initial analysis of human hMAO-B crystals diffracted to 3.0 Å resolution has been carried out by Binda et al in the 2001 [19,20], while a 3.0 Å structure of the adduct of human MAO-A with the acetylenic inhibitor clorgyline has been resolved more recently [21]. For what regard hMAO-B crystal structure, the enzyme is tightly bound to the outer mitochondrial membrane, with the C-terminal region being responsible for this membrane attachment. Analysis of the hMAO-B amino acid sequence suggests that a 27-amino acid transmembrane helix formed by residues 489-515 is the primary structural element responsible for membrane integration [22, 23, 24] Interestingly, further studies have shown that the C-terminal region may contain additional membrane interaction sites; in fact, it seemed that the truncation of this region does not completely abolish the enzyme's ability to bind to the membrane. The crystal structure of hMAO-B reveals that the C-terminal residues form an extended polypeptide chain (461-488) that traverses the monomer surface, followed by an α-helix that corresponds to the predicted transmembrane segment [21]. The orientation of the transmembrane helix, with its axis approximately parallel to the molecular two-fold axis of the MAO-B dimer, suggests that the enzyme binds to the membrane with its two-fold axis perpendicular to the membrane plane. The presence of an arginine residue in the second helix turn, oriented towards the anionic phospholipid headgroups, further supports the importance of electrostatic interactions in the

membrane attachment of hMAO-B. While the C-terminal helix is predicted to extend to residue 515, the electron density in this region is interrupted at Ile496, indicating the possibility of static and/or dynamic disorder in this portion of the helix which results probably due to the absence of membrane bilayer Interestingly, it has been noticed from the study of Binda et al., that together with the C-terminal region, other site could be involved in the membrane binding such as residues 481-488 and other hydrophobic chains such as Phe 481, Leu 482, Leu 486 and Pro 487 point towards the membrane. These structural insights into the membrane attachment of hMAO-B provide a valuable foundation for understanding the enzyme's localization and function within the mitochondrial membrane. [22-29]

The analysis of the electron density map of hMAO-B co-crystalized with pargyline, shows that the inhibitor binds covalently to the N5 atom of the flavin in a solvent-inaccessible environment.[30] The substrate binding site is a flat cavity with a volume of 420 $Å^3$, lined by aromatic and aliphatic amino acids that provide the highly hydrophobic environment predicted by studies of substrate specificity and structure-activity relationships [31]. Adjacent to the substrate cavity there is a smaller, separate hydrophobic cavity lined by residues Phe 103, Pro 104, Trp 119, Leu 164, Leu 167, Phe 168, Leu 171, Ile 199, Ile 316, and Tyr 326. This second cavity is situated between the active site and the protein surface, shielded from solvent by loop 99–112. Residues Tyr 326, Ile 199, Leu 171, and Phe 168 separate the two cavities. These observations suggest a mechanism where the substrate initially accesses the smaller "entrance cavity" through the movement of loop 99–112, and then transiently moves past the four separating residues to reach the active site. The total distance of substrate migration from the entrance cavity surface to the flavin ring is approximately 20 Å. Loop 99–112 may function as a "gating switch" to the entrance cavity, and its proximity to the membrane binding region suggests the substrate must access the catalytic site from the protein surface oriented towards the membrane. [21]

On the other hand, crystallographic structure of hMAO-A has been developed lately compared to the isoform B. Initially, thanks to Ma et al. studies, rat MAO-A (rMAO-A) structure has been

defined, albeit rMAO-A crystals initially prepared only diffracted to 3.2 Å, limiting the level of detail that can be attained about the molecular structure of its active site. However, these results showed that the enzyme used to pack in a tetrameric formation which form a dimeric structure *in vivo* in a way like MAO-B. [2]

It also has been predicted that the C-terminal regions of hMAO-B and rMAO-A are transmembrane α-helices that anchor the enzymes to the mitochondrial outer membrane, with the rest of the protein exposed to the cytoplasm.

Only in 2005, at Berkeley University, De Colimbus and his research group finally discovered the three-dimensional structure of hMAO-A reported as its clorgyline-inhibited adduct [ref de Colimbus [22]. Based on this research, it has been seen that hMAO-A structure is quite similar to both hMAO-B and rMAO-A. However, it also has been noticed that some important differences define the hMAO-A structure as unique in this field. Starting from the cavity-shaping loop 210-216, which represent a fundamental part for hMAO-A active-site. Another unique feature has been represented by the fact that hMAO-A crystalize as a monomer in fact, crystal structures of hMAO-A showing that Lys-151 is located remote from the active site on the protein surface (**Figure**). This surface location is proximal to a cluster of charged residues involved in monomer-monomer contacts to form the dimer in hMAO-B and rMAO-A. No other significant alterations are observed when comparing the residues involved in the dimerization of rMAO-A or hMAO-B with the corresponding residues in hMAO-A. However, the structural data support the intriguing hypothesis [22] that a specific mutation in hMAO-A destabilizes its dimeric state, resulting in its observed monomeric form. The interaction in the active site of the enzyme is between the flavin N5 and the clorgyline. In particular, the binding site is represented by a cavity that start from the flavin ring and arrive to the loop of the residues 210-216. With a volume of around 550 Å and a composition of 11 aliphatic and 5 aromatic residues, this cavity, similar to hMAO-B, showed to be quite hydrophobic. Close to the entrance of the catalytic site two residues of cysteine (Cys-321 and Cys-323) has been found. It has been seen,

during different mass spectrometry and mutagenic studies, that mutations on these two residues seemed to not influence the catalytic activity of the enzyme. [22,23]

To better understand the crystal structure and inhibitory activity of the enzyme, the two isoforms has been compared. The structures of the covalent FAD coenzymes and the two tyrosines constituting the "aromatic cage" [21,23] in the active sites were found to be identical. Since this region of the active sites is directly involved in substrate oxidation, this similarity supports the idea that both enzymes follow the same catalytic mechanisms [23]. However, significant differences were observed in the active site areas opposite the flavin, which govern substrate recognition, where it has been noticed, seven residues differ in identity. Additionally, there is a major alteration in the conformation of loop 210–216, resulting in C movements up to 6 Å due to a more extended loop conformation in hMAO-A. Consequently, the shapes and sizes of the active site cavities differ due to a combination of amino acid replacements and conformational changes. As matter of fact, hMAO-A has a single substrate cavity of 550 Å^3, which is shorter and wider than the longer and narrower cavity in hMAO-B, which has a size of 700 Å^3. Substrate entry into hMAO-B involves entrance and substrate cavities that fuse when certain inhibitors (including deprenyl) are bound. On the other hand, the structural data show that the active site cavity of hMAO-A does not exhibit such a bipartite nature. [22]

Based on these studies, seems clear that understanding the three-dimensional structures of hMAO-A and hMAO-B has offered new insights into how these enzymes interact with substrates and inhibitors. Further research in this area could help clarify the observed species variations in substrate specificity and inhibitor sensitivity, paving the way for the development of more effective hMAOs inhibitors for therapeutic use. [32]

1.4 Pathological role of hMAOs and their inhibitors

Monoamine oxidase enzymes are responsible for the degradation of biologically important amines including neurotransmitters, including neurotransmitters (norepinephrine, epinephrine, serotonin, and dopamine), trace amines, and neurotoxins. Although even if it has

been nearly 100 years since they were first described, there is still a lot to learn about their role in the healthy brain and how they are altered in various disease states. [31]

Monoamines play a unique role in neural development. In addition, to acting as neurotransmitters throughout prenatal life, they also contribute to neural differentiation and morphogenesis. hMAOs are therefore positioned to indirectly impact morphological features of the brain and its neural circuitry.

Tong et al. (2013) conducted a survey of regional hMAO distribution in healthy human brains, spanning 38 regions. The expression of hMAOs was heterogenous, though both isoforms were most highly expressed in the *hypothalamus, nucleus basalis, and the hippocampal uncus.* Across all brain regions examined, hMAO-B was significantly more abundant, with the B:A ratio ranging from 2:6 in the occipital cortex to 17:8 in the caudal corpus callosum [32]. This study revealed three developmental phases for hMAOs in the frontal cortex of healthy human brains. These included an infant phase (up to 1 year), a toddler phase (1–4 years), and the years thereafter. At birth, hMAO-A levels were 78 % of adult levels and increased 50 % above adult levels by 7 months, after which levels declined and stabilized. hMAO-B was barely detectable at birth but increased significantly over the first two years of life. From 18 years of age and up, hMAO-B increased ~20 % per decade, whilst hMAO-A remained stable. Using autoradiography, [34] also observed a significant increase in hMAO-B with age across 18 brain structures. In contrast, to the steady increase in hMAO-B that was observed by Tong et al. (2013), their data showed that hMAO-B began to increase between ages 50–60.

hMAOs were recognized for their role in mood and behaviour regulation in the 1950s. Clinical studies investigating the efficacy of the human monoamine oxidase inhibitor (hMAOI) iproniazid in tuberculosis patients revealed that individuals who were administered the drug became more active and social. The stimulating effect of iproniazid was initially considered a side-effect, and its use as a treatment for depression was quickly pursued. Subsequent studies demonstrated its effectiveness [35] and led to the development of additional hMAOIs to treat depression [36, 37, 38]. hMAOIs are no longer widely prescribed today due to adverse side

effects and drug interactions, however, they are considered good options for treatment of resistant and atypical depression [39,40,41]

hMAO substrates cooperatively mediate a wide range of behaviours and cognitive processes, including aggression [42] motivation [43], and movement; moreover, their metabolites and molecular byproducts also have substantial effects on a wide range of neural functions. Substrate oxidation by both hMAOs produces hydrogen peroxide and ammonia, which are implicated in the pathophysiology of various neurological disorders [44]. hMAOs are also crucial to the formation and function of neurotoxins. hMAO-B mediates the conversion of 1-methyl-4-- phenyl-1,2,3,6-tetrahydropyridine (MPTP) to its neurotoxic metabolite 1-methyl-4-phenylpyridinium (**MPTP)**, which is known to induce PD symptoms and pathology [45]. This compound was obtained as impurity during the attempt to synthesise the meperidine analogue **MPPP** (1-methyl-4-phenyl4-propionoxy-piperidine, **Figure 1.4.1**). MPTP is a "pro-toxin" because exerts neurotoxicity only after its conversion by means of MAO-B, affording MPDP$^+$ which in turn, undergoes spontaneous oxidation to MPP$^+$ provided with neurotoxic properties (**Figure 1.4.1**) [46-48]
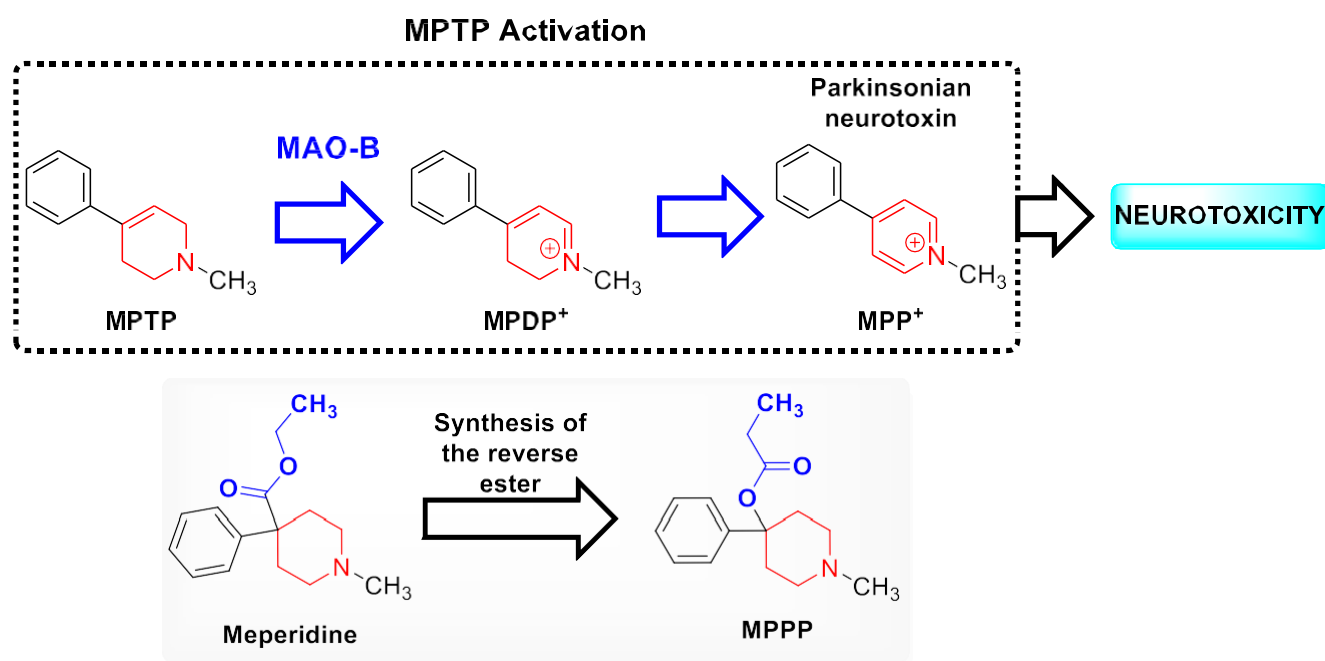
Figure 1.4.1. Structural formula of meperidine analogues and MPTP activation mechanisms.

1.5 MAOs in neurodegenerative diseases

Neurodegenerative disease is a leading cause of disability in elderly populations . Alzheimer's disease (AD) and Parkinson's disease (PD) are the most prevalent neurodegenerative diseases worldwide, affecting an estimated 24 million and 6.1 million people, respectively [49,50]. PD is a heterogenous disease of genetic and sporadic origin that is characterized by progressive loss of dopaminergic neurons in the *substantia nigra pars compacta* [51]. Loss of this neuronal population results in striatal dopamine denervation, leading to motor problems such as rigidity, bradykinesia, resting tremor, and postural instability. Hallmark motor symptoms are often what led to the diagnosis, however, sleep disturbances, depression, and cognitive impairment are often present for years prior to the discovery [52]. Another pathological feature that is often observed in, but not specific to, PD, are Lewy Bodies, intracellular neuronal aggregates that are made up of the protein α-synuclein[53, 54]. Currently, the most common and effective treatment for PD is based on dopamine (DA) replacement, which is achieved through administration of Levodopa (L-dopa), a direct precursor of DA.

However, during the years, clinical studies had shown that rasagiline treatment reduced functional decline in both the short- and long-term treatment [55]. These results suggested that inhibition of hMAO-B in PD is effective because it increases extracellular DA in the striatum and aids in preventing cell death. As matter of fact, hMAO-B inhibitors (hMAO-Bis) continue to be used in the treatment of PD [56,57]. Additional research on the effects of hMAO inhibition in PD is warranted, particularly regarding its role in inflammatory signalling and astrocyte activation. hMAO-B was recently shown to drive NLRP3 inflammasome activation [58]which is known to play a crucial role in PD neural pathology [59]. Additionally, high levels of hMAO-B in astrocytes was observed to induce PD-like pathology in a mouse model [60]. Using quantitative immunoblotting, [33] measured hMAO-A and hMAO-B protein concentration in postmortem brains from individuals diagnosed with PD, multiple systems atrophy (MSA), and progressive supranuclear palsy (PSP). MSA and PSP are considered "Parkinson's-plus" disorders due to their similarities with PD in addition to more widespread, unique pathological

features [61]. Tong et al. (2017) observed significantly elevated hMAO-B expression in the putamen in MSA, in the substantia nigra, caudate, putamen, and frontal cortex in PSP, and in the frontal cortex in PD. hMAO-A levels were significantly decreased in the putamen in MSA and significantly increased in the caudate in PSP and putamen in PD. Their findings demonstrate distinct hMAO dysregulation patterns in three similar neurodegenerative diseases. An unexpected finding in this study was the observation that hMAO-A was elevated in the putamen in PD. DA denervation of the striatum is a pathological feature of PD and hMAO-A is thought to mainly be expressed in dopaminergic neurons [62]. This unexpected increase may be due to hyperexpression of hMAO-A by the surviving dopaminergic neurons, which may function as a compensatory mechanism.

The other neurodegenerative disorders, particularly Alzheimer's disease (AD), impose significant psychological and economic burdens on patients. One of the key factors contributing to cognitive dysfunction in AD is the activation of the hMAO enzymes. Research has demonstrated that monoamine neurotransmitter systems play a crucial role in cognition at the biomolecular level, particularly in functions such as attention, memory, paranoid thinking, orientation, behaviour, and emotion. hMAO enzyme activity disrupts several chemical neurotransmitters, including cholinesterase, glutamate, serotonin (5-HT), and norepinephrine (NE), leading to cognitive impairments. [63,64].

Extensive research has shown that the hMAO-A isoform affecting predominantly NE and 5-HT, regulates cognition, intellect, and motivation, all of which are essential for social interactions. hMAO-A activation negatively impacts the NE pathway, contributing to the symptoms of impaired cognitive functions. Similarly, hMAO-A activation disrupts the cholinergic system, which is closely linked to memory and emotion.

Recent studies have highlighted a significant interaction between hMAO and catechol-O-methyltransferase genotypes, suggesting that increased prefrontal catecholamine availability is correlated with improved working memory. While there is no direct evidence linking neurotransmitter systems and hMAO in AD, several reports indicate that hMAO activation

indirectly affects neurotransmitter systems, contributing to cognitive impairment in AD. Oxidative stress related to hMAO-A activation is a well-known cause of neurotransmitter dysfunction, particularly in the cholinergic system and NE, both of which play critical roles in cognition. [65,66,67]

Neuroinflammation is another critical factor in cognitive decline, serving as an intermediary for oxidative stress. In AD, hMAO may act as a proinflammatory mediator, exacerbating cognitive loss. The activation of hMAO increases levels of monoamines in the brain, disrupting other neurotransmitter systems and leading to cognitive impairments. [68,69]

It has been proposed that monoaminergic dysfunction may play a role in the early stages of depression, while aggression and anxiety in individuals with mild cognitive impairment could indicate a progression to AD. Initially, elevated hMAO-A activity was observed in the platelets and brains of AD patients, with MAO-B activity increasing with age. Compared to age- and gender-matched controls, hMAO-A activity was significantly higher in the platelets of AD patients with dementia, and hMAO-B activity was notably higher in the cortex of the *gyrus cinguli* and *hippocampus* of AD patients. [68]

Evidence has shown that the interaction between clinical features, platelet hMAO-B activity, and cerebrospinal fluid (CSF) monoamine metabolites underscores the importance of platelet hMAO-B activity as a biological marker of AD. Increased hMAO-B activity may indicate a susceptibility to behavioural disorders. Studies using the Mini-Mental State Examination (MMSE) to assess patients in different stages of AD found significant correlations between MMSE scores, age, and hMAO-B activity, suggesting that these markers may reflect the severity or therapeutic progress of AD. [70]

hMAO-A activation also contributes to the formation of amyloid plaques, a hallmark of AD. Research on AD pathogenesis has demonstrated that oxidative damage is prevalent in AD patients, leading to amyloid plaque formation [71-74].Increased hMAO-B activity in the cerebral cortex and hippocampus of AD patients correlates with the presence of these plaques. In astrocytes, elevated MAO-B levels, which are markers of oxidative stress, are believed to

contribute to the excessive deamination of monoamines, releasing more oxygen radicals and hydrogen peroxide (H_2O_2), thus advancing AD progression. [75-79]

Monoamines also influence the symptoms of neuropsychiatric diseases in AD, particularly through the cleavage of amyloid precursor protein (APP). The generation of amyloid-beta (Aβ) involves two successive cleavages of APP by beta-secretase (BACE) and gamma-secretase, a process influenced by MAO-Activity. Aβ production is further affected by 5-HT stimulation of receptors like 5-HT4, 5-HT2c, and 5-HT2a. Moreover, the levels of monoamine metabolites are closely related to cerebrospinal amyloid-beta levels, with increased MAO-B activity in plaques associated with astrocytes being a critical indicator of AD progression. [80]

This association has been recently confirmed through imaging studies in AD mouse models. Given these findings, MAO-B has emerged as a potential therapeutic target for Alzheimer's disease. [81]

1.6 Other neurodegenerative disorders

Neurodegenerative disorders like Huntington's disease and amyotrophic lateral sclerosis (ALS) share several pathological features with Parkinson's and Alzheimer's diseases. These commonalities include oxidative stress, iron accumulation, excitotoxicity, inflammatory processes, and the misfolding of toxic proteins that resist degradation even after ubiquitination. While *R*-(–)-Deprenyl has not shown success in treating ALS, rasagiline and CGP 3466 have demonstrated effectiveness in mouse models of ALS. Additionally, a single-patient study suggested that combining *R*-(–)-Deprenyl with the 5-HT reuptake inhibitor fluoxetine may have beneficial effects in Huntington's disease. [82,83]

1.7 MAOs inhibitors as a therapeutic agent

In recent years, significant progress has been made in developing effective compounds targeting hMAO enzymes, resulting in the creation of various new chemical entities with promising properties. hMAO inhibitors are typically categorized as either selective or non-

selective, and as reversible or irreversible inhibitors. hMAO-A inhibitors (hMAO-AIs) are particularly useful for treating depression, while hMAO-B inhibitors (hMAO-BIs) are valuable in managing Parkinson's disease (PD) especially when combined with L-DOPA (**Figure 1.7.1**) or dopamine agonists, and Alzheimer's disease (AD). However, the challenge of achieving selectivity and affinity for specific isoforms has led to several side effects. Irreversible inhibitors, for instance, cause prolonged enzyme inhibition, which can lead to toxicities such as hypertensive crises, hypotension, and hepatotoxicity—collectively known as the cheese effect. hMAO-A irreversible inhibitors tend to induce the cheese reaction, while hMAO-B inhibitors, at selective doses, generally do not. [84-86]

First-generation hMAO inhibitors are mechanism-based inactivators that act through reactive electrophilic intermediates, which covalently modify proteins. Recent advancements have focused on developing newer, reversible, and selective hMAO inhibitors. Selective irreversible hMAOIs have been designed by adding substituents to the nitrogen atom of selective isozyme substrates, which are metabolized by hMAOs into electrophilic intermediates that alkylate the enzyme's active site. These *N*-substituents include allyl, amino (hydrazines), cyclobutyl, cyclopropyl, trialkylsilanyl, furanoyl, and oxazolidinonyl groups. Modifying the distance between the aromatic ring and the electron-rich centre, or introducing bulky groups on the aromatic ring, has led to the development of selective irreversible hMAO-A inhibitors. This is evident in the structural differences between the hMAO-B selective inhibitor (*R*)-(–)-Deprenyl and the hMAO-A selective inhibitor Clorgyline (**Figure 1.7.1**) [85-87]. Understanding the distinct binding sites within the active centre has helped mitigate some of the issues associated with non-selective inhibitors, particularly the cheese effect. The selectivity of these compounds is attributed to differences in substrate or inhibitor binding sites within the active site, rather than an alternative irreversible linkage to the FAD cofactor. However, it remains unclear whether these recognition sites are due to specific protein structures, lipid microenvironments, or MAO-Binding to certain locations on the outer mitochondrial membrane. [88-91]
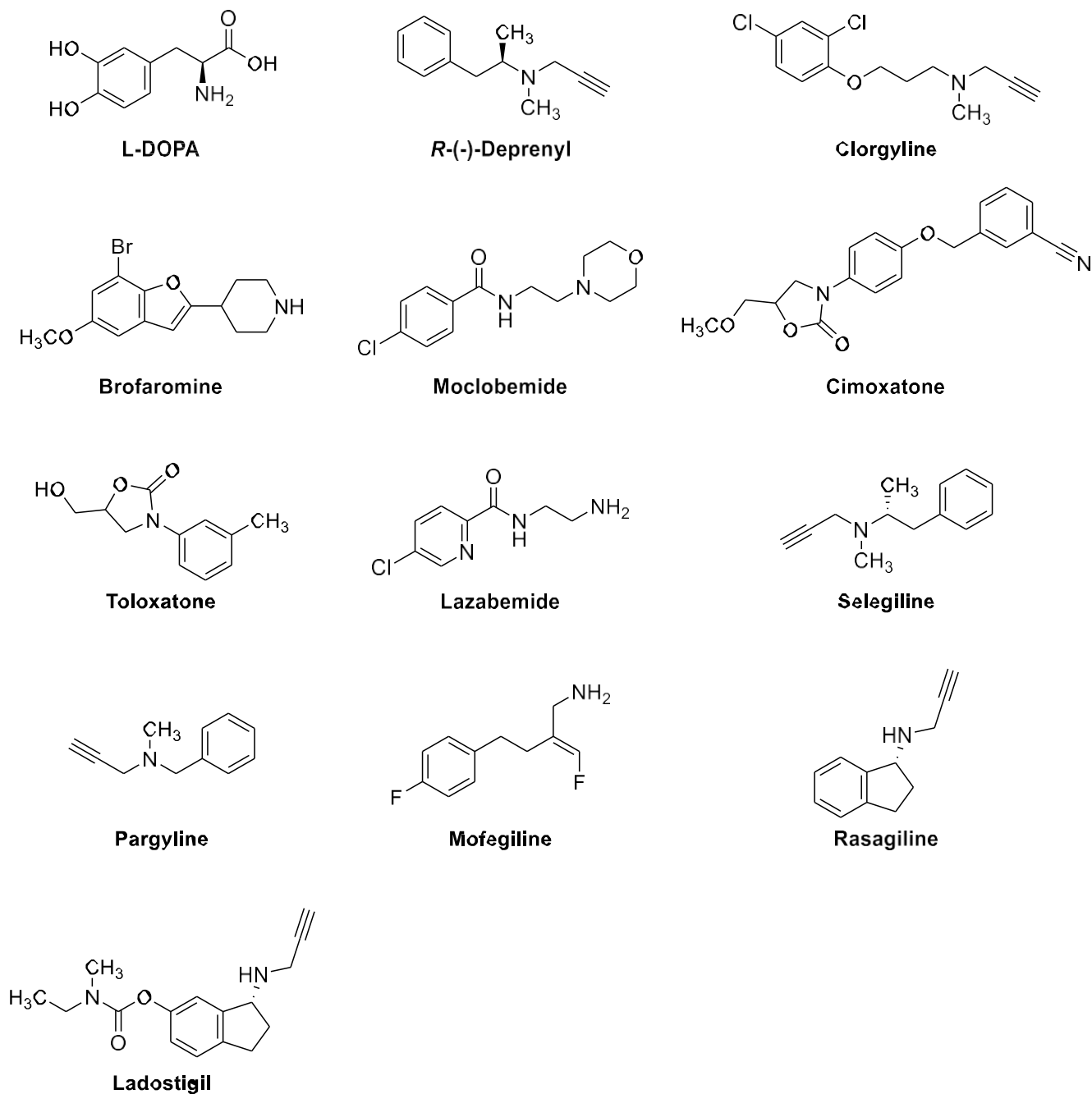
Figure 1.7.1. Structure of some hMAO-A and B inhibitors.

Reversible hMAO inhibitors can be further classified into competitive and slow, tight-binding inhibitors based on their kinetic behaviour. Competitive inhibitors form a readily reversible inhibitor-enzyme complex, while slow, tight-binding inhibitors undergo a time-dependent transformation into an activated complex, resulting in strong binding to the enzyme and a

conformational change in the enzyme structure. The development of reversible hMAO-A inhibitors, such as brofaromine and moclobemide (4-chloro-*N*-(2-morpholin-4-ylethyl)benzamide), as antidepressants, and potential anti-Parkinson's candidates with limited tyramine potentiation, relies on the displacement of the inhibitor by amine from the enzyme binding site (**Figure 1.7.1**). [90]

Chemically, the first reversible hMAO-A inhibitors included morpholine derivatives (moclobemide), benzofuranylpiperidine derivatives (brofaromine), 2-aminoethylcarboxamide derivatives, and oxazolidinone derivatives (cimoxatone, toloxatone) (**Figure 1.7.1**). Numerous other compounds with hMAO-A inhibitory activity, featuring various chemical structures, are currently undergoing preclinical evaluation. Moclobemide, a reversible hMAO-A inhibitor, has been shown to produce up to 80% inhibition in the liver and brain within 30 minutes of administration, with nearly 100% enzyme activity recovery after a 16-hour washout period in ex vivo experiments. Brofaromine's reversibility lasts 24-48 hours, while cimoxatone's lasts approximately 24 hours. In contrast, the irreversible inhibitor tranylcypromine allows only partial recovery of hMAO-A activity (about 50%) within 48 hours, with complete recovery taking much longer and causing prolonged side effects [88, 91]Lazabemide is one of the few examples of reversible hMAO-B inhibitors, while others like selegiline, pargyline, mofegiline, and rasagiline are selective irreversible inhibitors. A significant pharmacological advancement was made by inhibiting both hMAO-A and hMAO-B isoforms to fully exploit the functional activity of amine neurotransmitters without triggering the cheese reaction. This was achieved with the development of the cholinesterase-brain selective hMAO-A and hMAO-B inhibitor Ladostigil (*N*-propargyl-(3R)-aminoindan-5-yl-ethyl methylcarbamate hemitartrate), a carbamate derivative of rasagiline. [93-95] Pharmacologically similar to moclobemide, with limited tyramine potentiation, Ladostigil has demonstrated antidepressant, anti-Alzheimer, and anti-Parkinson activities in specific models through its inhibition of both hMAO-A and hMAO-B (**Figure 1.7.1**). Therapeutic strategies that can reverse, prevent, or even slow neuronal loss remain a critical unmet need in the treatment of neurodegenerative disorders, including

Parkinson's disease (PD). In this context, preclinical studies have clearly shown that the therapeutic benefits of hMAO-B inhibitors in PD extend beyond their primary mechanism of action, namely the inhibition of dopamine metabolism. Specifically, the neurotrophic and neuroprotective properties of hMAO-B inhibitors have garnered significant interest from both the scientific and clinical communities. However, despite strong preclinical evidence, efforts to establish neuroprotective or disease-modifying effects of hMAO-B inhibitors in PD have not yielded positive results. [96-98]

Research on hMAO-A and its inhibitors has significantly advanced the understanding of aminergic neurotransmission, highlighting the crucial role of hMAOs in brain development and function. These studies have led to the clinical use of hMAO inhibitors as antidepressants and anti-parkinsonian drugs. Additionally, further research has driven the development of other enzyme inhibitors for treating Parkinson's and Alzheimer's diseases, including the design of molecules that combine different inhibitory functions. Despite these advances, many questions about hMAO remain unanswered.

Chapter 2

Design and synthesis of carboxamide analogues of benzo[b]thiophene-3-oles

2.1. Design of the novel inhibitors

In 2019 we reported the benzo[*b*]thiophen-3-ol core as a convenient tool for the development of novel neuroprotective agents, the compounds endowed with this scaffold exhibiting promising biological activities on rat cortex synaptosome (*ex vivo* models) in LPS- induced inflammation conditions. The molecular design of benzothiophenes was influenced by the structure of analogues like isatin and indoles, which demonstrated selectivity in inhibiting different isoforms of hMAO enzymes, targeting hMAO-B and hMAO-A, respectively. While the size of the molecules may help explain their varying affinities for the hMAO isoforms, it is important to highlight that differences in the electron density of the molecular structures play a significant role in determining enzymatic selectivity. By focusing on the isosteric substitution of nitrogen in the indole system with an oxygen atom or a methylene group, aurone and indanone derivatives are obtained, respectively. [94-99-100] To explore new structures for the inhibition of hMAO, a novel scaffold based on the benzo[*b*]thiophen-3-ol structure has been developed (**Figure 2.1.1**).
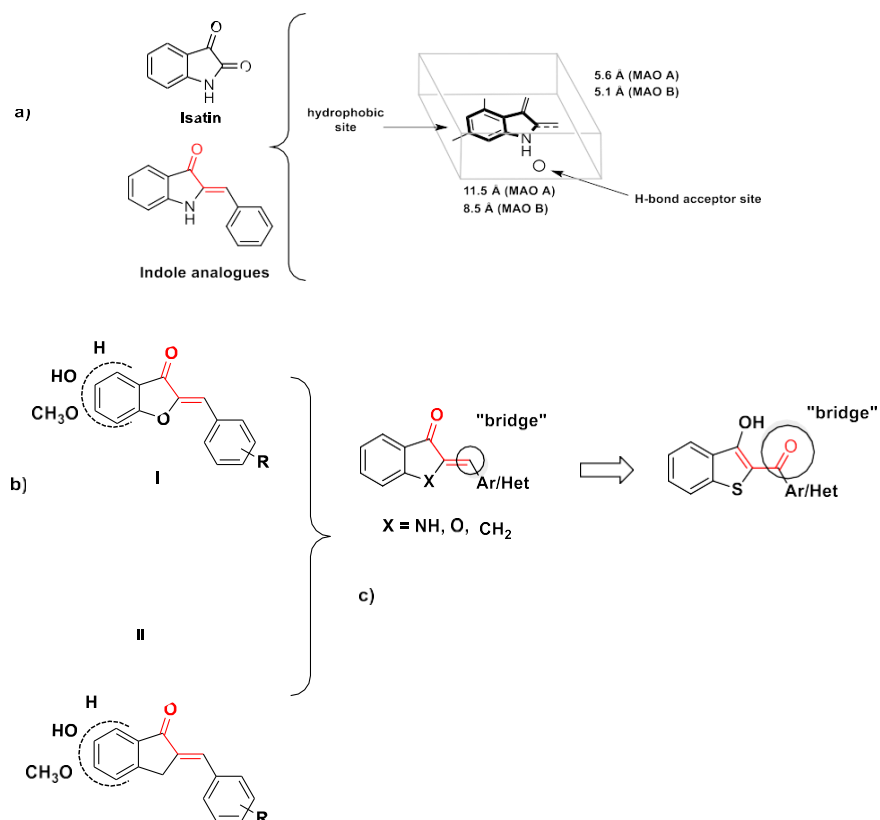
Figure 2.1.1. Design of the benzo[*b*]thiophen-3-ole scaffold.

This scaffold maintained some similarities with the previously discussed compounds (i.e., aurone, indanone and indole scaffolds), such as the presence of a bicyclic system connected by a "bridge" to an aromatic or heteroaromatic ring. In the case of indole, aurone, and indanone derivatives, the bridge is formed by the β-carbon of the α,β-unsaturated ketone. In contrast, for the benzo[*b*]thiophen-3-ol structure, the carbonyl group of the α,β-unsaturated ketone serves as the bridge.

Taking advantage of a straightforward one-step synthetic procedure (see below), the compounds PM1-PM20 (**Figure 2.1.2**) were synthesised and evaluated against the two isoforms of human monoamine oxidase. Only PM2, PM17, and PM18 slightly favored hMAO-A inhibition, while the others were more selective for hMAO-B, with IC_{50} values ranging from micromolar to low micromolar.
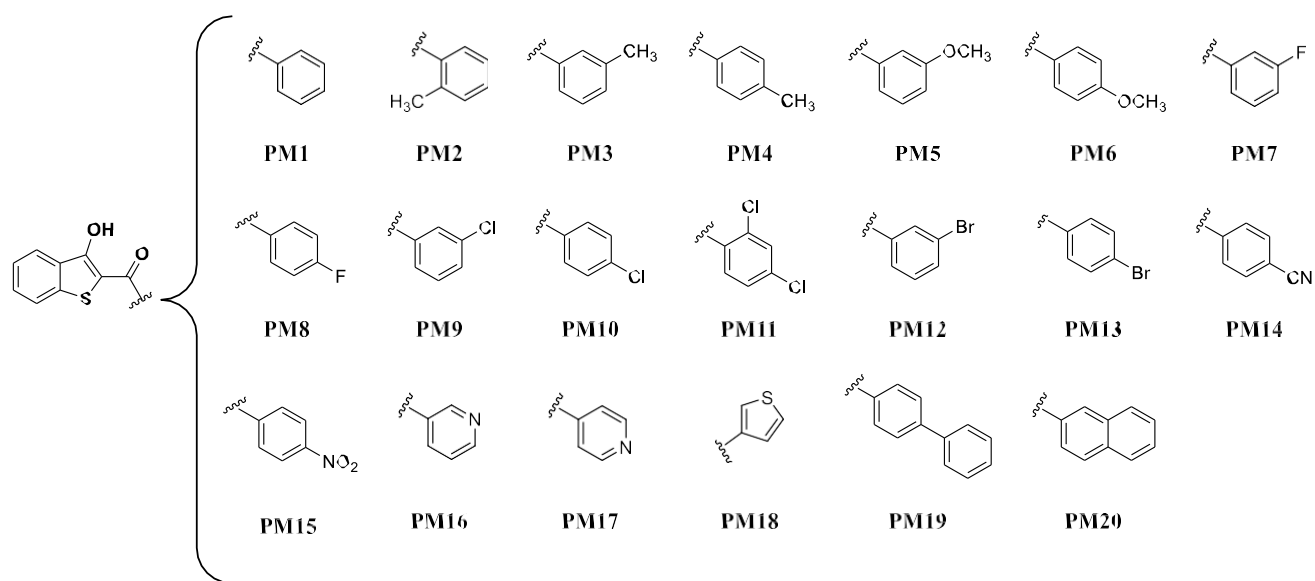
Figure 2.1.2. Structure of the compounds PM1-PM20.

PM1, the simplest compound, showed low selectivity, inhibiting both isoforms similarly. Substituting the phenyl ring altered activity depending on the substituent's position and type. For instance, adding a methyl group, an electron donor, at the *meta* and *para* positions improved hMAO-B inhibition, particularly in PM4, which also showed better hMAO-A inhibition. In contrast, *ortho*-substitution reduced inhibition toward both isoforms.

Methoxy groups followed a similar trend, with the *para* position enhancing hMAO-B inhibition and the *meta* position increasing selectivity by lowering hMAO-A inhibitory activity. Halogen-substituted compounds, particularly PM12, demonstrated increased hMAO-B inhibition and selectivity as halogen size increased. Compounds PM14 and PM15, with CN and NO_2 at the *para* position, inhibited hMAO-B but lacked selectivity. Introducing a heterocyclic ring in PM16-PM19 decreased hMAO-B inhibition, whereas substituting the phenyl ring with a bulky naphthyl group, as in PM20, enhanced both inhibition and selectivity for hMAO-B.

Molecular docking studies were conducted in order to unravel the molecular attributes responsible for inhibitory activity and selectivity. Several compounds of this series have been developed with variations in substituents, including bromobenzene, which appears to help hMAO-B inhibition. This preference could be attributed to the intermolecular hydrogen bond

with the Tyr326 side chain in the binding pocket. Additionally, the benzothiophene portion of the compounds is involved in $\pi-\pi$ stacking interactions with Tyr407, further contributing to selective inhibitory activity.

Regarding the binding of other derivatives, visual analysis revealed that the benzothiophene portion could adopt different modes of interaction within the hMAO-B active site, either maintaining or not maintaining the molecular hydrogen bond. Some derivatives oriented the benzothiophene portion towards the FAD cofactor, establishing $\pi-\pi$ interactions with the aromatic amino acids in the active site. In contrast, the benzothiophene portion of other compounds was directed towards the mouth of the active site gorge, positioning the hydroxyl group near the Tyr326 side chain or the Ile199 residue. Consequently, the docking results indicated that both $\pi-\pi$ interactions and hydrogen bonds with Tyr326 could play a crucial role in binding to hMAO-B. [1]

With the aim to deeply investigate the potential of the 2-aroyl-benzo[b]thiophen-3-ole scaffold, we evaluated some chemical modification of this structure. In the 2016 Reis and colleagues evaluated a series of chromone-based compounds substituted at the position 3 with different spacers (carboxamide, ester, thioester, amine and vinyl, **Figure 2.1.3**) [101-102] Structure Activity Relationship (SAR) studies concerning the spacers introduced between the γ-pyrone and the exocyclic ring showed that the most active and selective derivatives were the ones endowed with amide function, the other spacers resulting in derivatives with significantly lower potency and selectivity. Taking inspiration by this work, we designed a series of carboxamide analogues of the 2-aroyl-benzo[b]thiophen-3-oles by replacing the carbonyl spacer with the amidic one (**Figure 2.1.3**).
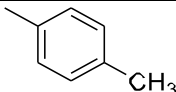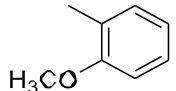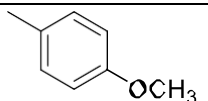
Previous work from Reis *et al*:

This work:
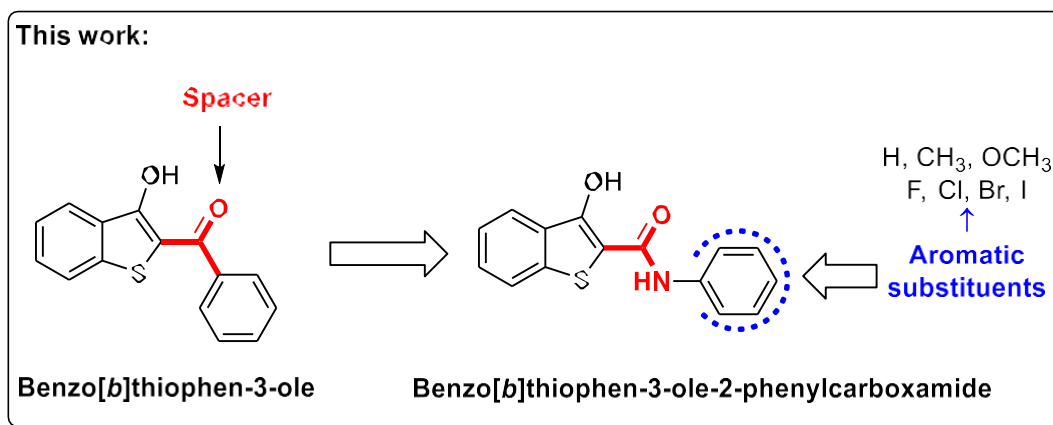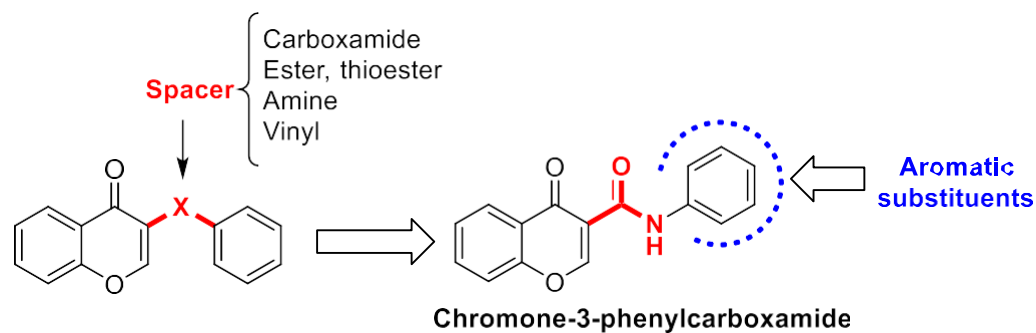
Figure 2.1.3. Design of the 2-phenylcarboxamide analogues of 2-aroyl-benzo[*b*]thiophen-3-oles.

2.2. *Chemistry*

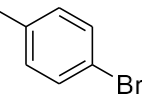The compounds reported in this thesis project have been synthesised through a multi-step synthetic approach (**Scheme 2.2.1**). In the first step (**I**), methyl thiosalicylate was reacted with ethyl 2-bromoacetate in the presence of potassium carbonate (K_2CO_3) as base. The reaction was performed in acetonitrile (CH_3CN) at refluxing conditions to afford the ethyl ester of the 3-hydroxybenzo[*b*]thiophene-2-carboxylic acid (intermediate **A**, **Scheme 2.2.1**). The hydroxyl group of the intermediate A was successively masked (**II**) by employing chloromethyl methyl ether as protecting agent (intermediate **B**, **Scheme 2.2.1**). This step was mandatory because, in the absence of protective moiety, the formation of a pseudo-cycle between the 2-carboxylic moiety and the vicinal 3-hydroxyl prevent ester hydrolysis, also in harsh conditions. The reaction (**II**) was performed in dry dichloromethane (DCM) in the presence of *N*,*N'*-diisopropylethylamine (DIPEA) as base, at room temperature (RT). Consequently, the obtained

intermediate **B** was easily hydrolyzed (**III**) using lithium hydroxide (LiOH) in a mixture of tetrahydrofuran (THF), methanol (MeOH) and water (H_2O), in the volume ratio of 3:1:1, to afford the intermediate **C** (**Scheme 2.2.1**).

Once intermediate **C** has been synthesized the successive steps (**IV** and **V**, **Scheme 2.2.1**) led to the final compounds. In the former (**IV**), the coupling reaction between the carboxylic acid (intermediate **C**) and the proper (un)substituted anilines, took place. The reactions were performed using ethyl chloroformate as coupling agent, in the presence of an excess of triethylamine (Et_3N) in dry THF, at room temperature and under nitrogen (N_2) atmosphere. In the latter step (**V**) the eleven intermediates obtained earlier (**D1**-**D11**) underwent the removal of the protecting group to afford the final compounds **1**-**11**. The "de-protection" reactions were performed in MeOH in the presence of concentrated hydrochloric acid (6M), at room temperature.
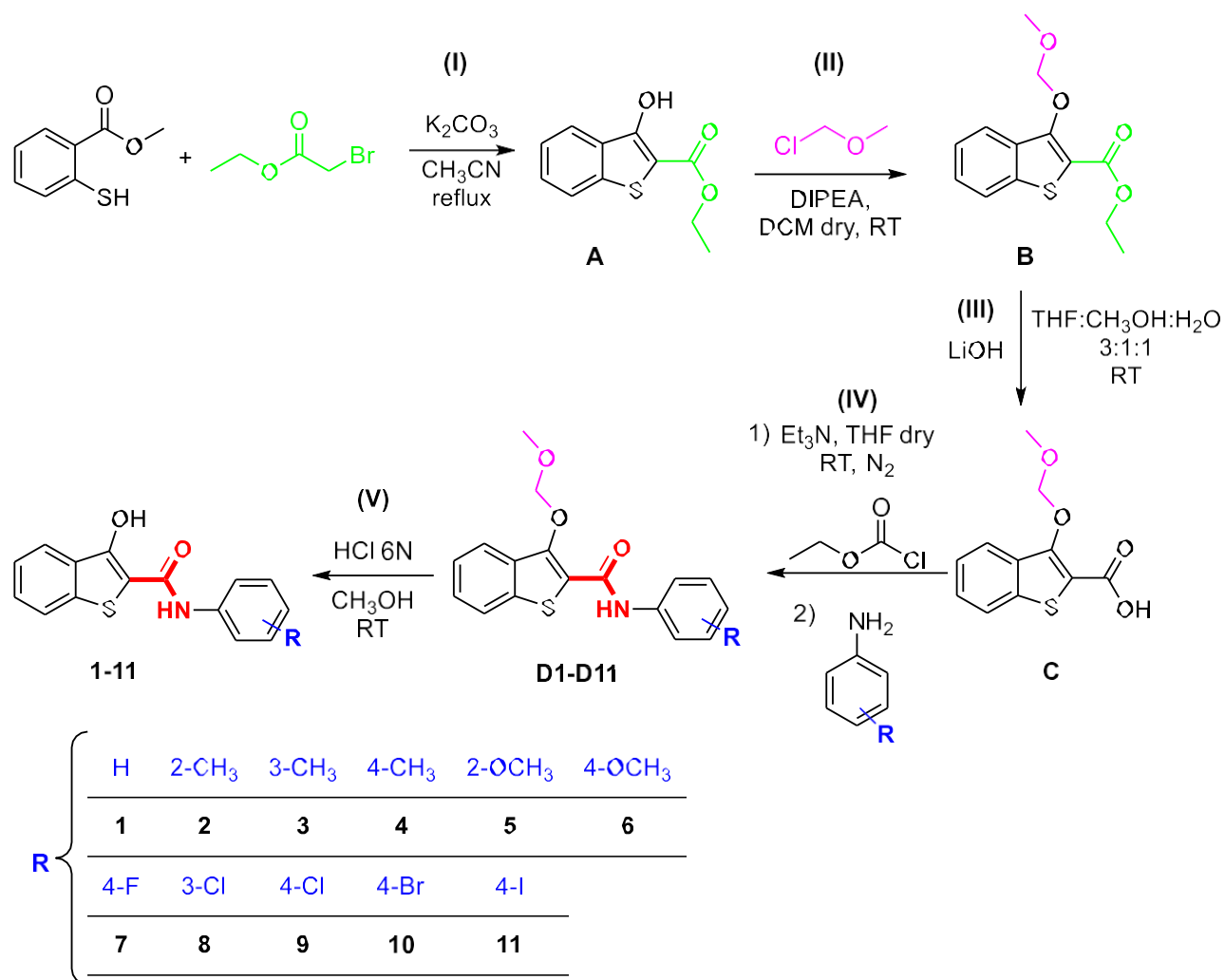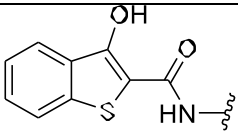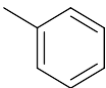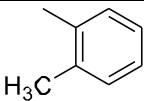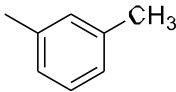
Scheme 2.2.1. Synthesis of the 2-phenylcarboxamide analogues of 2-aroyl-benzo[*b*]thiophen-3-oles
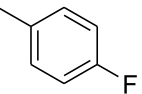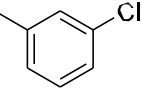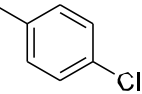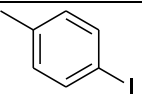
2.3. In vitro MAOs inhibition study

The compounds **1-11** have been appraised against both hMAO-A and hMAO-B (**Table 2.3.1**). A first screening has been performed at a fixed concentration of the inhibitors (10 µM) to determine the ones able to inhibit the two isoforms at the level equal or superior to 50%, our threshold value to determine IC_{50}. These preliminary results show that most of the compounds are selective for isoform B, with derivative **5** endowed with 2-methoxy group as substituent, exhibiting the complete inhibition (100%) of this isoform. Interestingly, the change of position of this group to the *para* position (compound **6**), led to the dramatic loss of affinity against B isoform (**Table 2.3.1**). Interesting results were also observed with the compound **4** bearing *para-*

methyl group exhibiting 65.31% inhibition against hMAO-B; on the contrary, the same substituent located at the positions *ortho* and *meta* (compounds **2** and **3**, respectively) was poor tolerated leading to weaker inhibitors (percentage of inhibition < 50%). With the exception of compound **11**, encouraging results were observed with halogen substituted derivatives, also showing a trend in the inhibitory activity results against hMAO-B (**7-10**). In particular, *para-*bromo compound (**10**) exhibited highest inhibitory activity among the halogen-substituted compounds, followed by *para*-chloro and *para*-fluoro derivatives. So, it is quite clear that increasing the halogen dimension led to the improvement of the inhibitory activity against hMAO-B. However, this trend did not include iodine (compound **11**), whose presence at the *para* position of the phenyl ring had detrimental effects.

Table 2.3.1. Inhibitory activity (%) of compounds **1-11** towards hMAO-A and hMAO-B

Compound	Substituent	Inhibition (%)*, §	
		hMAO-A	hMAO-B
1		26.0	17.0
2		7.9	3.4
3		23.5	40.5
4		0	**65.3**
5		14.0	**100.0**
6		0	15.1

7	(4-F phenyl)	0	**69.8**
8	(3-Cl phenyl)	23.1	**51.8**
9	(4-Cl phenyl)	27.3	**70.1**
10	(4-Br phenyl)	15.1	**82.8**
11	(4-I phenyl)	41.6	38.4
*Percentage inhibition evaluated at fixed concentration (10 µM) of inhibitor; §Errors are in the range of ±5% of the reported values, from three different assays			

2.4. Conclusions

The reported project has been based on the synthesis and evaluation of a series of carboxamide analogues of 2-aroyl-benzo[*b*]thiophen-3-oles, developed through a multi-step synthetic approach, based on the previous successful work carried out by Guglielmi et al in 2019, focused on the benzo[*b*]thiophene-3-ole scaffold. Additionally, to further explore the potential of the 2-aroyl-benzo[b]thiophen-3-ole scaffold, we examined several chemical modifications, drawing inspiration from the work of Reis et al. (2016), who investigated chromone-based compounds with various spacers. Their Structure-Activity Relationship (SAR) analysis revealed that carboxamide spacers produced the most potent and selective derivatives. Building on these findings, we designed a series of carboxamide analogues by replacing the carbonyl spacer with an amide group. This modification aimed to enhance the biological activity and selectivity of the compounds, laying the foundation for future development of neuroprotective agents.

The eleven obtained compounds were synthesized and characterized by means NMR spectroscopy (^{1}H and ^{13}C) and evaluated for their biological activity through enzymatic inhibitory essays. The biological evaluation revealed that many of the synthesized compounds

exhibited selective inhibition towards the hMAO-B isoform. Specifically, derivative 5 (3-hydroxy-N-(2-methoxyphenyl)benzo[*b*]thiophene-2-carboxamide), with a 2-methoxy substituent, demonstrated complete inhibition of hMAO-B at a concentration of 10 μM. Encouraging results were found with halogen-substituted derivatives (7 to 10, respectively: N-(4-fluorophenyl)-3-hydroxybenzo[*b*]thiophene-2-carboxamide, *N*-(3-chlorophenyl)-3-hydroxybenzo[*b*]thiophene-2-carboxamide, *N*-(4-chlorophenyl)-3-hydroxybenzo[*b*]thiophene-2-carboxamide , *N*-(4-bromophenyl)-3 hydroxybenzo[*b*]thiophene-2-carboxamide) , showing a clear trend in hMAO-B inhibitory activity. The *para*-bromo compound (**10**) exhibited the highest inhibition (82.8 %), followed by *para*-chloro and *para*-fluoro derivatives, indicating that larger halogens seem to improve the activity. However, this trend did not extend to iodine (compound **11**), which had a detrimental effect on inhibition.

This research underscores the potential of these compounds as selective hMAO-B inhibitors, paving the way for further investigation, including the determination of IC_{50} values for the most promising derivatives. It also establishes a solid foundation for the continued development of neuroprotective agents aimed at treating neurodegenerative diseases.

2.5. Material and methods

2.5.1. General

Unless otherwise indicated, all reactions were carried out under a positive nitrogen pressure (balloon pressure) in washed and oven-dried glassware. Solvents and reagents were used as supplied without further purification. All melting points were measured on a Stuart® melting point apparatus SMP1 and are uncorrected (temperatures are reported in °C). Fluorescence spectrophotometry was carried out with a Varian Cary Eclipse fluorescence spectrophotometer. ^{1}H and ^{13}C NMR spectra were recorded at 400 and 101 MHz, respectively, on a Bruker spectrometer using CDCl$_3$ and DMSO-d_6 as the solvents at room temperature. The samples were analysed with a final concentration of ~30 mg/mL. Chemical shifts are expressed as δ units (parts per million) relative to the solvent signal. ^{1}H spectra are reported as follows: δ_H (spectrometer frequency, solvent): chemical shift/ppm (multiplicity, J-coupling constant(s), number of protons, assignment). ^{13}C spectra are reported as follows: δ_C (spectrometer frequency, solvent): chemical shift/ppm (J-coupling constant C-F, assignment). Multiplicity is abbreviated as follows: br – broad; s – singlet; d – doublet; t – triplet; q – quartet; m – multiplet. Coupling constants J are given in Hertz (Hz). The processing and analyses of the NMR data were carried out with MestreNova. Column chromatography was carried out using Sigma-Aldrich® silica gel (high purity grade, pore size 60 Å, 230–400 mesh particle size). All the purifications and reactions were monitored by TLC which was performed on 0.2 mm thick silica gel-aluminium backed plates (60 F$_{254}$, Merck). Visualization was carried out under ultra-violet irradiation (254 nm). Where given, systematic compound names are those generated by ChemBioDraw Ultra 12.0 following IUPAC conventions. Recombinant hMAO-A and hMAO-B (5 mg protein/mL) and kynuramine dihydrobromide were obtained from Sigma-Aldrich.

2.5.2. Chemistry

Synthesis of ethyl-3-hydroxybenzo[b]thiophene-2-carboxylate derivative (A)

To synthesize the ethyl-3-hydroxybenzo[*b*]thiophene-2-carboxylate derivative (**A**), methyl thiosalicylate (1.0 equivalent) was reacted with ethyl bromoacetate (1.2 equivalents) in the presence of potassium carbonate (1.2 equivalents) as a base, with acetonitrile as the solvent. The reaction mixture was stirred overnight and monitored by thin-layer chromatography (TLC), using a petroleum ether/ethyl acetate mixture (9:1) as the mobile phase. Upon completion, the reaction mixture was treated with water and ice, followed by acidification to neutral pH with 2N HCl. The product was extracted three times with dichloromethane (DCM), and the organic layer was washed with brine, dried over anhydrous sodium sulfate, filtered, and concentrated under reduced pressure. The crude product was purified by column chromatography on silica gel, using a petroleum ether/ethyl acetate mixture (25:1) as the eluent. The final product was obtained as a white solid in 78% yield.

Synthesis of ethyl 3-(methoxymethoxy)benzo[b]thiophene-2-carboxylate (B)

In a round-bottom flask, ethyl 3-hydroxybenzo[*b*]thiophene-2-carboxylate (**A**) (1.0 equivalent) was reacted with chloromethyl methyl ether (1.0 equivalent) in 50 mL of anhydrous dichloromethane (DCM) at room temperature. *N,N*-diisopropylethylamine (1.5 equivalents) was then added dropwise at 0 °C. The reaction mixture was stirred overnight at room temperature under an inert atmosphere. Upon completion, the reaction mixture was extracted three times with a saturated sodium bicarbonate (NaHCO$_3$) solution and dichloromethane. The organic layer was washed with brine, dried over anhydrous sodium sulfate, filtered, and concentrated using a rotary evaporator. The crude product was used in the subsequent reaction step without further purification.

*General procedure for the synthesis of the 3-(methoxymethoxy)benzo[b]thiophene-2-carboxylic acid derivative (C)*

In a 250 mL flask, ethyl 3-(methoxymethoxy)benzo[*b*]thiophene-2-carboxylate (1.0 equivalent)

was treated with lithium hydroxide monohydrate (4.0 equivalents) in a solvent mixture of tetrahydrofuran, methanol, and water (3:1:1 ratio, 1 mL/mmol). The reaction proceeded at room temperature overnight, with its progress monitored via TLC using a petroleum ether/ethyl acetate (4:1) mobile phase, until the disappearance of the reactant spots indicated completion. Afterward, THF and methanol were removed by rotary evaporation, and water was added to the remaining mixture. The solution was then acidified with 2N HCl, precipitating 3-(methoxymethoxy)benzo[b]thiophene-2-carboxylic acid as a light pink solid. This solid was collected by vacuum filtration and directly used in the subsequent step to synthesize 3-(methoxymethoxy)-N-phenylbenzo[b]thiophene-2-carboxamide, with a yield of 57%.

General procedure for the synthesis of the 3-(methoxymethoxy)-N-phenylbenzo[b]thiophene-2-carboxamide derivatives (D1-D11)

In a 250 mL flask, under an inert atmosphere, 1.0 equivalent of the **C** intermediate in anhydrous tetrahydrofuran was combined with triethylamine (3.0 equivalents) and ethyl chloroformate (1.0 equivalent). After approximately 10 minutes, 1.2 equivalents of aniline, substituted at various positions, were added to the reaction mixture. The reaction was stirred for 5 hours and monitored via TLC, using a petroleum ether/ethyl acetate mixture (6:1) as the mobile phase. Upon completion, water and ice were added, and the mixture was acidified with 2N HCl to a pH of 5. The organic product was extracted twice with dichloromethane, and the organic phase was washed with brine, dried over anhydrous sodium sulfate, filtered, and concentrated using a rotary evaporator. The resulting dark viscous oil was purified via column chromatography on silica gel, using petroleum ether/ethyl acetate mixtures (ratios of 4:1, 5:1, or 7:1) as the mobile phase. The final product, 3-(methoxymethoxy)-N-phenylbenzo[b]thiophene-2-carboxamide, was obtained as a white solid, with a yield ranging from 54% to 66%.

General procedure for the synthesis of the 3-hydroxy-N-phenylbenzo[b]thiophene-2-carboxamide derivatives 1-11

In a 100 mL flask, 3-(methoxymethoxy)-*N*-phenylbenzo[*b*]thiophene-2-carboxamide (1.0 equivalent) was treated with 6N HCl (5 mL/mmol) in methanol (10 mL/mmol) at room temperature for 2 hours. The reaction progress was monitored in real time by TLC, using a petroleum ether/ethyl acetate mixture (6:1) as the mobile phase. Upon completion, water was added, and the mixture was extracted with dichloromethane. The organic layer was washed with brine, dried over anhydrous sodium sulfate, filtered, and concentrated via rotary evaporation. The resulting solid was purified through column chromatography, employing a petroleum ether/ethyl acetate mixture (6:1) as the eluent. The purified fractions were collected and evaporated under reduced pressure, yielding a white solid with a yield between 43% and 68%.

2.6 Characterization data for the compounds 1-11
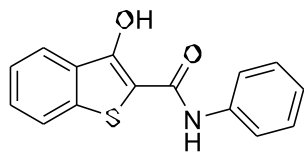
3-hydroxy-N-phenylbenzo[b]thiophene-2-carboxamide (1)

White solid, 37% yield. ^{1}H NMR (400MHz, CDCl$_3$) δ 7.63 – 7.35 (m, 6H), 7.76 (dd, J = 8.1, 1.1 Hz, 1H), 7.22 – 7.13 (m, 2H), 11.68 (s, OH, 1H), 7.98 (dt, J = 7.9, 1.1 Hz, NH, 1H). ^{13}C NMR (101MHz, CDCl$_3$) 117.5 (Benzothiophene) 118.7 (Benzothiophene) 120.98 (Benzothiophene), 121.5 (d, J= 11.0 Hz, 2C, Ar) (122.62 (Benzothiophene) 123.09 (Benzothiophene), 124.90 (Benzothiophene), 125.27 (Benzothiophene), 128.92 (d, J= 11.0 Hz, 2C, Ar), 129.01(Ar), 136.69 (Ar), 160.00 (C=O), 164.30 (C$_{benzothiophene}$ -OH).
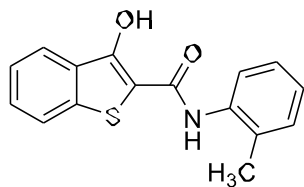
3-hydroxy-N-(o-tolyl)benzo[b]thiophene-2-carboxamide (2)

White solid, 41% yield. ^{1}H NMR (400MHz, DMSO-d_6) δ 6.95 (d, J = 7.5 Hz, 1H), 7.26 (t, J = 7.8 Hz, 1H), 7.57 – 7.42 (m, 4H), 7.96 (d, J = 8.0 Hz, 1H), 8.08 (d, J = 7.9 Hz, 1H), 9.89 (s, NH, 1H), 12.26 (s, OH, 1H), 2.32 (s, CH3, 3H). ^{13}C NMR (101MHz, DMSO-d_6) 21.63 (CH$_3$), 111.06 (Benzothiophene), 117.03 (Benzothiophene), 121.23 (Benzothiophene), 122.80 (Ar), 123.93 (Benzothiophene), 124.4 (Benzothiophene), 124.97 (Benzothiophene), 128.22 (Ar), 129.21 (Ar), 132.07 (Ar), 137.40 (Ar), 138.50 (Ar), 138.63 (Ar), 149.90 (Benzothiophene), 159.89 (C=O), 162.19 (C$_{benzothiophene}$ -OH).
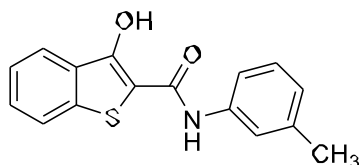
3-hydroxy-N-(m-tolyl)benzo[b]thiophene-2-carboxamide (3)

White solid, 39% yield. ^{1}H NMR (400 MHz, DMSO-d_6) δ 6.95 (d, J = 7.5 Hz, 1H), 7.26 (t, J = 7.8 Hz, 1H), 7.57 – 7.42 (m, 4H), 7.96 (d, J = 8.0 Hz, 1H), 8.08 (d, J = 7.9 Hz, 1H), 9.89 (s, NH, 1H), 12.26 (s, OH, 1H), 2.32 (s, CH3, 3H). ^{13}C NMR (101 MHz, DMSO-d_6) δ 21.63 (CH$_3$), 117.06 (Benzothiophene), 118.0 (Benzothiophene) 121.23 (Benzothiophene), 123.07(Benzothiophene), 123.93 (Benzothiophene), 124.97 (Benzothiophene), 125.15, 128.22, 129.21, 132.07, 137.40, 138.50, 138.63, 152.35 (Benzothiophene), 161.04 (C=O) 162.19 (C$_{benzothiophene}$ -OH).
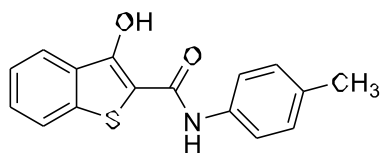
3-hydroxy-N-(p-tolyl)benzo[b]thiophene-2-carboxamide (4)

White solid, 43% yield. ^{1}H NMR (400 MHz, DMSO-d_6) δ 7.17 (d, J = 8.2 Hz, 2H), 7.62 – 7.41 (m, 4H), 7.95 (d, J = 8.0 Hz, 1H), 8.10 – 8.03 (m, 1H), 9.88 (s, NH, 1H), 12.25 (s, OH, 1H). ^{13}C NMR (101 MHz, DMSO-d_6) 20.96 (CH$_3$), 110.80 (Benzothiophene), 115.81 ((Benzothiophene) , 120.82 (Benzothiophene), 121.05 (2 2C, Ar) 123.03 (Benzothiophene), 123.91 (Benzothiophene), 124.96 (Benzothiophene), 129.74 (Ar), 136.03 (Ar), 137.37 (Benzothiophene), 152.50 (C=O), 162.23 (C$_{benzothiophene}$ -OH).
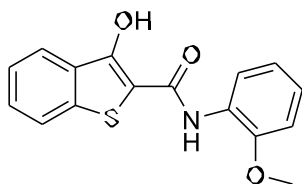
3-hydroxy-N-(2-methoxyphenyl)benzo[b]thiophene-2-carboxamide (5)

White solid, 33% yield. ^{1}H NMR (400 MHz, CDCl$_3$) δ 6.93 (dd, J = 8.1, 1.4 Hz, 1H), 7.02 (td, J = 7.8, 1.4 Hz, 1H), 7.51 (m, J = 8.2, 7.1, 1.3 Hz, 1H), 7.77 – 7.71 (m, 1H), 8.00 – 7.90 (m, 2H), 8.39 (dd, J = 7.9, 1.7 Hz, NH, 1H), 11.70 (s, OH, 1H). ^{13}C NMR (101MHz, CDCl$_3$) δ 56.60 (-OCH3) 111.47 (Benzothiophene), 112.8 (Ar), 113.99 (Benzothiophene), 117.3 (Benzothiophene) 119.61 (Benzothiophene), 121.21 (Benzothiophene), 123.21 (Benzothiophene), 123.91 (Benzothiophene), 124.87 (Ar), 128.05 (d, J = 30.7 Hz, Ar), 132.46 (Ar), 137.47 (Ar), 148.35 (Ar) , 149.93 (Benzothiophene), 160.79 (C=O), 164.0 (C$_{benzothiophene}$ -OH).
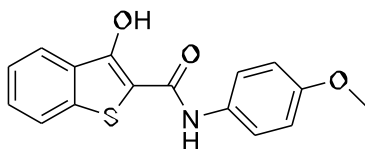
3-hydroxy-N-(4-methoxyphenyl)benzo[b]thiophene-2-carboxamide (6)

White solid, 38% yield. ^{1}H NMR (400 MHz, DMSO-d_6) δ 6.99 – 6.90 (m, 2H), 7.65 – 7.41 (m, 4H), 8.07 – 7.92 (m, 2H), 9.85 (s, NH, 1H), 12.22 (s, OH, 1H). ^{13}C NMR (101MHz, DMSO-d_6) 55.70 (OCH$_3$), 109.4 (Benzothiophene), 114.20 (Benzothiophene), 118.0 (Benzothiophene), 120.91 (d, J= 11.0 Hz, 2C, Ar), 122.53 (Benzothiophene), 122.85 (Benzothiophene), 128.16 (d, J= 11.0 Hz, 2C, Ar), 131.99 (Benzothiophene), 137.23 (Benzothiophene), 152.85 (Ar), 156.34 (Ar), 162.26 (C=O), 164.0 (C$_{benzothiophene}$ -OH).
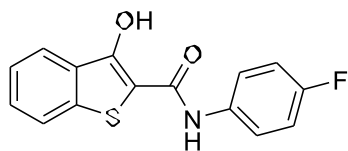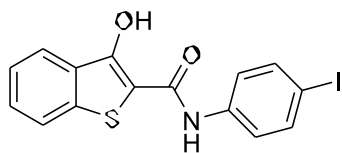
N-(4-fluorophenyl)-3-hydroxybenzo[b]thiophene-2-carboxamide (7)

White solid, 45% yield. ^{1}H NMR (400 MHz, DMSO-d_6) δ 7.27 – 7.16 (m, 2H), 7.49 (m, J = 26.5, 8.2, 7.1, 1.2 Hz, 2H), 7.80 – 7.68 (m, 2H), 7.96 (d, J = 8.0 Hz, 1H), 8.10 – 8.04 (m, 1H), 9.98 (s, NH, 1H), 12.22 (s, OH,1H). ^{13}C NMR (101 MHz, DMSO-d_6) 110.38 (benzothiophene), 115.80 (benzothiophene), 116.03 (benzothiophene), 121.9 (d, J= 11.0 Hz, 2C, Ar), 123.07 (benzothiophene), 123.94 (benzothiophene), 124.1 (benzothiophene), 124.6 (benzothiophene), 128.31 (d, J= 11.0 Hz, 2C, Ar), 131.99 (Ar), 152.83 (C=O), 162.38 (C$_{benzothiophene}$ -OH), 162.90 (Ar) .
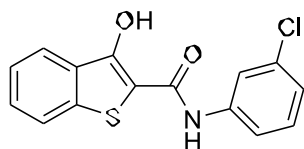
N-(3-chlorophenyl)-3-hydroxybenzo[b]thiophene-2-carboxamide (8)

White solid, 43% yield. ^{1}H NMR (400MHz, CDCl$_3$) δ 7.23 – 7.11 (m, 2H), 7.23 – 7.11 (m, 2H), 7.50 – 7.41 (m, 2H), 7.54 (ddd, J = 8.3, 7.1, 1.3 Hz, 1H), 7.79 – 7.72 (m, 2H), 7.98 (d, J = 8.0 Hz, 1H), 11.54 (s, 1H). ^{13}C NMR (101 MHz, DMSO-d_6) 116.64 (Benzothiophene), 119.19 (Benzothiophene), 120.21 (Ar) , 122.8 (Benzothiophene), 123.21 (Benzothiophene), 124.02 (Benzothiophene), 124.5 (Benzothiophene) 125.03 (Benzothiophene), 128.41 (Ar), 130.99 (Ar), 132.02 (Ar), 133.62 (Ar), 137.57 (Ar), 140.11 (Ar), 152.75 (C=O), 164.52 (C$_{benzothiophene}$ -OH)
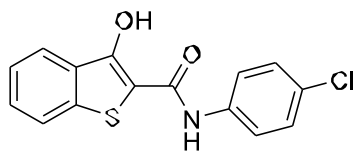
N-(4-chlorophenyl)-3-hydroxybenzo[b]thiophene-2-carboxamide (9)

White solid, 39% yield. ^{1}H NMR (400 MHz, DMSO-d_6) δ 7.23 – 7.11 (m, 2H), 7.32 (t, J = 8.1 Hz, 1H), 7.50 – 7.41 (m, 2H), 7.54 (m, J = 8.3, 7.1, 1.3 Hz, 1H), 7.79 – 7.72 (m, 2H), 7.98 (d, J = 8.0 Hz, NH, 1H), 11.54 (s, OH, 1H). ^{13}C NMR (101MHz, DMSO-d_6) δ 115.64 (Benzothiophene), 119.19 (Benzothiophene), 120.21 d, J= 11.0 Hz, 2C, Ar), 123.21 (Benzothiophene), 124.02 (Benzothiophene), 124.8 (Benzothiophene), 125.03 (Benzothiophene), 130.99 (d, J= 11.0 Hz, 2C, Ar) ,133.1 (Ar), 136.23 (Ar) 149.11 (Benzothiophene), 157.75 (C=O), 165.38 (C$_{benzothiophene}$ -OH)
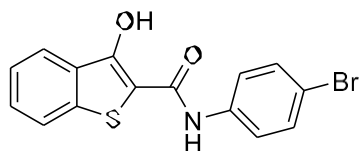
N-(4-bromophenyl)-3-hydroxybenzo[b]thiophene-2-carboxamide (10)

White solid, 35% yield. ^{1}H NMR (400 MHz, DMSO-d_6) δ 7.60 – 7.52 (m, 3H), 7.75 – 7.67 (m, 2H), 7.96 (d, J = 8.0 Hz, 1H), 8.09 (d, J = 7.9 Hz, 1H), 10.02 (s, NH, 1H), 12.26 (s, OH, 1H). ^{13}C NMR (101 MHz, DMSO-d_6) 114.68 (Benzothiophene), 116.08 (Benzothiophene), 122.8 (Benzothiophene), 123.16 (Benzothiophene), 123.95 (Benzothiophene), 125.02 (Benzothiophene), 126.36 (d, J= 11.0 Hz, 2C, Ar), 132.01 (d, J= 11.0 Hz, 2C, Ar), 147.08 (Benzothiophene), 152.69 (C=O), 162.30 (C$_{benzothiophene}$ -OH).

3-hydroxy-N-(4-iodophenyl)benzo[b]thiophene-2-carboxamide (11)

White solid, 41% yield. ^{1}H NMR (400 MHz, DMSO-d_6) δ 7.61 – 7.42 (m, 4H), 7.75 – 7.67 (m, 2H), 7.96 (d, J = 8.0 Hz, 1H), 8.12 – 8.05 (m, 1H), 10.00 (s, NH, 1H), 12.26 (s, OH, 1H). ^{13}C NMR (101 MHz, DMSO-d_6) 86.11 (C$_{Ar}$-I) 113.77 (Benzothiophene), 117.9 (Benzothiophene), 122.89 (Benzothiophene), 123.15 (Benzothiophene), 123.95 (Benzothiophene), 124.1 (Benzothiophene), 136.9 36 (d, J= 11.0 Hz, 2C, Ar) ,138.48 (Benzothiophene), 160.8 (C=O), 164.27 (C$_{benzothiophene}$ -OH).

2.5.3 Evaluation of human monoamine oxidase (hMAO) inhibitory activity

The assay for the evaluation of the inhibitory activity of the compounds is based on the measurement of the conversion rate of a hMAO-substrate, kynuramine, into its oxidized metabolite, 4-quinolinol (4HQ), that absorbs at 316 nm. The assay has been performed as previously described1.First, a calibration curve was created using 4-quinolinol solutions at different concentrations (ranging from 0,1 nM to 10 mM). Then, the kinetic properties (specific activity, Michaelis-Menten constant K_M, and maximum speed V_{max}) of the two isoforms were evaluated using solutions with different enzyme concentrations (X to X) for the measurement of the specific activity, and kynuramine solutions with at least six different concentration levels (Y to Y) for the measurement of K_M and V_{max}. After having fully characterized the enzymes, the inhibitory activity of the compounds was measured. Compound solutions were pipetted in a 96-wells plate, together with kynuramine solution (concentration = 2 x K_M in the well), phosphate buffer (pH = 7.4) and the plate was then incubated at 37°C for 10 minutes. Absorbance of the wells was measured every minute and the last read (t = 10 min) was used as blank. Then, the enzyme was added (the amount of enzyme added depended on the specific activity, Vmax = 50 pmol/min) and the plate was incubated at 37°C for 30 minutes. The formation of 4-quinolinol was analysed and the production formation rate, or initial velocity V0, was obtained from the slope of the *n (4HQ) = f(t)* curves. Inhibition percentages at 10 μM

were obtained from the comparison between the initial speed of the control well (no inhibitor) and the initial speed of the inhibitor. All compounds have been screened at 10 µM, those whose inhibition was ≥ 50%, were further investigated and their IC_{50} was measured as follows. Different concentrations for each inhibitor were tested and analysed as previously described. Dose-response curves were created using the percentage of inhibition as a function of the logarithm of the concentration of the inhibitor. The IC_{50} value was extrapolated from the curve. The results have been expressed as mean value ± standard deviation. All experiments have been performed in triplicate and conducted three times.

Chapter 3: from benzo[b]thiophene-3-oles to the open-structure analogues

3.1. Design of the novel inhibitors

The observations made on benzo[*b*]thiophen-3-ol derivatives both in terms of IC$_{50}$ and enzyme binding, prompted interest in studying open-structure analogues of this scaffold. The goal was to evaluate whether opening the ring could afford a more favourable interactions within the enzymes active site. As stated above, the compounds PM1-PM20 were obtained through a novel and efficient one-step synthetic procedure (**Scheme 3.1.1**), albeit several research groups also proposed synthetic strategies to obtain this class of compounds [104-105] Methyl 2-mercaptobenzoate and the proper α-bromo ketone in equimolar amount, were reacted in methanol in the presence of potassium hydroxide. The reaction was performed in a nitrogen atmosphere and at room temperature for 1-2 h. After this time, an excess of potassium hydroxide was added, and the temperature was raised to 60 °C. The completion of reactions was usually reached in 4-5 h producing all the compounds PM1-PM20 in high yields (**Scheme 3.1.1**, **I**). The reaction mechanism proposed for this synthesis underlined the importance of the intermediate **W**, obtained through the nucleophilic attack of the deprotonated thiol group on the α-position of the ketone (**Scheme 3.1.1**, **II**).
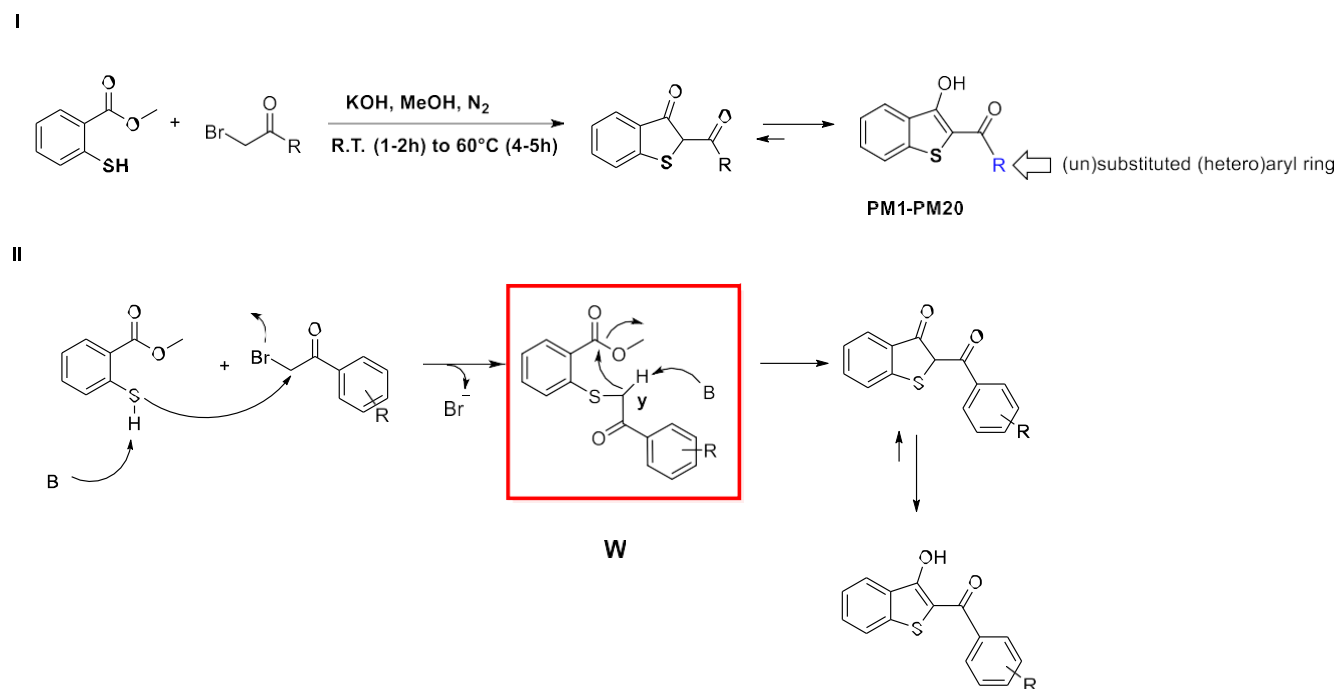
Scheme 3.1.1. I) Synthesis of the benzo[*b*]thiophen-3-oles. **II**) Proposed mechanism of reaction.

49

After that, an intramolecular crossed aldolic reaction between the methylene group (**y** in the **Scheme 3.1.1**, **II**) and methyl ester functional group with consequent methanol elimination occurred, affording the benzo[*b*]thiophen-3-ol core. The intermediate **W** inspired us for the development of the novel open-structure analogues of benzo[*b*]thiophen-3-oles, based on the methyl 2-(benzylthio)benzoate scaffold (red square in **Scheme 3.1.1**), that has been further explored through different chemical modifications. Indeed, the ester moiety (red in **Figure 3.1.1**) has been replaced with carboxylic acid functionality in order to evaluate how the different hydrogen-bond acceptor/donator profiles affect both inhibitory activity and selectivity. The phenyl ring (**blue in Figure 3.1.1**) has been substituted with groups having different electronic/steric properties. Finally, the role of the oxidation state of sulfur atom has also been challenged by synthesising three different sub-libraries of compounds, i.e. sulfide, sulfoxides and sulfones.
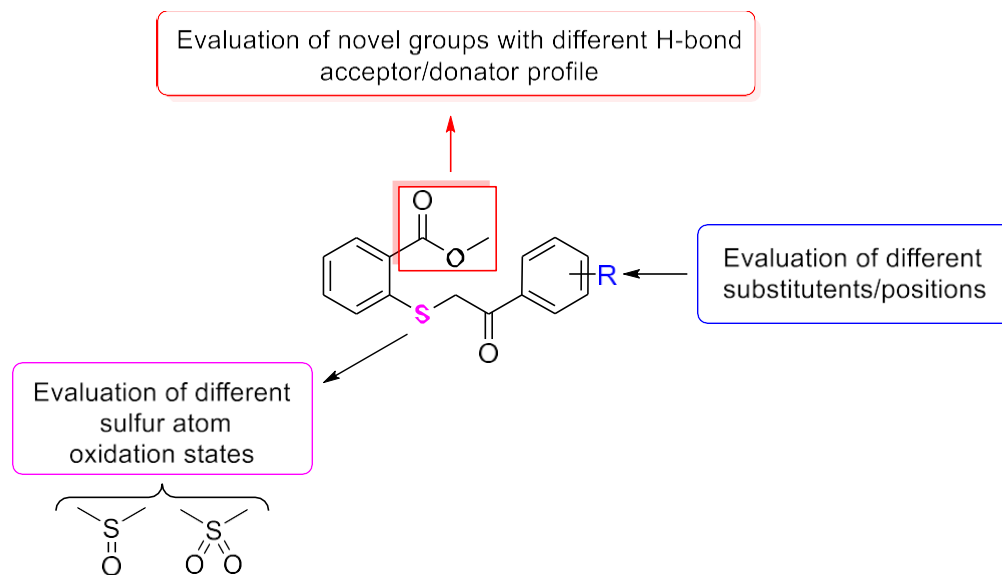
Figure 3.1.1. Design of the novel open-analogues of 2-aroyl-benzo[*b*]thiophen-3-oles.

3.2. Chemistry

The compounds reported in this thesis project have been synthesised through a multi-step synthetic approach developed on the basis of the results obtained in the preliminary stages. We hypothesized to employ the synthetic approach showed in the **Scheme 3.2.1**, at first. This approach was based on the initial synthesis of the ester derivatives (**Library I, Scheme 3.2.1**), whose hydrolysis was supposed to afford the acidic compounds belonging to the **Library II** (**Scheme 3.2.1**). After that, oxidation with *meta*-chloroperbenzoic acid (*m*-CPBA) at room temperature of the Libraries I and II, should have led to the sulfoxide and sulfone derivatives of the ester and carboxylic acid analogues, respectively (**Libraries IA**, **IB**, **IIA** and **IIB**).
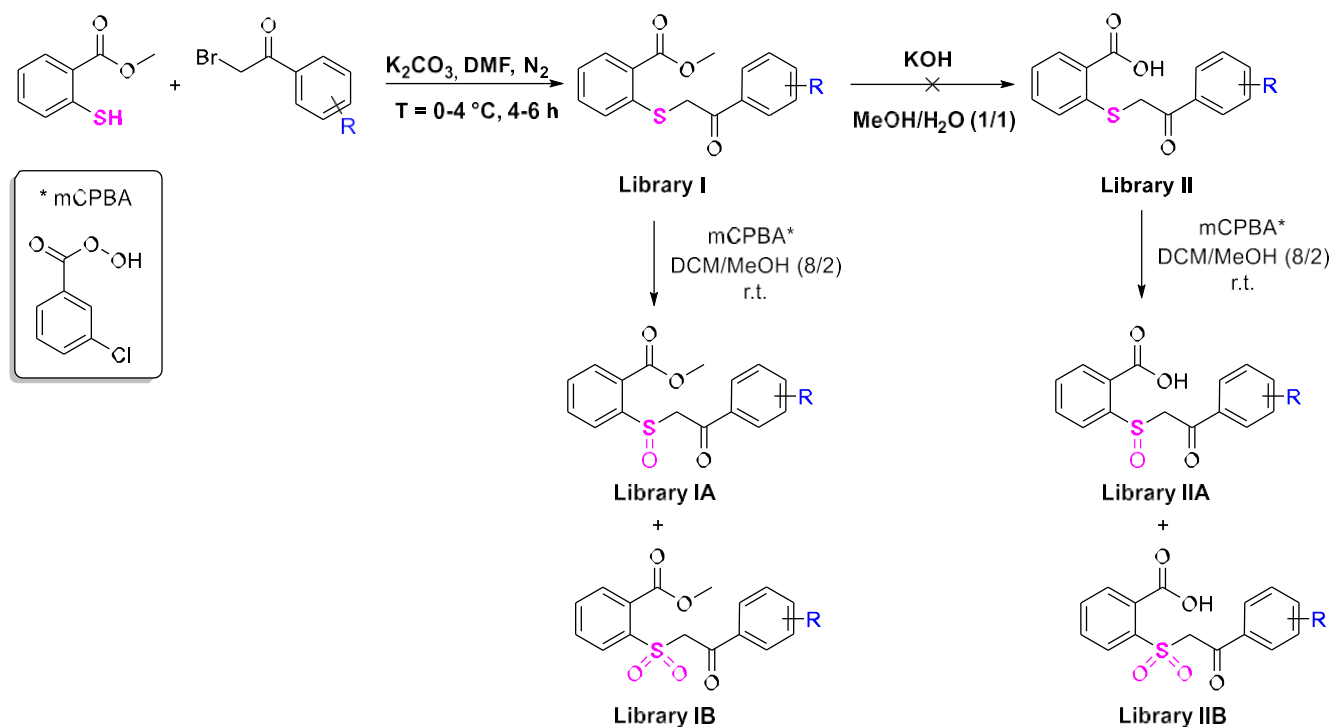
Scheme 3.2.1. Synthetic approach initially proposed for the target compounds.

However, the attempts performed to obtain the hydrolysis of the esters belonging to **Library I** always led to the respective benzo[*b*]thiophen-3-oles regardless the temperature as well as the base employed. Indeed, we tried to perform classical hydrolysis step at mild (40 °C) as well as

higher temperature (60 °C), with different bases such as KOH, NaOH and LiOH in a mixture with varying ratios of H_2O/THF. However, no or small amount of acids have been obtained.

As an alternative method, hydrolysis in the presence of lithium chloride (LiCl) and DMF was considered. This reaction, conducted using microwave irradiation, offers the advantage of reducing reaction times and enabling hydrolysis reactions on molecules with groups sensitive to acidic or basic environments [108]. Various parameters were analysed: temperature, time, and equivalents of LiCl and *N,N'*-dimethylformamide (DMF) used. Initially, 5 equivalents of LiCl and 5 equivalents of DMF were used at 150 °C for 10 minutes. Subsequently, the temperature was maintained at 150 °C, and the reaction time was extended to 30 minutes, using both 5 and 10 equivalents of LiCl and DMF. Finally, the temperature was reduced to 50 °C, keeping the reaction time the same, and 5 and then 10 equivalents of LiCl and DMF were employed. However, no significant differences have been observed in terms of yields, with the cyclic by-product being the main product. So, with the aim to overcome this issue, we designed a new synthetic strategy (**Schemes 3.2.2** and **3.2.4**).
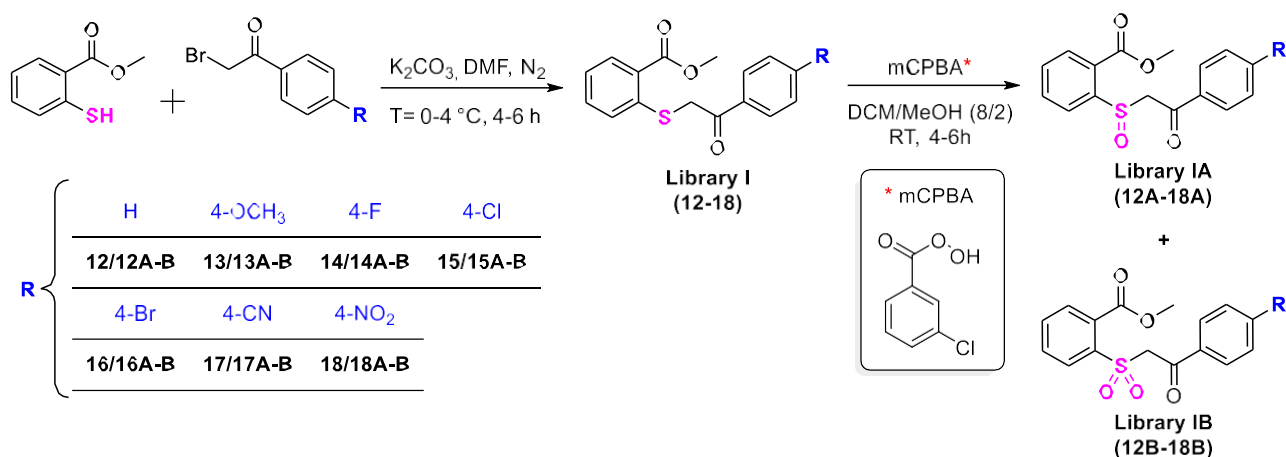
Scheme 3.2.2. Synthetic approach employed for the synthesis of the Libraries I, IA and IB.

As regard the ester derivatives (**Libraries I**, **IA** and **IB**), the synthetic procedure was similar to the one previously described, based on the synthesis of sulfides (**Library I**), followed by their transformation into sulfones and sulfoxides via the oxidation of the sulfur atom(**Library IIA**

and **IIIA**). Briefly, to obtain **Library I**, methylthiosalicylate was reacted with the proper (un)substituted α-bromoacetophenone in anhydrous DMF at ice-bath temperature, using potassium carbonate as the base for a period spanning from 2 to 4 hours. The synthesized sulfides were subsequently subjected to the oxidation step. This reaction was carried out at room temperature in a mixture of dichloromethane (DCM) and methanol, using *m*-chloroperbenzoic acid as the oxidizing agent. The use of *m*-CPBA, allow to obtain both the sulfoxide and sulfone in the same reaction step, by controlling the amount of oxidant added during the synthesis (**Library IA** and **IB**, **Scheme 3.2.2**). The couple of sulfoxide and sulfone contained in the crude obtained by reaction are easily isolable through chromatographic approaches, to achieve the title compounds.
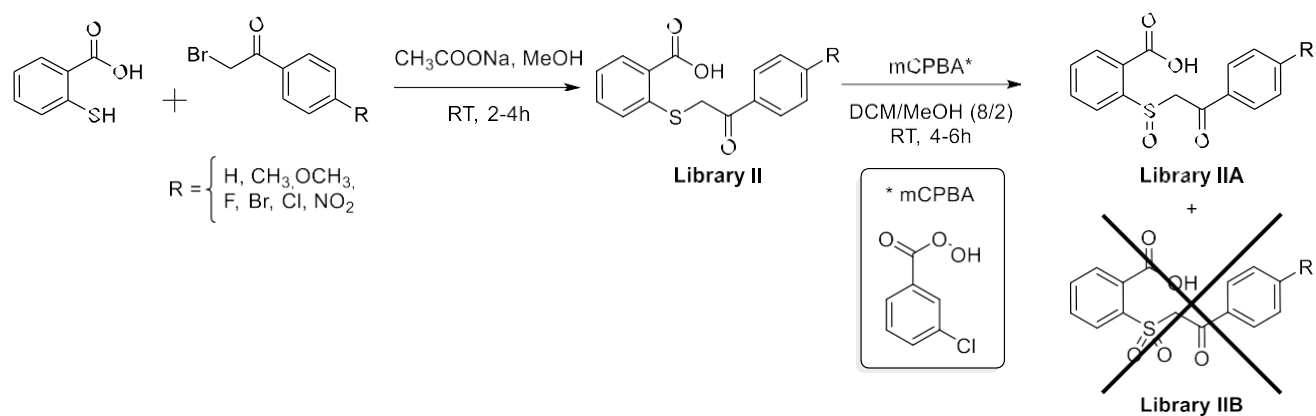
Scheme 3.2.3. Synthetic approach initially proposed for the compounds of Libraries II, IIA and IIB.

For the compounds endowed with carboxylic acid group we changed the synthetic approach with respect to the envisaged one. Indeed, we performed the synthesis of the sulfide derivatives (**Library II**) through the reaction between thiosalicylic acid and the proper α-bromoacetophenone; the reactions were performed in methanol, at room temperature and in the presence of sodium acetate (CH₃COONa). The obtained compounds were employed in the successive oxidative step to obtain sulfoxides (**Library IIA**) and sulfones (**Library IIB**). However, differing from the ester analogues, the synthesis performed with *m*-CPBA only afforded the sulfoxide derivatives (**Library IIA**, **Scheme 3.2.3**). Moreover, the presence of
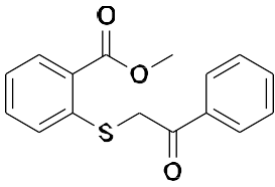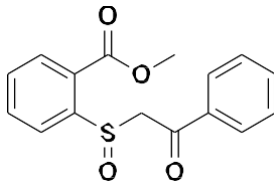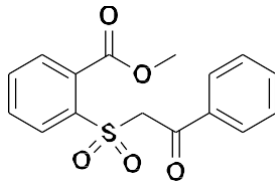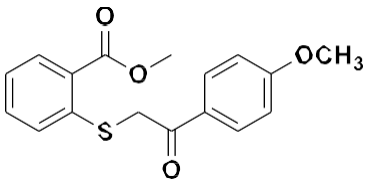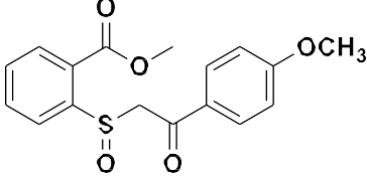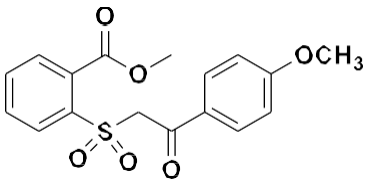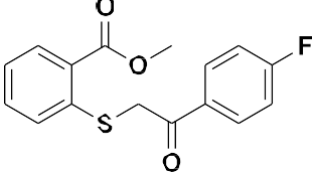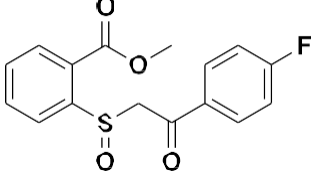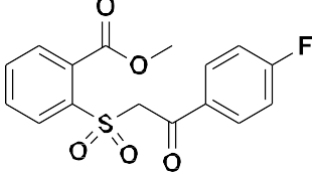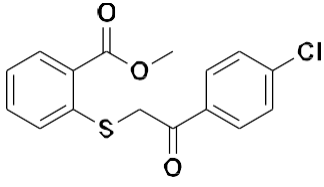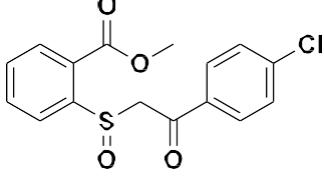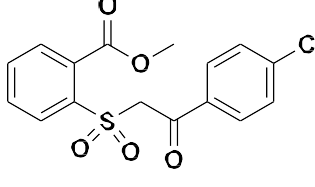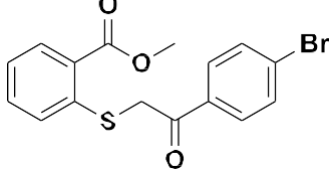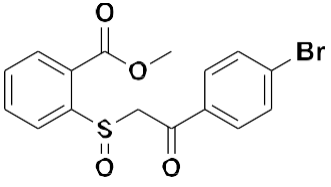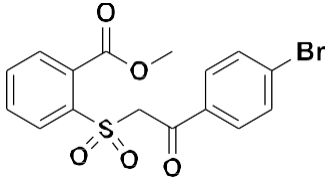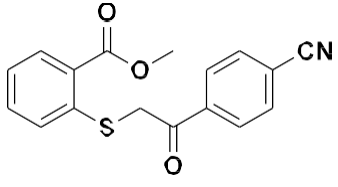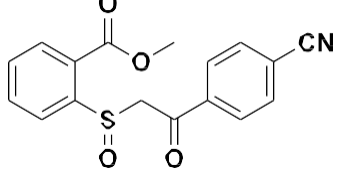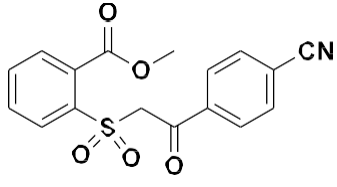
another acid (*m*-CPBA) over the sulfur/sulfoxides ones, get more difficult the successive purification step. So, we evaluated a different approach for the synthesis of sulfoxides and sulfones (**Scheme 3.2.4**).
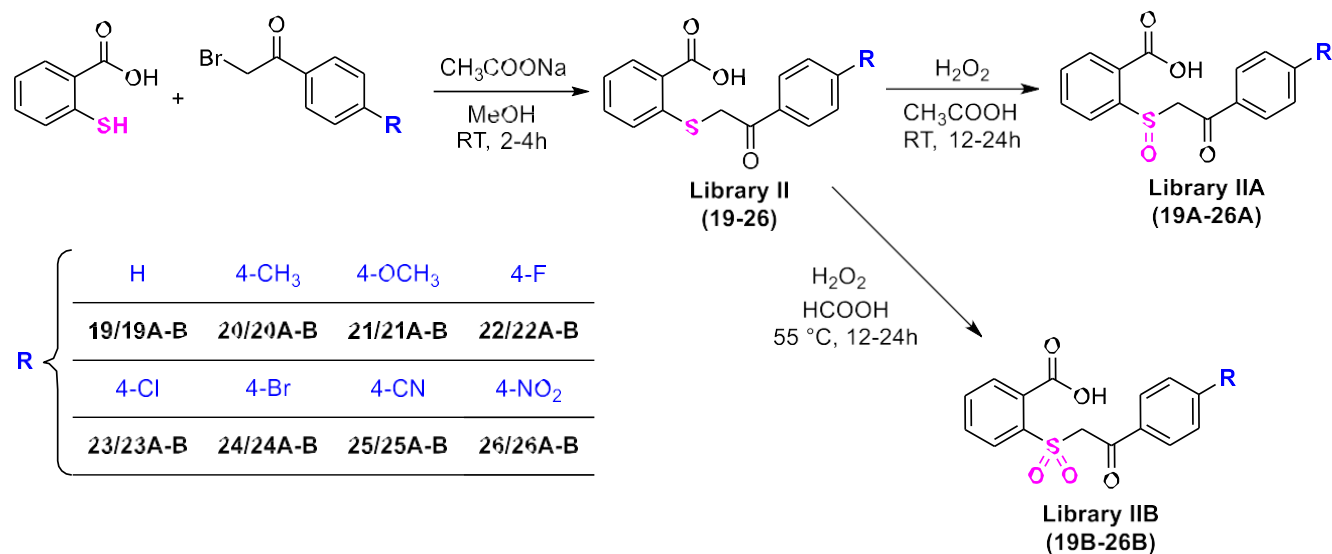
Scheme 3.2.4. Synthetic approach employed for the synthesis of the **Libraries II**, **IIA** and **IIB**.

The sulfoxide derivatives (**Library IIA**, **19A-25A**) were achieved by reacting the sulfides with equimolar amount of 33% hydrogen peroxide in the presence of glacial acetic acid at room temperature. The synthesis of the sulfones (**Library IIB**, **19B-25B**) requested the same oxidating agent (33% hydrogen peroxide) albeit in excess and employing formic acid despite acetic acid higher temperature (55 °C). The novel synthesised compounds belonging to the **Libraries I-II A/B,** have been characterized by means NMR method (^{1}H NMR and ^{13}C NMR) and evaluated for their hMAO-A and hMAO-B inhibitory activity by employing previously reported methods [106-107]. Tables **3.2.1** and **3.2.2**, reports the structures of the synthesised compounds.

Table 3.2.1. Structure of the compounds belonging to **Libraries I**, **IA** and **IB**.

Library I	Library IA	Library IB
12	**12A**	**12B**
13	**13A**	**13B**
14	**14A**	**14B**
15	**15A**	**15B**
16	**16A**	**16B**
17	**17A**	**17B**

| 18 | 18A | 18B |
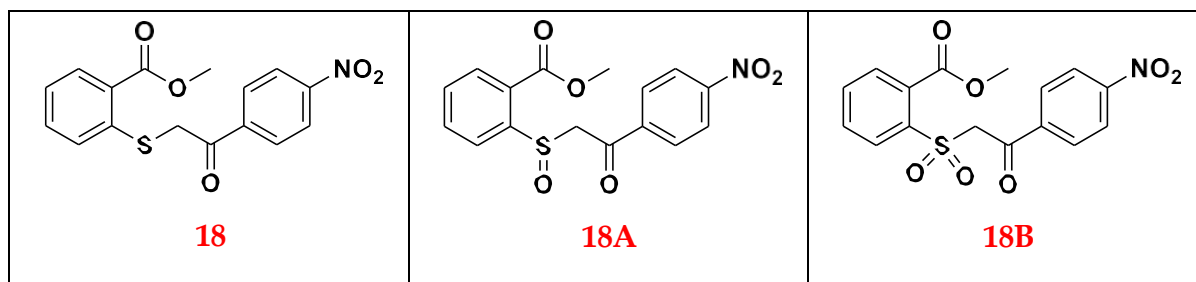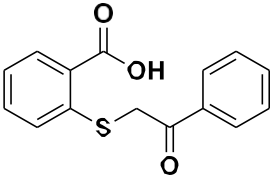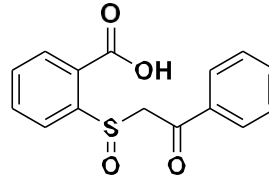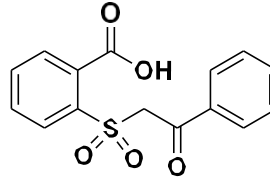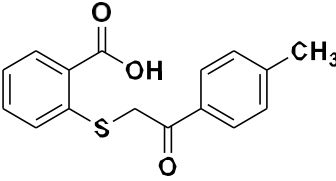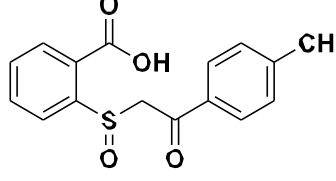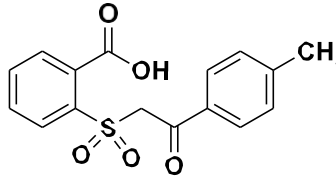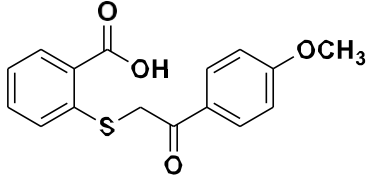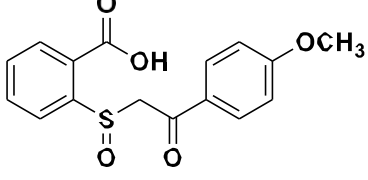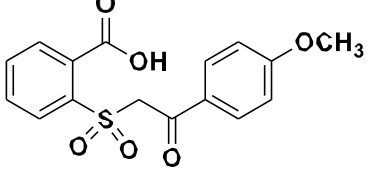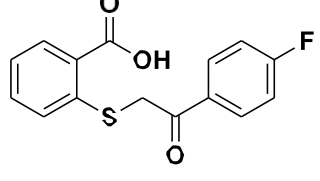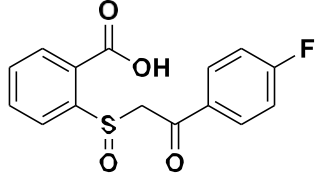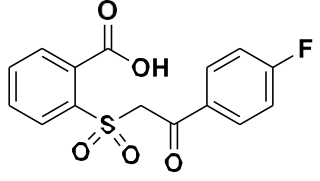
Table 3.2.2. Structure of the compounds belonging to **Libraries II**, **IIA** and **IIB**

Library II	Library IIA	Library IIB
19	19A	8B
20	20A	20B
21	21A	21B
22	22A	22B

23	23A	23B
24	24A	24B
25	25A	25B
26	26A	26B
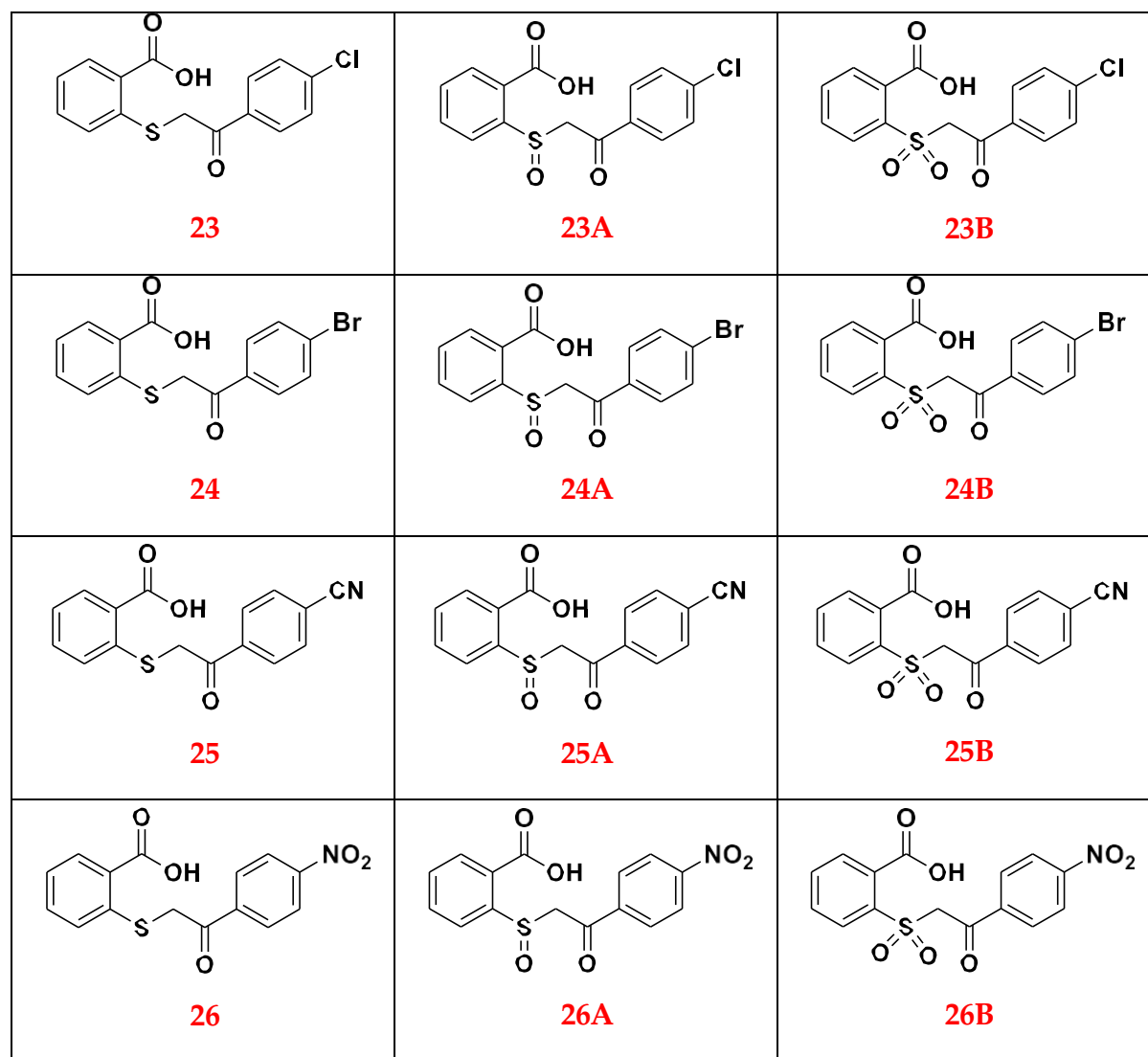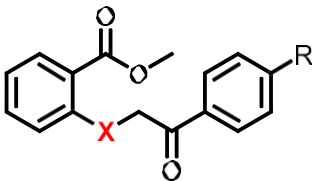
3.3. In vitro MAOs inhibition study

The compounds belonging to the **Libraries I**, **IA** and **IB** and **II**, **IIA** and **IIB** were evaluated manly to the A isoform, the inhibition towards the isoform B being appraised only for compounds **16**, **16A** and **16B (Tables 3.3.1** and **3.3.2)**. A first screening has been performed at a fixed concentration of the inhibitors (10 μM) to determine the ones able to inhibit the two isoforms at the level equal or superior to 50% (our threshold value to determine IC_{50}). With regards to the ester derivatives (**Table 3.3.1)**, the derivatives with sulfur in the oxidized states (S=O and O=S=O) tend to show higher inhibition of hMAO-A compared to those with unoxidized one (S). For instance, the *p*-Br derivative with sulfone group shows the highest

hMAO-A inhibition (87.91%) and with a micromolar IC_{50} value (1.20 µM), indicating strong inhibitory activity. In contrast, the sulfur analogue bearing the same R group, showed a lower inhibition of 78.6% with a higher IC_{50} of 3.01 µM. Similarly, the p-NO_2 derivative with S=O demonstrates a significant inhibition of 90.70% against hMAO-A with an IC_{50} of 2.86 µM, highlighting the importance of the sulfur oxidation state in enhancing hMAO-A inhibition. Regarding hMAO-B inhibition, the data currently available are not sufficient to define a precise SAR. However, the *p*-Br derivative with O=S=O stands out with 54.90% inhibition of MAO-B, contrasting sharply with the corresponding S and S=O derivatives, which exhibit very low or no inhibition. This suggests that the oxidation state of sulfur also plays a role in MAO-B selectivity.

Table 3.3.1. Inhibitory activity (%) of selected compounds belonging to **Libraries I** towards hMAO-A and hMAO-B

Cmpnd	R	X	Inhibition (%) [*],[§] MAO-A	IC_{50} MAO-A[§]	Inhibition (%) [*],[§] MAO-B
12		S	4.3		
12A	H	S=O	33.3		
12B		O=S=O	14.9		
14		S	0.0		
14A	p-F	S=O	0.0		
14B		O=S=O	0.00		
15		S	21.2		
15A	p-Cl	S=O	25.3		
15B		O=S=O	31.2		

16		**S**	78.6	3,01 µM	3.0%
16A	**p-Br**	**S=O**	68.8	3,16 µM	0.0%
16B		**O=S=O**	87.9	1,20 µM	54.9%
17		**S**	12.4		
17A	**p-CN**	**S=O**	16.7		
17B		**O=S=O**	14.2		
18		**S**	28.6		
18A	**p-NO₂**	**S=O**	90.7	2,86 µM	
18B		**O=S=O**	10.0		
* Percentage inhibition evaluated at fixed concentration (10 µM) of inhibitor; §Errors are in the range of ±5% of the reported values, from three different assays					

Table 3.3.2 summarizes the inhibitory activity of various derivatives, each featuring different R-group substitutions, such as p-CH₃, p-OCH₃, p-Cl, p-Br, p-F, p-NO₂, p-CN, and H and distinct sulfur oxidation states (S, S=O, and O=S=O) against MAO-A.

The data indicated that most derivatives exhibit low levels of hMAO-A inhibition, with few compounds exceeding 10% inhibition. For example, the *p*-CH₃ and *p*-Cl derivatives show minimal inhibition irrespective to sulfur oxidation states, with values not surpassing 2.2%. In contrast, the *p*-Br derivative with O=S=O demonstrates the highest inhibition at 10.20%, while the corresponding forms with unoxidized sulfur (S) or S=O show no inhibition. Similarly, the *p*-F derivative with O=S=O exhibits relatively higher inhibition at 16.10% compared to its other oxidation states. Overall, derivatives containing unoxidized sulfur (S) tend to show slightly higher inhibition than those with oxidized sulfur (S=O or O=S=O), though the inhibitory activity remains weak. Additionally, substitutions like *p*-CN, *p*-NO₂, and H result in very low or negligible inhibition, irrespective to the sulfur oxidation state.

These findings suggest that neither the R-group substitutions nor the sulfur oxidation state substantially enhance hMAO-A inhibition for most derivatives, making them generally weak

inhibitors of hMAO-A.

Table 3.3.2. Inhibitory activity (%) of selected compounds belonging to **Libraries II**, **IIA** and **IIB** towards hMAO-A and hMAO-B

Cmpnd	R	X	Inhibition (%) [*, §] MAO-A
19	H	S	4.4
19A		S=O	0
19B		O=S=O	0
20	p-CH$_3$	S	2.2
20A		S=O	0
20B		O=S=O	0
21	p-OCH$_3$	S	6.1
21A		S=O	7.5
21B		O=S=O	4.9
22	p-F	S	1.6
22A		S=O	0
22B		O=S=O	16.1
23	p-Cl	S	2.2
23A		S=O	1.4
23B		O=S=O	0
24	p-Br	S	0
24A		S=O	0

24B		O=S=O	10.2
25		S	0
25A	p-CN	S=O	0
25B		O=S=O	0.30
26		S	5.1
26A	p-NO$_2$	S=O	0
26B		O=S=O	0

* Percentage inhibition evaluated at fixed concentration (10 μM) of inhibitor; §Errors are in the range of ±5% of the reported values, from three different assays
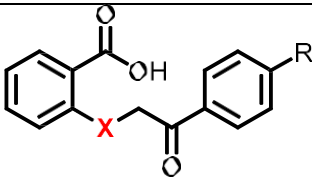
3.4. Conclusions

The design, synthesis and biological evaluation of a series of open-based analogues of 2-aroyl-benzo[*b*]thiophen-3-oles have been proposed. The selected synthetic approaches led to the obtainment of the titled compounds in moderate to good yields. Different chemical modifications of the novel scaffold have been proposed. In particular, the ester moiety has been replaced with carboxylic acid functionality in order to evaluate how the different hydrogen-bond acceptor/donator profiles affect both inhibitory activity and selectivity. The phenyl ring has been substituted with groups having different electronic/steric properties. Finally, the role of the oxidation state of sulfur atom has also been challenged by synthesising three different sub-libraries of compounds, i.e. sulfide, sulfoxides and sulfones. The preliminary data mainly available for the A isoform, show that most of the compounds are ineffective against hMAO-A with the exception of the compounds belonging to the Library I and endowed with p-Br substituent group. On the other hand, the results obtained against hMAO-B are insufficient to define a clear SAR and further inhibitory activity analysis will shed light on the potential of these compounds.

3.5. Material and methods

3.5.1. General

Unless otherwise indicated, all reactions were carried out under a positive nitrogen pressure (balloon pressure) in washed and oven-dried glassware. Solvents and reagents were used as supplied without further purification. All melting points were measured on a Stuart® melting point apparatus SMP1 and are uncorrected (temperatures are reported in °C). Fluorescence spectrophotometry was carried out with a Varian Cary Eclipse fluorescence spectrophotometer. ^{1}H and ^{13}C NMR spectra were recorded at 400 and 101 MHz, respectively, on a Bruker spectrometer using CDCl$_3$ and DMSO-d_6 as the solvents at room temperature. The samples were analysed with a final concentration of ~30 mg/mL. Chemical shifts are expressed as δ units (parts per million) relative to the solvent signal. ^{1}H spectra are reported as follows: δ_H (spectrometer frequency, solvent): chemical shift/ppm (multiplicity, J-coupling constant(s), number of protons, assignment). ^{13}C spectra are reported as follows: δ_C (spectrometer frequency, solvent): chemical shift/ppm (J-coupling constant C-F, assignment). Multiplicity is abbreviated as follows: br – broad; s – singlet; d – doublet; t – triplet; q – quartet; m – multiplet. Coupling constants J are given in Hertz (Hz). The processing and analyses of the NMR data were carried out with MestreNova. Column chromatography was carried out using Sigma-Aldrich® silica gel (high purity grade, pore size 60 Å, 230–400 mesh particle size). All the purifications and reactions were monitored by TLC which was performed on 0.2 mm thick silica gel-aluminium backed plates (60 F$_{254}$, Merck). Visualization was carried out under ultra-violet irradiation (254 nm). Where given, systematic compound names are those generated by ChemBioDraw Ultra 12.0 following IUPAC conventions. Recombinant hMAO-A and hMAO-B (5 mg protein/mL) and kynuramine dihydrobromide were obtained from Sigma-Aldrich.

3.5.2. Chemistry

Synthesis of the methyl 2-((2-oxo-2-phenylethyl)thio)benzoate derivatives

In a round-bottom flask, 1 equivalent of methylthiosalicylate and 1.1 equivalents of potassium carbonate were dissolved in anhydrous dimethylformamide (DMF). After stirring for 5 minutes, 1 equivalent of *para*-substituted α-bromoacetophenone was added to the solution. The reaction mixture was stirred at room temperature for 2-4 hours, with progress monitored using thin-layer chromatography (TLC). Upon completion, water was added to the flask, and the pH was adjusted to 3. The resulting yellow solid was filtered and purified via column chromatography. A pale-yellow solid was obtained, with yields ranging from 47% to 78%.

Synthesis of methyl 2-((2-oxo-2-phenylethyl)sulfinyl)benzoate and methyl 2-((2-oxo-2-phenylethyl)sulfonyl)benzoate

In an oven-dried flask, derivatives from 2-((2-oxo-2-phenylethyl)thio)benzoate library (Library I) were dissolved in a mixture of dichloromethane and methanol. Once the solid was fully dissolved, 1.1 eq of meta-chloroperoxybenzoic acid (mCPBA) was added. The reaction mixture was stirred at room temperature for 2 to 4 hours, and its progress was monitored using thin-layer chromatography (TLC). Upon completion, the solution was extracted three times with sodium carbonate, washed with brine, dried over anhydrous sodium sulfate, and concentrated under reduced pressure using a rotary evaporator. The two derivatives were isolated by column chromatography.

Synthesis of 2-((2-oxo-2-phenylethyl)thio)benzoic acid (Library II)

In a round-bottom flask, 1 equivalent of methylthiosalicylic acid and 1.1 equivalents of sodium acetate (CH_3COONa) were dissolved in 10 ml of methanol. After 5 minutes, 1 equivalent of para-substituted α-bromoacetophenone was added. The reaction mixture was stirred at room temperature overnight. Upon completion, water was added, leading to the formation of a white solid. The precipitate was collected by vacuum filtration and dried. Yields: 53%-61%

Synthesis of 2-((2-oxo-2-phenylethyl)sulfinyl)benzoic acid (Library IIA)

In a round bottom flask, 1 equivalent of 2-((2-oxo-2-phenylethyl)thio)benzoic acid from Library II was dissolved in 5 mL of acetic acid and 1 mL of hydrogen peroxide. The reaction mixture was stirred at room temperature for 12-24 hours. Once complete, water was added to the solution, and the resulting a white precipitate was collected by vacuum filtration. Yields: 48%-63%.

Synthesis of 2-((2-oxo-2-phenylethyl)sulfonyl)benzoic acid (Library IIB)

Compounds deriving from Library IIA (1 equivalent) was dissolved in 10 mL of formic acid and 3 mL of hydrogen peroxide 33%. The reaction mixture was stirred at room temperature for 24 hours. After the reaction was complete, water was added to the solution, and the resulting precipitate was collected by vacuum filtration. Yields: 47%-55%.

Characterization data for the compounds 12-26B
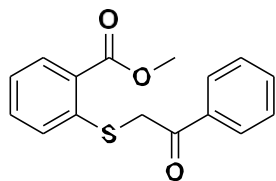
methyl 2-((2-oxo-2-phenylethyl)thio)benzoate. (12) White solid, yield 76%.

^{1}H NMR (400 MHz, DMSO-d_6): δ 3.92 (s, 3H, CH$_3$), 4.54 (s, 2H, CH$_2$), 7.25 – 7.32 (m, 1H, Ar), 7.47 (d, J = 8.1 Hz, 1H, Ar), 7.50 – 7.57 (m, 1H, Ar), 7.64 (d, J = 8.4 Hz, 2H, Ar), 8.04 (dt, J = 7.8, 1.3 Hz, 1H, Ar), 8.14 (dt, J = 7.8, 1.3 Hz, 2H).

^{13}C NMR (101 MHz, DMSO-d_6): δ 39.5 (CH$_3$), 52.6 (CH$_2$), 125,0 (Ar), 127.1 (Ar), 127.8 (Ar), 129.4 (2 x Ar), 131.0 (2 x Ar), 131.2 (Ar), 133.2 (Ar), 134.7 (Ar), 139.1 (Ar), 140.1 (Ar), 166.6 (COOCH3), 194.1 (CO).
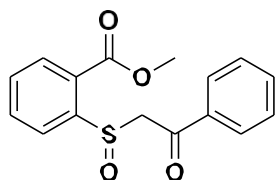
methyl 2-((2-oxo-2-phenylethyl)sulfinyl)benzoate (12A). White solid, yield: 68%

^{1}H NMR (400 MHz, CDCl$_3$): δ 3.90 (s, 3H, CH$_3$), 4.04 (s, 2H, CH$_2$), 7.21 (ddd, J = 7.8, 6.4, 2.1 Hz, 1H), 7.42 – 7.51 (m, 2H, Ar), 758 – 7.63 (m, 2H, Ar), 7.83 – 7.90 (m, 2H, Ar), 7.93 – 7.97 (m, 1H, Ar). ^{13}C NMR (101 MHz, DMSO-d_6): δ 39.5 (CH$_3$), 52.6 (CH$_2$), 125,0 (Ar), 127.1 (Ar), 127.8 (Ar), 129.4 (2 x Ar), 131.0 (2 x Ar), 131.2 (Ar), 133.2 (Ar), 134.7 (Ar), 139.1 (Ar), 140.1 (Ar), 166.6 (COOCH3), 194.1 (CO).
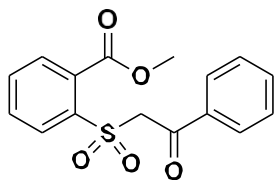
methyl 2-((2-oxo-2-phenylethyl)sulfonyl)benzoate (12B) White solid, 71% yield. ^{1}H NMR (400 MHz, CDCl$_3$): δ 3.90 (s, 3H, CH$_3$), 4.67 (s, 2H, CH$_2$), 7.10 – 7.17 (m, 2H, Ar), 7.20 (ddd, J = 7.8, 6.9, 1.5 Hz, 1H, Ar), 7.42 – 7.52 (m, 2H, Ar), 7.95 (dd, J = 7.8, 1.5 Hz, 1H, Ar), 8.01 – 8.08 (m, 2H, Ar).

^{13}C NMR (101 MHz, DMSO-d_6): δ 39.5 (CH$_3$), 52.6 (CH$_2$), 125,0 (Ar), 127.1 (Ar), 127.8 (Ar), 129.4 (2 x Ar), 131.0 (2 x Ar), 131.2 (Ar), 133.2 (Ar), 134.7 (Ar), 139.1 (Ar), 140.1 (Ar), 166.6 (COOCH3), 194.1 (CO).
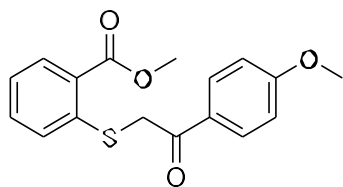
Methyl 2-((2-(4-methoxyphenyl)-2-oxoethyl)thio)benzoate (13). White solid, 57% yield.

^{1}H NMR (400 MHz, CDCl$_3$): δ 3.90 (d, J = 8.6 Hz, 6H, CH$_3$), 4.31 (s, 2H, CH$_2$), 6.93 – 7.00 (m, 2H, Ar), 7.21 (ddd, J = 7.8, 7.2, 1.3 Hz, 1H, Ar), 7.42 – 7.50 (m, 1H, Ar), 7.52 (dd, J = 8.2, 1.3 Hz, 1H, Ar), 7.97 (dd, J = 7.8, 1.6 Hz, 1H), 7.99 – 8.06 (m, 2H,Ar).

^{13}C NMR (101 MHz, DMSO-d$_6$): δ 53.71 (CH$_2$), 55.8 (OCH$_3$), 63.54 (CH$_2$), 116.3 (d, J = 21.8 Hz, 2 x Ar), 130.0 (Ar), 131.6 (Ar), 127.8 (Ar), 131.9 (Ar), 132.8 (2 x Ar), 133.1 (Ar), 135.0 (Ar), 137.0 (Ar), 165.3 (Ar), 167.8 (COOCH3), 187.9 (CO).
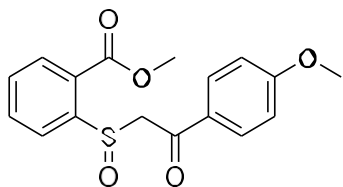
Methyl 2-((2-(4-methoxyphenyl)-2-oxoethyl)sulfinyl)benzoate (13A). White solid, 67% yield.

^{1}H NMR (400 MHz, CDCl$_3$): δ 3.85 (s, 3H, CH$_3$), 3.94 (s, 3H, CH$_3$), 4.19 (d, J = 13.6 Hz, 1H, CH$_2$), 4.69 (d, J = 13.6 Hz, 1H, CH$_2$), 6.86 – 6.97 (m, 2H, Ar), 7.56 (td, J = 7.6, 1.2 Hz, 1H, Ar), 7.76 (td, J = 7.7, 1.4 Hz, 1H, Ar), 7.92 – 7.99 (m, 2H, Ar), 8.08 (dd, J = 7.7, 1.4 Hz, 1H, Ar), 8.20 (dd, J = 8.0, 1.3 Hz, 1H, Ar).

^{13}C NMR (101 MHz, DMSO-d$_6$): δ 53.71 (CH$_3$), 55.8 (OCH$_3$), 63.54 (CH$_2$), 116.3 (d, J = 21.8 Hz, 2 x Ar), 130.0 (Ar), 131.6 (Ar), 127.8 (Ar), 131.9 (Ar), 132.8 (2 x Ar), 133.1 (Ar), 135.0 (Ar), 137.0 (Ar), 165.3 (Ar), 167.8 (COOCH3), 187.9 (CO).

Methyl 2-((2-(4-methoxyphenyl)-2-oxoethyl)sulfinyl)benzoate (13B): White solid, 65% yield.

^{1}H NMR (400 MHz, CDCl$_3$): δ 3.85 (s, 3H, CH$_3$), 3.94 (s, 3H, CH$_3$), 4.19 (d, J = 13.6 Hz, 1H, CH$_2$), 4.69 (d, J = 13.6 Hz, 1H, CH$_2$), 6.86 – 6.97 (m, 2H, Ar), 7.56 (td, J = 7.6, 1.2 Hz, 1H, Ar), 7.76 (td, J = 7.7, 1.4 Hz, 1H, Ar), 7.92 – 7.99 (m, 2H, Ar), 8.08 (dd, J = 7.7, 1.4 Hz, 1H, Ar), 8.20 (dd, J = 8.0, 1.3 Hz, 1H, Ar).

^{13}C NMR (101 MHz, DMSO-d$_6$): δ 53.71 (CH$_3$), 55.8 (OCH$_3$), 63.54 (CH$_2$), 116.3 (d, J = 21.8 Hz, 2 x Ar), 130.0 (Ar), 131.6 (Ar), 127.8 (Ar), 131.9 (Ar), 132.8 (2 x Ar), 133.1 (Ar), 135.0 (Ar), 137.0 (Ar), 165.3 (Ar), 167.8 (COOCH3), 187.9 (CO).

Methyl 2-((2-(4-fluorophenyl)-2-oxoethyl)thio)benzoate (14). White solid, 73% yield.

^{1}H NMR (400 MHz, DMSO-d_6): δ 3.83 (s, 3H, CH3), 4.74 (s, 2H, CH2), 7.20 – 7.32 (m, 1H, Ar), 7.34 – 7.43 (m, 2H, Ar), 7.60 – 7.44 (m, 2H, Ar), 7.89 (dt, J = 7.8, 1.2 Hz, 1H, Ar), 8.12 – 8.20 (m, 2H, Ar). ^{13}C NMR (101 MHz, DMSO-d_6): δ 39.4 (CH$_3$), 52.6 (CH$_2$), 116.34 (d, J = 21.8 Hz, 2 x Ar), 125.0 (Ar),), 127.1 (Ar), 127.8 (Ar), 131.2 (Ar), 132.2 (2 x Ar), 132.7 (Ar), 133.2 (Ar), 140.2 (Ar), 164.9 (Ar), 166.6 (COOCH3), 193.6 (CO).
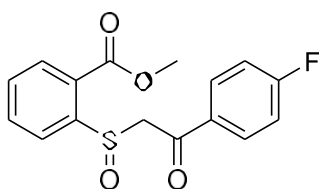
Methyl 2-((2-(4-fluorophenyl)-2-oxoethyl)sulfinyl)benzoate (14A). White solid, 71%. ^{1}H NMR (400 MHz, DMSO-d_6): δ 3.87 (s, 3H, CH3), 4.36 (d, J = 15.2 Hz, 2H, CH2), 4.95 (d, J = 15.2 Hz, 2H, CH2), 7.36 (t, J = 8.8 Hz, 2H, Ar), 7.72 (t, J = 7.5 Hz, 1H, Ar), 7.93 (t, J = 7.7 Hz, 1H, Ar), 8.00 – 8.18 (m, 2H, Ar). ^{13}C NMR (101 MHz, DMSO-d_6): δ 39.5 (CH$_3$), 52.6 (CH$_2$), 116.3 (d, J = 21.8 Hz, 2 x Ar), 125.0 (Ar), 127.1 (Ar), 127.8 (Ar), 131.2 (Ar), 132.2 (2 x Ar), 132.7 (Ar), 133.2 (Ar), 140.2 (Ar), 164.9 (Ar), 166.6 (COOCH3), 193.6 (CO).
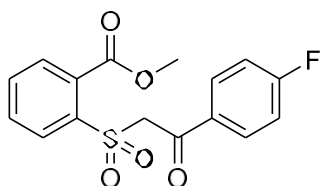
Methyl 2-((2-(4-fluorophenyl)-2-oxoethyl)sulfonyl)benzoate (**14B**). White solid, 55% yield.

^{1}H NMR (400 MHz, DMSO-d_6): δ 3.90 (s, 3H, CH$_3$) , 5.43 (s, 2H, CH$_2$), 7.39 (t, J = 8.8 Hz, 2H, Ar), 7.75 – 7.82 (m, 2H, Ar), 7.84 – 7.90 (m, 1H, Ar), 7.94 (d, J = 7.7 Hz, 1H, Ar), 8.09 (dd, J = 8.6, 5.5 Hz, 2H, Ar). $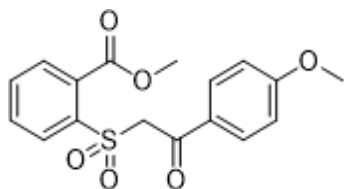^{13}$C NMR (101 MHz, DMSO-d$_6$): δ 53.71 (CH$_3$), 63.54 (CH$_2$), 116.3 (d, *J* = 21.8 Hz, 2 x Ar), 130.0 (Ar), 131.6 (Ar), 127.8 (Ar), 131.9 (Ar), 132.8 (2 x Ar), 133.1 (Ar), 135.0 (Ar), 137.0 (Ar), 165.3 (Ar), 167.8 (COOCH3), 187.9 (CO).
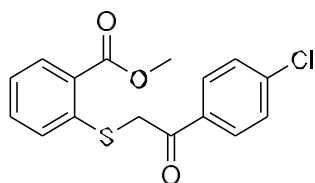
 Methyl 2-((2-(4-chlorophenyl)-2-oxoethyl)thio)benzoate (15). White solid, 71% yield.

^{1}H NMR (400 MHz, DMSO-d_6): δ 3.83 (s, 3H, CH3), 4.74 (s, 2H, CH$_2$), 7.22 – 7.30 (m, 1H, Ar), 7.47 (d, J = 8.1 Hz, 1H, Ar), 7.50 – 7.57 (m, 1H, Ar), 7.64 (d, J = 8.4 Hz, 2H, Ar), 7.89 (dt, J = 7.8, 1.3 Hz, 1H, Ar), 7.89 (dt, J = 7.8, 1.3 Hz, 2H). ^{13}C NMR (101 MHz, DMSO-d_6): δ 39.5 (CH$_3$), 52.6 (CH$_2$), 125,0 (Ar), 127.1 (Ar), 127.8 (Ar), 129.4 (2 x Ar), 131.0 (2 x Ar), 131.2 (Ar), 133.2 (Ar), 134.7 (Ar), 139.1 (Ar), 140.1 (Ar), 166.6 (COOCH3), 194.1 (CO).

Methyl2-((2-(4-chlorophenyl)-2-oxoethyl)sulfinyl)benzoate (15A). White solid, 57%. ^{1}H NMR (400 MHz, CDCl$_3$): δ 3.96 (s, 3H, CH$_3$), 4.23 (d, J = 13.6 Hz, 1H, CH$_2$), 4.72 (d, J = 13.5 Hz, 1H, CH$_2$), 7.39 – 7.47 (m, 2H, Ar), 7.58 (td, J = 7.6, 1.2 Hz, 1H, Ar), 7.77 (td, J = 7.7, 1.4 Hz, 1H, Ar), 7.89 – 7.97 (m, 2H, Ar), 8.10 (dd, J = 7.7, 1.4 Hz, 1H, Ar), 8.18 (dd, J = 8.0, 1.3 Hz, 1H, Ar).
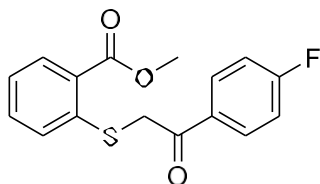
^{13}C NMR (101 MHz, DMSO-d_6): δ 39.5 (CH$_3$), 52.6 (CH$_2$), 125,0 (Ar), 127.1 (Ar), 127.8 (Ar), 129.4 (2 x Ar), 131.0 (2 x Ar), 131.2 (Ar), 133.2 (Ar), 134.7 (Ar), 139.1 (Ar), 140.1 (Ar), 166.6 (COOCH3), 194.1 (CO).
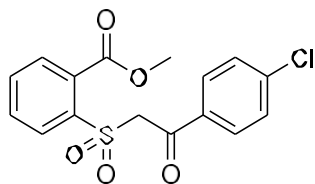
Methyl-2-((2-(4-chlorophenyl)-2-oxoethyl)sulfonyl)benzoate (15B). White solid, 55% yield. 1H NMR (400 MHz, CDCl$_3$): δ 3.89 (s, 3H, CH$_3$), 4.28 (s, 2H, CH$_2$), 7.21 (ddd, J = 7.8, 6.4, 2.1 Hz, 1H), 7.42 – 7.51 (m, 2H, Ar), 758 – 7.63 (m, 2H, Ar), 7.83 – 7.90 (m, 2H, Ar), 7.93 – 7.97 (m, 1H, Ar). ^{13}C NMR (101 MHz, DMSO-d_6): δ 39.5 (CH$_3$), 52.6 (CH$_2$), 125,0 (Ar), 127.1 (Ar), 127.8 (Ar), 129.4 (2 x Ar), 131.0 (2 x Ar), 131.2 (Ar), 133.2 (Ar), 134.7 (Ar), 139.1 (Ar), 140.1 (Ar), 166.6 (COOCH3), 194.1 (CO).
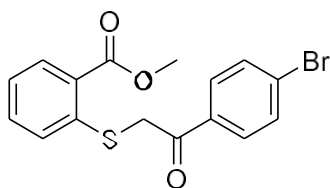
Methyl 2-((2-(4-bromophenyl)-2-oxoethyl)thio)benzoate (**16**). White solid, 61% yield.

^{1}H NMR (400 MHz, CDCl$_3$): δ 4.01 (s, 3H, CH$_3$), 5.22 (s, 2H, CH$_2$), 7.56 – 7.62 (m, 2H, Ar), 7.64 (dd, J = 7.8, 1.6 Hz, 1H, Ar), 7.71 (td, J = 7.5, 1.3 Hz, 1H, Ar), 7.76 (dd, J = 7.5, 1.6 Hz, 1H, Ar), 7.82 – 7.89 (m, 2H, Ar), 8.06 (dd, J = 7.9, 1.3 Hz, 1H, Ar).

^{13}C NMR (101 MHz, DMSO-d_6): δ 39.5 (CH$_3$), 52.6 (CH$_2$), 125,0 (Ar), 127.1 (Ar), 127.8 (Ar), 129.4 (2 x Ar), 131.0 (2 x Ar), 131.2 (Ar), 133.2 (Ar), 134.7 (Ar), 139.1 (Ar), 140.1 (Ar), 166.6 (COOCH3), 194.1 (CO).
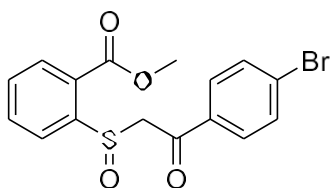
Methyl 2-((2-(4-bromophenyl)-2-oxoethyl)sulfinyl)benzoate (**16A**). White solid, 55% yield. ^{1}H NMR (400 MHz, DMSO-d_6): δ 3.86 (s, 3H, CH$_3$), 4.37 (d, J = 15.3 Hz, 1H, CH$_2$), 7.69 – 7.79 (m, 3H, Ar), 7.86 – 7.98 (m, 3H, Ar), 8.10 (ddd, J = 13.1, 7.8, 1.3 Hz, 2H).

^{13}C NMR (101 MHz, DMSO-d_6): δ 39.5 (CH$_3$), 52.6 (CH$_2$), 125,0 (Ar), 127.1 (Ar), 127.8 (Ar), 129.4 (2 x Ar), 131.0 (2 x Ar), 131.2 (Ar), 133.2 (Ar), 134.7 (Ar), 139.1 (Ar), 140.1 (Ar), 166.6 (COOCH3), 194.1 (CO).
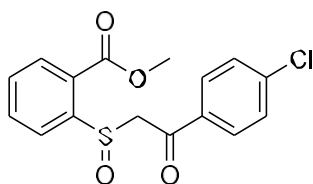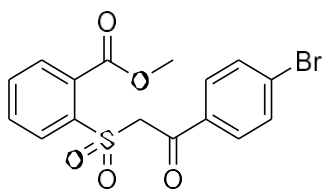
Methyl 2-((2-(4-bromophenyl)-2-oxoethyl)sulfonyl)benzoate (**16B**). White solid, 51% yield. ^{1}H NMR (400 MHz, CDCl$_3$): δ 3.89 (s, 3H, CH$_3$), 4.29 (s, 2H, CH$_2$), 7.10 – 7.17 (m, 2H, Ar), 7.20 (ddd, J = 7.8, 6.9, 1.5 Hz, 1H, Ar), 7.42 – 7.52 (m, 2H, Ar), 7.95 (dd, J = 7.8, 1.5 Hz, 1H, Ar), 8.01 – 8.08 (m, 2H, Ar).^{13}C NMR (101 MHz, DMSO-d_6): δ 39.5 (CH$_3$), 52.6 (CH$_2$), 125,0 (Ar), 127.1 (Ar), 127.8 (Ar), 129.4 (2 x Ar), 131.0 (2 x Ar), 131.2 (Ar), 133.2 (Ar), 134.7 (Ar), 139.1 (Ar), 140.1 (Ar), 166.6 (COOCH3), 194.1 (CO).
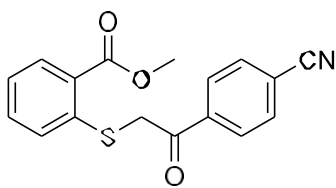
Methyl 2-((2-(4-cyanophenyl)-2-oxoethyl)thio)benzoate (17). Yellow solid, 47% yield.

^{1}H NMR (400 MHz, CDCl$_3$): δ 3.89 (s, 3H, CH$_3$), 5.50 (s, 2H, CH$_2$), 7.77 – 7.82 (m, 2H, Ar), 7.83 – 7.95 (m, 2H, Ar), 8.03 (d, J = 8.2 Hz, 2H, Ar), 8.14 (d, J = 8.1 Hz, 2H, Ar). ^{13}C NMR (101 MHz, DMSO-d$_6$): δ 53.6 (CH$_3$), 63.7 (CH$_2$), 116.2 (d, J = 21.8 Hz, 2 x Ar), 118.4 (CN), 128.4 (Ar), 129.3 (Ar), 130.2 (Ar), 131.9 (2 x Ar), 133.3 (Ar), 137.5 (Ar), 139.3 (Ar), 166.9 (Ar), 167.6 (COOCH3), 188.8 (CO).
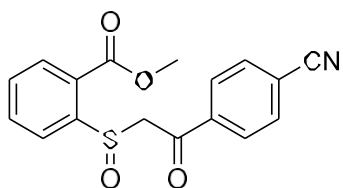
Methyl 2-((2-(4-cyanophenyl)-2-oxoethyl)sulfinyl)benzoate (**17A**). Yellow solid, 53% yield. ^{1}H NMR (400 MHz, DMSO-d_6): δ 3.85 (s, 3H, CH$_3$), 4.44 (d, J = 15.2 Hz, 1H, CH$_2$), 5.02 (d, J = 15.2 Hz, 1H, CH$_2$), 7.71 (tt, J = 7.6, 1.2 Hz, 1H, Ar), 7.92 (td, J = 7.6, 1.2 Hz, 1H, Ar), 8.00 (d, J = 8.2 Hz, 2H, Ar), 8.05 (dd, J = 8.0, 1.3 Hz, 1H, Ar), 8.07 – 8.13 (m, 3H, Ar). ^{13}C NMR (101 MHz, DMSO-d$_6$): δ 53.3 (CH$_3$), 65.4 (CH$_2$), 116.3 (d, J = 21.8 Hz, 2 x Ar), 118.6 (CN),124.1 (Ar), 125.3 (Ar), 127.0 (Ar), 131.2 (Ar), 132.4 (2 x Ar), 133.4 (Ar), 134.5 (Ar), 139.5 (Ar), 147.9 (Ar), 165.7 (COOCH3), 192.7 (CO).
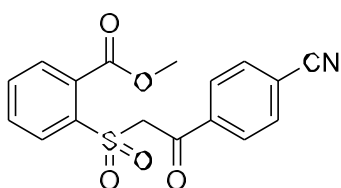
Methyl 2-((2-(4-cyanophenyl)-2-oxoethyl)sulfonyl)benzoate (**17B**). Yellow solid, 51% yield. ^{1}H NMR (400 MHz, DMSO-d_6): δ 3.90 (s, 3H, CH$_3$), 5.52 (s, 2H, CH$_2$), 7.78 – 7.83 (m, 2H, Ar), 7.85 – 7.89 (m, 1H, Ar), 7.92 – 7.97 (m, 1H, Ar), 8.05 (d, J = 8.5 Hz, 2H, Ar), 8.19 – 8.12 (m, 2H, Ar). ^{13}C NMR (101 MHz, DMSO-d$_6$): δ 53.7 (CH$_3$), 63.7 (CH$_2$), 116.5 (d, J = 21.8 Hz, 2 x Ar), 118.5 (CN), 130.1 (Ar), 131.3 (Ar), 131.9 (Ar), 133.1 (2 x Ar), 132.0 (Ar), 133.4 (Ar), 135.1 (Ar), 137.5 (Ar), 139.4 (Ar), 167.7 (COOCH$_3$), 188.9 (CO).
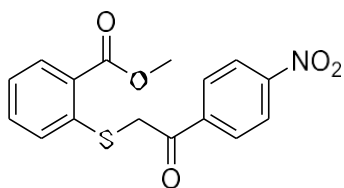
Methyl 2-((2-(4-nitrophenyl)-2-oxoethyl)thio)benzoate (18). Red solid, 56% yield.

^{1}H NMR (400 MHz, DMSO-d_6): δ 3.83 (s, 3H, CH$_3$), 4.04 (s, 2H, CH$_2$), 7.28 (t, J = 7.5 Hz, 1H, Ar), 7.46 – 7.57 (m, 2H, Ar), 7.90 (d, J = 7.8 Hz, 1H, Ar), 8.29 (d, J = 8.5 Hz, 2H, Ar), 8.38 (d, J = 8.5 Hz, 2H, Ar).

^{13}C NMR (101 MHz, DMSO-d_6): δ 39.7 (CH$_2$), 52.7 (CH$_3$), 124.2 (d, J = 21.8 Hz, 2 x Ar), 125.2 (Ar),), 127.2 (Ar), 130.2 (Ar), 131.3 (Ar), 133.2 (2 x Ar), 139.7 (Ar), 140.7 (Ar), 150.6 (Ar), 164.9 (Ar), 166.6 (COOCH3), 194.2 (CO).
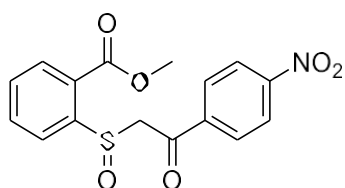
Methyl 2-((2-(4-nitrophenyl)-2-oxoethyl)sulfinyl)benzoate (**18A**). yellow solid, 51% yield.

^{1}H NMR (400 MHz, DMSO-d_6): δ 3.88 (d, J = 0.9 Hz, 3H, CH$_3$), 4.19 (s, 2H, CH$_2$), 7.28 – 7.34 (m, 1H, Ar), 7.40 – 7.48 (m, 2H, Ar), 7.52 (d, J = 8.1 Hz, 1H, Ar), 7.58 (tt, J = 7.0, 1.2 Hz, 1H, Ar), 7.94 (dt, J = 7.8, 1.2 Hz, 1H, Ar), 8.24 – 8.17 (m, 2H, Ar).

^{13}C NMR (101 MHz, DMSO-d_6): δ 53.3 (CH$_3$), 65.6 (CH$_2$), 124.2 (d, J = 21.8 Hz, 2 x Ar), 125.2 (Ar), 127.0 (Ar), 130.7 (Ar), 131.5 (2xAr), 134.5 (Ar) 141.0 (2xAr), 147.8 (Ar), 150.8 (Ar), 165.7 (COOCH3), 192.6 (CO).
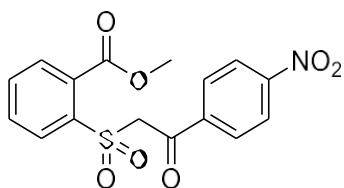
Methyl 2-((2-(4-nitrophenyl)-2-oxoethyl)sulfonyl)benzoate (18B). Yellow solid, 61% yield. ^{1}H NMR (400 MHz, DMSO-d_6): δ 3.95 (s, 3H, CH$_3$), 4.90 (s, 2H, CH$_2$), 7.83 – 7.89 (m, 2H, Ar), 7.92 (d, J = 7.3 Hz, 1H, Ar), 8.00 (d, J = 7.8 Hz, 1H, Ar), 8.29 (d, J = 8.7 Hz, 2H, Ar), 8.41 (d, J = 8.6 Hz, 2H, Ar). ^{13}C NMR (101 MHz, DMSO-d_6): δ 53.7 (CH$_3$), 63.9 (CH$_2$), 124.3 (d, J = 21.8 Hz, 2 x Ar), 130.2 (Ar), 131.1 (Ar), 131.3 (Ar), 132.0 (2xAr), 133.1 (Ar) 135.1 (2xAr), 140.7 (Ar), 150.9 (Ar), 165.7 (COOCH3), 188.8 (CO).
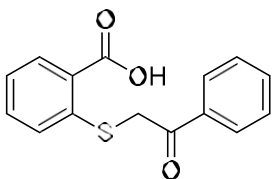
2-((2-oxo-2-phenylethyl)thio)benzoic acid (19). White solid, 43% yield. ^{1}H NMR (400 MHz, DMSO-d_6): δ 4.70 (s, 2H, CH$_2$), 7.18 – 7.23 (m, 1H, Ar), 7.48 (ddd, J = 13.3, 8.2, 6.7 Hz, 2H, Ar), 7.56 (t, J = 7.6 Hz, 2H, Ar), 7.64 – 7.74 (m, 1H, Ar), 7.91 (dd, J = 7.8, 1.6 Hz, 1H, Ar), 8.08 (dd, J = 8.1, 1.5 Hz, 2H, Ar), 13.10 (s, 1H, COOH). ^{13}C NMR (101 MHz, DMSO-d_6): δ 39.3 (CH$_2$), 124.6 (Ar), 126.4 (Ar), 128.4 (Ar), 129.0 (2xAr), 129.2 (2xAr), 131.4 (Ar), 132.8 (Ar), 134.1 (Ar), 135.9 (Ar), 140.5 (Ar), 167.9 (COOH), 195.1 (CO).
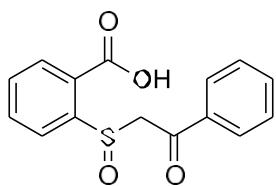
2-((2-oxo-2-phenylethyl)sulfinyl)benzoic acid (19A). White solid, 47% yield. ^{1}H NMR (400 MHz, DMSO-d_6): δ 4.23 (d, J = 14.7 Hz, 2H, CH$_2$), 7.53 (t, J = 7.6 Hz, 2H, Ar), 7.69 (q, J = 7.6 Hz, 2H, Ar), 7.91 (td, J = 7.8, 1.5 Hz, 1H, Ar), 8.02 (d, J = 7.6 Hz, 2H, Ar), 8.06 – 8.15 (m, 2H, Ar), 13.81 (s, 1H, COOH). ^{13}C NMR (101 MHz, DMSO-d_6): δ 38.9 (CH$_2$), 125.0 (Ar), 128.2 (Ar), 129.2 (2xAr), 129.3 (2xAr), 131.1 (Ar), 131.4 (Ar), 134.0 (Ar), 134.4 (Ar), 136.3 (Ar), 148.3 (Ar), 167.2 (COOH), 193.0 (CO).
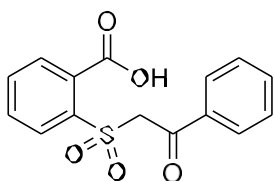
2-((2-oxo-2-phenylethyl)sulfonyl)benzoic acid White solid, 49% yield. ^{1}H NMR (400 MHz, DMSO-d_6): δ 4.67 (d, J = 14.7 Hz, 2H, CH$_2$), 7.54 (t, J = 7.6 Hz, 2H, Ar), 7.70 (q, J = 7.6 Hz, 2H, Ar), 7.91 (td, J = 7.8, 1.5 Hz, 1H, Ar), 8.02 (d, J = 7.6 Hz, 2H, Ar), 8.06 – 8.15 (m, 2H, Ar), 12.75 (s, 1H, COOH). ^{13}C NMR (101 MHz, DMSO-d_6): δ 69.6. (CH$_2$), 125.0 (Ar), 128.2 (Ar), 129.2 (2xAr), 129.3 (2xAr), 131.1 (Ar), 131.4 (Ar), 134.0 (Ar), 134.4 (Ar), 136.3 (Ar), 148.3 (Ar), 167.2 (COOH), 193.0 (CO).
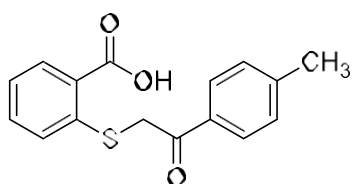
2-((2-oxo-2-(p-tolyl)ethyl)thio)benzoic acid (20). Solido bianco. ^{1}H NMR (400 MHz, DMSO-d_6): δ 2.39 (s, 3H, CH$_3$), 4.64 (s, 2H, CH$_2$), 7.22 (t, J = 7.3 Hz, 1H, Ar), 7.36 (d, J = 7.9 Hz, 2H, Ar), 7.47 (dt, J = 15.1, 4.8 Hz, 2H, Ar), 7.90 (d, J = 7.7 Hz, 1H, Ar), 7.98 (d, J = 7.8 Hz, 2H, Ar), 13.09 (s, 1H, COOH). ^{13}C NMR (101 MHz, DMSO-d_6): δ 21.6 (CH$_3$), 39.1 (CH$_2$), 124.5 (Ar), 126.4 (Ar), 128.3 (Ar), 129.1 (2xAr), 129.7 (2xAr), 131.4 (Ar), 132.8 (Ar), 133.5 (Ar), 140.6 (Ar), 144.6 (Ar), 167.9 (COOH), 194.7 (CO).
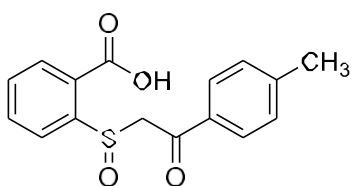
2-((2-oxo-2-(p-tolyl)ethyl)sulfinyl)benzoic acid (20A). Solido bianco. ^{1}H NMR (400 MHz, DMSO-d_6): δ 2.39 (s, 3H, CH$_3$), 4.08 (s, 2H, CH$_2$), 7.53 (t, J = 7.6 Hz, 2H, Ar), 7.69 (q, J = 7.6 Hz, 2H, Ar), 7.91 (td, J = 7.8, 1.5 Hz, 1H, Ar), 8.02 (d, J = 7.6 Hz, 1H, Ar), 8.06 – 8.15 (m, 2H, Ar), 13.81 (s, 1H, COOH). ^{13}C NMR (101 MHz, DMSO-d_6): δ 21.7 (CH$_3$), 66.0 (CH$_2$), 125.0 (Ar), 128.2 (Ar), 129.2 (2xAr), 129.3 (2xAr), 131.1 (Ar), 131.4 (Ar), 134.0 (Ar), 134.4 (Ar), 136.3 (Ar), 148.3 (Ar), 167.2 (COOH), 192.4 (CO).
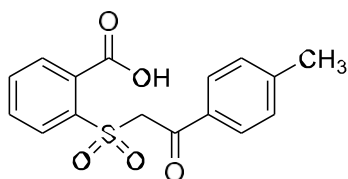
2-((2-oxo-2-(p-tolyl)ethyl)sulfonyl)benzoic acid 1H NMR (400 MHz, CDCl3) δ 2.62 (s, 3H, CH$_3$), 4.67 (s, 2H, CH$_2$), 6.72- 6.78 (m, 2H, Ar), 7.87-7.87 (m, 2H, Ar), 8.07-7.87 (m, 3H, Ar), 8.52 (m, 1H, Ar), 12.75 (s, -COOH). ^{13}C NMR (101 MHz, DMSO-d_6): δ 21.6 (CH$_3$), 39.1 (CH$_2$), 124.5 (Ar), 126.4 (Ar), 128.3 (Ar), 129.1 (2xAr), 129.7 (2xAr), 131.4 (Ar), 132.8 (Ar), 133.5 (Ar), 140.6 (Ar), 144.6 (Ar), 167.9 (COOH), 194.7 (CO).

2-((2-(4-methoxyphenyl)-2-oxoethyl)thio)benzoic acid (21). Solido bianco. ^{1}H NMR (400 MHz, DMSO-d_6): δ 3.86 (s, 3H, CH$_3$), 4.61 (s, 2H, CH$_2$), 7.07 (d, *J* = 8.6 Hz, 2H, Ar), 7.14 – 7.31 (m, 1H, Ar), 7.41 – 7.60 (m, 2H, Ar), 7.62 (dd, *J* = 8.8, 3.0 Hz, 2H, Ar), 7.90 (dd, *J* = 7.7, 1.5 Hz, 1H, Ar), 8.06 (d, *J* = 8.9 Hz, 2H, Ar), 13.09 (s, 1H, COOH). ^{13}C NMR (101 MHz, DMSO-d_6): δ 38.9 (CH$_3$), 58.0 (CH$_2$), 114.4 (2xAr), 124.5 (Ar), 126.4 (Ar), 128.3 (Ar), 128.8 (Ar), 131.4 (Ar), 131.5 (2xAr), 132.7 (Ar), 140.8 (Ar), 163.9 (Ar), 167.9 (COOH), 193.5 (CO).

2-((2-(4-methoxyphenyl)-2-oxoethyl)sulfinyl)benzoic acid (21A). White solid, 57% yield. ^{1}H NMR (400 MHz, DMSO-d_6): δ 3.86 (s, 3H, CH$_3$), 4.04 (d, J = 14.7 Hz, 1H, CH$_2$), 7.53 (t, J = 7.6 Hz, 2H, Ar), 7.69 (q, J = 7.6 Hz, 2H, Ar), 7.91 (td, J = 7.8, 1.5 Hz, 1H, Ar), 8.02 (d, J = 7.6 Hz, 2H, Ar), 8.06 – 8.15 (m, 2H, Ar), 13.81 (s, 1H, COOH). ^{13}C NMR (101 MHz, DMSO-d_6): δ 40.1 (CH$_3$), 65.8 (CH$_2$), 125.0 (Ar), 128.2 (Ar), 129.2 (2xAr), 129.3 (2xAr), 131.1 (Ar), 131.4 (Ar), 134.0 (Ar), 134.4 (Ar), 136.3 (Ar), 148.3 (Ar), 167.2 (COOH), 191.1 (CO).

2-((2-(4-methoxyphenyl)-2-oxoethyl)sulfonyl)benzoic acid 1H NMR (400 MHz, DMSO) δ δ 3.91 (s, 3H, CH$_3$), 4.14 (d, J = 14.7 Hz, 1H, CH$_2$), 4.67 (d, J = 14.7 Hz, 1H, CH$_2$), 7.53 (t, J = 7.6 Hz, 2H, Ar), 7.73 (q, J = 7.6 Hz, 2H, Ar), 7.94 (td, J = 7.8, 1.5 Hz, 1H, Ar), 8.02 (d, J = 7.6 Hz, 2H, Ar), 8.06 – 8.15 (m, 2H, Ar), 13.78 (s, 1H, COOH). ^{13}C NMR (101 MHz, DMSO-d_6): δ 38.9 (-OCH$_3$), 56.0 (CH$_2$), 114.4 (2xAr), 124.5 (Ar), 126.4 (Ar), 128.3 (Ar), 128.8 (Ar), 131.4 (Ar), 131.5 (2xAr), 132.7 (Ar), 140.8 (Ar), 163.9 (Ar), 167.9 (COOH), 193.5 (CO).
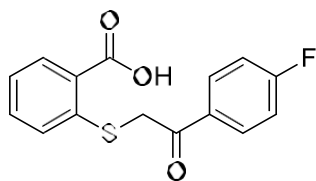
2-((2-(4-fluorophenyl)-2-oxoethyl)thio)benzoic acid (22). White solid, 51% yield. ^{1}H NMR (400 MHz, DMSO-d_6): δ 4.69 (s, 2H, CH$_2$), 7.22 (t, J = 7.4 Hz, 1H, Ar), 7.35 – 7.42 (m, 2H, Ar), 7.43 – 7.54 (m, 2H, Ar), 7.90 (d, J = 7.7 Hz, 1H, Ar), 8.17 (dd, J = 8.5, 5.5 Hz, 2H, Ar), 13.10 (s, 1H, COOH). ^{13}C NMR (101 MHz, DMSO-d_6): δ 39.2 (CH$_2$), 116.1 (Ar), 116.3 (Ar), 124.6 (Ar), 126.5 (Ar), 128.4 (Ar), 131.4 (Ar), 132.1 (Ar), 132.7 (Ar), 132.8 (Ar), 140.4 (Ar), 164.4 (Ar), 166.9 (Ar), 167.9 (COOH), 193.8 (CO).


2-((2-(4-fluorophenyl)-2-oxoethyl)sulfinyl)benzoic acid (22A). White solid, 57% yield. ^{1}H NMR (400 MHz, DMSO-d_6): δ 4.24 (d, J = 14.7 Hz, 1H, CH$_2$), 4.98 (d, J = 14.7 Hz, 1H, CH$_2$), 7.53 (t, J = 7.6 Hz, 2H, Ar), 7.69 (q, J = 7.6 Hz, 2H, Ar), 7.91 (td, J = 7.8, 1.5 Hz, 1H, Ar), 8.02 (d, J = 7.6 Hz, 2H, Ar), 8.06 – 8.15 (m, 2H, Ar), 13.85 (s, 1H, COOH). ^{13}C NMR (101 MHz, DMSO-d_6): δ 65.7 (CH$_2$), 125.0 (Ar), 128.2 (Ar), 129.2 (2xAr), 129.3 (2xAr), 131.1 (Ar), 131.4 (Ar), 134.0 (Ar), 134.4 (Ar), 136.3 (Ar), 148.3 (Ar), 167.2 (COOH), 191.6 (CO)
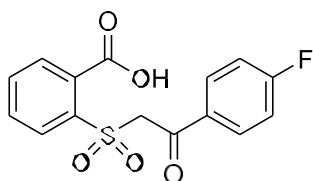
2-((2-(4-fluorophenyl)-2-oxoethyl)sulfonyl)benzoic acid White solid, 48% yield ^{1}H NMR (400 MHz, DMSO-d_6): δ 5.46 (s, 2H, CH2), 7.07 (d, J = 8.6 Hz, 2H, Ar), 7.14 – 7.31 (m, 1H, Ar), 7.41 – 7.60 (m, 2H, Ar), 7.62 (dd, J = 8.8, 3.0 Hz, 2H, Ar), 7.90 (dd, J = 7.7, 1.5 Hz, 1H, Ar), 8.06 (d, J = 8.9 Hz, 2H, Ar), 13.09 (s, 1H, COOH). ^{13}C NMR (101 MHz, DMSO-d_6): δ 65.9 (CH$_2$), 125.0 (Ar), 128.2 (Ar), 129.2 (2xAr), 129.3 (2xAr), 131.1 (Ar), 131.4 (Ar), 134.0 (Ar), 134.4 (Ar), 136.3 (Ar), 148.3 (Ar), 167.2 (COOH), 193.0 (CO).
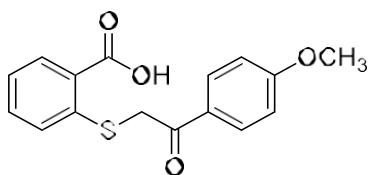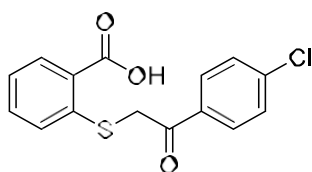

2-((2-(4-chlorophenyl)-2-oxoethyl)thio)benzoic acid (23). White solid, 51% yield. ^{1}H NMR (400 MHz, DMSO-d_6): δ 4.69 (s, 2H, CH$_2$), 7.22 (t, J = 7.4 Hz, 1H, Ar), 7.47 (dt, J = 14.9, 4.7 Hz, 2H, Ar), 7.62 (dd, J = 8.8, 3.0 Hz, 2H, Ar), 7.90 (dd, J = 7.8, 1.7 Hz, 1H, Ar), 8.08 – 8.12 (m, 2H, Ar), 13.11 (s, 1H, COOH). ^{13}C NMR (101 MHz, DMSO-d_6): δ 39.2 (CH$_2$), 124.6 (Ar), 126.5 (Ar), 128.4 (Ar), 129.3 (2xAr), 130.9 (2xAr), 131.4 (Ar), 132.8 (Ar), 134.6 (Ar), 139.0 (Ar), 140.3 (Ar), 167.9 (COOH), 194.2 (CO).
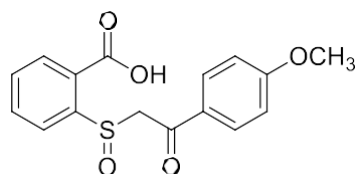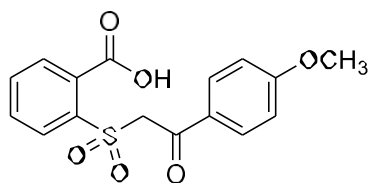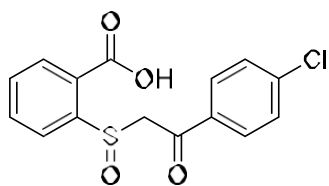
2-((2-(4-chlorophenyl)-2-oxoethyl)sulfinyl)benzoic acid (23A). White solid, 55% yield. ^{1}H NMR (400 MHz, DMSO-d_6): δ 4.26 (d, J = 14.7 Hz, 1H, CH$_2$), 4.98 (d, J = 14.7 Hz, 1H, CH$_2$), 7.59 (t, J = 7.6 Hz, 2H, Ar), 7.70 (dt, J = 7.6, 1.3 Hz, 2H, Ar), 7.90 (td, J = 7.8, 1.5 Hz, 1H, Ar), 8.00 (d, J = 7.6 Hz, 2H, Ar), 8.08 8.08 (t, J = 7.7 Hz, 2H, Ar), 13.84 (s, 1H, COOH). ^{13}C NMR (101 MHz, DMSO-d_6): δ 65.6 (CH$_2$), 125.0 (Ar), 128.2 (Ar), 129.2 (2xAr), 129.3 (2xAr), 131.1 (Ar), 131.4 (Ar), 134.0 (Ar), 134.4 (Ar), 136.3 (Ar), 148.3 (Ar), 167.2 (COOH), 192.1 (CO).

2-((2-(4-chlorophenyl)-2-oxoethyl)sulfonyl)benzoic acid White solid, 61% yield ^{1}H NMR (400 MHz, DMSO-d_6): δ 5.49 (s, CH$_2$, 2H), 7.53 (t, J = 7.6 Hz, 2H, Ar), 7.69 (q, J = 7.6 Hz, 2H, Ar), 7.91 (td, J = 7.8, 1.5 Hz, 1H, Ar), 8.02 (d, J = 7.6 Hz, 2H, Ar), 8.06 – 8.15 (m, 2H, Ar), 13.97 (s, 1H, COOH). ^{13}C NMR (101 MHz, DMSO-d_6): δ 65.7 (CH$_2$), 125.0 (Ar), 128.2 (Ar), 129.2 (2xAr), 129.3 (2xAr), 131.1 (Ar), 131.4 (Ar), 134.0 (Ar), 134.4 (Ar), 136.3 (Ar), 148.3 (Ar), 167.2 (COOH), 191.6 (CO).

2-((2-(4-bromophenyl)-2-oxoethyl)thio)benzoic acid (24). White solid, 57% yield. ^{1}H NMR (400 MHz, DMSO-d_6): δ 4.68 (s, 2H, CH$_2$), 7.17 – 7.28 (m, 1H, Ar), 7.48 (ddd, J = 16.7, 8.4, 6.9 Hz, 2H, Ar), 7.76 (d, J = 8.3 Hz, 2H, Ar), 7.90 (dd, J = 7.8, 1.5 Hz, 1H, Ar), 7.97 – 8.04 (m, 2H, Ar), 13.11 (s, 1H, COOH). ^{13}C NMR (101 MHz, DMSO-d_6): δ 39.2 (CH$_2$), 124.6 (Ar), 126.5 (Ar), 128.2 (Ar), 128.4 (Ar), 131.0 (2xAr), 131.4 (Ar), 132.2 (2xAr), 132.8 (Ar), 134.9 (Ar), 140.3 (Ar), 167.9 (COOH), 194.4 (CO).
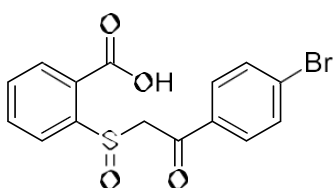

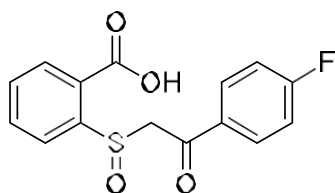**2-((2-(4-bromophenyl)-2-oxoethyl)sulfinyl)benzoic acid (24A).** White solid, 56% yield. ^{1}H NMR (400 MHz, DMSO-d_6): δ 4.25 (d, J = 14.7 Hz, 1H, CH$_2$), 4.97 (d, J = 14.7 Hz, 1H, CH$_2$), 7.53 (t, J = 7.6 Hz, 2H, Ar), 7.69 (q, J = 7.6 Hz, 2H, Ar), 7.91 (td, J = 7.8, 1.5 Hz, 1H, Ar), 8.02 (d, J = 7.6 Hz, 2H, Ar), 8.06 – 8.15 (m, 2H, Ar), 13.83 (s, 1H, COOH). ^{13}C NMR (101 MHz, DMSO-d_6): δ 65.6 (CH$_2$), 125.0 (Ar), 128.2 (Ar), 129.2 (2xAr), 129.3 (2xAr), 131.1 (Ar), 131.4 (Ar), 134.0 (Ar), 134.4 (Ar), 136.3 (Ar), 148.3 (Ar), 167.1 (COOH), 192.3 (CO).
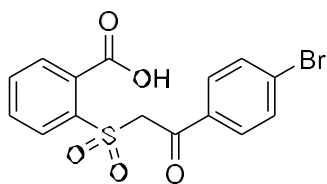
2-((2-(4-bromophenyl)-2-oxoethyl)sulfonyl)benzoic acid White solid, 45% yield yield ^{1}H NMR (400 MHz, DMSO-d_6): δ 4.87 (s, CH$_2$, 2H), 7.53 (t, J = 7.6 Hz, 2H, Ar), 7.69 (q, J = 7.6 Hz, 2H, Ar), 7.91 (td, J = 7.8, 1.5 Hz, 1H, Ar), 8.02 (d, J = 7.6 Hz, 2H, Ar), 8.06 – 8.15 (m, 2H, Ar), 13.97 (s, 1H, COOH). ^{13}C NMR (101 MHz, DMSO-d_6): δ 65.6 (CH$_2$), 125.0 (Ar), 128.2 (Ar), 129.2 (2xAr), 129.3 (2xAr), 131.1 (Ar), 131.4 (Ar), 134.0 (Ar), 134.4 (Ar), 136.3 (Ar), 148.3 (Ar), 167.2 (COOH), 192.1 (CO).
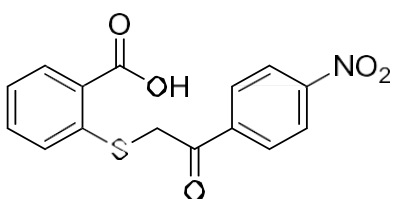

2-((2-(4-nitrophenyl)-2-oxoethyl)thio)benzoic acid (25). Yellow solid, 71% yield. ^{1}H NMR (400 MHz, DMSO-d_6): δ 4.79 (s, 2H, CH$_2$), 7.24 (t, J = 7.4 Hz, 1H, Ar), 7.41 – 7.59 (m, 2H, Ar), 7.90 (dd, J = 7.7, 1.5 Hz, 1H, Ar), 8.29 (d, J = 8.5 Hz, 2H, Ar), 8.36 (d, J = 8.5 Hz, 2H, Ar), 13.11 (s, 1H, COOH). ^{13}C NMR (101 MHz, DMSO-d_6): δ 39.6 (CH$_2$), 124.2 (2xAr), 124.8 (Ar), 126.6 (Ar), 128.5 (Ar), 130.4 (2xAr), 131.4 (Ar), 132.8 (Ar), 139.9 (Ar), 140.6 (Ar), 150.5 (Ar), 167.9 (COOH), 194.4 (CO).
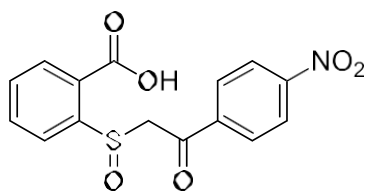
2-((2-(4-nitrophenyl)-2-oxoethyl)sulfinyl)benzoic acid (25A). yellow solid, 67% yield. ^{1}H NMR (400 MHz, DMSO-d_6): δ 4.40 (d, J = 14.7 Hz, 1H, CH$_2$), 5.07 (d, J = 14.7 Hz, 1H, CH$_2$), 7.53 (t, J = 7.6 Hz, 2H, Ar), 7.69 (q, J = 7.6 Hz, 2H, Ar), 7.91 (td, J = 7.8, 1.5 Hz, 1H, Ar), 8.02 (d, J = 7.6 Hz, 2H, Ar), 8.06 – 8.15 (m, 2H, Ar), 13.85 (s, 1H, COOH). ^{13}C NMR (101 MHz, DMSO-d_6): δ 65.6 (CH$_2$), 125.0 (Ar), 128.2 (Ar), 129.2 (2xAr), 129.3 (2xAr), 131.1 (Ar), 131.4 (Ar), 134.0 (Ar), 134.4 (Ar), 136.3 (Ar), 148.3 (Ar), 167.2 (COOH), 192.4 (CO).
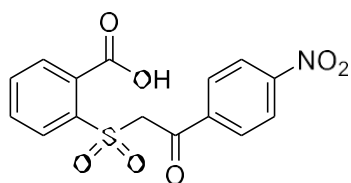
2-((2-(4-nitrophenyl)-2-oxoethyl)sulfonyl)benzoic acid . yellow solid, 57% yield ^{1}H NMR (400 MHz, DMSO-d_6): δ 5.49 (s, CH$_2$, 2H), 7.17 – 7.28 (m, 1H, Ar), 7.48 (ddd, J = 16.7, 8.4, 6.9 Hz, 2H, Ar), 7.76 (d, J = 8.3 Hz, 2H, Ar), 7.90 (dd, J = 7.8, 1.5 Hz, 1H, Ar), 7.97 – 8.04 (m, 2H, Ar), 13.11 (s, 1H, COOH). ^{13}C NMR (101 MHz, DMSO-d_6): δ 65.6 (CH$_2$), 125.0 (Ar), 128.2 (Ar), 129.2 (2xAr), 129.3 (2xAr), 131.1 (Ar), 131.4 (Ar), 134.0 (Ar), 134.4 (Ar), 136.3 (Ar), 148.3 (Ar), 167.1 (COOH), 192.3 (CO).
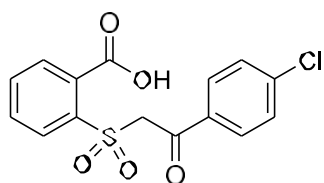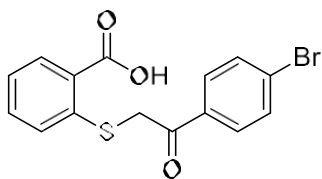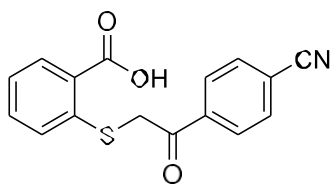
2-((2-(4-cyanophenyl)-2-oxoethyl)thio)benzoic acid White solid, 55% yield ^{1}H NMR (400 MHz, DMSO-d_6): δ 4.39 (s, CH$_2$, 2H), 7.17 – 7.28 (m, 1H, Ar), , 7.76 (d, J = 8.3 Hz, 2H, Ar), 7.90 (dd, J = 7.8, 1.5 Hz, 1H, Ar), 8.03 – 8.08 (m, 4H, Ar), 13.11 (s, 1H, COOH). ^{13}C NMR (101 MHz, DMSO-d_6): δ 38.5 (CH$_2$), 118.6 (CN),125.0 (Ar), 128.2 (Ar), 129.2 (2xAr), 129.3 (Ar), 132.4 (2Ar), 134.0 (Ar), 134.4 (Ar), 136.3 (Ar), 168.1 (COOH), 192.3 (CO).
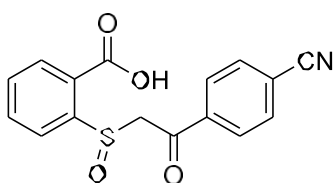
2-((2-(4-cyanophenyl)-2-oxoethyl)sulfinyl)benzoic acid White solid, 52% yield ^{1}H NMR (400 MHz, DMSO-d_6): δ 4.04 (s, CH$_2$, 2H), 7.17 – 7.28 (m, 1H, Ar), , 7.76 (d, J = 8.3 Hz, 2H, Ar), 7.90 (dd, J = 7.8, 1.5 Hz, 1H, Ar), 8.03 – 8.08 (m, 4H, Ar), 12.75 (s, 1H, COOH). ^{13}C NMR (101 MHz, DMSO-d_6): δ 63.3 (CH$_2$), 118.6 (CN),125.0 (Ar), 128.2 (Ar), 129.2 (2xAr), 129.3 (Ar), 132.4 (2Ar), 134.0 (Ar), 134.4 (Ar), 136.3 (Ar), 169.31 (COOH), 189.00 (CO).
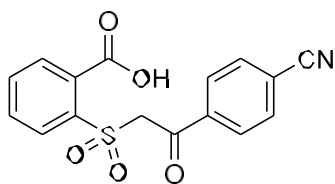
2-((2-(4-cyanophenyl)-2-oxoethyl)sulfonyl)benzoic acid White solid, 49% yield ^{1}H NMR (400 MHz, DMSO-d_6): δ 4.67 (s, CH$_2$, 2H), 7.17 – 7.28 (m, 1H, Ar), , 7.76 (d, J = 8.3 Hz, 2H, Ar), 7.90 (dd, J = 7.8, 1.5 Hz, 1H, Ar), 8.03 – 8.08 (m, 4H, Ar), 12.95 (s, 1H, COOH). ^{13}C NMR (101 MHz, DMSO-d_6): δ 69.9 (CH$_2$), 118.6 (CN),125.0 (Ar), 128.2 (Ar), 129.2 (2xAr), 129.3 (Ar), 132.4 (2Ar), 134.0 (Ar), 134.4 (Ar), 136.3 (Ar), 169.31 (COOH), 189.00 (CO).

### *Evaluation of human monoamine oxidase (hMAO) inhibitory activity*

The assay for the evaluation of the inhibitory activity of the compounds is based on the measurement of the conversion rate of a hMAO-substrate, kynuramine, into its oxidized metabolite, 4-quinolinol (4HQ), that absorbs at 316 nm [106]. The assay has been performed as previously described1.First, a calibration curve was created using 4-quinolinol solutions at different concentrations (ranging from 0,1 nM to 10 mM). Then, the kinetic properties (specific activity, Michaelis-Menten constant K_M, and maximum speed V_{max}) of the two isoforms were evaluated using solutions with different enzyme concentrations (X to X) for the measurement of the specific activity, and kynuramine solutions with at least six different concentration levels (Y to Y) for the measurement of K_M and V_{max}. After having fully characterized the enzymes, the inhibitory activity of the compounds was measured. Compound solutions were pipetted in a 96-wells plate, together with kynuramine solution (concentration = 2 x K_M in the well), phosphate buffer (pH = 7.4) and the plate was then incubated at 37°C for 10 minutes. Absorbance of the wells was measured every minute and the last read (t = 10 min) was used as blank. Then, the enzyme was added (the amount of enzyme added depended on the specific activity, Vmax = 50 pmol/min) and the plate was incubated at 37°C for 30 minutes. The formation of 4-quinolinol was analysed and the production formation rate, or initial velocity V0, was obtained from the slope of the *n (4HQ) = f(t)* curves. Inhibition percentages at 10 μM were obtained from the comparison between the initial speed of the control well (no inhibitor) and the initial speed of the inhibitor. All

compounds have been screened at 10 μM, those whose inhibition was ≥ 50%, were further investigated and their IC$_{50}$ was measured as follows. Different concentrations for each inhibitor were tested and analysed as previously described. Dose-response curves were created using the percentage of inhibition as a function of the logarithm of the concentration of the inhibitor. The IC$_{50}$ value was extrapolated from the curve. The results have been expressed as mean value ± standard deviation. All experiments have been performed in triplicate and conducted three times.

Chapter 4: Photocatalytic Functionalization of Dehydroalanine-Derived Peptides in Batch and Flow

4.1 Introduction

Peptide and protein therapeutics are currently experiencing a significant breakthrough, setting them on par with small molecules as potential drug candidates.[110] Late-stage functionalization (LSF) of biomolecules and drug scaffolds has proven to be a powerful strategy for efficiently exploring the chemical landscape, eliminating the need for expensive and resource-intensive de novo methodologies.[111-113] Consequently, the site- and chemoselective LSF of peptides has garnered substantial interest from both academic researchers and the pharmaceutical industry. Within this context, the incorporation of unnatural amino acids into peptides can significantly modify their bioactivity and enhance proteolytic stability.[114-117] For the LSF of peptides to be effective, it necessitates highly selective and mild reaction.

Conditions capable of forging bonds with high precision amidst the complex array of functional groups inherent to peptides. To overcome this challenge, a diverse array of synthetic strategies has been utilized, encompassing classical condensations and (cyclo)additions,[118] transition-metal catalysis,[119] click chemistry,[120] photochemistry,[121] and more recently electrochemistry.[8] Notably, among the proteinogenic amino acids, those with nucleophilic side chains have been most extensively investigated for photochemical LSF.[123] Key examples include cysteine,[124] tryptophan,[125] methionine,[126] and tyrosine.[127] In contrast, dehydroalanine (Dha) represents an electrophilic residue that, although not proteinogenic, occurs naturally and is prevalent in a host of antimicrobial peptides.[128] It presents an alternative avenue for functionalization, as depicted in **Figure** 1a.[129-131] The recent advancement in photochemical LSF of Dha-enriched peptides has facilitated targeted and chemoselective processes such as alkylation, fluoroalkylation, acylation, and to a more limited degree, arylation.[132-135] Prior arylation approaches typically demanded aryl bromides as coupling agents, necessitating complex and laborious de novo synthesis to produce a variety of functionalized partners. However, recent studies by the groups of Ritter,[110] Procter, and Alcarazo [136-139] has highlighted the utility of arylsulfonium salts. These salts enable straightforward preparation routes leading to intricate aryl electrophiles,[140] which

are instrumental for both transition metal-catalyzed cross coupling chemistry[141-146] and photochemical applications.[147-151] Building on this, vinyl-sulfonium salts have recently been employed for various polar transformations.[154] Therefore, we were intrigued by the prospect of developing a photocatalytic LSF approach for Dha-containing peptides using the highly versatile and modular arylthianthrenium salts, as illustrated in **Figure** 1b. This transformation was accomplished by the single electron transfer (SET) reduction of these salts, which generates an exceptionally reactive aryl radical. This radical readily adds to the α,β-unsaturated moiety within the Dha backbone. To guarantee gentle reaction conditions and minimize reaction times—key factors for ensuring broad functional group compatibility and scalability—we also devised a continuous-flow protocol.[28] Notably, our method facilitates the efficient ligation of peptides and their conjugation with various drug scaffolds.
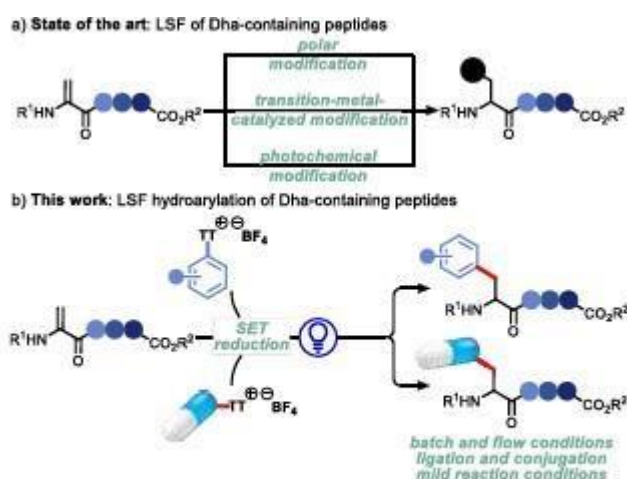
Figure 1. a) Dha diversification. b) Photocatalytic LSF of Dha-containing peptides with arylthianthrenium salts.

Our initial efforts in achieving regioselective arylation of Dha-derivative 2 focused on the use of arylthianthrenium salt 1 (For detailed optimization, see Supporting Information). We employed DIPEA as the stoichiometric reductant and eosin Y as a photocatalyst, with the reaction driven by visible light irradiation at a wavelength of 456 nm (Table 1). The reaction proceeded efficiently (72% isolated yield) in a solvent mixture of MeCN:HFIP (7:1) at room temperature over 4 hours (Table 1, Entry 1). Other protic or aprotic polar solvents failed to provide satisfactory conversions (Table 1, Entries 2 and 3). It became evident that the choice

of solvent was critical; variations in the solvent system composition, containing different ratios between MeCN and HFIP, resulted in decreased yields (Table 1, Entry 4). A control experiment demonstrated the essential role of DIPEA (entry 5). Other potential reductants, including various amines and dihydropyridines, were also tested but failed to effectively produce the target product 3 (Table 1, Entries 6 and 7). Furthermore, we explored a range of photo-organocatalysts and metal-based photocatalysts, which unfortunately led to less efficient processes (Table 1, Entries 8 and 9). Gratifyingly, the synthesis of the unnatural amino acid 3 could be smoothly performed in a continuous-flow photoreactor in a significantly reduced reaction Table 1. Optimization of the photocatalytic arylation of the Dha-derivative 2 with arylthianthrenium salt 1.[a] Entry Deviation from the standard conditions 1 2 3 4 5 6 7 None MeOH/i-PrOH/HFIP/DMF/DMSO as solvent MeCN as solvent MeCN:HFIP (1:1)/(3:1)/(19:1) as solvent without DIPEA TEA/TBA/DABCO/TEOA instead of DIPEA hantzsch ester (2.0 equiv) instead of DIPEA 8 9 10 eosin Y-Na2/fluorescein/rhodamine B/Ru(bpy)3Cl2 as photocatalyst Ir(ppy)3/10-phenylphenothiazine as photocatalyst under flow conditions tR = 20 min Yield [%][b] 72 40/38/nd/nd/nd 45 36/63/49 nd 37/29/nd/55 23 68/47/52/45 nd/10[c] 69 [a] Reaction conditions: 1 (0.20 mmol), 2 (1.0 mmol), eosin Y (5.0 mol%), DIPEA (1.0 mmol), MeCN:HFIP (7:1, 4.0 mL), at room temperature, 456 nm for 4 h. [b] Yield of isolated product. [c] Yield determined by 1H-NMR spectroscopy using trichloroethylene as external standard. HFIP: 1,1,1,3,3,3-hexafluoro-2 propanol, DMF: N,N-dimethylformamide, DMSO: dimethyl sulfoxide, DIPEA: N,N-diisopropylethylamine, TEA: triethylamine, TBA: tributylamine, DABCO: 1,4-diazabicyclo[2.2.2]octane, TEOA: 2-(bis(2-hydroxyethyl)amino)ethanol, bpy: 2,2'-bipyridine, ppy: 2-phenylpyridine. time (tR = 20 min) with comparable efficiency (Table 1, Entry 10).

Batch or Continuous-Flow
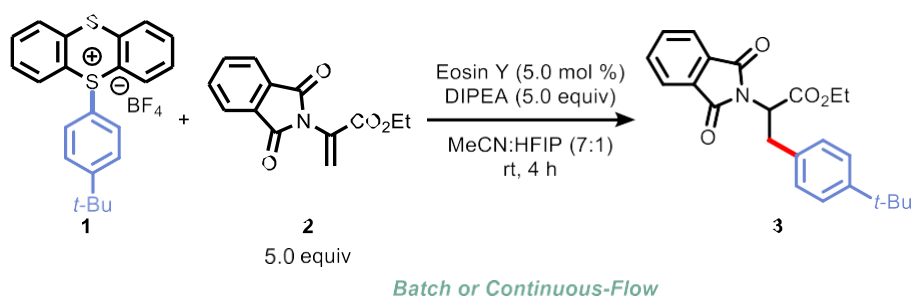
Entry	Deviation from the standard conditions	Yield [%][b]
1	none	72
2	MeOH/i-PrOH/HFIP/DMF/DMSO as solvent	40/38/nd/nd/nd
3	MeCN as solvent	45
4	MeCN:HFIP (1:1)/(3:1)/(19:1) as solvent	36/63/49
5	without DIPEA	nd
6	TEA/TBA/DABCO/TEOA instead of DIPEA	37/29/nd/55
7	hantzsch ester (2.0 equiv) instead of DIPEA	23
8	eosin Y-Na$_2$/fluorescein/rhodamine B/Ru(bpy)$_3$Cl$_2$ as photocatalyst	68/47/52/45
9	Ir(ppy)$_3$/10-phenylphenothiazine as photocatalyst	nd/10[c]
10	under flow conditions t_R = 20 min	69

Table 1. [a] Reaction conditions: 1 (0.20 mmol), 2 (1.0 mmol), eosin Y (5.0 mol%), DIPEA (1.0 mmol), MeCN:HFIP (7:1, 4.0 mL), at room temperature, 456 nm for 4 h. [b] Yield of isolated product. [c] Yield determined by 1H-NMR spectroscopy using trichloroethylene as external standard. HFIP: 1,1,1,3,3,3-hexafluoro-2-propanol, DMF: N,N-dimethylformamide, DMSO: dimethyl sulfoxide, DIPEA: N,N-diisopropylethylamine, TEA: triethylamine, TBA: tributylamine, DABCO: 1,4-diazabicyclo[2.2.2]octane, TEOA: 2-(bis(2-hydroxyethyl)amino)ethanol, bpy: 2,2'-bipyridine, ppy: 2-phenylpyridine.

Building upon the established optimal conditions for the photocatalytic arylation of Dha 2, both in batch and flow (Table 1, Entries 1 and 10), we sought to evaluate the versatility and scope of our method. Hereto, we applied various arylthianthrenium salts 4 to the established protocol, as delineated in Scheme 1. Scaling up our model reaction using arylthianthrenium salt 1 and Dha derivative 2 via flow technology was successful, achieving a 71% isolated yield at a 1.0 mmol scale under our standard conditions.

We then extended our approach to include alkyl-substituted arylthianthrenium salts 4, which served as competent reaction partners into our protocol, yielding the anticipated products 7-12 in good to excellent isolated yields. Notably, the synthesis of biaryl unnatural amino acids 13-15 was achieved in excellent yields. These amino acids bear functional groups amenable to subsequent synthetic manipulations, such as condensations and transition-metal catalyzed cross-couplings. Impressively, the aryl iodide bond, typically sensitive to reduction under photocatalytic conditions, proved to be compatible with our process. The method's adaptability was further underscored by its application to heteroatom-containing arylthianthrenium salts 4, leading to an array of phenylalanine derivatives (16-24). The yields were moderate to excellent, maintaining both high chemo- and regioselectivity. Additionally, our methodology demonstrated its robust functional group tolerance by facilitating access to a diverse set of heterocycle-containing amino acids. This collection of compounds included structures with dihydrobenzofuran, benzodioxole, chromanone, xanthone, pyridine, carbazole, indoline, and quinazoline-dione, showcasing the broad applicability and robustness of the synthetic strategy. In addition, our methodology enabled the synthesis of diverse amino acid derivatives for peptide synthesis, incorporating orthogonal protecting groups, requiring only minor adjustments to reaction conditions. We evaluated acid-, base- and hydrogenation-labile protecting groups, including tert -butyloxycarbonyl (Boc), fluorenylmethyloxycarbonyl (Fmoc), and benzyloxycarbonyl (Cbz) resulting in the successful preparation of the desired building blocks 33-35.
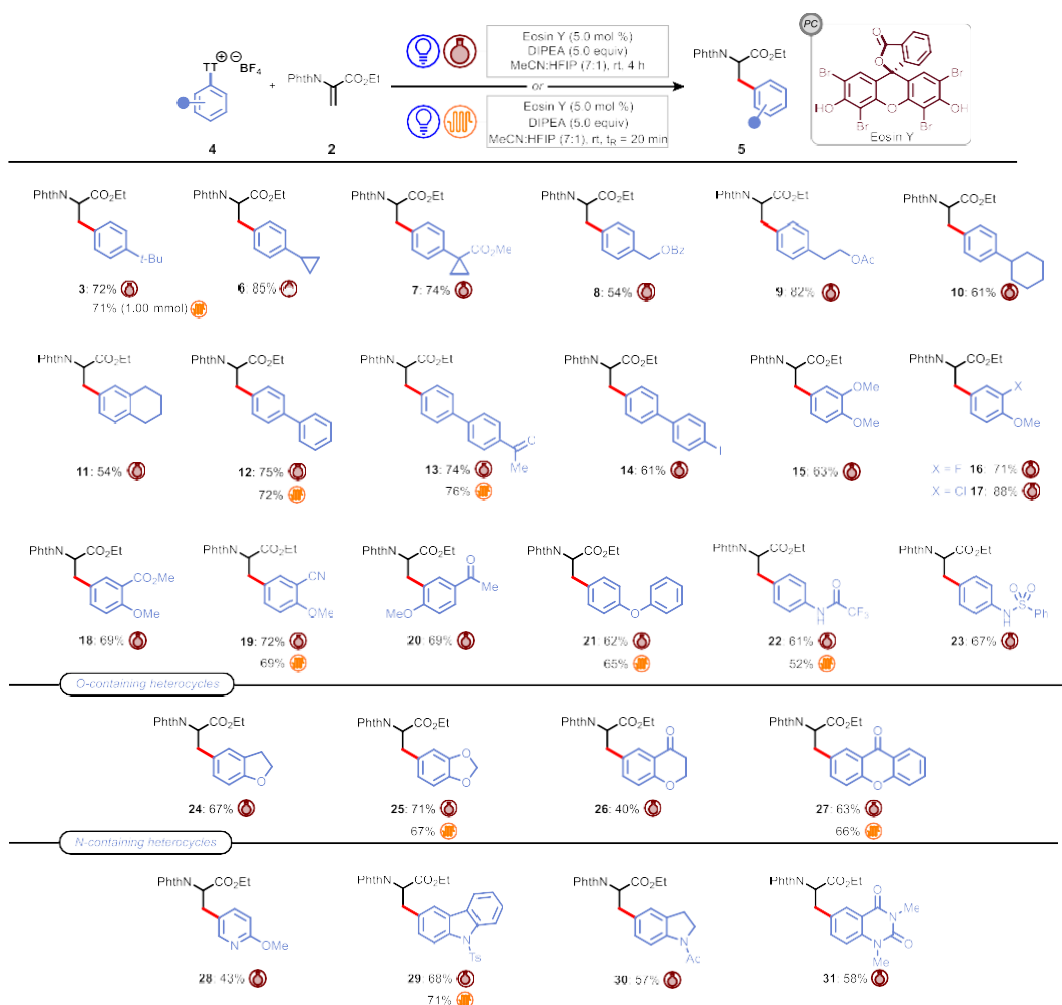
Scheme 1. Synthesis of unnatural amino acids via radical addition to Dha derivative 2. For further experimental details see the Supporting Information.

The streamlined and selective synthesis of arylthianthrenium salts prompted us to investigate their application with drug scaffolds and natural product derivatives, numbered as 36, within our photocatalytic protocol, aiming to create distinctive conjugates as depicted in Scheme 2. The process proved to be of high value, allowing for the seamless integration of a variety of drugs onto the Dha-backbone, yielding an array of novel amino acid/drug conjugates 38. The mild conditions of our photocatalytic hydroarylation were evidenced by the complete preservation of vulnerable heterocyclic structures, such as those found in pyriproxyphen, bifonazole, boscalid, and benzbromarone. The successful incorporation of drug scaffolds onto amino acid backbones led us to extend our strategy to the chemical ligation of peptides. We utilized an arylthianthrenium salt derivative of phenylalanine

under our standard conditions, which afforded the targeted unnatural dipeptide 47 with excellent chemo- and regioselectivity.
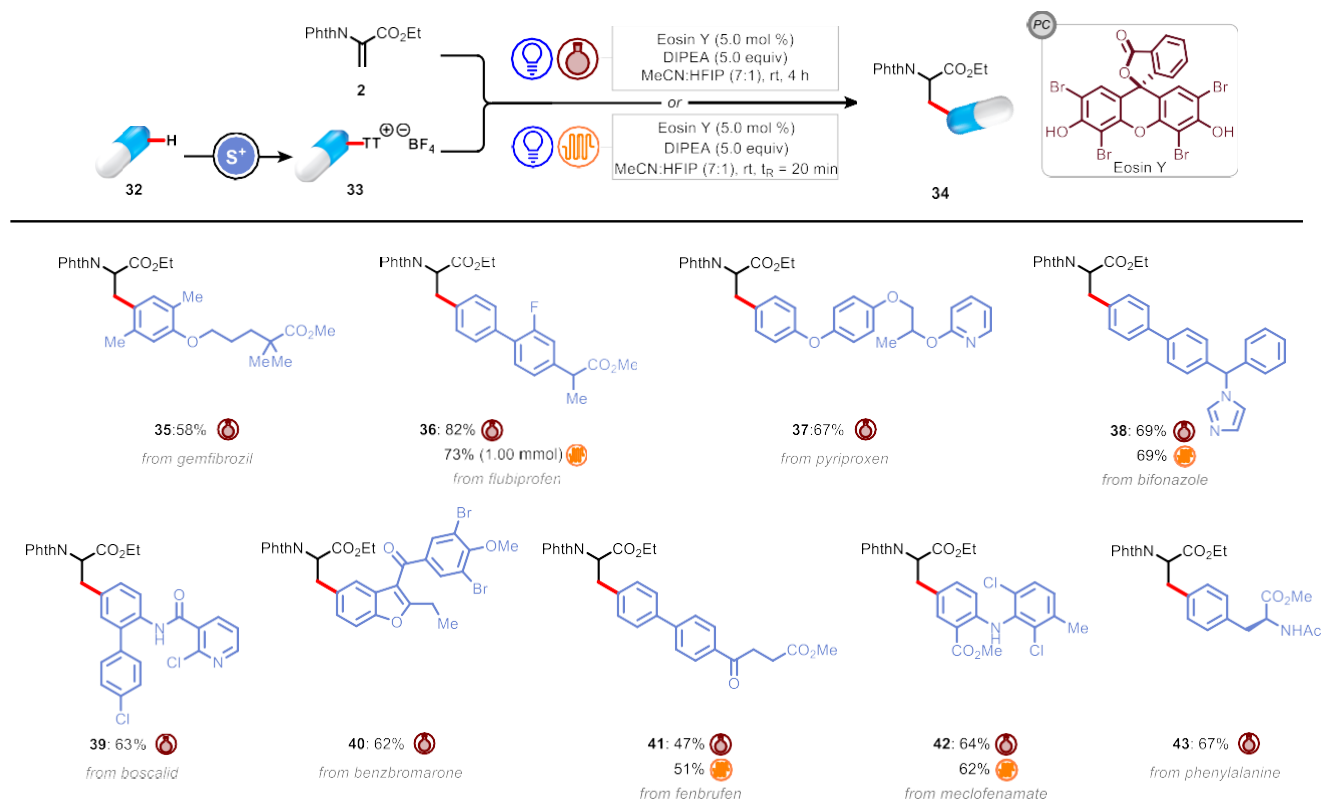
Scheme 2. Synthesis of conjugated and ligated unnatural amino acids via radical addition to Dha derivative 2. For further experimental details see the Supporting Information.

Furthermore, we synthesized a series of conjugates employing continuous-flow conditions, achieving similar success even when scaling up the reactions, which underscores the practicality and scalability of our synthetic approach. We then advanced to the late-stage functionalization of more complex peptide structures 48, applying our photocatalytic conditions detailed in Scheme 3. We were able to precisely and selectively functionalize a variety of di-,tri-, penta- and hexapeptides, decorating them with a multitude of functional groups derived from the aromatic core. Notably, peptides containing residues with sensitive functionalities like thioether, phenol, and indole groups were tolerated without any interference from photocatalytic single electron transfer (SET) processes or hydrogen atom transfer reactions, which typically present significant deleterious side pathways. In addition, our protocol was not hindered by the position of the Dha residue in the peptide, as the functionalization at N-, C-terminus as well as inside the peptide sequence was

96

accomplished. Furthermore, our methodology facilitated the rapid synthesis of a tripeptide 66, which showcased an atypical linkage, demonstrating the applicability of our ligation techniques. This process also proved to be highly capable at integrating drug scaffolds with peptides, further emphasizing the remarkable functional group compatibility of our system, even within the intricate context of peptide conjugation.
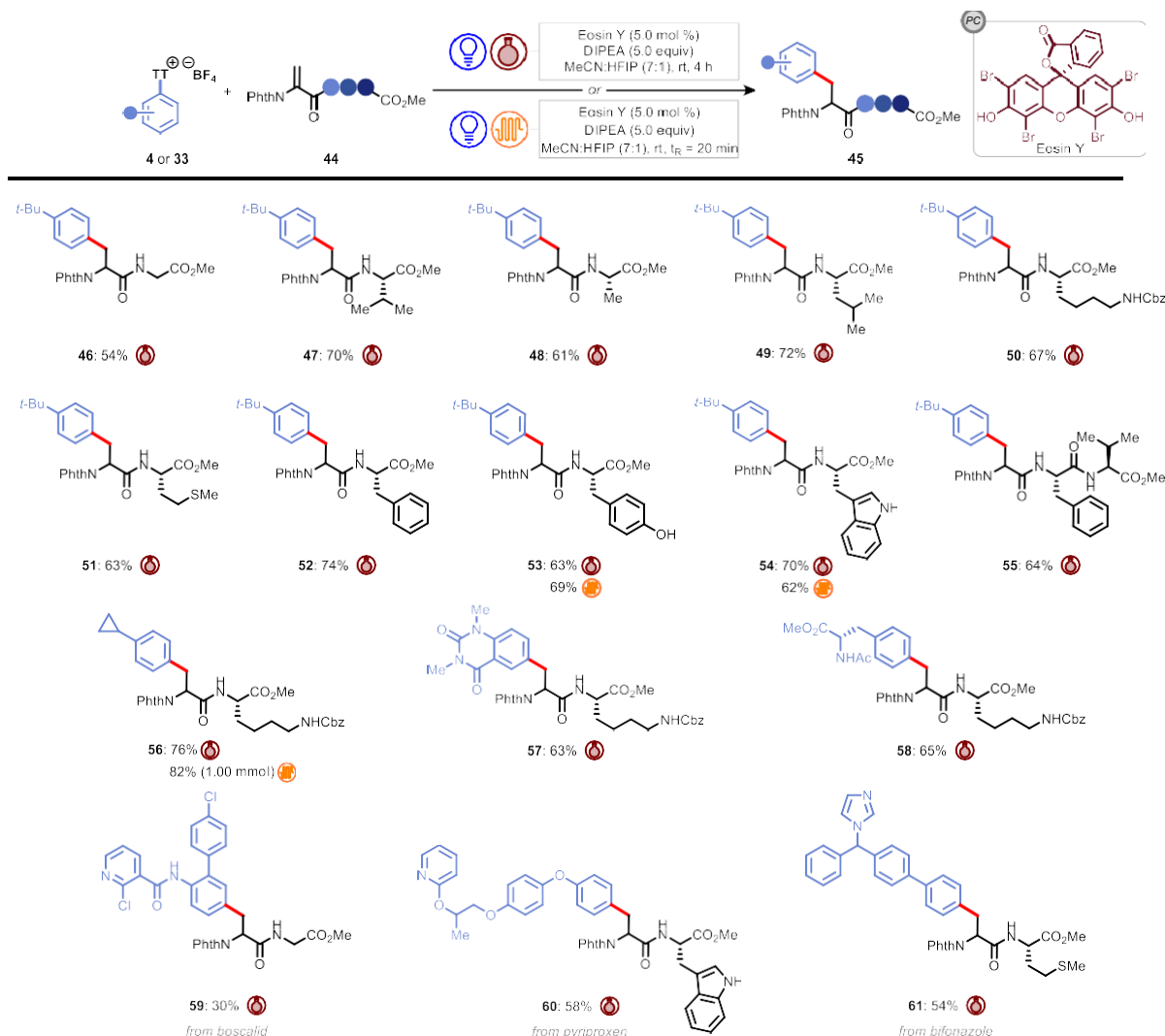
Scheme 3. LSF of Dha-containing peptides 44 leading to conjugation and ligation. For further experimental details see the Supporting Information.

In conclusion, we have successfully developed a photocatalytic hydroarylation protocol that efficiently targets the Dha-backbone utilizing versatile arylthianthrenium salts. This novel strategy has demonstrated its versatility in synthesizing a diverse array of unnatural amino acids, with the potential for straightforward scale-up under a continuous-flow regime. The remarkable functional group tolerance of our methodology enables the preservation of

97

delicate chemical structures during synthesis, broadening the scope of compatible coupling partners. Furthermore, the precise site- and chemoselectivity of this technique showcase its utility in the modification of peptides bearing a variety of sensitive residues. Looking forward, this mild photocatalytic approach is poised to impact the late-stage functionalization of complex peptides and proteins, offering new avenues for biochemical research and therapeutic development.

4.2 Materials and Methods

Reagents and consumables. All reagents and solvents were bought from Sigma Aldrich, TCI, Flurochem, VWR International and Biosolv and used as received. Disposable syringes were purchased from Laboratory Glass Specialist. Syringe pumps were purchased from Chemix Inc. model Fusion 200 Touch. All capillary tubing, microfluidic fittings and Back Pressure Regulator (BPR) were purchased from IDEX Health & Science. Product isolation was performed manually, using silica (P60, SILICYCLE). TLC analysis was performed using Silica on aluminum foils TLC plates (F254, SILICYCLE) with visualization under ultraviolet light (254 nm and 365 nm) or appropriate TLC staining (potassium permanganate or cerium ammonium molybdate). The HPLC pump used was Shimadzu LC-20AD.

Starting materials. Arylthianthrenium salts 4 and 37 were prepared according to literature.[1] Dha derivative 2 and Dha-containing peptides 48 were prepared according to literature.[2] NMR spectroscopy. 1H (400 MHz or 300 MHz), 13C (101 MHz or 75 MHz), 19F (376 MHz or 282) spectra were recorded unless stated otherwise on ambient temperature using a Bruker AV400 or a Bruker AV300. 1H NMR spectra are reported in parts per million (ppm) downfield relative to CDCl3 (7.26 ppm) or DMSO-d6 (2.50 ppm) and all 13C NMR spectra are reported in ppm relative to CDCl3 (77.16 ppm) or DMSO-d6 (39.52 ppm) unless stated otherwise. The multiplicities of signals are designated by the following abbreviations: s (singlet), d (doublet), t (triplet), q (quartet), m (multiplet), dd (doublet of doublets), dt (doublet of triplets), td (triplet of doublets), tt (triplets of triplets), ddd (doublet of doublet of doublets), qd (quartet of doublet). Coupling constants (J) are reported in hertz (Hz). NMR data was processed using the MestReNova 14 software package. Known products were

characterized by comparing to the corresponding 1H NMR, 13C NMR, and 19F NMR with those available in the literature.

Mass spectrometry. High resolution mass spectra (HRMS) were collected on an AccuTOF LC, JMS-T100LP Mass spectrometer (JEOL, Japan) or on an AccuTOF GC v 4g, JMS-T100GCV Mass spectrometer (JEOL, Japan), or on a 7200 GC−qTOF (Agilent Technologies).

4.3 Reactor design

4.3.1 UFO reactor

For all batch experiments a homemade, 3D-printed reactor was adopted. The reactor was designed to fit reaction vials and to be equipped with a Kessil lamp PR160L series (⊚em = 456 nm). The reactor was designed in Adobe Inventor 2021 with 4 different parts. The lid (100 mm × 12 mm) is designed to host up to 8 reactions vials and holds the Kessil lamp in the center (**Figure** S1A); a fan (SUNON DCLüfter 24 V; 50x50x15 Vapo RoHS) is mounted on the bottom of the reactor for cooling. The box is designed with holes to allow the air flow to escape the reactor and keep the temperature stable around 30−33 °C (**Figure** S1B), as measured by an external thermometer. A reflector is situated underneath the lamp and reflects the photons inside the box to have homogeneous light distribution (**Figure** S1C). Finally, the stirring plate adapter (**Figure** S1D) was added to fix the system on a stirring plate and provide homogeneous stirring (**Figure** S1E). It also spaces the reflector from the plate to ensure a continuous air flow from the top to the bottom of the system. All the inside surfaces were covered with reflective tape. An overview of the assembled reactor is shown in **Figure** S2.
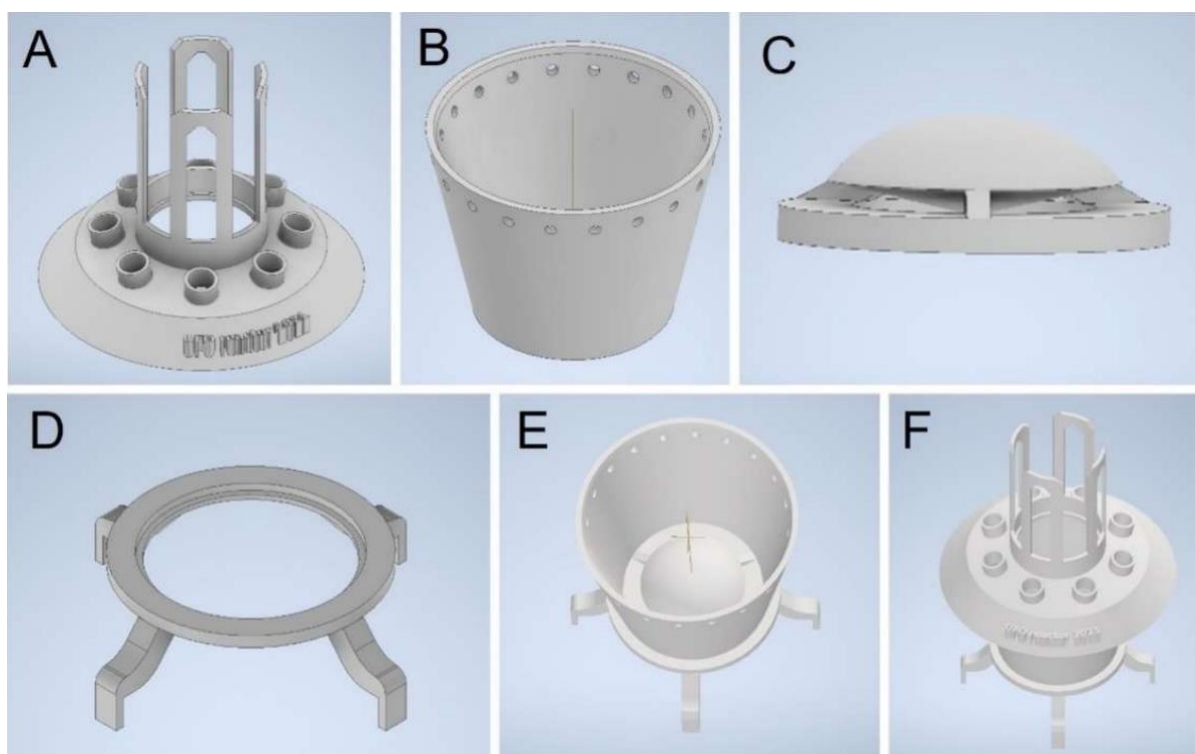
Figure S1. Overview of the 3D-printed reactor: A) lid designed to host up to 8 reactions vials and hold the Kessil lamp in the center; B) body of the reactor; C) light reflector: it is coated with reflective tape; D) adapter for stirring plate; E) inside of the reactor; G) overall reactor.
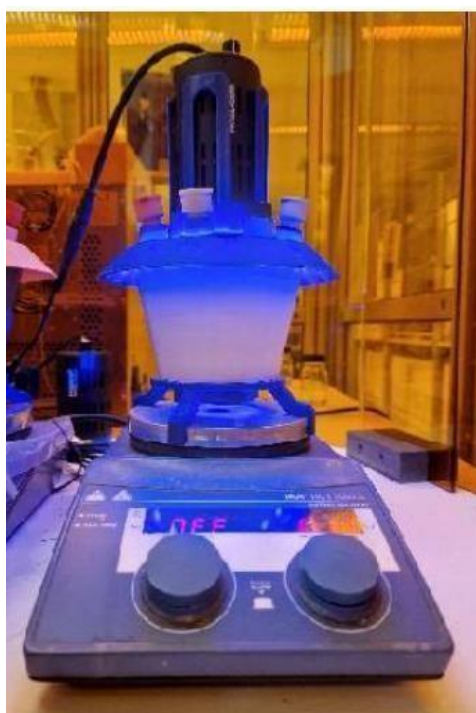
Figure S2. Picture of the assembled reactor equipped with a Kessil lamp (λem = 456 nm).

4.3.2 Flow reactor (UFlow)

For all flow experiments a homemade, 3D-printed reactor was adopted (**Figure** S3, left). The reactor consists of a lid to host the Kessil lamp and a support around which a PFA tubing (0.8 mm inner diameter) is coiled (**Figure** S3, middle); a fan (SUNON DCLüfter 24 V; 50x50x15 Vapo RoHS) is mounted on the bottom of the reactor for cooling. The coil is inserted in a S7 cylindrical plastic body **Figure** S3, right) with holes to allow the air flow to escape the reactor and keep the temperature stable around 30–33 °C. Additional details on the reactor will be published elsewhere.

Figure S3. Overview of the 3D-printed flow reactor: left: overall reactor; middle: inside of the reactor (flow loop) and holder for the Kessil lamp in the center; right: main body, internally coated with reflective tape. A fan is mounted on the bottom to keep the temperature stable around 30–33 °C.

4.4 Optimization Studies

Optimization Studies: Solvent effects [a]
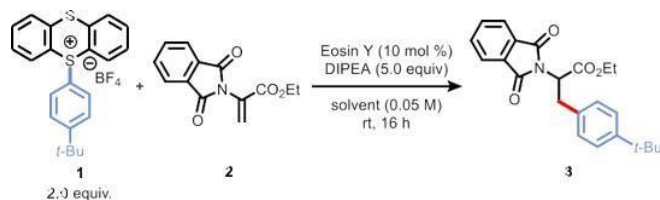
Entry	Solvent	Yield[b]
1	MeOH	47%
2	MeOH (reverse stoichiometry)	51%
3	EtOH	36%
4	i-PrOH	46%
5	t-BuOH	31%
6	HFIP	traces
7	DMF	3%
8	DMA	5%
9	DMSO	16%
10	Et$_2$O	24%
11	1,4-dioxane	13%
12	DCM	15%
13	MeCN	48%
14	MeCN (reverse stoichiometry)	31%
15	MeOH/HFIP (6/4)	29%
16	MeCN/HFIP (6/4)	32%

[a] Reaction conditions: 1 (0.40 mmol), 2 (0.20 mmol), eosin Y (10 mol%), DIPEA (1.0 mmol), solvent (4.0 mL, 0.05 M), at room temperature, 456 nm for 4 h. [b] Yield determined by 1H-NMR spectroscopy using trichloroethylene as external standard.

Optimization Studies: Amount of DIPEA [a]
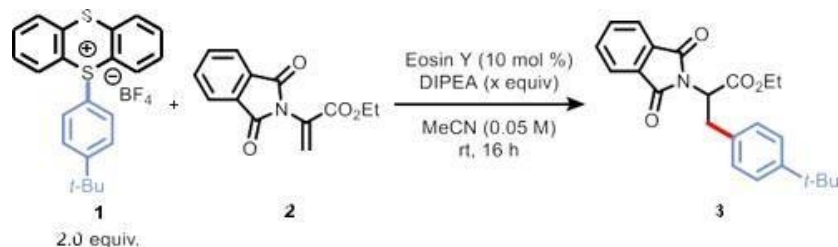
Entry	Equivalents	Yield[b]
1	1.0	21%
2	2.0	35%
3	3.0	39%
4	5.0	48%

[a] Reaction conditions: 1 (0.40 mmol), 2 (0.20 mmol), eosin Y (10 mol%), DIPEA (x equiv.), MeCN (4.0 mL, 0.05 M), at room temperature, 456 nm for 4 h. [b] Yield determined by 1H- NMR spectroscopy using trichloroethylene as external standard.

Optimization Studies: Screening of reductants [a]
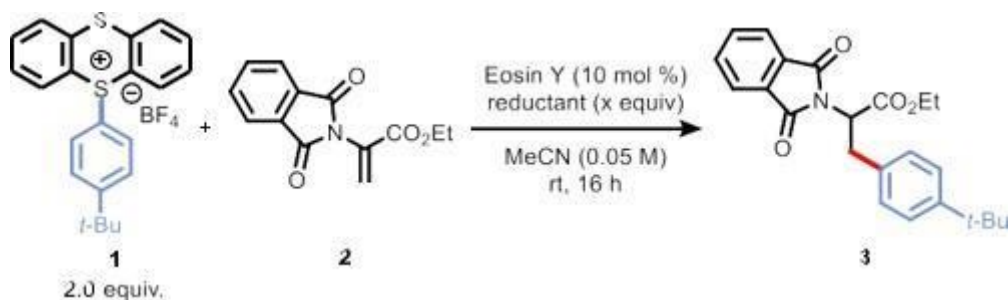
Entry	Amine	Yield
1	DIPEA	48%
2	DIPEA (no photocat.)	4%
3	DIPEA (no photocat. at 390 nm)	24%
4	DIPEA and AcOH (2 eq.)	48%
5	DIPEA and AcOH (2 eq) in MeOH	34%
6	TEA	19%%
7	DABCO	traces
8	DABCO (no photocat.)	traces
9	triethanolamine	30%

[a] Reaction conditions: 1 (0.40 mmol), 2 (0.20 mmol), eosin Y (10 mol%), DIPEA (x equiv.), MeCN (4.0 mL, 0.05 M), at room temperature, 456 nm for 4 h. [b] Yield determined by 1H-NMR spectroscopy using trichloroethylene as external standard.

Optimization Studies: Screening of hantzsch ester (diethyl 1,4-dihydro-2,6-dimethyl-3,5-pyridinedicarboxylate) as reductant [a]
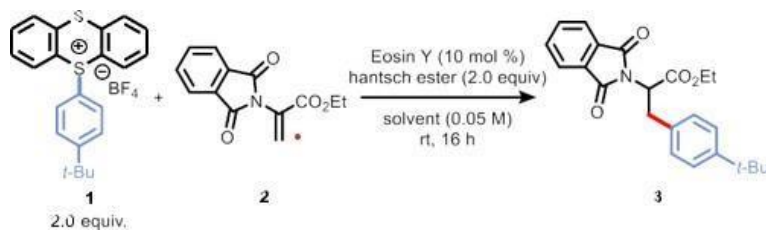
Entry	Solvent	Yield[b]
1	MeCN	16%
2	DCM	21%
3	DMF	traces
4	DMSO	traces
5	HFIP	traces
6	MeOH	traces

[a]   Reaction conditions: 1 (0.40 mmol), 2 (0.20 mmol), eosin Y (10 mol%), hantsch ester (2.0 equiv.), solvent (4.0 mL, 0.05 M), at room temperature, 456 nm for 4 h. [b] Yield determined by 1H-NMR spectroscopy using trichloroethylene as external standard.

Optimization Studies: Arylthianthrenium salt 1 as limiting agent [a]
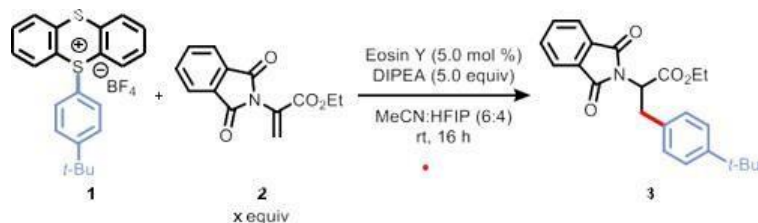
Entry	equivalents	Yield[b]
1	2.0	36%
2	3.0	55%
3	10	75%[c]

[a] Reaction conditions: 1 (0.20 mmol), 2 (x equiv.), eosin Y (5.0 mol%), DIPEA (5.0 equiv.), solvent (4.0 mL, 0.05 M), at room temperature, 456 nm for 4 h. [b] Yield determined by 1H-NMR spectroscopy using trichloroethylene as external standard. [c] Yield of isolated product.

Optimization Studies: Solvent screening with arylthianthrenium salt 1 as limiting agent [a]
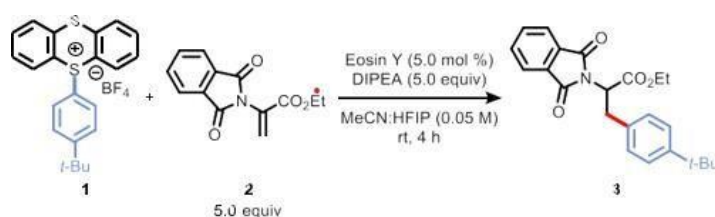
Entry	Solvent ratio	Yield[b]
1	1.5/2.5	27%
2	2.0/2.0	36%

3	2.5/1.5	64%
4	3.0/1.0	63%
5	3.5/0.5	72%
6	3.6/0.4	61%
7	3.7/0.3	63%
8	3.8/0.2	62%
9	3.9/0.1	49%

[a]   Reaction conditions: 1 (0.20 mmol), 2 (5.0 equiv.), eosin Y (5.0 mol%), DIPEA (5.0 equiv.), solvent (4.0 mL, 0.05 M), at room temperature, 456 nm for 4 h. [b] Yield of isolated product.

4.5 General procedures

General procedure 1 (GP1) for the photocatalytic radical addition of arylthianthrenium salts to Dha in batch

In a typical experiment, to an oven-dried 7 mL vial equipped with a stirring bar were added arylthianthrenium salt 4 or 37 (0.2 mmol, 1.0 equiv.), Eosin Y (6.5 mg, 5.0 mol%) and Dha derivative 5 or Dha-containing peptide 48 (1.0 mmol, 5.0 equiv). The vial was sealed with a rubber septum and the solids were dissolved in MeCN:HFIP (7:1, 4.0 mL, 0.05 M). Then, DIPEA was added (173 µL, 5.0 equiv.). The vial was then stirred and irradiated in the UFO photochemical reactor for 4 h, while the temperature was maintained at 30 °C. The solvent was evaporated under reduced pressure and the crude reaction mixture was purified by flash column chromatography on silica gel.

General procedure 1 (GP2) for the photocatalytic radical addition of arylthianthrenium salts to Dha in flow

In a typical experiment, to an oven-dried 7 mL vial equipped with a stirring bar were added arylthianthrenium salt 4 or 37 (0.2 mmol, 1.0 equiv.), eosin Y (6.5 mg, 5.0 mol%) and Dha derivative 5 or Dha-containing peptide 48 (1.0 mmol, 5.0 equiv). The vial was sealed with a rubber septum and the solids were dissolved in MeCN:HFIP (7:1, 4.0 mL, 0.05 M). Then, DIPEA was added (173 μL, 5.0 equiv.). The solution was loaded to a filling loop (FEP capillary tubing: 1.6 mm OD, 0.8 mm ID, 5 mL volume), that had been sparged with N2. By using an HPLC pump the solution was delivered to the flow reactor (UFlow) with a PFA coil (FEP capillary tubing: 1.6 mm OD, 0.8 mm ID, 4.0 mL volume) prefilled with CH3CN. The solution was pumped with a total flow rate of 0.20 mL/min flow rate (20 minutes of residence time) and after 60 min the collected solution was evaporated under reduced pressure and the crude reaction mixture was purified by flash column chromatography on silica gel.

General procedure 3 (GP3) for the arylthianthrenium salts 4 and 37

Following a modified literature procedure,[3] under an ambient atmosphere, a round-bottom flask was charged sequentially with the arene (1.1 equiv.), thianthrene 5-oxide (1.0 equiv.), and anhydrous MeCN (0.10 - 0.25 M). The solution was cooled to 0 °C, followed by the addition of HBF4·Et2O (1.5 equiv.) and trifluoroacetic anhydride (3.0 equiv.). The mixture was stirred at 0 °C for 1 h and subsequently at 25 °C for 16 h. At this point, the reaction mixture was concentrated under reduced pressure and diluted with dichloromethane (0.05 M). The CH2Cl2 phase was poured onto a saturated aqueous NaHCO3 solution. The mixture was poured into a separatory funnel, and the layers were separated. The CH2Cl2 layer was washed with aqueous NaBF4 solution (2 X, 5 % w/w), and with water (2 X). The CH2Cl2 layer was dried over Na2SO4, filtered, and the solvent was

removed under reduced pressure. The solvent was evaporated under reduced pressure and the crude reaction mixture was purified by flash column chromatography on silica gel.

General procedure 4 (GP4) for the preparation of Dha-containing peptides 48

Following a modified literature procedure,[2a] Phth-Ser-OH (1.5 equiv.) was dissolved in dry CH2Cl2 (0.2 M) and the solution cooled to 0 °C. The amino acid methyl ester hydrochloride (1.0 equiv) was then added followed by DIPEA (adjusted pH > 8), EDCI.HCl (1.1 eq.) HOBt (1.1 equiv.). The reaction mixture was slowly warmed to room temperature and stirred overnight. The reaction mixture was then washed with brine, HCl 1M (2 X), brine, sat NaHCO3 (2 X), brine, and dried over MgSO4 and evaporated under reduced pressure. The crude product was then used in the next reaction forward without further purification. The crude residue was re-dissolved in CH2Cl2 (0.2 M) and placed under an atmosphere of nitrogen. Then, EDCI.HCl (1.1 eq.) and CuCl (0.33 eq.) were added, and the reaction stirred at room temperature for 18 hours. The solution was then washed with two portions of water (2 × 10 mL), dried over MgSO4 and evaporated under reduced pressure. The crude product was purified flash column chromatography on silica gel.

4.6 Characterization data for the synthesized compounds

Characterization data for the unnatural amino acids 6
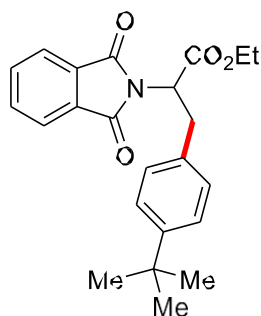
Ethyl 3-(4-(tert-butyl)phenyl)-2-(1,3-dioxoisoindolin-2-yl)propanoate (3)

Prepared according to the GP1, using 5-(4-(tert-butyl)phenyl)-5H-thianthren-5-ium tetrafluoroborate (87.3 mg, 0.20 mmol, 1.0 equiv.) and ethyl 2-(1,3-dioxoisoindolin-2-yl)acrylate (245.2 mg, 1.0 mmol, 5.0 equiv.). The crude mixture was purified by flash column chromatography (n-pentane/EtOAc: 19/1 → 5/1) to afford product 3 (54.5 mg, 72% yield) as white solid. Following the GP2 on 1.00 mmol scale the product 3 was isolated in 71% yield. Spectroscopic data are in accordance with the literature.[4]

1H-NMR (400 MHz, CDCl3) δ 7.71 (dd, J = 5.5, 3.1 Hz, 1H), 7.61 (dd, J = 5.5, 3.1 Hz, 1H), 7.12 (d, J = 8.3 Hz, 1H), 7.02 (d, J = 8.3 Hz, 1H), 5.07 (dd, J = 10.8, 5.6 Hz, 1H), 4.22 – 4.11 (m, 2H), 3.50 (dd, J = 14.6, 5.6 Hz, 1H), 3.44 (dd, J = 14.6, 10.8 Hz, 1H), 1.17 (t, J = 7.1 Hz, 3H), 1.14 (s, 9H).

13C-NMR (101 MHz, CDCl3) δ 169.0, 167.6, 149.6, 134.0, 133.7, 131.7, 128.5, 125.4, 123.4, 62.0, 53.4, 34.3, 34.1, 31.3, 14.1.

HRMS (ESI) m/z calcd for C23H26NO4+: 380.1856; found: 380.1870.
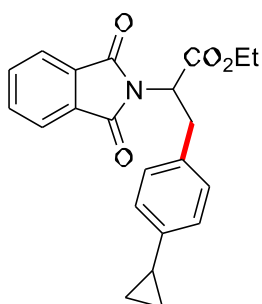
Ethyl -3-(4-cyclopropylphenyl)-2-(1,3-dioxoisoindolin-2-yl)propanoate (7)

Prepared according to the GP1, using 5-(4-cyclopropylphenyl)-5H-thianthren-5-ium tetrafluoroborate (84.1 mg, 0.20 mmol, 1.0 equiv.) and ethyl 2-(1,3-dioxoisoindolin-2-yl)acrylate (245.2 mg, 1.0 mmol, 5.0 equiv.). The crude mixture was purified by flash column chromatography (n-pentane/EtOAc: 19/1 → 5/1) to afford product 7 (61.7 mg, 85% yield) as white solid.

1H-NMR (400 MHz, CDCl3) δ 7.79 (dd, J = 5.5, 3.1 Hz, 2H), 7.69 (dd, J = 5.6, 3.1 Hz, 2H), 7.07 (d, J = 7.9 Hz, 2H), 6.90 (d, J = 7.9 Hz, 2H), 5.14 (dd, J = 10.8, 5.7 Hz, 1H), 4.36 – 4.14 (m, 2H), 3.68 – 3.42 (m, 2H), 1.90 – 1.65 (m, 1H), 1.27 (t, J = 7.1 Hz, 2H), 0.98 – 0.79 (m, 2H), 0.69 – 0.47 (m, 2H).

13C-NMR (101 MHz, CDCl3) δ 168.9, 167.6, 142.4, 134.1, 133.7, 131.7, 128.7, 125.8, 123.4, 62.0, 53.5, 34.2, 15.0, 14.1, 9.1, 9.1.

HRMS (ESI) m/z calcd for $C_{22}H_{22}NO_4^+$: 364.1543; found: 364.1557.
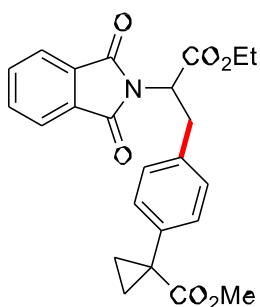
Methyl -1-(4-(2-(1,3-dioxoisoindolin-2-yl)-3-ethoxy-3-oxopropyl)phenyl)cyclopropane-1-carboxylate (8)

Prepared according to the GP1, using 5-(4-(1-(methoxycarbonyl)cyclopropyl)phenyl)-5H-thianthren-5-ium tetrafluoroborate (95.6 mg, 0.20 mmol, 1.0 equiv.) and ethyl 2-(1,3-dioxoisoindolin-2-yl)acrylate (245.2 mg, 1.0 mmol, 5.0 equiv.). The crude mixture was purified by flash column chromatography (toluene/EtOAc: 100/0 → 97/3) to afford product 8 (62.3 mg, 74% yield) as white solid.

1H-NMR (400 MHz, CDCl3) δ 7.79 (dd, J = 5.4, 3.1 Hz, 2H), 7.70 (dd, J = 5.4, 3.1 Hz, 2H), 7.16 (d, J = 8.2 Hz, 2H), 7.11 (d, J = 8.2 Hz, 2H), 5.14 (dd, J = 10.8, 5.5 Hz, 1H), 4.42 – 4.11 (m, 2H), 3.68 – 3.42 (m, 5H), 1.56 – 1.42 (m, 2H), 1.25 (t, J = 7.1 Hz, 3H), 1.16 – 1.00 (m, 2H).

13C-NMR (101 MHz, CDCl3) δ 175.1, 168.9, 167.5, 138.0, 135.8, 134.1, 131.7, 130.6, 128.6, 123.4, 62.1, 53.3, 52.3, 34.3, 28.6, 16.6, 16.6, 14.1.

HRMS (ESI) m/z calcd for C24H24NO6+: 422.1598; found: 422.1610.
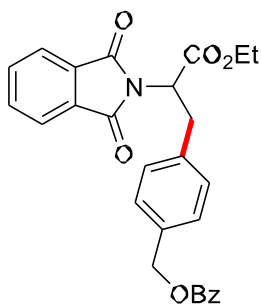
4-(2-(1,3-Dioxoisoindolin-2-yl)-3-ethoxy-3-oxopropyl)benzyl benzoate (9)

Prepared according to the GP1, using 5-(4-((benzoyloxy)methyl)phenyl)-5H-thianthren-5-ium tetrafluoroborate (102.8 mg, 0.20 mmol, 1.0 equiv.) and ethyl 2-(1,3-dioxoisoindolin-2-yl)acrylate (245.2 mg, 1.0 mmol, 5.0 equiv.). The crude mixture was purified by flash column chromatography (n-pentane/EtOAc: 19/1 → 5/1) to afford product 9 (49.3 mg, 54% yield) as white solid.

1H-NMR (400 MHz, CDCl3) δ 7.93 (d, J = 8.0 Hz, 2H), 7.70 (dd, J = 5.5, 3.1 Hz, 2H), 7.59 (dd, J = 5.5, 3.1 Hz, 2H), 7.46 (t, J = 7.4 Hz, 1H), 7.33 (dd, J = 8.0, 7.4 Hz, 2H), 7.20 (d, J = 8.0 Hz, 2H), 7.12 (d, J = 8.0 Hz, 2H), 5.17 (s, 2H), 5.08 (dd, J = 10.9, 5.6 Hz, 1H), 4.28 – 4.08 (m, 2H), 3.60 – 3.42 (m, 2H), 1.18 (t, J = 7.1 Hz, 3H).

13C-NMR (101 MHz, CDCl3) δ 168.8, 167.5, 166.4, 137.0, 134.6, 134.1, 133.0, 131.6, 130.1, 129.7, 129.1, 128.4, 128.4, 123.5, 66.3, 62.1, 53.3, 34.4, 14.1.

HRMS (ESI) m/z calcd for C27H24NO6+: 458.1598; found: 458.1597.
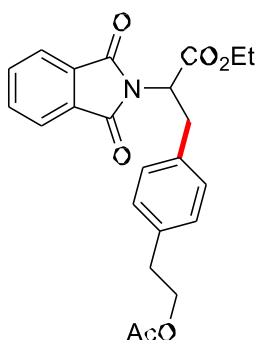
Ethyl -3-(4-(2-acetoxyethyl)phenyl)-2-(1,3-dioxoisoindolin-2-yl)propanoate (10)

Prepared according to the GP1, using 5-(4-(2-acetoxyethyl)phenyl)-5H-thianthren-5-ium tetrafluoroborate (93.2 mg, 0.20 mmol, 1.0 equiv.) and ethyl 2-(1,3-dioxoisoindolin-2-yl)acrylate (245.2 mg, 1.0 mmol, 5.0 equiv.). The crude mixture was purified by flash column chromatography (n-pentane/EtOAc: 19/1 → 5/1) to afford product 10 (76.3 mg, 82% yield) as white solid.

1H-NMR (400 MHz, CDCl3) δ 7.78 (dd, J = 5.5, 3.1 Hz, 2H), 7.68 (dd, J = 5.5, 3.1 Hz, 2H), 7.10 (d, J = 8.1 Hz, 2H), 7.02 (d, J = 8.1 Hz, 2H), 5.12 (dd, J = 11.0, 5.4 Hz, 1H), 4.30 – 4.20 (m, 2H), 4.16 (t, J = 7.1 Hz, 2H), 3.57 (dd, J = 14.4, 5.4 Hz, 1H), 3.50 (dd, J = 14.4, 11.0 Hz, 1H), 2.81 (t, J = 7.1 Hz, 2H), 1.97 (s, 3H), 1.25 (t, J = 7.1 Hz, 3H).

13C-NMR (101 MHz, CDCl3) δ 171.0, 168.8, 167.5, 136.2, 135.1, 134.1, 131.6, 129.1, 129.0, 123.5, 64.8, 62.0, 53.4, 34.6, 34.3, 20.9, 14.1.

HRMS (ESI) m/z calcd for $C_{23}H_{24}NO_6^+$: 410.1598; found: 410.1596.
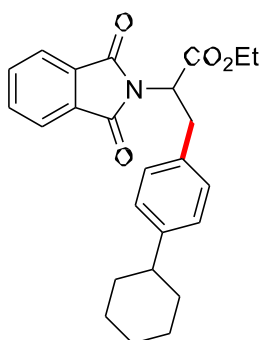
Ethyl -3-(4-cyclohexylphenyl)-2-(1,3-dioxoisoindolin-2-yl)propanoate (11)

Prepared according to the GP1, using 5-(4-cyclohexylphenyl)-5H-thianthren-5-ium tetrafluoroborate (92.4 mg, 0.20 mmol, 1.0 equiv.) and ethyl 2-(1,3-dioxoisoindolin-2-yl)acrylate (245.2 mg, 1.0 mmol, 5.0 equiv.). The crude mixture was purified by flash column chromatography (n-pentane/EtOAc: 19/1 → 9/1) to afford product 11 (48.3 mg, 60% yield) as white solid.

1H-NMR (400 MHz, CDCl3) δ 7.70 (dd, J = 5.5, 3.1 Hz, 2H), 7.60 (dd, J = 5.5, 3.1 Hz, 2H), 7.00 (d, J = 8.0 Hz, 2H), 6.94 (d, J = 8.0 Hz, 2H), 5.05 (dd, J = 10.9, 5.5 Hz, 1H), 4.30 – 3.98 (m, 2H), 3.49 (dd, J = 14.4, 5.5 Hz, 1H), 3.42 (dd, J = 14.4, 10.9 Hz, 1H), 2.30 (ddd, J = 11.7, 8.5, 3.2 Hz, 1H), 1.77 – 1.54 (m, 5H), 1.37 – 1.02 (m, 8H).

13C-NMR (101 MHz, CDCl3) δ 169.0, 167.6, 146.5, 134.1, 134.0, 131.7, 128.7, 126.9, 123.4, 62.0, 53.5, 44.1, 34.4, 34.3, 34.2, 26.9, 26.1, 14.1.

HRMS (ESI) m/z calcd for C25H28NO4+: 406.2013; found: 406.2029.
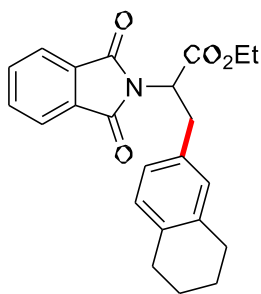
Ethyl 2-(1,3-dioxoisoindolin-2-yl)-3-(5,6,7,8-tetrahydronaphthalen-2-yl)propanoate (12)

Prepared according to the GP1, using 5-(5,6,7,8-tetrahydronaphthalen-2-yl)-5H-thianthren-5- ium tetrafluoroborate (92.4 mg, 0.20 mmol, 1.0 equiv.) and ethyl 2-(1,3-dioxoisoindolin-2-yl)acrylate (245.2 mg, 1.0 mmol, 5.0 equiv.). The crude mixture was purified by flash column chromatography (n-pentane/EtOAc: 19/1 → 5/1) to afford product 12 (40.7 mg, 54% yield) as white solid.

1H-NMR (400 MHz, CDCl3) δ 7.80 (dd, J = 5.4, 3.1 Hz, 2H), 7.70 (dd, J = 5.4, 3.1 Hz, 2H), 6.92 – 6.82 (m, 3H), 5.12 (dd, J = 10.9, 5.5 Hz, 1H), 4.33 – 4.18 (m, 2H), 3.53 (dd, J = 14.4, 5.5 Hz, 1H), 3.46 (dd, J = 14.4, 10.9 Hz, 1H), 2.74 – 2.59 (m, 3H), 2.58 – 2.46 (m, 1H), 1.77 – 1.63 (m, 4H), 1.26 (t, J = 7.2 Hz, 3H).

13C-NMR (101 MHz, CDCl3) δ 169.0, 167.6, 137.2, 135.5, 134.0, 133.7, 131.8, 129.5, 129.2, 125.8, 123.4, 62.0, 53.6, 34.2, 29.2, 28.9, 23.1, 23.1, 14.1.

HRMS (ESI) m/z calcd for C23H24NO4+: 378.1700; found: 378.1704.
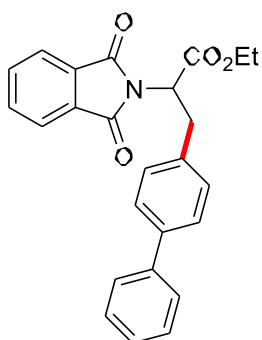
Ethyl 3-([1,1'-biphenyl]-4-yl)-2-(1,3-dioxoisoindolin-2-yl)propanoate (13)

Prepared according to the GP1, using 5-([1,1'-biphenyl]-4-yl)-5H-thianthren-5-ium tetrafluoroborate (91.3 mg, 0.20 mmol, 1.0 equiv.) and ethyl 2-(1,3-dioxoisoindolin-2-yl)acrylate (245.2 mg, 1.0 mmol, 5.0 equiv.). The crude mixture was purified by flash column chromatography (n-pentane/EtOAc: 19/1 → 5/1) to afford product 13 (59.8 mg, 75% yield) as white solid. Following the GP2 on 0.20 mmol scale the product 13 was isolated in 72% yield. Spectroscopic data are in accordance with the literature.[4]

1H-NMR (400 MHz, CDCl3) δ 7.71 (dd, J = 5.5, 3.1 Hz, 2H), 7.61 (dd, J = 5.5, 3.1 Hz, 2H), 7.46 – 7.39 (m, 2H), 7.35 (d, J = 8.1 Hz, 2H), 7.30 (t, J = 7.6 Hz, 2H), 7.22 – 7.14 (m, 3H), 5.12 (dd, J = 10.8, 5.8 Hz, 1H), 4.31 – 4.08 (m, 2H), 3.56 (dd, J = 14.7, 5.8 Hz, 1H), 3.51 (dd, J = 14.7, 10.9 Hz, 1H), 1.19 (t, J = 7.1 Hz, 3H).

13C-NMR (101 MHz, CDCl3) δ 168.9, 167.6, 140.6, 139.6, 135.9, 134.1, 131.6, 129.3, 128.7, 127.2, 127.2, 126.9, 123.5, 62.1, 53.4, 34.3, 14.1.

HRMS (ESI) m/z calcd for C25H22NO4+: 400.1543; found: 400.1547.
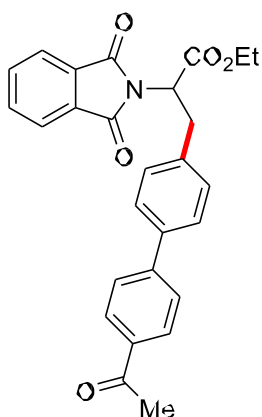
Ethyl -3-(4'-acetyl-[1,1'-biphenyl]-4-yl)-2-(1,3-dioxoisoindolin-2-yl)propanoate (14)

Prepared according to the GP1, using 5-(4'-acetyl-[1,1'-biphenyl]-4-yl)-5H-thianthren-5-ium tetrafluoroborate (99.6 mg, 0.20 mmol, 1.0 equiv.) and ethyl 2-(1,3-dioxoisoindolin-2-yl)acrylate (245.2 mg, 1.0 mmol, 5.0 equiv.). The crude mixture was purified by flash column chromatography (n-pentane/EtOAc: 9/1 → 3/1) to afford product 14 (65.3 mg, 74% yield) as white solid. .Following the GP2 on 0.20 mmol scale the product 14 was isolated in 76% yield.

1H-NMR (400 MHz, CDCl3) δ 7.99 (d, J = 8.1 Hz, 2H), 7.82 (dd, J = 5.5, 3.1 Hz, 2H), 7.72 (dd, J = 5.5, 3.1 Hz, 2H), 7.62 (d, J = 8.1 Hz, 2H), 7.49 (d, J = 7.8 Hz, 2H), 7.30 (d, J = 7.8 Hz, 2H), 5.22 (dd, J = 10.8, 5.7 Hz, 1H), 4.41 – 4.15 (m, 2H), 3.75 – 3.53 (m, 2H), 2.63 (s, 3H), 1.29 (t, J = 7.0 Hz, 3H).

13C-NMR (101 MHz, CDCl3) δ 197.8, 168.7, 167.6, 145.2, 138.2, 137.1, 135.8, 134.2, 131.6, 129.5, 128.9, 127.4, 127.0, 123.5, 62.2, 53.3, 34.4, 26.6, 14.1.

HRMS (ESI) m/z calcd for C27H24NO5+: 442.1649; found: 442.1662.
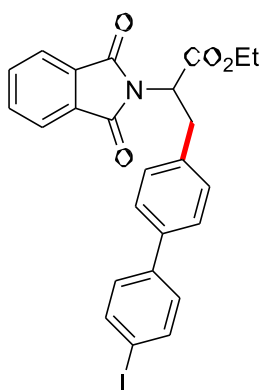
Ethyl   -2-(1,3-dioxoisoindolin-2-yl)-3-(4'-iodo-[1,1'-biphenyl]-4-yl)propanoate   (15)

Prepared according to the GP1, using 5-(4'-iodo-[1,1'-biphenyl]-4-yl)-5H-thianthren-5-ium tetrafluoroborate (116.4 mg, 0.20 mmol, 1.0 equiv.) and ethyl 2-(1,3-dioxoisoindolin-2-yl)acrylate (245.2 mg, 1.0 mmol, 5.0 equiv.). The reaction was run for 20 min. The crude mixture was purified by flash column chromatography (n-pentane/EtOAc: 19/1 → 5/1) to afford product 15 (64.0 mg, 61% yield) as white solid.

1H-NMR (400 MHz, CDCl3) δ 7.80 (dd, J = 5.5, 3.1 Hz, 2H), 7.73 – 7.67 (m, 4H), 7.39 (d, J = 8.2 Hz, 2H), 7.25 – 7.23 (m, 4H), 5.19 (dd, J = 10.7, 5.7 Hz, 1H), 4.39 – 4.18 (m, 2H), 3.73 – 3.50 (m, 2H), 1.27 (t, J = 7.1 Hz, 3H).

13C-NMR (101 MHz, CDCl3) δ 168.8, 167.6, 140.2, 138.4, 137.8, 136.5, 134.1, 131.6, 129.4, 128.8, 127.0, 123.5, 92.9, 62.1, 53.3, 34.3, 14.1.

HRMS (ESI) m/z calcd for C25H21INO +: 526.0510; found: 526.0528.
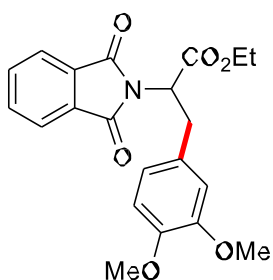
Ethyl -3-(3,4-dimethoxyphenyl)-2-(1,3-dioxoisoindolin-2-yl)propanoate (16)

Prepared according to the GP1, using 5-(3,4-dimethoxyphenyl)-5H-thianthren-5-ium tetrafluoroborate (88.1 mg, 0.20 mmol, 1.0 equiv.) and ethyl 2-(1,3-dioxoisoindolin-2-yl)acrylate (245.2 mg, 1.0 mmol, 5.0 equiv.). The crude mixture was purified by flash column chromatography (n-pentane/EtOAc: 8/2 → 7/3) to afford product 16 (48.2 mg, 63% yield) as white solid. Spectroscopic data are in accordance with the literature.[5]

1H-NMR (400 MHz, CDCl3) δ 7.77 (dd, J = 5.5, 3.1 Hz, 2H), 7.68 (dd, J = 5.5, 3.1 Hz, 2H), 6.76 – 6.58 (m, 3H), 5.13 (dd, J = 11.1, 5.7 Hz, 1H), 4.38 – 4.14 (m, 2H), 3.77 (s, 3H), 3.69 (s, 3H), 3.60 – 3.39 (m, 2H), 1.26 (t, J = 7.1 Hz, 3H).

13C-NMR (101 MHz, CDCl3) δ 168.8, 167.5, 148.7, 147.7, 134.1, 131.6, 129.2, 123.4, 121.0, 111.8, 111.2, 62.0, 55.7, 55.7, 53.4, 34.1, 14.1.

HRMS (ESI) m/z calcd for C21H22NO6+: 384.1442; found: 384.1446.
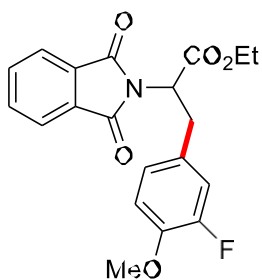
Ethyl -2-(1,3-dioxoisoindolin-2-yl)-3-(3-fluoro-4-methoxyphenyl)propanoate (17)

Prepared according to the GP1, using 5-(3-fluoro-4-methoxyphenyl)-5H-thianthren-5-ium tetrafluoroborate (85.6 mg, 0.20 mmol, 1.0 equiv.) and ethyl 2-(1,3-dioxoisoindolin-2-yl)acrylate (245.2 mg, 1.0 mmol, 5.0 equiv.). The crude mixture was purified by flash column chromatography (n-pentane/EtOAc: 10/1 → 5/1) to afford product 17 (52.7 mg, 71% yield) as white solid.

1H-NMR (400 MHz, CDCl3) δ 7.79 (dd, J = 5.5, 3.1 Hz, 2H), 7.69 (dd, J = 5.5, 3.1 Hz, 2H), 6.93 – 6.83 (m, 2H), 6.77 (t, J = 8.6 Hz, 1H), 5.07 (dd, J = 11.1, 5.5 Hz, 1H), 4.31 – 4.18 (m, 2H), 3.78 (s, 3H), 3.53 (dd, J = 14.5, 5.5 Hz, 1H), 3.46 (dd, J = 14.5, 11.1 Hz, 1H), 1.25 (t, J = 7.1 Hz, 3H).

13C NMR (101 MHz, CDCl3) δ 168.6, 167.5, 152.1 (d, $^1J_{C-F}$ = 246.0 Hz), 146.4 (d, $^2J_{C-F}$ = 10.5 Hz), 134.2, 131.6, 129.7 (d, $^3J_{C-F}$ = 6.2 Hz), 124.5 (d, $^3J_{C-F}$ = 3.6 Hz), 123.5, 116.6 (d, $^2J_{C-F}$ = 18.3 Hz), 113.4 (d, $^4J_{C-F}$ = 2.2 Hz), 62.1, 56.1, 53.3, 33.8, 14.1.

19F NMR (376 MHz, CDCl3) δ -135.06 (dd, J = 12.1, 8.7 Hz).

HRMS (ESI) m/z calcd for C20H19FNO5+: 372.1242; found: 372.1253.

Ethyl -2-(1,3-dioxoisoindolin-2-yl)-3-(3-chloro-4-methoxyphenyl)propanoate (18)

Prepared according to the GP1, using 5-(3-chloro-4-methoxyphenyl)-5H-thianthren-5-ium tetrafluoroborate (88.9 mg, 0.20 mmol, 1.0 equiv.) and ethyl 2-(1,3-dioxoisoindolin-2-yl)acrylate (245.2 mg, 1.0 mmol, 5.0 equiv.). The crude mixture was purified by flash column chromatography (n-pentane/EtOAc: 10/1 → 5/1) to afford product 18 (68.1 mg, 88% yield) as white solid.

1H-NMR (400 MHz, CDCl3) δ 7.79 (dd, J = 5.5, 3.1 Hz, 1H), 7.69 (dd, J = 5.5, 3.1 Hz, 1H), 7.17 (d, J = 2.2 Hz, 1H), 7.03 (dd, J = 8.4, 2.2 Hz, 1H), 6.75 (d, J = 8.4 Hz, 1H), 5.07 (dd, J = 11.1, 5.4 Hz, 1H), 4.33 – 4.17 (m, 2H), 3.79 (s, 3H), 3.52 (dd, J = 14.5, 5.4 Hz, 1H), 3.44 (dd, J = 14.5, 11.1 Hz, 1H), 1.25 (t, J = 7.1 Hz, 3H).

13C NMR (101 MHz, CDCl3) δ 168.6, 167.5, 153.8, 134.2, 131.6, 130.7, 129.9, 128.0, 123.5, 122.3, 112.1, 62.1, 56.0, 53.3, 33.6, 14.1.

HRMS (ESI) m/z calcd for C20H19ClNO +: 388.0946; found: 388.0956.

Methyl 5-(2-(1,3-dioxoisoindolin-2-yl)-3-ethoxy-3-oxopropyl)-2-methoxybenzoate (19)

Prepared according to the GP1, using 5-(4-methoxy-3-(methoxycarbonyl)phenyl)-5H-thianthren-5-ium tetrafluoroborate (93.6 mg, 0.20 mmol, 1.0 equiv.) and ethyl 2-(1,3-dioxoisoindolin-2-yl)acrylate (245.2 mg, 1.0 mmol, 5.0 equiv.). The crude mixture was purified by flash column chromatography (n-pentane/EtOAc: 10/1 → 2/1) to afford product 19 (56.4 mg, 69% yield) as white solid.

1H-NMR (400 MHz, CDCl3) δ 7.80 (dd, J = 5.5, 3.1 Hz, 2H), 7.70 (dd, J = 5.5, 3.1 Hz, 2H), 7.58 (d, J = 2.4 Hz, 1H), 7.30 (dd, J = 8.5, 2.4 Hz, 1H), 6.82 (d, J = 8.5 Hz, 1H), 5.09 (dd, J = 11.0, 5.5 Hz, 1H), 4.30 – 4.21 (m, 2H), 3.82 (s, 3H), 3.77 (s, 3H), 3.56 (dd, J = 14.5, 5.5 Hz, 1H), 3.49 (dd, J = 14.5, 11.0 Hz, 1H), 1.26 (t, J = 7.1 Hz, 3H).

13C-NMR (101 MHz, CDCl3) δ 168.6, 167.5, 166.2, 158.1, 134.1, 133.8, 132.1, 131.6, 128.4, 123.5, 119.8, 112.2, 62.1, 55.9, 53.3, 51.9, 33.6, 14.1.

HRMS (ESI) m/z calcd for $C_{22}H_{22}NO_7^+$: 412.1391; found: 412.1403.
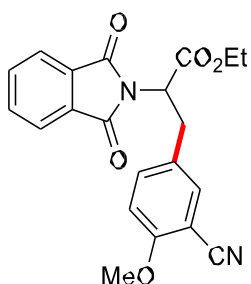
Ethyl 3-(3-cyano-4-methoxyphenyl)-2-(1,3-dioxoisoindolin-2-yl)propanoate (20)

Prepared according to the GP1, using 5-(3-cyano-4-methoxyphenyl)-5H-thianthren-5-ium tetrafluoroborate (87.0 mg, 0.20 mmol, 1.0 equiv.) and ethyl 2-(1,3-dioxoisoindolin-2-yl)acrylate (245.2 mg, 1.0 mmol, 5.0 equiv.). The crude mixture was purified by flash column chromatography (n-pentane/EtOAc: 10/1 → 2/1) to afford product 20 (54.4 mg, 72% yield) as white solid. Following the GP2 on 0.20 mmol scale the product 20 was isolated in 69% yield. 1H-NMR (400 MHz, CDCl3) δ 7.81 (dd, J = 5.5, 3.1 Hz, 2H), 7.72 (dd, J = 5.5, 3.1 Hz, 2H),7.38 (dd, J = 8.7, 2.3 Hz, 1H), 7.33 (d, J = 2.3 Hz, 1H), 6.83 (d, J = 8.7 Hz, 1H), 5.05 (dd, J = 11.0, 5.5 Hz, 1H), 4.34 – 4.16 (m, 2H), 3.84 (s, 3H), 3.55 (dd, J = 14.5, 5.5 Hz, 1H), 3.47 (dd, J = 14.5, 11.0 Hz, 1H), 1.25 (t, J = 7.1 Hz, 3H).

13C-NMR (101 MHz, CDCl3) δ 168.4, 167.5, 160.2, 134.9, 134.4, 133.9, 131.4, 129.5, 123.7, 116.2, 111.6, 101.8, 62.2, 56.0, 53.1, 33.5, 14.1.

HRMS (ESI) m/z calcd for C H N O +: 379.1288; found: 379.1307.
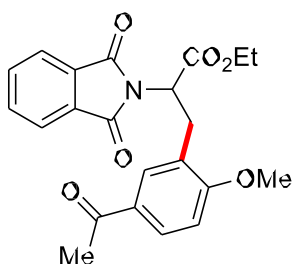
Ethyl 3-(5-acetyl-2-methoxyphenyl)-2-(1,3-dioxoisoindolin-2-yl)propanoate (21)

Prepared according to the GP1, using 5-(5-acetyl-2-methoxyphenyl)-5H-thianthren-5-ium tetrafluoroborate (90.4 mg, 0.20 mmol, 1.0 equiv.) and ethyl 2-(1,3-dioxoisoindolin-2-yl)acrylate (245.2 mg, 1.0 mmol, 5.0 equiv.). The crude mixture was purified by flash column chromatography (n-pentane/EtOAc: 10/1 → 2/1) to afford product 21 (54.5 mg, 69% yield) as white solid.

1H-NMR (400 MHz, CDCl3) δ 7.83 – 7.74 (m, 3H), 7.69 (dd, J = 5.5, 3.1 Hz, 2H), 7.63 (d, J = 2.3 Hz, 1H), 6.82 (d, J = 8.6 Hz, 1H), 5.32 (dd, J = 11.2, 4.7 Hz, 1H), 4.27 (q, J = 7.1 Hz, 2H), 3.84 (s, 3H), 3.68 (dd, J = 14.0, 4.7 Hz, 1H), 3.45 (dd, J = 14.0, 11.2 Hz, 1H), 2.36 (s, 3H), 1.27 (t, J = 7.1 Hz, 3H).

13C-NMR (101 MHz, CDCl3) δ 196.6, 169.0, 167.4, 161.6, 134.1, 131.6, 129.9, 129.7, 125.3, 123.3, 109.8, 62.0, 55.6, 51.2, 30.6, 26.2, 14.1.

HRMS (ESI) m/z calcd for C22H22NO6+: 396.1442; found: 396.1444.

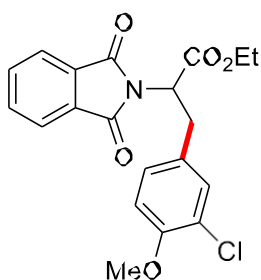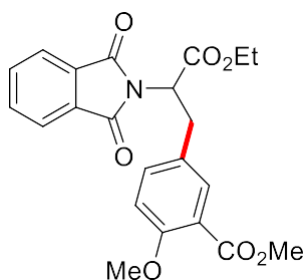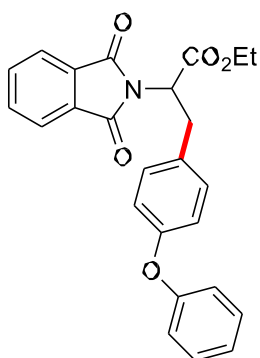**Ethyl -2-(1,3-dioxoisoindolin-2-yl)-3-(4-phenoxyphenyl)propanoate (22)**

Prepared according to the GP1, using 5-(4-phenoxyphenyl)-5H-thianthren-5-ium tetrafluoroborate (94.4 mg, 0.2 mmol, 1.0 equiv.) and ethyl 2-(1,3-dioxoisoindolin-2-yl)acrylate (245.2 mg, 1.0 mmol, 5 equiv.). The crude mixture was purified by flash column chromatography (n-pentane/EtOAc: 19/1 → 5/1) to afford product 22 (51.5 mg, 62% yield) as white solid. Following the GP2 on 0.20 mmol scale the product 22 was isolated in 65% yield. 1H-NMR (400 MHz, CDCl3) δ 7.73 (dd, J = 5.4, 3.1 Hz, 2H), 7.63 (dd, J = 5.4, 3.1 Hz, 2H),7.22 – 7.19 (m, 1H), 7.18 (d, J = 5.9 Hz, 1H), 7.05 (d, J = 8.4 Hz, 2H), 7.01 – 6.93 (m, 1H), 6.85 – 6.78 (m, 2H), 6.75 (d, J = 8.4 Hz, 2H), 5.04 (dd, J = 11.0, 5.6 Hz, 1H), 4.32 – 4.07 (m, 2H), 3.50 (dd, J = 14.4, 5.6 Hz, 1H), 3.44 (dd, J = 14.4, 11.0 Hz, 1H), 1.19 (t, J = 7.1 Hz, 3H). 13C-NMR (101 MHz, CDCl3) δ 168.8, 167.5, 157.3, 155.9, 134.1, 131.8, 131.6, 130.2, 129.6, 123.5, 123.1, 119.2, 118.6, 62.1, 53.5, 34.0, 14.1.

HRMS (ESI) m/z calcd for C25H22NO5+: 416.1492; found: 416.1504.
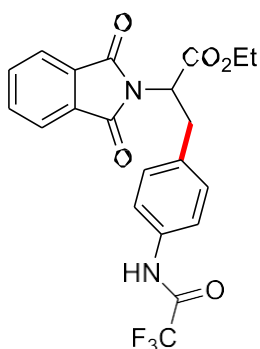
Ethyl 2-(1,3-dioxoisoindolin-2-yl)-3-(4-(2,2,2-trifluoroacetamido)phenyl)propanoate (23)

Prepared according to the GP1, using 5-(4-acetamidophenyl)-5H-thianthren-5-ium tetrafluoroborate (98.2 mg, 0.20 mmol, 1.0 equiv.) and ethyl 2-(1,3-dioxoisoindolin-2-yl)acrylate (245.2 mg, 1.0 mmol, 5.0 equiv.). The crude mixture was purified by flash column chromatography (n-pentane/EtOAc: 9/1 → 2/1) to afford product 23 (52.9 mg, 61% yield) as white solid. Following the GP2 on 0.20 mmol scale the product 23 was isolated in 52% yield.

^{1}H-NMR (400 MHz, CDCl3) δ 8.07 (brs, 1H), 7.77 (dd, J = 5.5, 3.1 Hz, 2H), 7.69 (dd, J = 5.5, 3.1 Hz, 2H), 7.41 (d, J = 8.3 Hz, 2H), 7.17 (d, J = 8.3 Hz, 2H), 5.10 (dd, J = 10.9, 5.6 Hz, 1H), 4.45 – 4.09 (m, 2H), 3.65 – 3.44 (m, 2H), 1.25 (t, J = 7.2 Hz, 3H).

^{13}C-NMR (101 MHz, CDCl3) δ 168.6, 167.5, 154.6 (q, J = 37.4 Hz), 135.0, 134.3, 134.0, 131.5, 129.8, 123.6, 120.5, 115.6 (q, J = 288.8 Hz), 62.2, 53.3, 34.2, 14.1.

^{19}F NMR (376 MHz, CDCl3) δ -75.7.

HRMS (ESI) m/z calcd for C H F N O +: 435.1162; found: 435.1159.

127

Ethyl -2-(1,3-dioxoisoindolin-2-yl)-3-(4-(phenylsulfonamido)phenyl)propanoate (24)

Prepared according to the GP1, using 5-(4-(phenylsulfonamido)phenyl)-5H-thianthren-5-ium tetrafluoroborate (107.1 mg, 0.20 mmol, 1.0 equiv.) and ethyl 2-(1,3-dioxoisoindolin-2-yl)acrylate (245.2 mg, 1.0 mmol, 5.0 equiv.). The crude mixture was purified by flash column chromatography (n-pentane/acetone: 100/0 → 7/3) to afford product 24 (64.2 mg, 67% yield) as white solid.

1H-NMR (400 MHz, CDCl3) δ 7.78 (dd, J = 5.5, 3.1 Hz, 2H), 7.70 (dd, J = 5.5, 3.1 Hz, 2H), 7.64 – 7.59 (m, 2H), 7.52 – 7.42 (m, 1H), 7.34 (dd, J = 8.4, 7.3 Hz, 2H), 7.02 (d, J = 8.5 Hz, 2H), 6.87 (d, J = 8.5 Hz, 2H), 5.04 (dd, J = 11.0, 5.5 Hz, 1H), 4.35 – 4.12 (m, 2H), 3.57 – 3.36 (m, 2H), 1.23 (t, J = 7.1 Hz, 3H).

13C-NMR (101 MHz, CDCl3) δ 168.6, 167.5, 138.8, 135.1, 134.4, 134.2, 132.9, 131.5, 129.8, 128.9, 127.1, 123.5, 122.3, 62.1, 53.3, 34.0, 14.1.

HRMS (ESI) m/z calcd for C25H23N2O3S+: 479.1271; found: 479.1273.
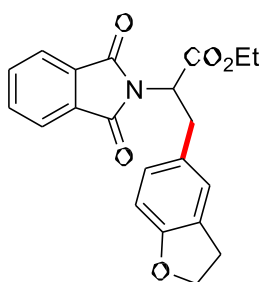
Ethyl 3-(2,3-dihydrobenzofuran-5-yl)-2-(1,3-dioxoisoindolin-2-yl)propanoate (25)

Prepared according to the GP1, using 5-(2,3-dihydrobenzofuran-5-yl)-5H-thianthren-5-ium tetrafluoroborate (84.4 mg, 0.20 mmol, 1.0 equiv.) and ethyl 2-(1,3-dioxoisoindolin-2-yl)acrylate (245.2 mg, 1.0 mmol, 5.0 equiv.). The crude mixture was purified by flash column chromatography (n-pentane/EtOAc: 19/1 → 5/1) to afford product 25 (48.9 mg, 67% yield) as white solid.

1H-NMR (400 MHz, CDCl3) δ 7.77 (dd, J = 5.5, 3.1 Hz, 2H), 7.68 (dd, J = 5.5, 3.1 Hz, 2H), 7.00 (d, J = 2.0 Hz, 1H), 6.85 (dd, J = 8.2, 2.0 Hz, 1H), 6.55 (d, J = 8.2 Hz, 1H), 5.07 (dd, J = 10.9, 5.6 Hz, 1H), 4.45 (ddd, J = 9.3, 8.1, 1.2 Hz, 2H), 4.29 – 4.16 (m, 2H), 3.57 – 3.37 (m, 2H), 3.18 – 2.89 (m, 2H), 1.24 (t, J = 7.1 Hz, 3H).

13C-NMR (101 MHz, CDCl3) δ 168.9, 167.6, 158.9, 134.1, 131.7, 128.7, 128.4, 127.3, 125.4, 123.4, 109.1, 71.1, 62.0, 53.8, 34.1, 29.6, 14.1.

HRMS (ESI) m/z calcd for C21H20NO5+: 366.1336; found: 366.1348.
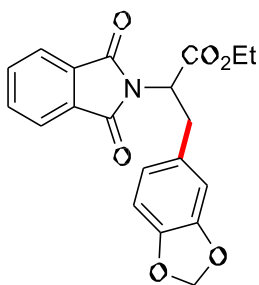
Ethyl 3-(benzo[d][1,3]dioxol-5-yl)-2-(1,3-dioxoisoindolin-2-yl)propanoate (26)

Prepared according to the GP1, using 5-(benzo[d][1,3]dioxol-5-yl)-5H-thianthren-5-ium tetrafluoroborate (84.8 mg, 0.20 mmol, 1.0 equiv.) and ethyl 2-(1,3-dioxoisoindolin-2-yl)acrylate (245.2 mg, 1.0 mmol, 5.0 equiv.). The crude mixture was purified by flash column chromatography (n-pentane/EtOAc: 9/1 → 4/1) to afford product 26 (52.2 mg, 71% yield) as white solid. Following the GP2 on 0.20 mmol scale the product 26 was isolated in 67% yield.Spectroscopic data are in accordance with the literature.[5]

1H-NMR (400 MHz, CDCl3) δ 7.78 (dd, J = 5.5, 3.1 Hz, 1H), 7.68 (dd, J = 5.5, 3.1 Hz, 1H), 6.66 (d, J = 1.4 Hz, 1H), 6.58 (d, J = 1.4 Hz, 1H), 5.91 – 5.67 (m, 1H), 5.06 (dd, J = 10.9, 5.5 Hz, 1H), 4.35 – 4.10 (m, 2H), 3.70 – 3.31 (m, 2H), 1.24 (t, J = 7.1 Hz, 3H).

13C-NMR (101 MHz, CDCl3) δ 168.8, 167.5, 147.7, 146.4, 134.1, 131.6, 130.5, 123.5, 122.0, 109.2, 108.3, 100.9, 62.0, 53.6, 34.4, 14.1.

HRMS (ESI) m/z calcd for $C_{20}H_{18}NO_6^+$: 368.1129; found: 368.1133.
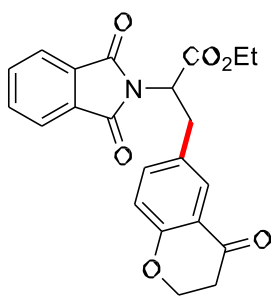
Ethyl -2-(1,3-dioxoisoindolin-2-yl)-3-(4-oxochroman-6-yl)propanoate (27)

Prepared according to the GP1, using 5-(4-oxochroman-6-yl)-5H-thianthren-5-ium tetrafluoroborate (90.2 mg, 0.20 mmol, 1.0 equiv.) and ethyl 2-(1,3-dioxoisoindolin-2-yl)acrylate (245.2 mg, 1.0 mmol, 5.0 equiv.). The crude mixture was purified by flash column chromatography (toluene/EtOAc: 100/0 → 9/1) to afford product 27 (31.8 mg, 40% yield) as white solid.

1H-NMR (400 MHz, CDCl3) δ 7.80 (dd, J = 5.5, 3.1 Hz, 2H), 7.74 – 7.67 (m, 3H), 7.33 – 7.27 (m, 1H), 6.81 (d, J = 8.5 Hz, 1H), 5.06 (dd, J = 11.0, 5.3 Hz, 1H), 4.45 (t, J = 6.2 Hz, 2H), 4.33

– 4.15 (m, 2H), 3.56 (dd, J = 14.4, 5.3 Hz, 1H), 3.48 (dd, J = 14.5, 11.0 Hz, 1H), 2.72 (t, J = 6.2 Hz, 2H), 1.25 (t, J = 7.1 Hz, 3H).

13C-NMR (101 MHz, CDCl3) δ 191.5, 168.6, 167.5, 160.7, 136.5, 134.2, 131.6, 130.0, 127.2, 123.6, 121.2, 118.2, 66.9, 62.1, 53.4, 37.6, 33.8, 14.1.

HRMS (ESI) m/z calcd for C22H20NO6+: 394.1285; found: 394.1290.

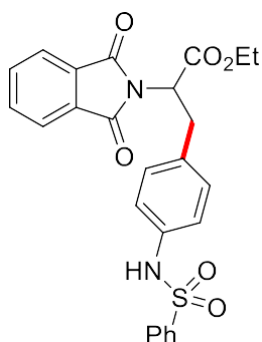**Ethyl -2-(1,3-dioxoisoindolin-2-yl)-3-(9-oxo-9H-xanthen-2-yl)propanoate (28)**

Prepared according to the GP1, using 5-(9-oxo-9H-xanthen-2-yl)-5H-thianthren-5-ium tetrafluoroborate (99.7 mg, 0.20 mmol, 1.0 equiv.) and ethyl 2-(1,3-dioxoisoindolin-2-yl)acrylate (245.2 mg, 1.0 mmol, 5.0 equiv.). The crude mixture was purified by flash column chromatography (n-pentane/EtOAc: 9/1 → 3/1) to afford product 28 (55.6 mg, 63% yield) as white solid. Following the GP2 on 0.20 mmol scale the product 28 was isolated in 66% yield.

1H-NMR (400 MHz, CDCl3) δ 8.19 (d, J = 8.0 Hz, 1H), 8.06 (d, J = 2.2 Hz, 1H), 7.70 (dd, J = 5.5, 3.1 Hz, 2H), 7.64 – 7.55 (m, 3H), 7.49 (dd, J = 8.5, 2.2 Hz, 1H), 7.35 (d, J = 8.5 Hz, 1H), 7.31 – 7.18 (m, 2H), 5.10 (dd, J = 11.0, 5.1 Hz, 1H), 4.38 – 4.05 (m, 2H), 3.66 (dd, J = 14.5, 5.1 Hz, 1H), 3.58 (dd, J = 14.5, 11.0 Hz, 1H), 1.19 (t, J = 7.1 Hz, 3H).

13C-NMR (101 MHz, CDCl3) δ 176.9, 168.5, 167.4, 156.1, 155.1, 135.4, 134.8, 134.2, 132.9, 131.5, 126.7, 126.7, 123.9, 123.6, 121.8, 121.7, 118.4, 117.9, 62.2, 53.4, 34.2, 14.1.

HRMS (ESI) m/z calcd for C26H20NO6+: 442.1285; found: 442.1287.
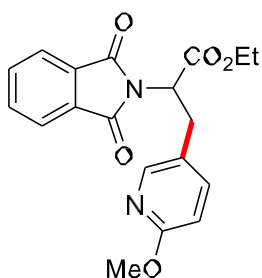
Ethyl -2-(1,3-dioxoisoindolin-2-yl)-3-(6-methoxypyridin-3-yl)propanoate (29)

Prepared according to the GP1, using 5-(6-methoxypyridin-3-yl)-5H-thianthren-5-ium tetrafluoroborate (82.2 mg, 0.20 mmol, 1.0 equiv.) and ethyl 2-(1,3-dioxoisoindolin-2-yl)acrylate (245.2 mg, 1.0 mmol, 5.0 equiv.). The crude mixture was purified by flash column chromatography (n-pentane/EtOAc: 9/1 → 8/2) to afford product 29 (30.4 mg, 43% yield) as white solid.

1H-NMR (400 MHz, CDCl3) δ 7.90 (d, J = 2.5 Hz, 1H), 7.78 (dd, J = 5.5, 3.1 Hz, 2H), 7.69 (dd, J = 5.5, 3.1 Hz, 2H), 7.42 (dd, J = 8.5, 2.5 Hz, 1H), 6.60 (d, J = 8.5 Hz, 1H), 5.04 (dd, J = 9.8, 6.6 Hz, 1H), 4.32 – 4.14 (m, 2H), 3.81 (s, 3H), 3.52 – 3.42 (m, 2H), 1.24 (t, J = 7.1 Hz, 3H).

13C-NMR (101 MHz, CDCl3) δ 168.5, 167.5, 163.3, 146.9, 139.1, 134.2, 131.5, 124.9, 123.6, 110.8, 62.1, 53.3, 53.2, 31.1, 14.1.

HRMS (ESI) m/z calcd for C H N O +: 355.1288; found: 355.1300.
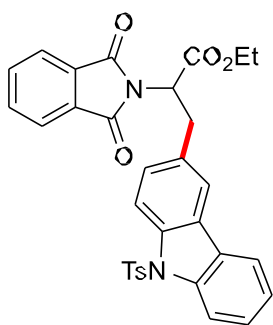
Ethyl 2-(1,3-dioxoisoindolin-2-yl)-3-(9-tosyl-9H-carbazol-3-yl)propanoate (30)

Prepared according to the GP1, using 5-(9-tosyl-9H-carbazol-3-yl)-5H-thianthren-5-ium tetrafluoroborate (124.7 mg, 0.20 mmol, 1.0 equiv.) and ethyl 2-(1,3-dioxoisoindolin-2-yl)acrylate (245.2 mg, 1.0 mmol, 5.0 equiv.). The crude mixture was purified by flash column chromatography (n-pentane/EtOAc: 9/1 → 3/1) to afford product 30 (77.1 mg, 68% yield) as white solid. Following the GP2 on 0.20 mmol scale the product 30 was isolated in 71% yield.

1H-NMR (400 MHz, CDCl3) δ 8.21 (d, J = 8.4 Hz, 1H), 8.11 (d, J = 8.4 Hz, 1H), 7.77 – 7.67 (m, 4H), 7.65 – 7.60 (m, 2H), 7.58 (d, J = 8.4 Hz, 2H), 7.40 (ddd, J = 8.5, 7.3, 1.3 Hz, 1H), 7.31 – 7.18 (m, 2H), 7.01 (d, J = 8.4 Hz, 2H), 5.19 (dd, J = 11.0, 5.4 Hz, 1H), 4.31 – 4.17 (m, 2H), 3.71 (dd, J = 14.5, 5.4 Hz, 1H), 3.64 (dd, J = 14.5, 11.0 Hz, 1H), 2.20 (s, 3H), 1.23 (t, J = 7.1 Hz, 3H).

13C-NMR (101 MHz, CDCl3) δ 168.8, 167.5, 144.8, 138.6, 137.3, 134.9, 134.1, 132.7, 131.6, 129.6, 128.1, 127.4, 126.7, 126.4, 126.1, 123.8, 123.5, 120.3, 120.0, 115.2, 115.1, 62.1, 53.6, 34.5, 21.5, 14.1.

HRMS (ESI) m/z calcd for $C_{32}H_{27}N_2O_6S^+$: 567.1584; found: 567.1594.
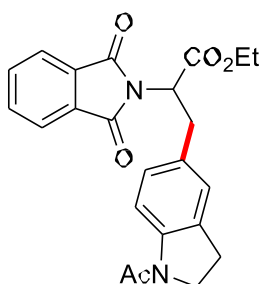
Ethyl -3-(1-acetylindolin-5-yl)-2-(1,3-dioxoisoindolin-2-yl)propanoate (31)
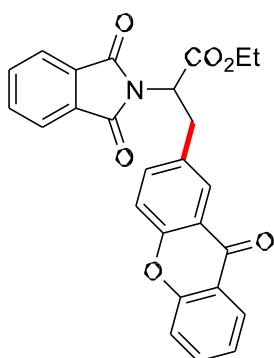
Prepared according to the GP1, using 5-(1-acetylindolin-5-yl)-5H-thianthren-5-ium tetrafluoroborate (92.7 mg, 0.20 mmol, 1.0 equiv.) and ethyl 2-(1,3-dioxoisoindolin-2-yl)acrylate (245.2 mg, 1.0 mmol, 5.0 equiv.). The crude mixture was purified by flash column chromatography (n-pentane/EtOAc: 9/1 → 3/1) to afford product 31 (46.3 mg, 57% yield) as white solid.

1H-NMR (400 MHz, CDCl3) δ 7.96 (d, J = 8.2 Hz, 1H), 7.78 (dd, J = 5.5, 3.1 Hz, 2H), 7.69 (dd, J = 5.5, 3.1 Hz, 2H), 7.03 (s, 1H), 6.92 (dd, J = 8.2, 1.9 Hz, 1H), 5.08 (dd, J = 10.3, 6.3 Hz, 1H), 4.31 – 4.16 (m, 2H), 3.97 (t, J = 8.2 Hz, 2H), 3.58 – 3.43 (m, 2H), 3.27 – 2.94 (m, 2H), 2.15 (s, 3H), 1.25 (t, J = 7.1 Hz, 3H).

13C-NMR (101 MHz, CDCl3) δ 168.8, 168.5, 167.5, 141.8, 134.1, 132.1, 131.6, 131.6, 128.1, 124.9, 123.5, 116.8, 62.0, 53.6, 48.8, 34.2, 27.8, 24.1, 14.1.

HRMS (ESI) m/z calcd for C H N O +: 407.1601; found: 407.1619.
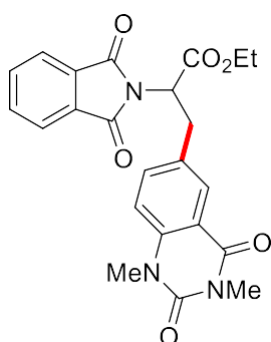
Ethyl -3-(1,3-dimethyl-2,4-dioxo-1,2,3,4-tetrahydroquinazolin-6-yl)-2-(1,3-dioxoisoindolin-2-yl)propanoate (32)

Prepared according to the GP1, using 5-(1,3-dimethyl-2,4-dioxo-1,2,3,4-tetrahydroquinazolin- 6-yl)-5H-thianthren-5-ium tetrafluoroborate (98.5 mg, 0.20 mmol, 1.0 equiv.) and ethyl 2-(1,3- dioxoisoindolin-2-yl)acrylate (245.2 mg, 1.0 mmol, 5.0 equiv.). The crude mixture was purified

by flash column chromatography (n-pentane/EtOAc: 9/1 → 3/1) to afford product 32 (50.6 mg, 58% yield) as white solid.

1H-NMR (400 MHz, CDCl3) δ 8.04 (d, J = 2.2 Hz, 1H), 7.79 (dd, J = 5.5, 3.0 Hz, 2H), 7.69 (dd, J = 5.5, 3.0 Hz, 2H), 7.49 (dd, J = 8.6, 2.2 Hz, 1H), 7.06 (d, J = 8.6 Hz, 1H), 5.13 (dd, J = 11.1, 5.1 Hz, 1H), 4.35 – 4.18 (m, 2H), 3.72 – 3.56 (m, 2H), 3.52 (s, 3H), 3.42 (s, 3H), 1.26 (t, J = 7.1 Hz, 3H).

13C-NMR (101 MHz, CDCl3) δ 168.4, 167.4, 161.6, 151.1, 139.3, 135.6, 134.2, 131.9, 131.5, 129.0, 123.6, 115.5, 113.9, 62.2, 53.3, 33.9, 30.7, 28.5, 14.1.

HRMS (ESI) m/z calcd for C H N O +: 436.1503; found: 436.1511.
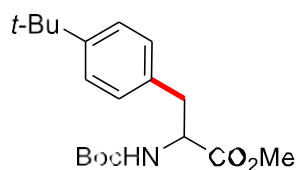
methyl 2-((tert-butoxycarbonyl)amino)-3-(4-(tert-butyl)phenyl)propanoate (33)

Prepared according to the GP1, 5-(4-(tert-butyl)phenyl)-5H-thianthren-5-ium tetrafluoroborate

261.9 mg, 0.60 mmol, 3.0 equiv.) and methyl 2-((tert-butoxycarbonyl)amino)acrylate (20.1 mg, 0.20 mmol, 1.0 equiv.). The crude mixture was purified by flash column chromatography (n-pentane/EtOAc: 9/1 → 7/3) to afford product 33 (34.8 mg, 52% yield) as white solid. Spectroscopic data are in accordance with the literature.[6]

1H-NMR (400 MHz, CDCl3) δ 7.31 (d, J = 8.0 Hz, 2H), 7.05 (d, J = 8.0 Hz, 2H), 4.98 (d, J = 8.5 Hz, 1H), 4.58 (dt, J = 8.5, 6.0 Hz, 1H), 3.72 (s, 3H), 3.09 (dd, J = 13.9, 5.6 Hz, 1H), 3.01 (dd, J = 13.9, 6.3 Hz, 1H), 1.41 (s, 9H), 1.30 (s, 9H).

13C-NMR (101 MHz, CDCl3) δ 172.6, 155.2, 149.9, 133.0, 129.1, 125.6, 80.0, 54.5, 52.3, 37.9, 34.5, 31.5, 28.4.

HRMS (ESI) m/z calcd for $C_{19}H_{30}NO_4^+$: 336.2169; found: 336.2188.
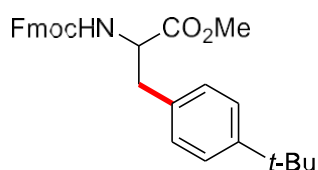
Methyl 2-((((9H-fluoren-9-yl)methoxy)carbonyl)amino)-3-(4-(tert-butyl)phenyl)propanoate (34)

Prepared according to the GP1, 5-(4-(tert-butyl)phenyl)-5H-thianthren-5-ium tetrafluoroborate

261.9 mg, 0.60 mmol, 3.0 equiv.) and methyl 2-((((9H-fluoren-9-yl)methoxy)carbonyl)amino)acrylate (32.3 mg, 0.20 mmol, 1.0 equiv.). The crude mixture was purified by flash column chromatography (n-pentane/EtOAc: 9/1 → 7/3) to afford product 34 (39.3 mg, 43% yield) as white solid.

1H-NMR (400 MHz, CDCl3) δ 7.79 (d, J = 7.5 Hz, 2H), 7.60 (t, J = 7.5 Hz, 2H), 7.43 (t, J = 7.5 Hz, 2H), 7.37 – 7.29 (m, 4H), 7.05 (d, J = 7.9 Hz, 2H), 5.32 (d, J = 8.3 Hz, 1H), 4.70 (dt, J = 8.3, 5.8 Hz, 1H), 4.48 (dd, J = 10.5, 7.1 Hz, 1H), 4.35 (dd, J = 10.5, 7.1 Hz, 1H), 4.23 (t, J = 7.1 Hz, 1H), 3.77 (s, 3H), 3.16 (dd, J = 14.0, 5.7 Hz, 1H), 3.10 (dd, J = 14.0, 6.1 Hz, 1H), 1.32 (s, 9H).

13C-NMR (101 MHz, CDCl3) δ 172.1, 155.6, 150.0, 143.9, 143.9, 141.4, 132.6, 129.0, 127.8, 127.1, 125.6, 125.2, 125.1, 120.0, 120.0, 67.0, 54.8, 52.4, 47.2, 37.6, 34.5, 31.4.

HRMS (ESI) m/z calcd for C29H32NO4+: 458.2326; found: 458.2338.
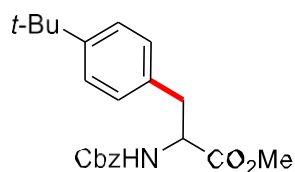
Methyl 2-(((benzyloxy)carbonyl)amino)-3-(4-(tert-butyl)phenyl)propanoate (35)

Prepared according to the GP1, 5-(4-(tert-butyl)phenyl)-5H-thianthren-5-ium tetrafluoroborate

261.9 mg, 0.60 mmol, 3.0 equiv.) and methyl 2-(((benzyloxy)carbonyl)amino)acrylate (23.5 mg, 0.20 mmol, 1.0 equiv.). The crude mixture was purified by flash column chromatography (n-pentane/EtOAc: 9/1 → 7/3) to afford product 35 (28.2 mg, 38% yield) as white solid.

1H-NMR (400 MHz, CDCl3) δ 7.40 – 7.27 (m, 7H), 7.03 (d, J = 8.4 Hz, 2H), 5.22 (d, J = 8.3 Hz, 1H), 5.11 (s, 2H), 4.67 (ddd, J = 10.9, 8.3, 5.4 Hz, 1H), 3.17 – 3.01 (m, 2H), 1.32 – 1.26 (m, 9H).

13C-NMR (101 MHz, CDCl3) δ 172.1, 155.7, 150.0, 136.3, 132.5, 129.0, 128.5, 128.2, 128.1, 125.6, 67.0, 54.7, 52.3, 37.5, 34.5, 31.3.

HRMS (ESI) m/z calcd for C22H28NO4+: 370.2013; found: 370.2016.

Characterization data for the conjugated unnatural amino acids 38
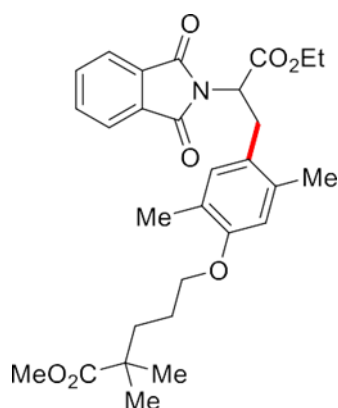
Methyl 5-(4-(2-(1,3-dioxoisoindolin-2-yl)-3-ethoxy-3-oxopropyl)-2,5-dimethylphenoxy)-2,2-dimethylpentanoate (39)

Prepared according to the GP1, using 5-(4-((5-methoxy-4,4-dimethyl-5-oxopentyl)oxy)-2,5-dimethylphenyl)-5H-thianthren-5-ium tetrafluoroborate (113.3 mg, 0.20 mmol, 1.0 equiv.) and ethyl 2-(1,3-dioxoisoindolin-2-yl)acrylate (245.2 mg, 1.0 mmol, 5.0 equiv.). The crude mixture was purified by flash column chromatography (n-pentane/EtOAc: 19/1 → 4/1) to afford product 39 (59.2 mg, 58% yield) as white solid.

1H-NMR (400 MHz, CDCl3) δ 7.78 (dd, J = 5.5, 3.1 Hz, 2H), 7.68 (dd, J = 5.5, 3.1 Hz, 2H), 6.72 (s, 1H), 6.50 (s, 1H), 5.08 (dd, J = 11.3, 5.0 Hz, 1H), 4.32 – 4.17 (m, 2H), 3.89 – 3.75 (m, 2H), 3.62 (s, 3H), 3.52 (dd, J = 14.6, 5.0 Hz, 1H), 3.39 (dd, J = 14.6, 11.3 Hz, 1H), 2.31 (s, 3H), 1.92 (s, 3H), 1.71 – 1.60 (m, 4H), 1.25 (t, J = 7.1 Hz, 3H), 1.18 (s, 6H).

13C-NMR (101 MHz, CDCl3) δ 178.3, 169.1, 167.5, 155.7, 134.7, 134.0, 132.0, 131.7, 126.2, 123.9, 123.4, 113.2, 67.9, 61.9, 52.1, 51.7, 42.1, 37.0, 31.5, 25.2, 25.1, 19.2, 15.3, 14.1.

HRMS (ESI) m/z calcd for C29H36NO7+: 510.2486; found: 510.2486.
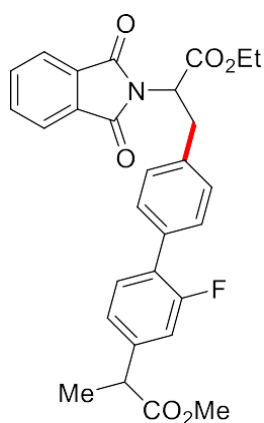
Ethyl -2-(1,3-dioxoisoindolin-2-yl)-3-(2'-fluoro-4'-(1-methoxy-1-oxopropan-2-yl)-[1,1'-biphenyl]-4-yl)propanoate (40)

Prepared according to the GP1, using 5-(2'-fluoro-4'-(1-methoxy-1-oxopropan-2-yl)-[1,1'-biphenyl]-4-yl)-5H-thianthren-5-ium tetrafluoroborate (112.1 mg, 0.20 mmol, 1.0 equiv.) and ethyl 2-(1,3-dioxoisoindolin-2-yl)acrylate (245.2 mg, 1.0 mmol, 5.0 equiv.). The crude mixture was purified by flash column chromatography (n-pentane/EtOAc: 19/1 → 3/1) to afford product 40 (82.5 mg, 82% yield) as white solid. Following the GP2 on 1.00 mmol scale the product 40 was isolated in 73% yield.

1H-NMR (400 MHz, CDCl3) δ 7.71 (dd, J = 5.5, 3.1 Hz, 2H), 7.60 (dd, J = 5.5, 3.1 Hz, 2H), 7.34 – 7.26 (m, 2H), 7.26 – 7.13 (m, 3H), 7.04 – 6.91 (m, 2H), 5.11 (dd, J = 10.8, 5.6 Hz, 1H), 4.30 – 4.09 (m, 2H), 3.64 (q, J = 7.2 Hz, 1H), 3.59 (s, 2H), 3.57 – 3.45 (m, 2H), 1.42 (d, J = 7.2 Hz, 3H), 1.18 (t, J = 7.1 Hz, 3H).

13C-NMR (101 MHz, CDCl3) δ 174.4, 168.8, 167.6, 159.6 (d, $^1J_{C-F}$ = 248.5 Hz), 141.7 (d, $^3J_{C-F}$ = 7.7 Hz), 136.4, 134.1, 133.9 (d, $^4J_{C-F}$ = 1.4 Hz), 131.6, 130.6 (d, $^3J_{C-F}$ = 4.0 Hz), 129.1 (d, $^1J_{C-F}$ = 3.0 Hz), 129.0, 127.3 (d, $^2J_{C-F}$ = 13.4 Hz), 123.5, 123.4, 115.2 (d, $^2J_{C-F}$ = 23.7 Hz), 62.1, 53.3, 52.2, 44.9, 34.4, 18.4, 14.1.

19F NMR (376 MHz, CDCl3) δ -117.38 – -117.50 (m)

HRMS (ESI) m/z calcd for C29H27FNO6+: 504.1817; found: 504.1832.
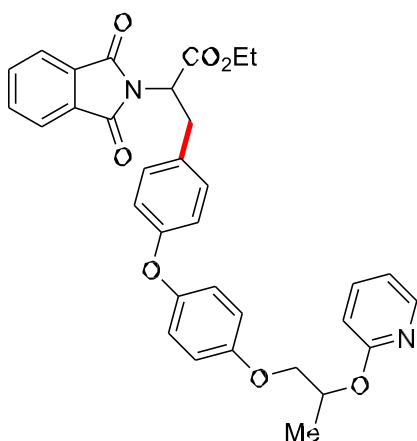
Ethyl 2-(1,3-dioxoisoindolin-2-yl)-3-(4-(4-(2-(pyridin-2

yloxy)propoxy)phenoxy)phenyl)propanoate (41)

Prepared according to the GP1, using 5-(4-(4-(2-(pyridin-2-yloxy)propoxy)phenoxy)phenyl)- 5H-thianthren-5-ium tetrafluoroborate (124.7 mg, 0.20 mmol, 1.0 equiv.) and ethyl 2-(1,3- dioxoisoindolin-2-yl)acrylate (245.2 mg, 1.0 mmol, 5.0 equiv.). The crude mixture was purified by flash column chromatography (n-pentane/EtOAc: 9/1 → 3/1) to afford product 41 (75.9 mg, 67% yield) as white solid.

1H-NMR (400 MHz, CDCl3) δ 8.16 (dd, J = 5.2, 1.9 Hz, 1H), 7.81 (dd, J = 5.5, 3.1 Hz, 2H), 7.72 (dd, J = 5.5, 3.1 Hz, 2H), 7.58 (ddd, J = 8.8, 7.1, 2.0 Hz, 1H), 7.10 (d, J = 8.6 Hz, 2H), 6.91 – 6.82 (m, 5H), 6.81 – 6.71 (m, 3H), 5.71 – 5.47 (m, 1H), 5.12 (dd, J = 10.9, 5.6 Hz, 1H), 4.33 – 4.21 (m, 2H), 4.18 (dd, J = 9.9, 5.3 Hz, 1H), 4.07 (dd, J = 9.9, 4.8 Hz, 1H), 3.64 – 3.45 (m, 2H), 1.49 (d, J = 6.4 Hz, 3H), 1.28 (t, J = 7.1 Hz, 3H).

13C-NMR (101 MHz, CDCl3) δ 168.8, 167.5, 163.2, 157.2, 155.1, 150.3, 146.8, 138.7, 134.1, 131.6, 130.9, 130.1, 123.5, 120.5, 117.9, 116.8, 115.7, 111.7, 71.1, 69.3, 62.0, 53.5, 33.9, 17.0, 14.1.

HRMS (ESI) m/z calcd for C33H31N2O7+: 567.2126; found: 567.2124.
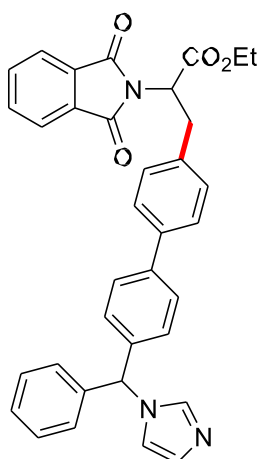
Ethyl -3-(4'-((1H-imidazol-1-yl)(phenyl)methyl)-[1,1'-biphenyl]-4-yl)-2-(1,3-dioxoisoindolin-2-yl)propanoate (42)

Prepared according to the GP1, using 5-(4'-((1H-imidazol-1-yl)(phenyl)methyl)-[1,1'-biphenyl]-4-yl)-5H-thianthren-5-ium tetrafluoroborate (122.5 mg, 0.20 mmol, 1.0 equiv.) and ethyl 2-(1,3-dioxoisoindolin-2-yl)acrylate (245.2 mg, 1.0 mmol, 5.0 equiv.). The crude mixture was purified by flash column chromatography (n-pentane/EtOAc: 9/1 → 2/1) to afford product 42 (76.8 mg, 69% yield) as white solid. Following the GP2 on 0.20 mmol scale the product 42 was isolated in 69% yield.

1H-NMR (400 MHz, CDCl3) δ 7.70 (dd, J = 5.5, 3.1 Hz, 2H), 7.60 (dd, J = 5.5, 3.1 Hz, 2H), 7.41 (d, J = 8.3 Hz, 2H), 7.36 – 7.24 (m, 6H), 7.19 – 7.15 (m, 2H), 7.07 – 6.99 (m, 5H), 6.78 (s, 1H), 6.45 (s, 1H), 5.11 (dd, J = 10.8, 5.7 Hz, 1H), 4.39 – 4.07 (m, 2H), 3.71 – 3.37 (m, 2H), 1.19 (t, J = 7.1 Hz, 3H).

13C-NMR (101 MHz, CDCl3) δ 168.8, 167.5, 140.7, 139.1, 138.6, 138.0, 137.4, 136.4, 134.1, 131.6, 129.4, 128.9, 128.5, 128.4, 128.1, 128.0, 127.3, 127.2, 123.5, 119.4, 64.8, 62.1, 53.3, 34.3, 14.1.

HRMS (ESI) m/z calcd for C35H30N3O4+: 556.2231; found: 556.2233.
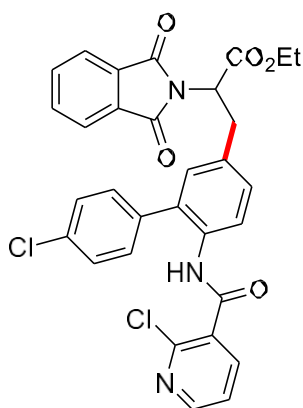
Ethyl 3-(4'-chloro-6-(2-chloronicotinamido)-[1,1'-biphenyl]-3-yl)-2-(1,3-dioxoisoindolin-2-yl)propanoate (43)

Prepared according to the GP1, using 5-(4'-chloro-6-(2-chloronicotinamido)-[1,1'-biphenyl]-3- yl)-5H-thianthren-5-ium tetrafluoroborate (129.1 mg, 0.20 mmol, 1.0 equiv.) and ethyl 2-(1,3- dioxoisoindolin-2-yl)acrylate (245.2 mg, 1.0 mmol, 5.0 equiv.). The crude mixture was purified by flash column chromatography (n-pentane/EtOAc: 9/1 → 1/1) to afford product 43 (74.1 mg, 63% yield) as white solid.

1H-NMR (400 MHz, CDCl3) δ 8.34 (dd, J = 4.7, 2.1 Hz, 1H), 8.18 (d, J = 8.4 Hz, 1H), 8.01 (dd, J = 7.8, 2.0 Hz, 1H), 7.97 (brs, 1H), 7.74 (dd, J = 5.5, 3.1 Hz, 2H), 7.65 (dd, J = 5.5, 3.1 Hz, 2H), 7.30 – 7.22 (m, 3H), 7.17 (dd, J = 8.6, 2.1 Hz, 1H), 7.03 (d, J = 8.2 Hz, 2H), 6.98 (d, J = 2.1 Hz, 1H), 5.08 (dd, J = 10.9, 5.5 Hz, 1H), 4.29 – 4.10 (m, 2H), 3.61 – 3.42 (m, 2H), 1.19 (t, J = 7.1 Hz, 3H).

13C-NMR (101 MHz, CDCl3) δ 168.6, 167.5, 162.3, 151.3, 146.6, 140.2, 135.9, 134.4, 134.2, 133.9, 133.1, 132.2, 131.6, 131.0, 130.7, 130.6, 129.4, 129.2, 123.6, 122.9, 122.1, 62.2, 53.3, 34.1, 14.1.

HRMS (ESI) m/z calcd for C H 35Cl N O +: 588.1088; found: 588.1093.
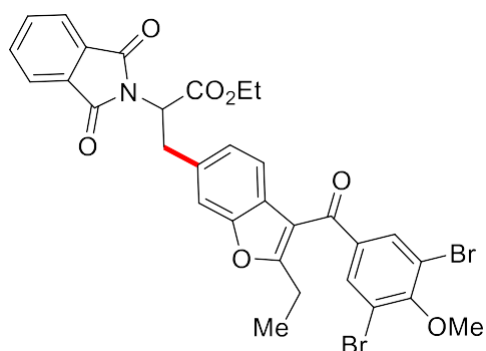
Ethyl 3-(3-(3,5-dibromo-4-methoxybenzoyl)-2-ethylbenzofuran-6-yl)-2-(1,3-dioxoisoindolin-2-yl)propanoate (44)

Prepared according to the GP1, using 5-(3-(3,5-dibromo-4-methoxybenzoyl)-2-ethylbenzofuran-5-yl)-5H-thianthren-5-ium tetrafluoroborate (148.0 mg, 0.20 mmol, 1.0 equiv.) and ethyl 2-(1,3-dioxoisoindolin-2-yl)acrylate (245.2 mg, 1.0 mmol, 5.0 equiv.). The crude mixture was purified by flash column chromatography (n-pentane/EtOAc: 9/1 → 1/1) to afford product 44 (84.8 mg, 62% yield) as white solid.

1H-NMR (400 MHz, CDCl3) δ 7.82 (s, 2H), 7.70 (dd, J = 5.6, 3.1 Hz, 2H), 7.60 (dd, J = 5.6, 3.1 Hz, 2H), 7.19 (s, 1H), 7.15 (d, J = 8.1 Hz, 1H), 6.97 (d, J = 8.1 Hz, 1H), 5.11 (dd, J = 11.0, 5.5 Hz, 1H), 4.27 – 4.10 (m, 2H), 3.87 (s, 3H), 3.70 – 3.45 (m, 2H), 2.74 (q, J = 7.5 Hz, 2H), 1.34 – 1.10 (m, 6H).

13C-NMR (101 MHz, CDCl3) δ 187.9, 168.7, 167.5, 167.0, 157.7, 153.9, 137.1, 134.2, 134.0, 133.6, 131.6, 125.2, 124.8, 123.6, 121.0, 118.4, 115.2, 111.5, 62.1, 60.9, 53.6, 34.7, 22.0, 14.1, 12.1.

HRMS (ESI) m/z calcd for C H 79Br NO +: 682.0071; found: 682.0085.
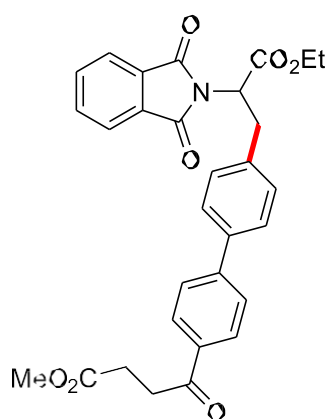
**Methyl -4-(4'-(2-(1,3-dioxoisoindolin-2-yl)-3-ethoxy-3-oxopropyl)-[1,1'-biphenyl]-4-yl)-4-oxobutanoate (45)**

Prepared according to the GP1, using 5-(4'-(4-methoxy-4-oxobutanoyl)-[1,1'-biphenyl]-4-yl)-5H-thianthren-5-ium tetrafluoroborate (114.1 mg, 0.20 mmol, 1.0 equiv.) and ethyl 2-(1,3-dioxoisoindolin-2-yl)acrylate (245.2 mg, 1.0 mmol, 5.0 equiv.). The crude mixture was purified by flash column chromatography (n-pentane/EtOAc: 9/1 → 1/1) to afford product 45 (48.3 mg, 47% yield) as white solid. Following the GP2 on 0.20 mmol scale the product 45 was isolated in 51% yield.

1H-NMR (400 MHz, CDCl3) δ 8.02 (d, J = 8.3 Hz, 2H), 7.82 (dd, J = 5.5, 3.1 Hz, 2H), 7.72 (dd, J = 5.5, 3.1 Hz, 2H), 7.62 (d, J = 8.3 Hz, 2H), 7.49 (d, J = 8.3 Hz, 2H), 7.30 (d, J = 8.3 Hz, 2H), 5.22 (dd, J = 10.7, 5.7 Hz, 1H), 4.37 – 4.15 (m, 2H), 3.73 (s, 3H), 3.71 – 3.52 (m, 2H), 3.35 (t, J = 6.6 Hz, 2H), 2.80 (t, J = 6.6 Hz, 2H), 1.29 (t, J = 7.1 Hz, 3H).

13C-NMR (101 MHz, CDCl3) δ 197.6, 173.4, 168.7, 167.6, 145.4, 138.2, 137.1, 135.1, 134.2, 131.6, 129.5, 128.6, 127.4, 127.0, 123.5, 62.2, 53.3, 51.9, 34.4, 33.4, 28.1, 14.1.

HRMS (ESI) m/z calcd for C30H28NO7+: 514.1860; found: 514.1864.
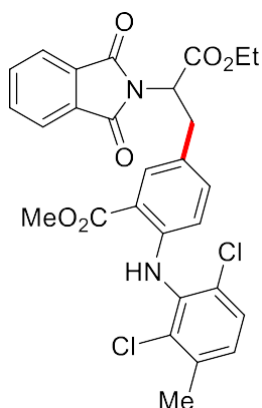
Methyl 2-((2,6-dichloro-3-methylphenyl)amino)-5-(2-(1,3-dioxoisoindolin-2-yl)-3-ethoxy-3-oxopropyl)benzoate (46)

Prepared according to the GP1, using 5-(4-((2,6-dichloro-3-methylphenyl)amino)-3-(methoxycarbonyl)phenyl)-5H-thianthren-5-ium tetrafluoroborate (114.1 mg, 0.20 mmol, 1.0 equiv.) and ethyl 2-(1,3-dioxoisoindolin-2-yl)acrylate (245.2 mg, 1.0 mmol, 5.0 equiv.). The crude mixture was purified by flash column chromatography (n-pentane/EtOAc: 9/1 → 1/1) to afford product 46 (78.4 mg, 64% yield) as white solid. Following the GP2 on 0.20 mmol scale the product 46 was isolated in 62% yield.

1H-NMR (400 MHz, CDCl3) δ 9.18 (s, 1H), 7.83 – 7.74 (m, 3H), 7.69 (dd, J = 5.5, 3.1 Hz, 2H), 7.23 (d, J = 7.6 Hz, 1H), 7.10 – 7.00 (m, 2H), 6.15 (d, J = 8.5 Hz, 1H), 5.07 (dd, J = 11.0, 5.6 Hz, 1H), 4.32 – 4.16 (m, 2H), 3.83 (s, 3H), 3.50 (dd, J = 14.5, 5.6 Hz, 1H), 3.43 (dd, J = 14.5, 11.0 Hz, 1H), 2.35 (s, 3H), 1.25 (t, J = 7.1 Hz, 3H).

13C-NMR (101 MHz, CDCl3) δ 168.8, 168.7, 167.5, 146.2, 136.4, 135.1, 134.4, 134.0, 133.9, 131.7, 131.6, 130.9, 128.3, 127.7, 125.4, 123.4, 114.2, 111.6, 62.0, 53.4, 51.8, 33.7, 20.6, 14.1.

HRMS (ESI) m/z calcd for $C_{28}H_{25}^{35}Cl_2N_2O_6^+$: 555.1084; found: 555.1084.
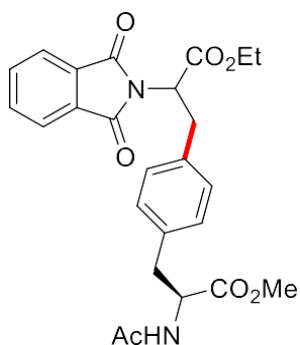
Ethyl 3-(4-((S)-2-acetamido-3-methoxy-3-oxopropyl)phenyl)-2-(1,3-dioxoisoindolin-2-yl)propanoate (47)

Prepared according to the GP1, using (S)-5-(4-(2-acetamido-3-methoxy-3-oxopropyl)phenyl)- 5H-thianthren-5-ium tetrafluoroborate (104.6 mg, 0.20 mmol, 1.0 equiv.) and ethyl 2-(1,3- dioxoisoindolin-2-yl)acrylate (245.2 mg, 1.0 mmol, 5.0 equiv.). The crude mixture was purified by flash column chromatography (n-pentane/EtOAc: 9/1 → 1/1) to afford product 47 (62.4 mg, 67% yield, 1/1 dr by 1H-NMR) as white solid.

1H-NMR (400 MHz, CDCl3) δ 7.81 – 7.73 (m, 2H), 7.72 – 7.64 (m, 2H), 7.13 – 7.01 (m, 2H), 7.02 – 6.80 (m, 2H), 5.89 (d, J = 7.8 Hz, 0.5H), 5.83 (d, J = 7.8 Hz, 0.5H), 5.15 – 4.98 (m, 1H), 4.81 – 4.70 (m, 1H), 4.30 – 4.13 (m, 2H), 3.61 (s, 1.5H), 3.56 (s, 1.5H), 3.54 – 3.40 (m, 2H), 3.12 – 2.85 (m, 2H), 1.93 (s, 1.5H), 1.88 (s, 1.5H), 1.24 (t, J = 7.1 Hz, 3H).

13C-NMR (101 MHz, CDCl3) δ 172.0, 171.9, 169.6, 169.5, 168.7, 168.7, 167.4, 167.4, 135.8, 135.7, 134.4, 134.3, 134.1*, 131.6, 131.5, 129.4, 129.4, 129.1*, 123.5, 123.5, 62.1*, 53.5, 53.4, 53.0, 53.0, 52.2, 52.1, 37.4, 37.4, 34.3, 34.3, 23.1, 23.0, 14.1*. *(Peaks denoted with * correspond to both diastereomers)*

HRMS (ESI) m/z calcd for C H N O +: 467.1813; found: 467.1818.
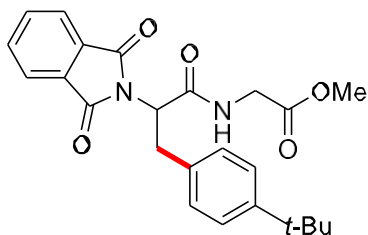
Methyl (3-(4-(tert-butyl)phenyl)-2-(1,3-dioxoisoindolin-2-yl)propanoyl)glycinate (50)

Prepared according to the GP1, using 5-(4-(tert-butyl)phenyl)-5H-thianthren-5-ium tetrafluoroborate (87.3 mg, 0.20 mmol, 1.0 equiv.) and methyl (2-(1,3-dioxoisoindolin-2-yl)acryloyl)glycinate (288.2 mg, 1.0 mmol, 5.0 equiv.). The crude mixture was purified by flash column chromatography (n-pentane/EtOAc: 7/3 → 1/1) to afford product 50 (45.6 mg, 54% yield) as white solid.

1H NMR (400 MHz, CDCl3) δ 7.78 (dd, J = 5.5, 3.1 Hz, 2H), 7.69 (dd, J = 5.5, 3.0 Hz, 2H), 7.22 – 7.15 (m, 2H), 7.14 – 7.03 (m, 2H), 6.73 (s, 1H), 5.16 (dd, J = 9.2, 7.4 Hz, 1H), 4.07 (d, J = 5.1 Hz, 2H), 3.73 (s, 3H), 3.60 – 3.48 (m, 2H), 1.19 (s, 9H).

13C NMR (101 MHz, CDCl3) δ 170.1, 168.9, 168.2, 150.0, 134.4, 133.4, 131.6, 128.7, 125.7, 123.6, 55.9, 52.6, 41.7, 34.5, 34.5, 31.4.

HRMS (ESI) m/z calcd for C H N O +: 423.1914; found: 423.1920.
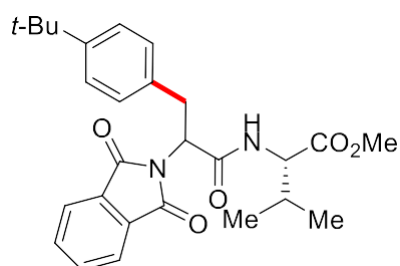
Methyl (3-(4-(tert-butyl)phenyl)-2-(1,3-dioxoisoindolin-2-yl)propanoyl)-L-valinate (51)

Prepared according to the GP1, using 5-(4-(tert-butyl)phenyl)-5H-thianthren-5-ium tetrafluoroborate (87.3 mg, 0.20 mmol, 1.0 equiv.) and methyl (2-(1,3-dioxoisoindolin-2- yl)acryloyl)-L-valinate (330.4 mg, 1.0 mmol, 5.0 equiv.). The crude mixture was purified by flash column chromatography (n-pentane/EtOAc: 7/3 → 1/1) to afford product 51 (65.1 mg, 70% yield, 1/1 dr by 1H-NMR) as white solid.

1H-NMR (400 MHz, CDCl3) δ 7.83 – 7.75 (m, 2H), 7.72 – 7.65 (m, 2H), 7.23 – 7.17 (m, 2H), 7.16 – 7.09 (m, 2H), 6.74 – 6.52 (m, 1H), 5.22 – 5.11 (m, 1H), 4.62 – 4.45 (m, 1H), 3.69 (s, 3H), 3.62 – 3.44 (m, 2H), 2.27 – 2.05 (m, 1H), 1.20 (s, 4.5H), 1.20 (s, 4.5H), 0.92 – 0.86 (m, 3H), 0.83 (d, J = 6.9 Hz, 1.5H), 0.80 (d, J = 6.9 Hz, 1.5H).

13C-NMR (101 MHz, CDCl3) δ 172.2, 172.1, 168.7, 168.6, 168.2, 168.2, 150.1*, 134.3, 134.3, 133.5, 133.4, 131.7*, 128.7, 128.7, 125.8, 125.7, 123.6*, 57.7, 57.5, 56.0, 55.9, 52.3*, 34.8, 34.6, 34.5*, 31.5, 31.3*, 31.2, 19.0, 19.0, 17.8, 17.7. *(Peaks denoted with * correspond to both diastereomers)*

HRMS (ESI) m/z calcd for $C_{27}H_{33}N_2O_5^+$: 465.2384; found: 465.2384.
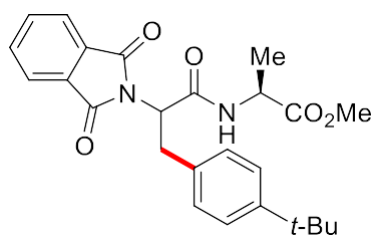
Methyl (3-(4-(tert-butyl)phenyl)-2-(1,3-dioxoisoindolin-2-yl)propanoyl)-L-alaninate (52)

Prepared according to the GP1, using 5-(4-(tert-butyl)phenyl)-5H-thianthren-5-ium tetrafluoroborate (87.3 mg, 0.20 mmol, 1.0 equiv.) and methyl (2-(1,3-dioxoisoindolin-2- yl)acryloyl)-L-alaninate (302.2 mg, 1.0 mmol, 5.0 equiv.). The crude mixture was purified by flash column chromatography (n-pentane/EtOAc: 7/3 → 5/4) to afford product 52 (53.2 mg, 61% yield, 1/1 dr by 1H-NMR) as white solid.

1H NMR (400 MHz, CDCl3) δ 7.79 – 7.73 (m, 2H), 7.70 – 7.63 (m, 2H), 7.20 – 7.13 (m, 2H), 7.11 – 7.04 (m, 2H), 6.66 (d, J = 7.2 Hz, 1H), 5.11 – 4.99 (m, 1H), 4.61 – 4.44 (m, 1H), 3.64 (s, 3H), 3.53 – 3.36 (m, 2H), 1.38 (d, J = 7.1Hz, 1.5H), 1.37 (d, J = 7.1Hz, 1.5H),1.12 (s, 9H).

13C NMR (101 MHz, CDCl3) δ 173.2, 173.2, 168.2, 168.2, 168.1, 168.1, 150.0, 149.9, 134.3*, 133.5*, 131.6*, 128.7*, 125.6, 125.6, 123.6, 123.6, 55.9, 55.8, 52.6*, 48.6, 48.5, 34.5*, 34.5*, 31.3*, 18.4, 18.4. *(Peaks denoted with * correspond to both diastereomers)*

HRMS (ESI) m/z calcd for C H N O +: 437.2071; found: 437.2076.

Methyl (3-(4-(tert-butyl)phenyl)-2-(1,3-dioxoisoindolin-2-yl)propanoyl)-L-leucinate (53)

Prepared according to the GP1, using 5-(4-(tert-butyl)phenyl)-5H-thianthren-5-ium tetrafluoroborate (87.3 mg, 0.20 mmol, 1.0 equiv.) and methyl (2-(1,3-dioxoisoindolin-2- yl)acryloyl)-L-leucinate (344.3 mg, 1.0 mmol, 5.0 equiv.). The crude mixture was purified by flash column chromatography (n-pentane/EtOAc: 7/3 → 2/1) to afford product 53 (68.9 mg, 72% yield, 1/1 dr by 1H-NMR) as white solid.

1H NMR (400 MHz, CDCl3) δ 7.81 – 7.74 (m, 2H), 7.71 – 7.64 (m, 2H), 7.21 – 7.16 (m, 2H), 7.14 – 7.07 (m, 2H), 6.58 – 6.43 (m, 1H), 5.23 – 5.07 (m, 1H), 4.69 – 4.54 (m, 1H), 3.67 (s, 3H), 3.62 – 3.41 (m, 2H), 1.66 – 1.43 (m, 3H), 1.20 (s, 4.5H), 1.19 (s, 4.5H), 0.95 – 0.81 (m, 6H).

13C NMR (101 MHz, CDCl3) δ 173.2, 173.2, 168.5, 168.4, 168.1, 168.1, 150.0, 150.0, 134.3, 134.3, 133.5, 133.5, 131.7*, 128.7, 128.7, 125.7*, 123.6*, 55.9, 55.8, 52.4*, 51.2, 51.2, 41.6, 41.6, 34.6*, 34.5*, 31.4*, 24.9, 24.9, 22.9, 22.8, 22.1, 22.0. *(Peaks denoted with * correspond to both diastereomers)*

HRMS (ESI) m/z calcd for C H N O +: 479.2540; found: 479.2546
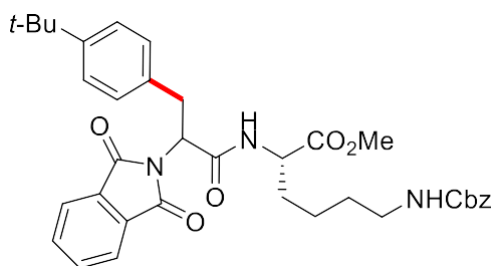
Methyl N6-((benzyloxy)carbonyl)-N2-(3-(4-(tert-butyl)phenyl)-2-(1,3-dioxoisoindolin-2-yl)propanoyl)-L-lysinate (54)

Prepared according to the GP1, using 5-(4-(tert-butyl)phenyl)-5H-thianthren-5-ium tetrafluoroborate (87.3 mg, 0.20 mmol, 1.0 equiv.) and methyl N6-((benzyloxy)carbonyl)-N2- (2-(1,3-dioxoisoindolin-2-yl)acryloyl)-L-lysinate (493.5 mg, 1.0 mmol, 5.0 equiv.). The crude mixture was purified by flash column chromatography (n-pentane/EtOAc: 9/1 → 1/1) to afford product 54 (84.0 mg, 67% yield, 1/1 dr by 1H-NMR) as white solid.

1H-NMR (400 MHz, CDCl3) δ 7.80 – 7.70 (m, 2H), 7.68 – 7.56 (m, 2H), 7.40 – 7.27 (m, 5H), 7.21 – 7.12 (m, 2H), 7.12 – 7.03 (m, 2H), 6.89 – 6.62 (m, 1H), 5.24 – 4.99 (m, 4H), 4.71 – 4.52 (m, 1H), 3.69 (s, 1.5H), 3.66 (s, 1.5H), 3.62 – 3.39 (m, 2H), 3.28 – 3.06 (m, 2H), 1.95 – 1.80 (m, 1H), 1.71 – 1.59 (m, 1H), 1.58 – 1.44 (m, 2H), 1.44 – 1.27 (m, 2H), 1.19 (s, 4.5H), 1.18 (s, 4.5H).

13C-NMR (101 MHz, CDCl3) δ 172.6, 172.5, 168.5, 168.4, 168.1, 168.1, 156.7, 156.6, 150.0, 149.9, 136.8, 136.8, 134.3, 134.3, 133.5, 133.3, 131.6, 131.6, 128.7, 128.6, 128.6, 128.6, 128.2*, 128.1, 125.6, 125.5, 123.6*, 66.7, 66.7, 55.6, 55.6, 52.6, 52.5, 52.4, 52.2, 40.7, 40.6, 34.4, 34.4*, 32.0, 31.8, 31.3*, 29.4, 29.2, 22.4, 22.1. *(Peaks denoted with * correspond to both diastereomers)*

HRMS (ESI) m/z calcd for C36H42N3O7+: 628.3017; found: 628.3013.
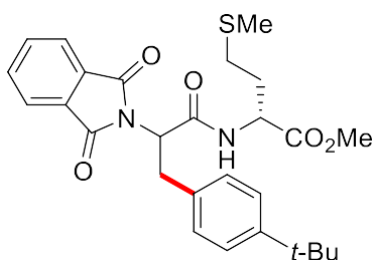
Methyl (3-(4-(tert-butyl)phenyl)-2-(1,3-dioxoisoindolin-2-yl)propanoyl)-L-methioninate (55)

Prepared according to the GP1, using 5-(4-(tert-butyl)phenyl)-5H-thianthren-5-ium tetrafluoroborate (87.3 mg, 0.20 mmol, 1.0 equiv.) and methyl (2-(1,3-dioxoisoindolin-2-yl)acryloyl)-L-methioninate (362.4 mg, 1.0 mmol, 5.0 equiv.). The crude mixture was purified by flash column chromatography (n-pentane/EtOAc: 7/3 → 1/2) to afford product 55 (62.5 mg, 63% yield, 1/1 dr by 1H-NMR) as white solid.

1H NMR (400 MHz, CDCl3) δ 7.80 – 7.74 (m, 2H), 7.72 – 7.65 (m, 2H), 7.22 – 7.13 (m, 2H), 7.13 – 7.04 (m, 2H), 6.94 – 6.83 (m, 1H), 5.19 – 5.08 (m, 1H), 4.75 – 4.66 (m, 1H), 3.71 (s, 1.5H), 3.69 (m, 1.5H), 3.61 – 3.41 (m, 2H), 2.48 – 2.41 (m, 2H), 2.15 – 2.09 (m, 1H), 2.03 (s, 1.5H), 2.00 (m, 1.5H), 1.99 – 1.90 (m, 1H), 1.19 (s, 4.5H), 1.18 (m, 4.5H).

13C NMR (101 MHz, CDCl3) δ 172.1, 172.1, 168.5, 168.4, 168.1, 168.0, 150.0, 149.9, 134.3, 134.3, 133.5, 133.4, 131.6, 131.6, 128.7, 128.7, 125.7, 125.6, 123.6, 123.6, 55.8, 55.6, 52.7, 52.7, 52.1, 52.0, 34.5, 34.4, 34.4, 34.4, 31.3*, 31.3, 31.3, 30.0, 29.9, 15.5, 15.5. *(Peaks denoted with * correspond to both diastereomers)*

HRMS (ESI) m/z calcd for $C_{27}H_{33}N_2O_5S^+$: 497.2105; found: 497.2110.
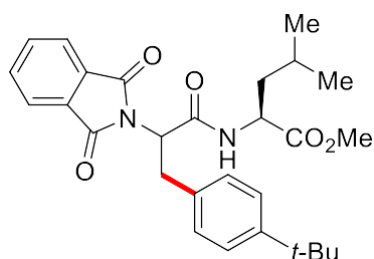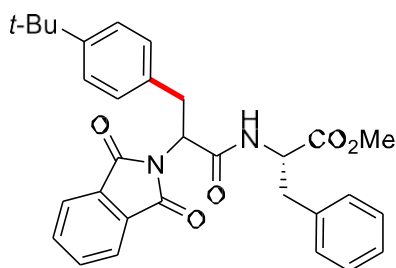
Methyl (3-(4-(tert-butyl)phenyl)-2-(1,3-dioxoisoindolin-2-yl)propanoyl)-L-phenylalaninate (56)

Prepared according to the GP1, using 5-(4-(tert-butyl)phenyl)-5H-thianthren-5-ium tetrafluoroborate (87.3 mg, 0.20 mmol, 1.0 equiv.) and methyl (2-(1,3-dioxoisoindolin-2-yl)acryloyl)-L-phenylalaninate (378.4 mg, 1.0 mmol, 5.0 equiv.). The crude mixture was purified by flash column chromatography (n-pentane/EtOAc: 9/1 → 1/1) to afford product 56

(75.8 mg, 74% yield, 1.6/1 dr by 1H-NMR) as white solid.

1H-NMR (400 MHz, CDCl3) δ 7.81 – 7.74 (m, 2H), 7.74 – 7.66 (m, 2H), 7.21 – 7.08 (m, 5H), 7.08 – 6.98 (m, 4H), 6.68 (d, J = 7.6 Hz, 0.4H), 6.51 (d, J = 7.6 Hz, 0.6H), 5.12 – 5.00 (m, 1H), 4.91 – 4.82 (m, 1H), 3.71 (s, 1.2H), 3.70 (s, 1.8H), 3.54 – 3.38 (m, 2H), 3.22 – 2.96 (m, 2H), 1.19 (s, 9H).

13C-NMR (101 MHz, CDCl3) δ 171.7, 171.7, 168.3, 168.2, 168.1, 168.0, 150.0, 149.9, 135.7*, 134.3, 134.3, 133.5, 133.4, 131.6, 131.6, 129.4, 129.3, 128.7, 128.6, 128.6, 128.6, 127.2, 127.2, 125.7, 125.6, 123.6, 123.6, 56.0, 55.6, 53.5*, 52.5, 52.5, 37.8, 37.6, 34.5*, 34.4, 34.2, 31.3*.

*(Peaks denoted with * correspond to both diastereomers)*

HRMS (ESI) m/z calcd for C H N O +: 513.2384; found: 513.2382.
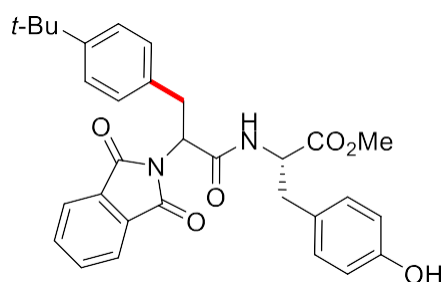
Methyl (3-(4-(tert-butyl)phenyl)-2-(1,3-dioxoisoindolin-2-yl)propanoyl)-L-tyrosinate (57)

Prepared according to the GP1, using 5-(4-(tert-butyl)phenyl)-5H-thianthren-5-ium tetrafluoroborate (87.3 mg, 0.20 mmol, 1.0 equiv.) and methyl (2-(1,3-dioxoisoindolin-2-yl)acryloyl)-L-tyrosinate (394.4 mg, 1.0 mmol, 5.0 equiv.). The crude mixture was purified by flash column chromatography (n-pentane/EtOAc: 9/1 → 1/1) to afford product 57 (66.5 mg, 63% yield, 1/1 dr by 1H-NMR) as white solid. Following the GP2 on 0.20 mmol scale the product 57 was isolated in 69% yield.

1H-NMR (400 MHz, CDCl3) δ 7.78 – 7.73 (m, 2H), 7.70 – 7.63 (m, 2H), 7.21 – 7.11 (m, 2H), 7.07 – 7.01 (m, 2H), 6.91 – 6.81 (m, 2H), 6.78 – 6.71 (m, 0.5H), 6.61 – 6.48 (m, 2.5H), 5.95 (brs, 1H), 5.18 – 5.01 (m, 1H), 4.93 – 4.75 (m, 1H), 3.71 (s, 1.5H), 3.70 (s, 1.5H), 3.55 – 3.40 (m, 2H), 3.21 – 2.88 (m, 2H), 1.19 (s, 4.5H), 1.18 (s, 4.5H).

13C-NMR (101 MHz, CDCl3) δ 172.0, 171.9, 168.5, 168.5, 168.2, 168.0, 155.2*, 150.0, 149.9, 134.4, 134.3, 133.4, 133.3, 131.5, 131.5, 130.5, 130.4, 128.7, 128.6, 127.1*, 125.7, 125.6, 123.6*, 115.6, 115.5, 56.0, 55.6, 53.7, 53.7, 52.6*, 37.1, 36.9, 34.5, 34.4, 34.4, 34.1, 31.3*.

*(Peaks denoted with * correspond to both diastereomers)*

HRMS (ESI) m/z calcd for C31H33N2O6+: 529.2333; found: 526.2337.
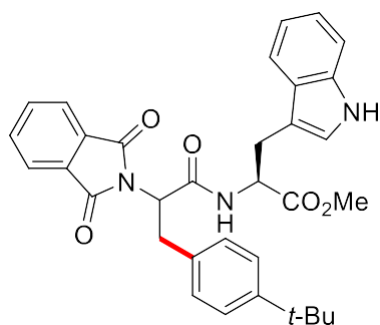
Methyl (3-(4-(tert-butyl)phenyl)-2-(1,3-dioxoisoindolin-2-yl)propanoyl)-L-tryptophanate (58)

Prepared according to the GP1, using 5-(4-(tert-butyl)phenyl)-5H-thianthren-5-ium tetrafluoroborate (87.3 mg, 0.20 mmol, 1.0 equiv.) and methyl (2-(1,3-dioxoisoindolin-2-yl)acryloyl)-L-tryptophanate (417.2 mg, 1.0 mmol, 5.0 equiv.). The crude mixture was purified by flash column chromatography (toluene/EtOAc: 7/3 → 2/1) to afford product 58 (77.2 mg, 70% yield, 1/1 dr by 1H-NMR) as white solid. Following the GP2 on 0.20 mmol scale the product 58 was isolated in 63% yield.

1H NMR (400 MHz, CDCl3) δ 8.27 – 8.12 (m, 1H), 7.77 – 7.28 (m, 4H), 7.49 – 7.43 (m, 1H), 7.32 – 6.88 (m, 8H), 6.78 (d, J = 7.8 Hz, 0.5H), 6.62 (d, J = 7.6 Hz, 0.5H), 5.18 – 5.03 (m, 1H), 5.00 – 4.87 (m, 1H), 3.66 (s, 1.5H), 3.65 (s, 1.5H), 3.51 – 3.38 (m, 2H), 3.37 – 3.24 (m, 2H), 1.18 (s, 9H).

13C NMR (101 MHz, CDCl3) δ 172.1, 172.0, 168.4, 168.4, 168.1, 168.0, 149.9, 149.8, 136.1, 136.0, 134.2, 134.1, 133.4, 133.3, 131.5, 131.5, 128.6, 128.6, 127.7, 127.5, 125.6, 125.5, 123.5, 123.5, 123.1, 123.1, 122.2, 122.2, 119.7, 119.7, 118.5, 118.4, 111.4, 111.2, 109.8, 109.7, 55.9, 55.6, 53.5*, 52.5, 52.5, 34.4*, 34.2*, 31.3*, 27.4, 27.4. *(Peaks denoted with * correspond to both diastereomers)*

HRMS (ESI) m/z calcd for C H N O +: 552.2493; found: 552.2498.
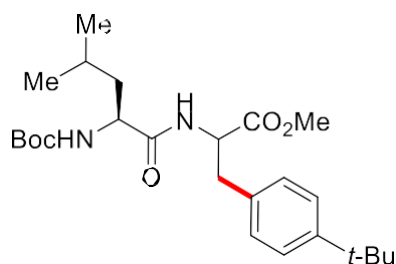
Methyl 2-((S)-2-((tert-butoxycarbonyl)amino)-4-methylpentanamido)-3-(4-(tert-butyl)phenyl)propanoate (59)

Prepared according to the GP1, 5-(4-(tert-butyl)phenyl)-5H-thianthren-5-ium tetrafluoroborate (261.9 mg, 0.60 mmol, 3.0 equiv.) and methyl (S)-2-(2-((tert-butoxycarbonyl)amino)-4- methylpentanamido)acrylate (31.4 mg, 0.20 mmol, 1.0 equiv.). The crude mixture was purified by flash column chromatography (n-pentane/EtOAc: 8/2 → 1/1) to afford product 59 (57.3 mg, 64% yield, 1/1 dr by 1H-NMR) as white solid.

1H-NMR (400 MHz, CDCl3) δ 7.25 (d, J = 8.0 Hz, 2H), 7.00 (d, J = 8.0 Hz, 2H), 6.64 (d, J = 7.9 Hz, 0.5H), 6.53 (d, J = 7.9 Hz, 0.5H), 4.90 (d, J = 8.1 Hz, 1H), 4.80 (ddd, J = 14.5, 8.4, 6.1 Hz, 1H), 4.23 – 3.96 (m, 1H), 3.72 – 3.59 (m, 3H), 3.23 – 2.85 (m, 2H), 1.68 – 1.48 (m, 2H), 1.43 – 1.35 (m, 10H), 1.25 (s, 9H), 0.93 – 0.75 (m, 6H).

13C-NMR (101 MHz, CDCl3) δ 172.2, 172.2, 171.9, 171.8, 155.6, 155.5, 149.9, 149.9, 132.7*, 129.0, 128.9, 125.5, 125.5, 79.9*, 53.1, 53.0, 52.9, 52.9, 52.3, 52.2, 41.3*, 37.3, 37.3, 34.4*, 31.3*, 28.3*, 24.7*, 22.9*, 22.0*. *(Peaks denoted with * correspond to both diastereomers)*

HRMS (ESI) m/z calcd for C H N O +: 449.3010; found: 449.3026.
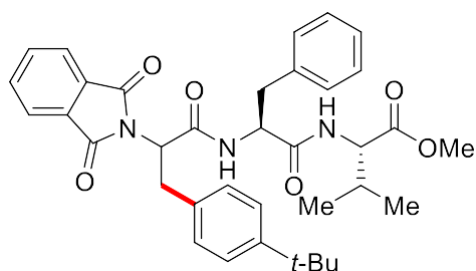
Methyl (3-(4-(tert-butyl)phenyl)-2-(1,3-dioxoisoindolin-2-yl)propanoyl)-L-phenylalanyl-L-valinate (60)

Prepared according to the GP1, using 5-(4-(tert-butyl)phenyl)-5H-thianthren-5-ium tetrafluoroborate (87.3 mg, 0.20 mmol, 1.0 equiv.) and methyl (2-(1,3-dioxoisoindolin-2-yl)acryloyl)-L-phenylalanyl-L-valinate (477.5 mg, 1.0 mmol, 5.0 equiv.). The crude mixture was purified by flash column chromatography (n-pentane/EtOAc: 9/1 → 1/1) to afford product 60 (94.2 mg, 77% yield, 2/1 dr by 1H-NMR) as white solid.

1H NMR (400 MHz, CDCl3) δ 7.78 – 7.64 (m, 4H), 7.18 – 6.98 (m, 9H), 6.79 (d, J = 7.2, 0.3H), 6.71 (d, J = 7.2, 0.7H), 5.14 – 5.00 (m, 1H), 4.75 – 4.62 (m, 1H), 4.44 – 4.35 (m, 1H), 3.70 (s, 2H), 3.66 (s, 1H), 3.52 – 3.34 (m, 2H), 3.22 – 3.07 (m, 1H), 3.07 – 2.95 (m, 1H), 2.20 – 2.04 (m, 1H), 1.19 (s, 3H), 1.17 (s, 6H), 0.90 – 0.76 (m, 6H).

13C NMR (101 MHz, CDCl3) δ 171.7*, 170.5, 170.4, 168.7, 168.7, 168.0, 167.9, 149.9*, 136.4, 136.2, 134.3, 134.3, 133.3*, 131.6, 131.5, 129.4*, 128.7, 128.6*, 128.6, 127.1, 127.0, 125.6, 125.6, 123.6, 123.6, 57.7, 57.6, 56.0, 55.6, 55.0, 54.4, 52.2, 52.2, 37.6, 37.5, 34.4, 34.4, 34.3, 34.2, 31.3, 31.3, 31.1, 31.1, 19.0, 18.9, 17.9, 17.8. (Peaks denoted with * correspond to both diastereomers)

HRMS (ESI) m/z calcd for C H N O +: 612.3068; found: 612.3074.
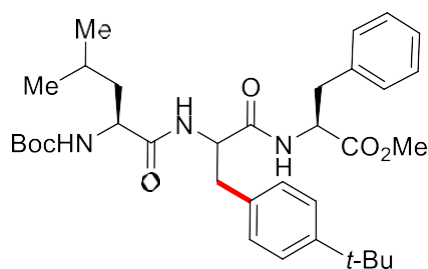
Methyl (2-((S)-2-((tert-butoxycarbonyl)amino)-4-methylpentanamido)-3-(4-(tert-butyl)phenyl)propanoyl)-L-phenylalaninate (61)

Prepared according to the GP1, 5-(4-(tert-butyl)phenyl)-5H-thianthren-5-ium tetrafluoroborate

261.9 mg, 0.60 mmol, 3.0 equiv.) and methyl (2-((S)-2-((tert-butoxycarbonyl)amino)-4-methylpentanamido)acryloyl)-L-phenylalaninate (46.1 mg, 0.20 mmol, 1.0 equiv.). The crude mixture was purified by flash column chromatography (n-pentane/EtOAc: 8/2 → 1/1) to afford product 61 (50.1 mg, 42% yield, 1/1 dr by 1H-NMR) as white solid.

1H-NMR (400 MHz, CDCl3) δ 7.26 – 7.09 (m, 5H), 7.04 (d, J = 8.3 Hz, 1H), 6.99 – 6.86 (m, 3.5H), 6.76 (d, J = 7.9 Hz, 1H), 6.54 (d, J = 7.6 Hz, 0.5H), 5.04 (d, J = 7.7 Hz, 0.5H), 4.97 (d, J = 7.6 Hz, 0.5H), 4.78 – 4.56 (m, 2H), 4.17 – 3.86 (m, 1H), 3.56 (s, 1.5H), 3.52 (s, 1.5H), 3.05 – 2.79 (m, 4H), 1.60 – 1.36 (m, 3H), 1.35 (s, 4.5H), 1.32 (s, 4.5H), 1.19 (s, 4.5H), 1.18 (s, 4.5H), 0.86 – 0.70 (m, 6H).

13C-NMR (101 MHz, CDCl3) δ 172.7, 172.5, 171.7, 171.3, 170.6, 170.4, 155.6*, 149.7, 149.7, 136.0, 135.8, 133.4, 133.3, 129.3, 129.2, 129.2, 129.1, 128.6, 128.5, 127.1, 127.1, 125.5*, 80.0, 79.9, 54.1, 54.0, 53.5*, 53.5, 53.3, 52.2, 52.2, 41.5, 41.4, 38.0, 37.9, 37.5, 37.4, 34.4*, 31.4*, 28.4*, 24.7, 24.6, 23.0, 22.9, 22.2, 21.9. (Peaks denoted with * correspond to both diastereomers)

HRMS (ESI) m/z calcd for C34H50N3O6+: 596.3694; found: 596.3695.
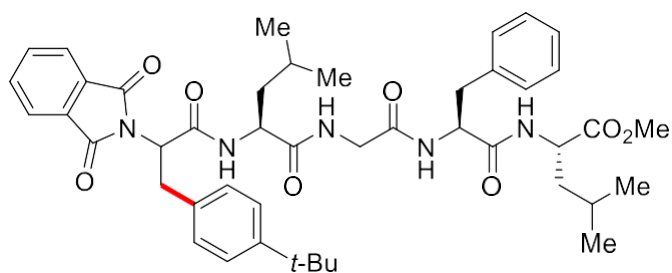
Methyl (3-(4-(tert-butyl)phenyl)-2-(1,3-dioxoisoindolin-2-yl)propanoyl)-L-leucylglycyl-L- phenylalanyl-L-leucinate (62)

Prepared according to the GP1, 5-(4-(tert-butyl)phenyl)-5H-thianthren-5-ium tetrafluoroborate (87.3 mg, 0.20 mmol, 1.0 equiv.) and methyl (2-(isoindolin-2-yl)acryloyl)-L-leucylglycyl-L- phenylalanyl-L-leucinate (633.4 mg, 1.0 mmol, 5.0 equiv.). The crude mixture was purified by flash column chromatography (CH2Cl2/EtOAc: 8/2 → 1/2) to afford product 62 (125.6 mg, 79% yield, 1/1 dr by 1H-NMR) as white solid.

1H-NMR (400 MHz, CDCl3) δ 7.76 – 7.39 (m, 5H), 7.23 – 7.05 (m, 11H), 7.01 (d, J = 8.0 Hz, 1H), 5.26 – 5.10 (m, 1H), 4.90 – 4.75 (m, 1H), 4.61 – 4.41 (m, 2H), 3.96 – 3.76 (m, 2H), 3.64 (s, 1.5H), 3.61 (s, 1.5H), 3.60 – 3.31 (m, 2H), 3.19 – 3.02 (m, 1H), 3.01 – 2.88 (m, 1H), 1.64 – 1.39 (m, 6H), 1.16 (s, 9H), 0.94 – 0.71 (m, 12H).

13C-NMR (101 MHz, CDCl3) δ 173.4, 173.3, 172.9, 172.7, 170.9, 170.9, 169.4, 169.3, 168.9, 168.8, 168.1, 168.0, 150.0, 149.9, 136.8, 136.7, 134.2, 134.2, 133.4, 133.3, 131.6, 131.5, 129.4*, 128.7, 128.6, 128.5, 128.4, 126.8*, 125.6, 125.5, 123.5, 123.4, 55.1*, 54.5, 54.5, 52.6, 52.6, 52.3*, 50.9*, 43.4, 43.1, 41.1, 41.0, 40.9, 40.5, 38.3, 38.1, 34.5*, 34.4, 34.4, 31.3*, 24.8, 24.8, 24.7*, 23.1, 23.0, 22.8, 22.8, 22.0*, 21.9*. (*Peaks denoted with * correspond to both diastereomers*)

HRMS (ESI) m/z calcd for C H N O +: 796.4280; found: 796.4283.
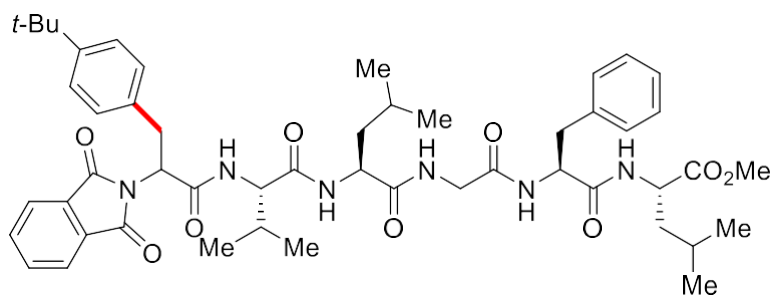
Methyl (3-(4-(tert-butyl)phenyl)-2-(1,3-dioxoisoindolin-2-yl)propanoyl)-L-valyl-L-leucylglycyl-L-phenylalanyl-L-leucinate (63)

Prepared according to the GP1, 5-(4-(tert-butyl)phenyl)-5H-thianthren-5-ium tetrafluoroborate (87.3 mg, 0.20 mmol, 1.0 equiv.) and methyl (2-(1,3-dioxoisoindolin-2-yl)acryloyl)-L-valyl-L- leucylglycyl-L-phenylalanyl-L-leucinate (760.2 mg, 1.0 mmol, 5.0 equiv.). The crude mixture was purified by flash column chromatography (CH2Cl2/EtOAc: 9/1 → 1/1) to afford product 63 (134.2 mg, 75% yield, 1/1 dr by 1H-NMR) as white solid.

1H-NMR (300 MHz, DMSO-d6) δ 9.42 (d, J = 8.5 Hz, 0.5H), 8.46 – 8.17 (m, 2.5H), 8.12 – 7.88 (m, 3H), 7.86 – 7.71 (m, 4H), 7.35 – 6.97 (m, 8H), 5.14 (dd, J = 11.4, 5.3 Hz, 0.5H), 5.03 (dd, J = 10.8, 5.5 Hz, 0.5H), 4.75 – 4.50 (m, 1H), 4.38 – 4.10 (m, 3H), 3.82 – 3.38 (m, 7H), 3.04 (dd, J = 13.9, 4.4 Hz, 1H), 2.76 (dd, J = 13.9, 9.3 Hz, 1H), 2.18 – 1.87 (m, 1H), 1.70 – 1.37 (m, 6H), 1.39 – 0.93 (m, 9H), 0.97 – 0.68 (m, 18H).

13C-NMR (101 MHz, CDCl3) δ 172.8*, 172.2, 172.0, 171.2, 170.9, 170.7, 169.5, 168.3, 168.3, 168.1, 168.0, 167.8, 167.7, 148.7, 148.7, 137.7, 137.7, 134.6*, 134.5, 134.5, 131.4, 131.2, 129.2*, 128.4, 128.4, 128.1*, 126.3*, 125.0, 124.9, 123.1, 123.0, 59.2, 58.7, 58.3, 55.2, 54.6, 53.6*, 51.9*, 51.3, 51.2, 50.4, 41.8, 41.8, 40.8, 40.8, 40.7, 37.7, 34.1, 34.0, 33.8, 33.6, 31.1*, 30.2, 29.9, 29.7, 24.2, 24.2, 24.1, 24.0, 23.0, 23.0, 23.0, 22.8, 21.6, 21.5, 21.4, 21.4, 19.4, 19.4, 19.1, 18.6, 18.3. (Peaks denoted with * correspond to both diastereomers) HRMS (ESI) m/z calcd for C H N O +: 895.4964; found: 895.4958.
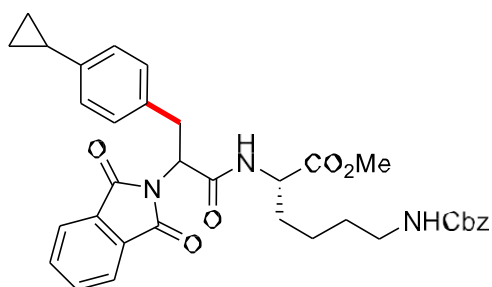
Methyl N6-((benzyloxy)carbonyl)-N2-(3-(4-cyclopropylphenyl)-2-(1,3-dioxoisoindolin-2-yl)propanoyl)-L-lysinate (64)

Prepared according to the GP1, using 5-(4-cyclopropylphenyl)-5H-thianthren-5-ium tetrafluoroborate (84.1 mg, 0.20 mmol, 1.0 equiv.) and methyl N6-((benzyloxy)carbonyl)-N2- (2-(1,3-dioxoisoindolin-2-yl)acryloyl)-L-lysinate (493.5 mg, 1.0 mmol, 5.0 equiv.). The crude mixture was purified by flash column chromatography (n-pentane/EtOAc: 9/1 → 1/1) to afford product 64 (92.9 mg, 76% yield, 1/1 dr by 1H-NMR) as white solid. Following the GP2 on 1.00 mmol scale the product 64 was isolated in 82% yield.

1H-NMR (400 MHz, CDCl3) δ 7.81 – 7.70 (m, 2H), 7.69 – 7.57 (m, 2H), 7.44 – 7.29 (m, 5H), 7.13 – 6.97 (m, 2H), 6.92 – 6.82 (m, 2H), 6.80 – 6.72 (m, 1H), 5.21 – 5.02 (m, 4H), 4.72 – 4.55 (m, 1H), 3.70 (s, 1.5H), 3.65 (s, 1.5H), 3.61 – 3.40 (m, 2H), 3.23 – 3.10 (m, 2H), 1.91 – 1.82 (m, 1H), 1.80 – 1.71 (m, 1H), 1.59 – 1.44 (m, 2H), 1.37 – 1.29 (m, 1H), 1.25 – 1.13 (m, 1H), 1.10 – 0.94 (m, 1H), 0.89 – 0.80 (m, 2H), 0.68 – 0.45 (m, 2H).

13C-NMR (101 MHz, CDCl3) δ 172.6, 172.5, 168.4, 168.4, 168.1, 168.0, 156.6, 156.6, 142.8, 142.7, 136.8, 136.8, 134.3, 134.3, 133.6, 133.3, 131.5, 131.5, 128.9, 128.8, 128.6, 128.6, 128.2, 128.1*, 126.0, 125.9, 123.6*, 66.6, 66.6, 55.6*, 52.6, 52.5, 52.4, 52.2, 40.6, 40.6, 34.5, 34.4, 31.9, 31.8, 29.3, 29.2, 22.3, 22.1, 15.1*, 9.3, 9.2*, 9.2. (Peaks denoted with * correspond to both diastereomers)

HRMS (ESI) m/z calcd for C H N O +: 612.2704; found: 612.2706.
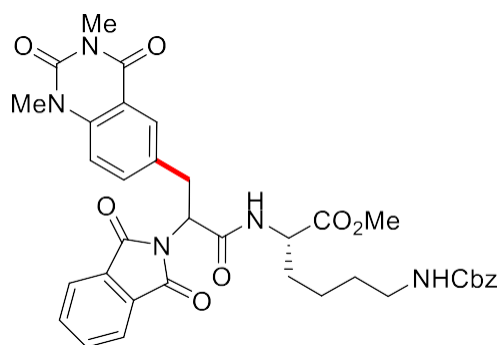
Methyl N6-((benzyloxy)carbonyl)-N2-(3-(1,3-dimethyl-2,4-dioxo-1,2,3,4-tetrahydroquinazolin-6-yl)-2-(1,3-dioxoisoindolin-2-yl)propanoyl)-L-lysinate (65)

Prepared according to the GP1, using 5-(1,3-dimethyl-2,4-dioxo-1,2,3,4-tetrahydroquinazolin- 6-yl)-5H-thianthren-5-ium tetrafluoroborate (98.5 mg, 0.20 mmol, 1.0 equiv.) and methyl N6- ((benzyloxy)carbonyl)-N2-(2-(1,3-dioxoisoindolin-2-yl)acryloyl)-L-lysinate (493.5 mg, 1.0 mmol, 5.0 equiv.). The crude mixture was purified by flash column chromatography (n- pentane/EtOAc: 9/1 → 1/1) to afford product 65 (85.9 mg, 63% yield, 1/1 dr by 1H-NMR) as white solid.

1H-NMR (400 MHz, CDCl3) δ 7.99 (dd, J = 8.1, 2.2 Hz, 1H), 7.78 – 7.71 (m, 2H), 7.67 – 7.57 (m, 2H), 7.54 – 7.47 (m, 1H), 7.37 – 7.27 (m, 5H), 7.07 – 6.97 (m, 1H), 6.87 (d, J = 7.8 Hz, 1H), 5.28 – 5.00 (m, 4H), 4.70 – 4.54 (m, 1H), 3.70 (s, 1.5H), 3.66 – 3.52 (m, 3.5H), 3.49 (s, 3H), 3.37 (s, 3H), 3.27 – 3.07 (m, 2H), 1.92 – 1.80 (m, 1H), 1.76 – 1.58 (m, 1H), 1.58 – 1.24 (m, 4H).

13C-NMR (101 MHz, CDCl3) δ 172.7, 172.6, 168.0*, 167.9, 167.9, 161.6*, 156.7, 156.6, 151.2, 151.1, 139.4, 139.4, 136.8, 136.8, 135.8, 135.7, 134.5, 134.5, 131.9, 131.7, 131.4, 131.4, 129.0*, 128.6, 128.6, 128.2*, 128.1*, 123.8*, 115.5, 115.5, 114.1, 114.1, 66.7, 66.7, 55.4, 55.4, 52.6, 52.6, 52.5, 52.3, 40.7, 40.6, 34.1, 33.9, 31.9, 31.7, 30.8*, 29.4, 29.2, 28.5*, 22.4, 22.2.

*(Peaks denoted with * correspond to both diastereomers)*

HRMS (ESI) m/z calcd for C H N O +: 684.2664; found: 684.2680.
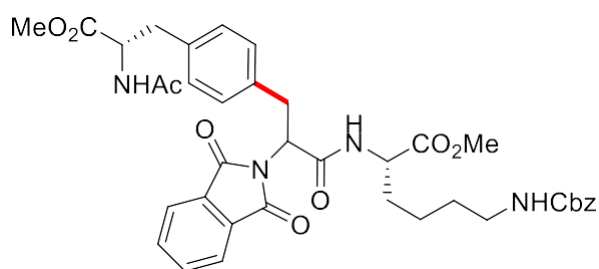
Methyl N2-(3-(4-((S)-2-acetamido-3-methoxy-3-oxopropyl)phenyl)-2-(1,3-dioxoisoindolin-2-yl)propanoyl)-N6-((benzyloxy)carbonyl)-L-lysinate (66)

Prepared according to the GP1, using (S)-5-(4-(2-acetamido-3-methoxy-3-oxopropyl)phenyl)- 5H-thianthren-5-ium tetrafluoroborate (104.6 mg, 0.20 mmol, 1.0 equiv.) and methyl N6- ((benzyloxy)carbonyl)-N2-(2-(1,3-dioxoisoindolin-2-yl)acryloyl)-L-lysinate (493.5 mg, 1.0 mmol, 5.0 equiv.). The crude mixture was purified by flash column chromatography (n- pentane/EtOAc: 9/1 → 1/1) to afford product 66 (92.9 mg, 65% yield, 1/1 dr by 1H-NMR) as white solid.

1H-NMR (400 MHz, CDCl3) δ 7.80 – 7.70 (m, 2H), 7.68 – 7.58 (m, 2H), 7.36 – 7.28 (m, 5H), 7.11 – 7.00 (m, 2H), 6.93 – 6.84 (m, 2H), 6.83 – 6.70 (m, 1H), 6.06 – 6.01 (m, 0.5H), 5.96 – 5.84 (m, 0.5H), 5.23 – 5.00 (m, 4H), 4.83 – 4.67 (m, 1H), 4.65 – 4.52 (m, 1H), 3.68 (s, 1.5H), 3.64 (s, 1.5H), 3.61 (s, 1.5H), 3.58 – 3.34 (m, 3.5H), 3.22 – 3.07 (m, 2H), 3.03 – 2.86 (m, 2H), 1.91 (s, 1.5H), 1.87 (s, 1.5H), 1.71 – 1.56 (m, 1H), 1.55 – 1.41 (m, 3H), 1.38 – 1.23 (m, 2H).

13C-NMR (101 MHz, CDCl3) δ 172.7, 172.7, 172.0, 171.9, 169.7, 169.7, 168.2, 168.2, 168.0, 167.9, 156.7, 156.6, 136.8, 136.7, 135.7, 135.4, 134.8, 134.6, 134.4, 134.4, 131.4*, 129.7, 129.5, 129.2, 129.1, 128.6, 128.6, 128.1, 128.1*, 128.1, 123.7*, 66.6, 66.6, 55.5, 55.4, 53.1, 53.0, 52.6, 52.5, 52.4, 52.3, 52.2, 52.2, 40.6, 40.6, 37.4, 37.4, 34.5, 34.5, 31.9, 31.7, 29.3, 29.2, 23.1, 23.0, 22.3, 22.1. (Peaks denoted with * correspond to both diastereomers)

HRMS (ESI) m/z calcd for C38H43N4O10+: 715.2974; found: 715.2985.
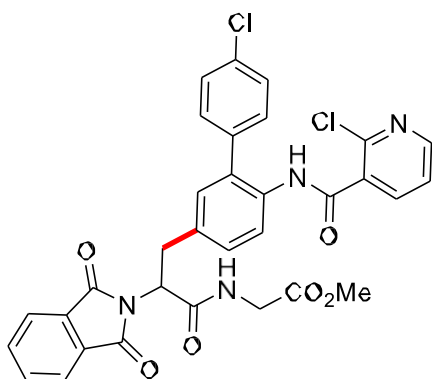
Methyl (3-(4'-chloro-6-(2-chloronicotinamido)-[1,1'-biphenyl]-3-yl)-2-(1,3-dioxoisoindolin-2-yl)propanoyl)glycinate (67)

Prepared according to the GP1, using 5-(4'-chloro-6-(2-chloronicotinamido)-[1,1'-biphenyl]-3- yl)-5H-thianthren-5-ium tetrafluoroborate (129.1 mg, 0.20 mmol, 1.0 equiv.) and methyl (2-

(1,3-dioxoisoindolin-2-yl)acryloyl)glycinate (288.2 mg, 1.0 mmol, 5.0 equiv.). The crude mixture was purified by flash column chromatography (n-pentane/EtOAc: 7/3 → 1/4) to afford product 67 (37.8 mg, 30% yield) as white solid.

1H NMR (400 MHz, CDCl3) δ 8.42 (dd, J = 4.8, 2.0 Hz, 1H), 8.26 (d, J = 8.5 Hz, 1H), 8.09 (dd, J = 7.7, 2.0 Hz, 1H), 8.03 (s, 1H), 7.82 (dd, J = 5.5, 3.1 Hz, 2H), 7.74 (dd, J = 5.5, 3.1 Hz, 2H), 7.38 – 7.28 (m, 3H), 7.26 – 7.22 (m, 1H), 7.13 – 6.99 (m, 3H), 6.76 (t, J = 5.2 Hz, 1H), 5.22 – 5.11 (m, 1H), 4.08 (d, J = 5.1 Hz, 2H), 3.74 (s, 3H), 3.64 – 3.52 (m, 2H).

13C NMR (101 MHz, CDCl3) δ 170.1, 168.6, 168.0, 162.4, 151.5, 146.7, 140.3, 135.9, 134.6, 133.7, 133.4, 132.4, 131.5, 131.0, 130.8, 130.7, 129.5, 129.4, 123.9, 123.0, 122.3, 55.8, 52.6, 41.7, 34.2.

HRMS (ESI) m/z calcd for C H 35Cl N O +: 631.1146; found: 631.1137.
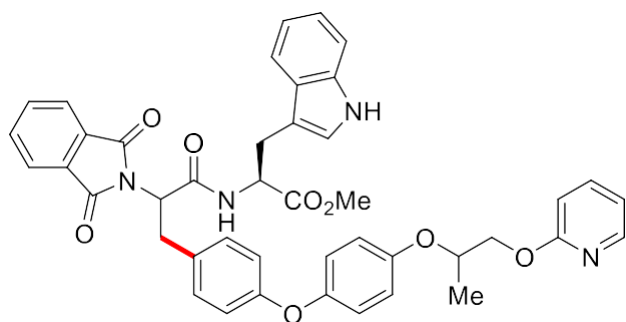
Methyl (2-(1,3-dioxoisoindolin-2-yl)-3-(4-(4-((1-(pyridin-2-yloxy)propan-2-yl)oxy)phenoxy)phenyl)propanoyl)-L-tryptophanate (68)

Prepared according to the GP1, using 5-(4-(4-(2-(pyridin-2-yloxy)propoxy)phenoxy)phenyl)- 5H-thianthren-5-ium tetrafluoroborate (124.7 mg, 0.20 mmol, 1.0 equiv.) and methyl (2-(1,3-

dioxoisoindolin-2-yl)acryloyl)-L-tryptophanate (417.2 mg, 1.0 mmol, 5.0 equiv.). The crude mixture was purified by flash column chromatography (toleuene/EtOAc: 7/3 → 2/1) to afford product 68 (85.6 mg, 58% yield, 1/1 dr by 1H-NMR) as white solid.

1H NMR (400 MHz, CDCl3) δ 8.17 – 8.07 (m, 2H), 7.77 – 7.62 (m, 4H), 7.59 – 7.50 (m, 1H), 7.51 – 7.42 (m, 1H), 7.32 – 7.15 (m, 1H), 7.14 – 6.89 (m, 5H), 6.89 – 6.50 (m, 9H), 5.63 – 5.50 (m, 1H), 5.11 – 4.99 (m, 1H), 4.99 – 4.82 (m, 1H), 4.18 – 4.12 (m, 1H), 4.07 – 4.01 (m, 1H), 3.68 (s, 1.5H), 3.65 (s, 1.5H), 3.49 – 3.37 (m, 2H), 3.37 – 3.22 (m, 2H), 1.47 (d, J = 6.4 Hz, 3H).

13C NMR (101 MHz, CDCl3) δ 172.1, 172.0, 168.2, 168.2, 168.0, 167.9, 163.3, 157.3, 157.2, 155.2, 150.5, 146.9, 138.8, 136.1, 136.0, 134.3, 134.2, 131.5, 131.5, 130.7, 130.6, 130.4, 130.2, 130.2, 127.7, 127.6, 127.2, 123.6, 123.6, 123.1, 123.0, 122.3, 122.3, 120.5, 119.8, 119.8, 118.5, 118.4, 118.1, 116.9, 115.8, 111.8, 111.3, 111.2, 109.9, 109.8, 71.2, 69.4, 56.0, 55.7, 53.6, 53.6, 53.5, 52.6, 52.6, 34.2, 34.0, 27.4, 27.3, 17.1.

HRMS (ESI) m/z calcd for C H N O +: 739.2762; found: 739.2768.
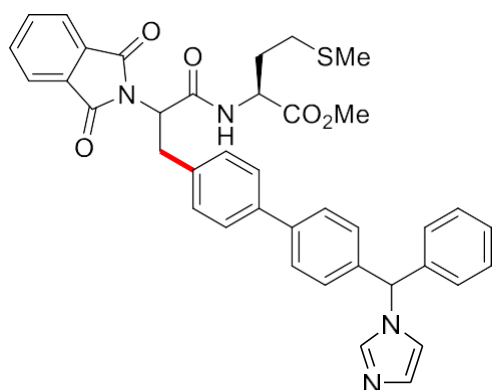
Methyl (3-(4'-((1H-imidazol-1-yl)(phenyl)methyl)-[1,1'-biphenyl]-4-yl)-2-(1,3-dioxoisoindolin-2-yl)propanoyl)-L-methioninate (69)

Prepared according to the GP1, using 5-(4'-((1H-imidazol-1-yl)(phenyl)methyl)-[1,1'-biphenyl]-4-yl)-5H-thianthren-5-ium tetrafluoroborate (122.5 mg, 0.20 mmol, 1.0 equiv.) and methyl (2-(1,3-dioxoisoindolin-2-yl)acryloyl)-L-methioninate (362.4 mg, 1.0 mmol, 5.0 equiv.). The crude mixture was purified by flash column chromatography (n-pentane/EtOAc: 1/4) to afford product 69 (72.6 mg, 54% yield, 1/1 dr by 1H-NMR) as white solid.

1H NMR (400 MHz, CDCl3) δ 7.72 – 7.66 (m, 2H), 7.60 (dd, J = 5.5, 3.1 Hz, 2H), 7.46 – 7.22 (m, 8H), 7.21 – 7.09 (m, 3H), 7.08 – 6.95 (m, 5H), 6.77 (s, 1H), 6.45 (s, 1H), 5.19 – 5.05 (m, 1H), 4.74 – 4.54 (m, 1H), 3.64 (s, 1.5H), 3.61 (s, 1.5H), 3.59 – 3.47 (m, 2H), 2.41 (t, J = 7.4 Hz, 2H), 2.13 – 2.03 (m, 1H), 1.98 – 1.85 (m, 4H).

13C NMR (101 MHz, CDCl3) δ 172.2, 172.1, 168.4, 168.3, 168.0, 167.9, 140.8, 140.7, 139.1*, 138.8, 138.7, 138.1, 138.1, 138.1*, 137.4*, 136.4, 136.2, 134.4*, 131.5, 131.5, 129.5, 129.5, 129.3*, 129.0*, 128.5, 128.5, 128.1, 128.1, 127.4*, 127.3, 127.3, 123.7, 123.6, 119.5*, 64.9*, 55.6, 55.4, 52.7, 52.7, 52.1, 52.1, 34.4*, 31.1*, 30.1, 30.0, 15.5, 15.5. (Peaks denoted with * correspond to both diastereomers)

HRMS (ESI) m/z calcd for C39H37N4O5S+: 673.2479; found: 673.2485

Characterization data for the arylthianthrenium salts 4 and 37
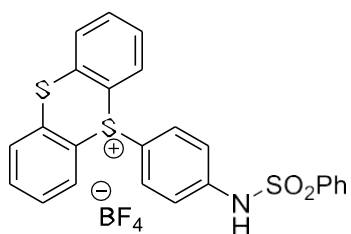
5-(4-(Phenylsulfonamido)phenyl)-5H-thianthren-5-ium tetrafluoroborate (4r)

Prepared according to the GP3, using N-phenylbenzenesulfonamide. The crude mixture was purified by flash column chromatography (CH2Cl2/MeOH: 100/0 → 8/2) to afford product 4r (71% yield) as white solid.

1H-NMR (400 MHz, DMSO-d6) δ 11.06 (brs, 1H), 8.48 (d, J = 7.8 Hz, 2H), 8.01 (d, J = 7.8 Hz, 2H), 7.88 (t, J = 7.3 Hz, 2H), 7.85 – 7.77 (m, 4H), 7.62 (t, J = 7.3 Hz, 1H), 7.55 (t, J = 7.6 Hz, 2H), 7.23 (d, J = 8.8 Hz, 2H), 7.13 (d, J = 8.8 Hz, 2H).

13C NMR (101 MHz, DMSO-d6) δ 142.4, 139.4, 135.8, 135.7, 135.1, 133.9, 130.7, 130.3, 130.1, 130.0, 127.2, 119.9, 118.1.

19F NMR (282 MHz, DMSO-d6) δ -151.66 (s), -151.71 (s).

HRMS (ESI) m/z calcd for C24H18O2S3+ [M-BF4]: 448.0494; found: 448.0490.
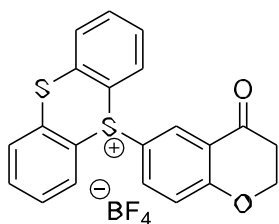
5-(4-Oxochroman-6-yl)-5H-thianthren-5-ium tetrafluoroborate (4u)

Prepared according to the GP3, using chroman-4-one. The crude mixture was purified by flash column chromatography (CH2Cl2/MeOH: 100/0 → 95/5) to afford product 4u (81% yield) as white solid.

1H-NMR (400 MHz, DMSO-d6) δ 8.59 (d, J = 7.8 Hz, 2H), 8.08 (d, J = 7.8 Hz, 2H), 7.93 (t, J = 7.6 Hz, 2H), 7.86 (t, J = 7.3 Hz, 2H), 7.59 (d, J = 2.5 Hz, 1H), 7.37 (dt, J = 9.1, 2.5 Hz, 1H), 7.23 (dd, J = 9.1, 2.5 Hz, 1H), 4.61 (t, J = 6.4 Hz, 2H), 2.82 (t, J = 6.4 Hz, 2H).

13C NMR (101 MHz, DMSO-d6) δ 189.9, 163.9, 135.5, 135.0, 134.8, 134.7, 130.2, 129.7, 127.4, 121.7, 120.8, 119.5, 116.7, 67.3, 36.4.

19F NMR (282 MHz, DMSO-d6) δ -148.23, -148.24.

HRMS (ESI) m/z calcd for C21H15O2S2+ [M-BF4]: 363.0508; found: 363.0520.
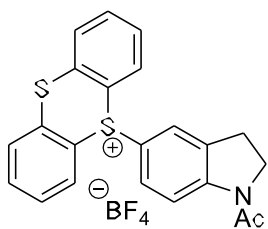
5-(1-Acetylindolin-5-yl)-5H-thianthren-5-ium tetrafluoroborate (4y)

Prepared according to the GP3, using 1-(indolin-1-yl)ethan-1-one. The crude mixture was purified by flash column chromatography (CH2Cl2/MeOH: 100/0 → 80/20) to afford product 4y (75% yield) as pale brown solid.

1H-NMR (400 MHz, DMSO-d6) δ 8.50 (d, J = 7.8 Hz, 2H), 8.11 – 8.03 (m, 3H), 7.91 (t, J = 7.7 Hz, 2H), 7.84 (t, J = 7.7 Hz, 2H), 7.21 (s, 1H), 7.12 (dd, J = 8.8, 2.5 Hz, 1H), 4.10 (t, J = 8.9 Hz, 2H), 3.09 (t, J = 8.9 Hz, 2H), 2.15 (s, 3H).

13C NMR (101 MHz, DMSO-d6) δ 169.8, 146.9, 135.2, 135.1, 135.0, 134.6, 130.2, 129.7, 128.6, 124.6, 119.8, 116.4, 48.6, 27.1, 24.0.

19F NMR (282 MHz, DMSO-d6) δ -148.18 (s), -148.19 (s).

HRMS (ESI) m/z calcd for C22H18NOS2+ [M-BF4]: 376.0824; found: 376.0840.
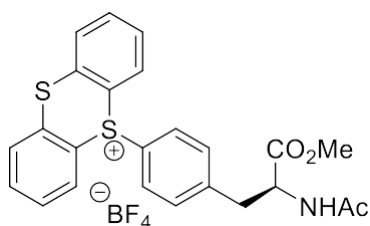
(S)-5-(4-(2-acetamido-3-methoxy-3-oxopropyl)phenyl)-5H-thianthren-5-ium tetrafluoroborate (37i)

Following a modified literature procedure,[7] a Schlenk flask was charged with thianthrene S- oxide (1.2 equiv.), CH2Cl2 (0.2 M) and Ac-Phe-OMe (1.0 equiv.) under a nitrogen atmosphere. The suspension was then cooled to -40 °C, followed by the dropwise addition of Tf2O (1.2 equiv.). The mixture was stirred at -40 °C for 1 h and subsequently at 25 °C for 16 h. At this point, the reaction mixture was concentrated under reduced pressure and diluted with dichloromethane (0.05 M). The CH2Cl2 phase was poured onto a saturated aqueous NaHCO3 solution. The mixture was poured into a separatory funnel, and the layers were separated. The CH2Cl2 layer was washed with aqueous NaBF4 solution (2 X, 5 % w/w), and with water (2 X). The CH2Cl2 layer was dried over Na2SO4, filtered, and the solvent was removed under reduced pressure. The solvent was evaporated under reduced pressure and he crude mixture was purified by flash column chromatography (CH2Cl2/MeOH: 100/0 → 80/20) to afford product 37i (26% yield) as pale brown solid.

1H-NMR (300 MHz, CDCl3) δ 8.52 (ddt, J = 7.0, 3.4, 1.3 Hz, 2H), 7.94 – 7.75 (m, 6H), 7.37 – 7.23 (m, 2H), 7.10 (d, J = 8.6 Hz, 2H), 6.53 (d, J = 7.9 Hz, 1H), 4.77 (ddd, J = 7.9, 7.0, 5.7 Hz, 1H), 3.69 (s, 3H), 3.27 – 3.01 (m, 2H), 1.94 (s, 3H).

13C NMR (75 MHz, CDCl3) δ 171.5, 170.6, 143.3, 136.7, 136.7, 135.4, 135.3, 135.1, 131.9, 130.5, 130.5, 130.4, 128.2, 121.8, 119.0, 119.0, 53.0, 52.7, 37.2, 23.0.

19F NMR (282 MHz, CDCl3) δ -150.65 (s), -150.66 (s).

HRMS (ESI) m/z calcd for C24H22NO3S2+ [M-BF4]: 436.1036; found: 436.1041.

Characterization data for the Dha-containing peptides 48
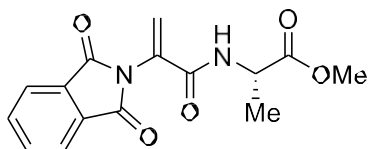
Methyl (2-(1,3-dioxoisoindolin-2-yl)acryloyl)-L-alaninate (48c)

Prepared according to the GP3, using Phth-Ser-OH (1.5 equiv.) and HCl·H-Ala-OMe (1.0 equiv.). The crude mixture was purified by flash column chromatography (n-pentane/EtOAc: 1/4) to afford product 48c (21% yield) as white solid.

1H NMR (400 MHz, CDCl3) δ 7.90 (dd, J = 5.5, 3.1 Hz, 2H), 7.77 (dd, J = 5.5, 3.1 Hz, 2H), 6.64 (d, J = 7.2 Hz, 1H), 6.20 (d, J = 1.4 Hz, 1H), 5.83 (d, J = 1.4 Hz, 1H), 4.67 (dq, J = 7.2, 7.1 Hz, 1H), 3.77 (s, 3H), 1.49 (d, J = 7.1 Hz, 3H).

13C NMR (101 MHz, CDCl3) δ 173.3, 166.5, 162.5, 134.7, 132.9, 131.9, 124.1, 120.4, 52.8, 48.7, 18.5.

HRMS (ESI) m/z calcd for C H N O +: 303.0975; found: 303.0981.
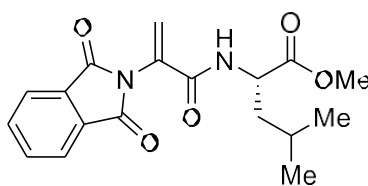
Methyl (2-(1,3-dioxoisoindolin-2-yl)acryloyl)-L-leucinate (48d)

Prepared according to the GP4, using Phth-Ser-OH (1.5 equiv.) and HCl·H-Leu-OMe (1.0 equiv.). The crude mixture was purified by flash column chromatography (n-pentane/EtOAc: 5/4) to afford product 48d (23% yield) as white solid.

1H NMR (400 MHz, CDCl3) δ 7.89 (dd, J = 5.5, 3.1 Hz, 2H), 7.76 (dd, J = 5.5, 3.0 Hz, 2H), 6.49 (d, J = 8.4 Hz, 1H), 6.19 (d, J = 1.4 Hz, 1H), 5.83 (d, J = 1.4 Hz, 1H), 4.73 (td, J = 8.4, 5.0 Hz, 1H), 3.75 (s, 3H), 1.79 – 1.68 (m, 2H), 1.66 – 1.56 (m, 1H), 0.98 – 0.93 (m, 6H).

13C NMR (101 MHz, CDCl3) δ 173.3, 166.5, 162.8, 134.7, 132.9, 131.9, 124.1, 120.3, 52.6, 51.3, 42.0, 24.9, 22.9, 22.1.

HRMS (ESI) m/z calcd for C H N O +: 345.1445; found: 345.1450.
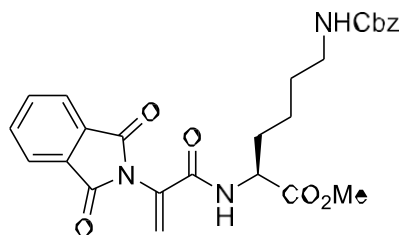
Methyl N6-((benzyloxy)carbonyl)-N2-(2-(1,3-dioxoisoindolin-2-yl)acryloyl)-L-lysinate (48e)

Prepared according to the GP4, using Phth-Ser-OH (1.5 equiv.) and HCl·H-Lys(Cbz)-OMe (1.0 equiv.). The crude mixture was purified by flash column chromatography (n-pentane/EtOAc: 1/1 → 1/4) to afford product 48e (36% yield) as white solid.

1H-NMR (400 MHz, CDCl3) δ 7.84 (dd, J = 5.5, 3.1 Hz, 2H), 7.68 (dd, J = 5.5, 3.1 Hz, 2H), 7.36 – 7.27 (m, 5H), 6.70 (d, J = 8.1 Hz, 1H), 6.17 (s, 1H), 5.81 (s, 1H), 5.25 (t, J = 5.7 Hz, 1H), 5.10 (d, J = 12.2 Hz, 1H), 5.04 (d, J = 12.2 Hz, 1H), 4.69 (td, J = 8.1, 4.6 Hz, 1H), 3.75 (s, 3H), 3.30 – 3.11 (m, 2H), 2.04 – 1.89 (m, 1H), 1.83 – 1.68 (m, 1H), 1.64 – 1.34 (m, 4H).

13C-NMR (101 MHz, CDCl3) δ 172.6, 166.4, 162.9, 156.7, 136.7, 134.6, 132.7, 131.7, 128.5, 128.0, 128.0, 124.0, 119.7, 66.5, 52.6, 52.3, 40.5, 31.9, 29.2, 22.1.

HRMS (ESI) m/z calcd for C H N O +: 494.1922; found: 494.1923.
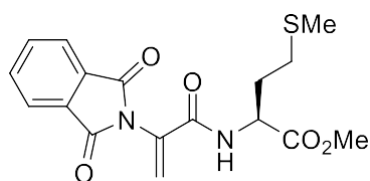
Methyl (2-(1,3-dioxoisoindolin-2-yl)acryloyl)-L-methioninate (48f)

Prepared according to the GP4, using Phth-Ser-OH (1.5 equiv.) and HCl·H-Met-OMe (1.0 equiv.). The crude mixture was purified by flash column chromatography (n-pentane/EtOAc: 1/4) to afford product 48f (19% yield) as white solid.

1H NMR (400 MHz, CDCl3) δ 7.89 (dd, J = 5.5, 3.1 Hz, 2H), 7.76 (dd, J = 5.5, 3.1 Hz, 2H), 6.87 (d, J = 7.7 Hz, 1H), 6.24 (d, J = 1.4 Hz, 1H), 5.84 (d, J = 1.4 Hz, 1H), 4.79 (td, J = 7.3, 4.9 Hz, 1H), 3.77 (s, 3H), 2.58 (t, J = 7.3 Hz, 2H), 2.30 – 2.19 (m, 1H), 2.08 (s, 3H), 2.08 – 2.00 (m, 1H).

13C NMR (101 MHz, CDCl3) δ 172.2, 166.4, 162.8, 134.7, 132.7, 131.8, 124.1, 120.7, 52.8, 52.2, 31.4, 30.0, 15.6.

HRMS (ESI) m/z calcd for C17H19N2O5S+: 363.1009; found: 363.1015.
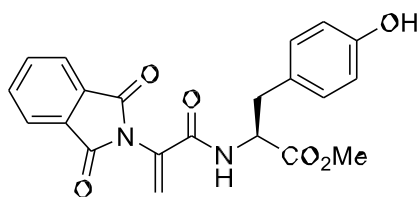
Methyl (2-(1,3-dioxoisoindolin-2-yl)acryloyl)-L-tyrosinate (48h)

Prepared according to the GP4, using Phth-Ser-OH (1.5 equiv.) and HCl·H-Tyr-OMe (1.0 equiv.). The crude mixture was purified by flash column chromatography (n-pentane/EtOAc: 1/1 → 1/3) to afford product 48h (23% yield) as white solid.

1H-NMR (300 MHz, CDCl3) δ 7.93 (dd, J = 5.5, 3.1 Hz, 2H), 7.79 (dd, J = 5.5, 3.1 Hz, 2H), 7.01 (d, J = 8.2 Hz, 2H), 6.69 (d, J = 8.2 Hz, 2H), 6.55 (d, J = 7.7 Hz, 1H), 6.12 (d, J = 1.5 Hz, 1H), 5.84 (d, J = 1.5 Hz, 1H), 5.65 – 5.27 (m, 1H), 4.95 (dt, J = 7.7, 5.2 Hz, 1H), 3.79 (s, 3H), 3.36 – 2.93 (m, 2H).

13C-NMR (101 MHz, CDCl3) δ 171.8, 166.5, 163.1, 155.5, 134.6, 132.2, 131.6, 130.4, 126.5, 124.0, 121.0, 115.5, 53.9, 52.6, 36.7.

HRMS (ESI) m/z calcd for C H N O +: 395.1238; found: 395.1238.
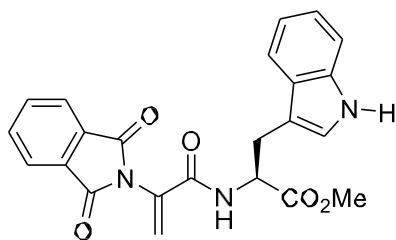
Methyl (2-(1,3-dioxoisoindolin-2-yl)acryloyl)-L-tryptophanate (48i)

Prepared according to the GP4, using Phth-Ser-OH (1.5 equiv.) and HCl·H-Trp-OMe (1.0 equiv.). The crude mixture was purified by flash column chromatography (n-pentane/EtOAc: 1/4) to afford product 48i (32% yield) as white solid.

1H NMR (400 MHz, CDCl3) δ 8.41 (s, 1H), 7.84 (dd, J = 5.5, 3.1 Hz, 2H), 7.72 (dd, J = 5.5, 3.1 Hz, 2H), 7.52 (d, J = 7.8 Hz, 1H), 7.31 – 7.27 (m, 1H), 7.14 – 7.01 (m, 3H), 6.67 (d, J = 7.8 Hz, 1H), 6.01 (d, J = 1.5 Hz, 1H), 5.74 (d, J = 1.5 Hz, 1H), 4.99 (dt, J = 7.8, 5.0 Hz, 1H), 3.69 (s, 3H), 3.44 – 3.34 (m, 2H).

13C NMR (101 MHz, CDCl3) δ 171.5, 166.1, 162.3, 135.7, 134.2, 132.3, 131.3, 127.2, 123.6, 123.2, 121.7, 120.2, 119.3, 118.1, 111.0, 109.0, 53.1, 52.2, 27.0.

HRMS (ESI) m/z calcd for C H N O +: 418.1397; found: 418.1403.
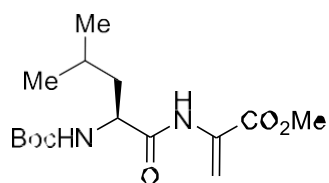
Methyl (S)-2-(2-((tert-butoxycarbonyl)amino)-4-methylpentanamido)acrylate (48j)

Prepared according to the GP4, using Boc-Leu-OH (1.0 equiv.) and HCl·H-Ser-OMe (1.5 equiv.). The crude mixture was purified by flash column chromatography (n-pentane/EtOAc: 8/2→ 1/1) to afford product 48j (56% yield) as white solid.

1H-NMR (400 MHz, CDCl3) δ 8.42 (s, 1H), 6.60 (d, J = 1.5 Hz, 1H), 5.90 (d, J = 1.5 Hz, 1H), 5.01 (d, J = 7.0 Hz, 1H), 4.29 – 4.14 (m, 1H), 3.84 (s, 6H), 1.77 – 1.64 (m, 2H), 1.58 – 1.49 (m, 1H), 1.45 (s, 9H), 1.03 – 0.86 (m, 6H).

13C-NMR (101 MHz, CDCl3) δ 171.6, 164.3, 155.7, 130.8, 109.2, 80.4, 53.9, 52.9, 41.0, 28.2, 24.8, 23.0, 21.8.

HRMS (ESI) m/z calcd for C15H27N2O5+: 315.1914; found: 315.1908.
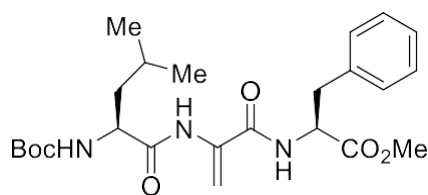
Methyl (2-((S)-2-((tert-butoxycarbonyl)amino)-4-methylpentanamido)acryloyl)-L-phenylalaninate (48l)

Prepared according to the GP4, using Boc-Leu-OH (1.0 equiv.) and TFA·H-Ser-Phe-OMe (1.5 equiv.). The crude mixture was purified by flash column chromatography (n-pentane/EtOAc: 8/2→ 1/2) to afford product 48l (45% yield) as white solid.

1H-NMR (400 MHz, CDCl3) δ 8.54 (s, 1H), 7.25 – 7.13 (m, 3H), 7.04 (d, J = 8.2 Hz, 2H), 6.79 (d, J = 7.6 Hz, 1H), 6.37 (s, 1H), 5.14 (s, 1H), 4.96 (d, J = 8.2 Hz, 1H), 4.80 (dt, J = 7.7, 6.0 Hz, 1H), 4.29 – 4.10 (m, 1H), 3.68 (s, 3H), 3.12 (dd, J = 13.9, 5.7 Hz, 1H), 3.06 (dd, J = 13.9, 6.3 Hz, 1H), 1.69 – 1.54 (m, 2H), 1.50 – 1.41 (m, 1H), 1.37 (s, 9H), 0.91 – 0.83 (m, 7H).

13C-NMR (101 MHz, CDCl3) δ 171.9, 171.8, 163.4, 155.7, 135.6, 133.7, 129.2, 128.7, 127.3, 102.5, 80.2, 53.9, 53.8, 52.6, 41.5, 37.6, 28.3, 24.8, 23.0, 21.7.

HRMS (ESI) m/z calcd for C H N O +: 462.2599; found: 462.2602.
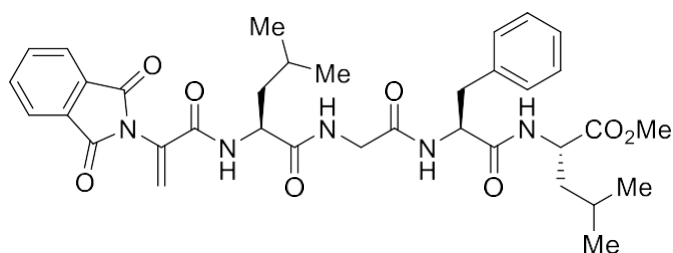
Methyl (2-(1,3-dioxoisoindolin-2-yl)acryloyl)-L-leucylglycyl-L-phenylalanyl-L-leucinate (48m)

Prepared according to the GP4, using Phth-Ser-OH (1.5 equiv.) and TFA·H-Leu-Gly-Phe-Leu- OMe (1.0 equiv.). The crude mixture was purified by flash column chromatography (CH2Cl2/EtOAc: 8/2 → 1/1) to afford product 48m (56% yield) as white solid.

1H-NMR (400 MHz, DMSO-d6) δ 8.57 (d, J = 7.9 Hz, 1H), 8.37 (d, J = 7.6 Hz, 1H), 8.04 (t, J = 5.8 Hz, 1H), 7.99 (d, J = 8.4 Hz, 1H), 7.95 – 7.86 (m, 4H), 7.30 – 7.14 (m, 5H), 6.39 (s, 1H), 5.83 (s, 1H), 4.55 (td, J = 8.8, 4.4 Hz, 1H), 4.37 (ddd, J = 9.7, 7.8, 4.9 Hz, 1H), 4.29 (ddd, J = 9.7, 7.5, 5.2 Hz, 1H), 3.71 (dd, J = 16.7, 5.8 Hz, 1H), 3.66 – 3.55 (m, 4H), 3.02 (dd, J = 13.9, 4.5 Hz, 1H), 2.74 (dd, J = 13.9, 9.4 Hz, 1H), 1.68 – 1.38 (m, 6H), 0.90 (d, J = 6.3 Hz, 3H), 0.87 – 0.81 (m, 9H).

13C-NMR (101 MHz, DMSO-d6) δ 173.2, 172.6, 171.6, 168.8, 167.0, 162.8, 138.1, 135.1, 132.6, 132.3, 129.6, 128.5, 126.7, 124.0, 123.9, 54.0, 52.3*, 50.8, 42.3*, 40.7, 38.1, 24.6, 24.5, 23.5, 23.2, 21.8, 21.8. (Peaks denoted with * correspond to two peaks)

HRMS (ESI) m/z calcd for C H N O +: 662.3184; found: 662.3192.
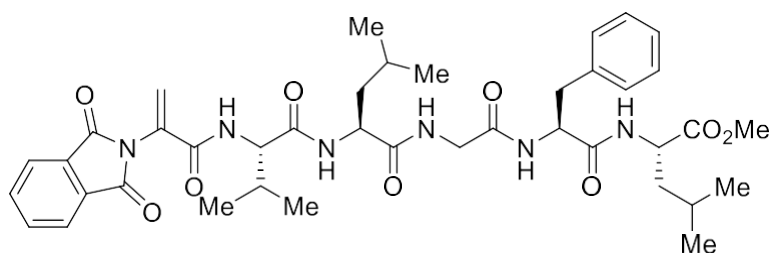
Methyl (2-(1,3-dioxoisoindolin-2-yl)acryloyl)-L-valyl-L-leucylglycyl-L-phenylalanyl-L-leucinate (48n)

Prepared according to the GP4, using Phth-Ser-OH (1.5 equiv.) and TFA·H-Val-Leu-Gly-Phe- Leu-OMe (1.0 equiv.). The crude mixture was purified by flash column chromatography (CH2Cl2/EtOAc: 8/2 → 1/1) to afford product 48n (48% yield) as white solid.

1H-NMR (400 MHz, DMSO-d6) δ 8.47 (d, J = 8.6 Hz, 1H), 8.39 (d, J = 7.6 Hz, 1H), 8.01 (d, J = 8.4 Hz, 1H), 7.98 – 7.85 (m, 6H), 7.29 – 7.14 (m, 5H), 6.35 (s, 1H), 5.82 (s, 1H), 4.56 (td, J = 8.9, 4.5 Hz, 1H), 4.36 – 4.22 (m, 2H), 4.17 (t, J = 8.5 Hz, 1H), 3.75 – 3.54 (m, 5H), 3.02 (dd, J = 13.9, 4.5 Hz, 1H), 2.75 (dd, J = 13.9, 9.4 Hz, 1H), 2.08 – 1.93 (m, 1H), 1.68 – 1.40 (m, 6H), 0.93 – 0.78 (m, 18H).

13C-NMR (101 MHz, DMSO-d6) δ 173.2, 172.6, 171.6, 171.1, 168.7, 167.0, 162.8, 138.1, 135.1, 132.8, 132.4, 129.6, 128.5, 126.7, 123.9, 123.6, 59.4, 53.9, 52.3, 51.6, 50.8, 42.2, 41.3, 38.2, 30.2, 24.6, 24.5, 23.5, 23.2, 22.0, 21.8, 19.8, 19.2.

HRMS (ESI) m/z calcd for $C_{40}H_{53}N_6O_9^+$: 761.3869; found: 761.3880.

References

1. Guglielmi P, Carradori S, Ammazzalorso A, Secci D. Novel approaches to the discovery of selective human monoamine oxidase-B inhibitors: is there room for improvement? *Expert Opin Drug Discov*. 2019 Oct;14(10):995-1035. doi: 10.1080/17460441.2019.1637415. Epub 2019 Jul 3. PMID: 31268358.

2. Youdim MBH. Monoamine oxidase inhibitors, and iron chelators in depressive illness and neurodegenerative diseases. *J Neural Transm (Vienna)*. 2018 Nov;125(11):1719-1733. doi: 10.1007/s00702-018-1942-9. Epub 2018 Oct 19. PMID: 30341696.

3. Wong W. Pathogenic putrescine. *Sci Signal.* 2022 Sep 13;15 (751). doi: 10.1126/scisignal.ade8161. Epub 2022 Sep 13. PMID: 36099340.

4. Blaschko, H.; Richter, D.; Schlossmann, H. The inactivation of adrenaline. *J. Physiol.* **1937**, *90*, 1–17.

5. Edmondson, D. E.; Binda, C. *Membrane Protein Complexes: Structure and Function*; Harris, J. R., Boekema, E. J., Eds.; Subcellular Biochemistry; Springer Singapore: Singapore, 2018; Vol. 87; ISBN 978-981-10-7756-2

6. Gesi, M.; Santinami, A.; Ruffoli, R.; Conti, G.; Fornai, F. Novel aspects of dopamine oxidative metabolism. *Pharmacol Toxicol.* **2001**, *89*, 217–224.

7. Edmondson, D. E.; Mattevi, A.; Binda, C.; Li, M.; Hubálek, F.; Hubalek, F. Structure and Mechanism of Monoamine Oxidase. Burger's Med. Chem. Drug Discov. 2004, 11, 1983–1993, doi:10.1002/0471266949.bmc111.

8. Miller, J. R.; Edmondson, D. E. Structure-activity relationships in the oxidation of para-substituted benzylamine analogues by recombinant human liver monoamine oxidase A. Biochemistry 1999, 38, 13670–13683, doi:10.1021/bi990920y.

9. Jonsson, T., Edmondson, D. E., & Klinman, J. P. (1994). Hydrogen tunneling in the flavoenzyme monoamine oxidase B. *Biochemistry*, *33*(49), 14871-14878.

10. Silverman, Richard B. "Radical ideas about monoamine oxidase." *Accounts of chemical research* 28.8 (1995): 335-342.

11. Silverman, Richard B., Stephen J. Hoffman, and William B. Catus III. "A mechanism for mitochondrial monoamine oxidase catalyzed amine oxidation." *Journal of the American Chemical Society* 102.23 (1980): 7126-7128.

12. Carradori S.; Gidaro M. C.; Petzer A.; Costa G.; Guglielmi P.; Chimenti P.; Alcaro S.; Petzer, J. P. Inhibition of Human Monoamine Oxidase: Biological and Molecular Modeling Studies on Selected Natural Flavonoids. J. Agric. Food Chem. 2016, 64, 9004–9011, doi:10.1021/acs.jafc.6b03529.

13. Shih JC, Chen K, Ridd MJ. Monoamine oxidase: from genes to behaviour. Annu Rev Neurosci. 1999;22:197–217.

14. SonSY, MaJ ,KondouY ,et al. Structure of human monoamine oxidase A at 2.2 A resolution: the control of opening the entry for substrates/ inhibitors. Proc Natl Acad Sci U S A. 2008;105:5739–5744.

15. Bach AW, Lan NC, Johnson DL, Abell CW, Bembenek ME, Kwan SW, Seeburg PH, Shih JC. cDNA cloning of human liver monoamine oxidase A and B: molecular basis of differences in enzymatic properties. Proc Natl Acad Sci U S A. 1988 Jul;85(13):4934-8.

16. Fowler, C.J., Wiberg, A., Oreland, L., Marcusson, J. & Winblad, B. J. Neural Transm. 49, 1–20 (1980).

17. Sohrabi S. The criminal gene: the link between MAOA and aggression (REVIEW). BMC Proc. 2015 Jan 14;9(Suppl 1):A49. doi: 10.1186/1753-6561-9-S1-A49. PMCID: PMC4306065.

18. Sharma, P., Jha, A. B., Dubey, R. S., & Pessarakli, M. (2012). Reactive oxygen species, oxidative damage, and antioxidative defense mechanism in plants under stressful conditions. *Journal of botany*, *2012*(1), 217037.

19. O'Carroll, AM., Fowler, C.J., Phillips, J.P. *et al.* The deamination of dopamine by human brain monoamine oxidase. *Naunyn-Schmiedeberg's Arch. Pharmacol.* **322**, 198–202 (1983). https://doi.org/10.1007/BF00500765

20. Binda, C., Newton-Vinson, P., Huba ́lek, F., Edmondson, D. E. & Mattevi, A. (2002) Nat. Struct. Biol. 9, 22–26.

21. Binda, C., Li, M., Huba ́lek, F., Restelli, N., Edmondson, D. E. & Mattevi, A. (2003) Proc. Natl. Acad. Sci. USA 100, 9750–9755.

22. De Colimbus L., Min L, Binda C., Lustig A, Edmondson D., Mattevi A. Three-dimensional structure of human monoamine oxidase A (MAO A): Relation to the structures of rat MAO A and human MAOB, 2005 vol. 102 no. 36, www.pnas.orgcgi doi 10.1073pnas.0505975102

23. Edmondson DE, Mattevi A, Binda C, Li M, Hubálek F. Structure and mechanism of monoamine oxidase. Curr Med Chem. 2004 Aug;11(15):1983-93. doi: 10.2174/0929867043364784. PMID: 15279562.

24. Ulmschneider MB, Sansom MS. Amino acid distributions in integral membrane protein structures. Biochim Biophys Acta. 2001 May 2;1512(1):1-14. doi: 10.1016/s0005-2736(01)00299-1. PMID: 11334619.

25. Kleywegt, G. J., & Jones, T. A. (1994). Detection, delineation, measurement and display of cavities in macromolecular structures. *Acta Crystallographica Section D: Biological Crystallography*, *50*(2), 178-185.

26. Murshudov, G. N., Vagin, A. A., & Dodson, E. J. (1997). Refinement of macromolecular structures by the maximum-likelihood method. *Acta Crystallographica Section D: Biological Crystallography*, *53*(3), 240-255.

27. Ma J, Yoshimura M, Yamashita E, Nakagawa A, Ito A, Tsukihara T. Structure of rat monoamine oxidase A and its specific recognitions for substrates and inhibitors. J Mol Biol. 2004 Apr 16;338(1):103-14. doi: 10.1016/j.jmb.2004.02.032. PMID: 15050826.

28. Tsugeno Y, Ito A. A key amino acid responsible for substrate selectivity of monoamine oxidase A and B. J Biol Chem. 1997 May 30;272(22):14033-6. doi: 10.1074/jbc.272.22.14033. PMID: 9162023.

29. Wang J, Edmondson DE. High-level expression and purification of rat monoamine oxidase A (MAO A) in Pichia pastoris: comparison with human MAO A. Protein Expr Purif. 2010 Apr;70(2):211-7. doi: 10.1016/j.pep.2009.10.013. Epub 2009 Oct 31. PMID: 19883764; PMCID: PMC2827670.

30. Newton-Vinson P, Hubalek F, Edmondson DE. High-level expression of human liver monoamine oxidase B in Pichia pastoris. Protein Expr Purif. 2000 Nov;20(2):334-45. doi: 10.1006/prep.2000.1309. PMID: 11049757.

31. Walker, M. C., & Edmondson, D. E. (1994). Structure-activity relationships in the oxidation of benzylamine analogs by bovine liver mitochondrial monoamine oxidase B. *Biochemistry*, *33*(23), 7088-7098. The role of monoamine oxidase enzymes in the pathophysiology of neurological disorders, Journal of Chemical

32. Nandigama, Ravi K., J. Richard Miller, and Dale E. Edmondson. "Loss of serotonin oxidation as a component of the altered substrate specificity in the Y444F mutant of recombinant human liver MAO A." *Biochemistry* 40.49 (2001): 14839-14846.

33. Tong J, Meyer JH, Furukawa Y, et al. Distribution of Monoamine Oxidase Proteins in Human Brain: Implications for Brain Imaging Studies. *Journal of Cerebral Blood Flow & Metabolism*. 2013;33(6):863-871.

34. Saura J, Andrés N, Andrade C, Ojuel J, Eriksson K, Mahy N (1997) Biphasic and region-specific MAO-B response to aging in normal human brain. Neurobiol Aging 18:497–507

35. LOOMER HP, SAUNDERS JC, KLINE NS. A clinical and pharmacodynamic evaluation of iproniazid as a psychic energizer. Psychiatr Res Rep Am Psychiatr Assoc. 1957 Dec 8:129-41. PMID: 13542681.

36. MAASS, A., NIMMO, M. A New Inhibitor of Serotonin Metabolism. *Nature* **184**, 547–548 (1959).

37. Tedeschi, R. E., Tedeschi, D. H., Mucha, A., Cook, L., Mattis, P. A., & Fellows, E. J. (1959). Effects of various centrally acting drugs on fighting behavior of mice. *Journal of Pharmacology and Experimental Therapeutics*, *125*(1), 28-34.

38. Robinson, D. S. (1975). Changes in monoamine oxidase and monoamines with human development and aging. *Biology of Aging and Development*, 203-212.

39. Robinson, D. S., Sourkes, T. L., Nies, A., Harris, L. S., Spector, S., Bartlett, D. L., & Kaye, I. S. (1977). Monoamine metabolism in human brain. *Archives of General Psychiatry*, *34*(1), 89-92.

40. López-Muñoz, F., Alamo, C., Juckel, G., & Assion, H. J. (2007). Half a century of antidepressant drugs: on the clinical introduction of monoamine oxidase inhibitors, tricyclics, and tetracyclics. Part I: monoamine oxidase inhibitors. *Journal of clinical psychopharmacology*, *27*(6), 555-559.

41. Menkes, D., Bosanac, P., & Castle, D. (2016). MAOIs–does the evidence warrant their resurrection?. *Australasian Psychiatry*, *24*(4), 371-373

42. Yanowitch R, Coccaro EF. The neurochemistry of human aggression. Adv Genet. 2011;75:151-69. doi: 10.1016/B978-0-12-380858-5.00005-8. PMID: 22078480.

43. Lammel S, Lim BK, Malenka RC. Reward and aversion in a heterogeneous midbrain dopamine system. Neuropharmacology. 2014 Jan;76 Pt B(0 0):351-9. doi: 10.1016/j.neuropharm.2013.03.019. Epub 2013 Apr 8. PMID: 23578393; PMCID: PMC3778102.

44. Okusaga OO. Accelerated aging in schizophrenia patients: the potential role of oxidative stress. Aging Dis. 2013 Dec 4;5(4):256-62. doi: 10.14336/AD.2014.0500256. PMID: 25110609; PMCID: PMC4113515.

45. Nonnekes J, Post B, Tetrud JW, Langston JW, Bloem BR. MPTP-induced parkinsonism: an historical case series. Lancet Neurol. 2018 Apr;17(4):300-301. doi: 10.1016/S1474-4422(18)30072-3. Epub 2018 Mar 13. Erratum in: Lancet Neurol. 2018 May;17(5):392. doi: 10.1016/S1474-4422(18)30120-0. PMID: 29553378.

46. Ferrucci M, Fornai F. MPTP Neurotoxicity: Actions, Mechanisms, and Animal Modeling of Parkinson's Disease BT - Handbook of Neurotoxicity. In: Kostrzewa RM, editor.

47. Ferrucci M, Fornai F., MPTP Neurotoxicity: Actions, Mechanisms, and Animal Modeling of Parkinson's Disease, Cham: Springer International Publishing; 2021, p. 1–41. doi:10.1007/978-3-030-71519-9_239-1.

48. Nonnekes J, Post B, Tetrud JW, Langston JW, Bloem BR. MPTP-induced parkinsonism: an historical case series. Lancet Neurol. 2018 Apr;17(4):300-301. doi: 10.1016/S1474-4422(18)30072-3. Epub 2018 Mar 13. Erratum in: Lancet Neurol. 2018 May;17(5):392. doi: 10.1016/S1474-4422(18)30120-0. PMID: 29553378.

49. Erkkinen MG, Kim MO, Geschwind MD. Clinical Neurology and Epidemiology of the Major Neurodegenerative Diseases. Cold Spring Harb Perspect Biol. 2018 Apr 2;10(4):a033118. doi: 10.1101/cshperspect.a033118. PMID: 28716886; PMCID: PMC5880171.

50. Reitz C, Brayne C, Mayeux R. Epidemiology of Alzheimer disease. Nat Rev Neurol. 2011 Mar;7(3):137-52. doi: 10.1038/nrneurol.2011.2. Epub 2011 Feb 8. PMID: 21304480; PMCID: PMC3339565.

51. Dickson DW. Parkinson's disease and parkinsonism: neuropathology. Cold Spring Harb Perspect Med. 2012 Aug 1;2(8):a009258. doi: 10.1101/cshperspect.a009258. PMID: 22908195; PMCID: PMC3405828.

52. Goldman J, Postuma R. Premotor and nonmotor features of Parkinson's disease. Curr Opin Neurol. 2014 Aug;27(4):434-41. doi: 10.1097/WCO.0000000000000112. PMID: 24978368; PMCID: PMC4181670.

53. Spillantini MG, Crowther RA, Jakes R, Hasegawa M, Goedert M. alpha-Synuclein in filamentous inclusions of Lewy bodies from Parkinson's disease and dementia with lewy bodies. Proc Natl Acad Sci U S A. 1998 May 26;95(11):6469-73. doi: 10.1073/pnas.95.11.6469. PMID: 9600990; PMCID: PMC27806.

54. Schneider SA, Alcalay RN. Neuropathology of genetic synucleinopathies with parkinsonism: Review of the literature. Mov Disord. 2017 Nov;32(11):1504-1523. doi: 10.1002/mds.27193. PMID: 29124790; PMCID: PMC5726430.

55. Blandini F. Neuroprotection by rasagiline: a new therapeutic approach to Parkinson's disease? CNS Drug Rev. 2005 Summer;11(2):183-94. doi: 10.1111/j.1527-3458.2005.tb00269.x. PMID: 16007239; PMCID: PMC6741719.

56. Stocchi F, Antonini A, Barone P, Tinazzi M, Zappia M, Onofrj M, Ruggieri S, Morgante L, Bonuccelli U, Lopiano L, Pramstaller P, Albanese A, Attar M, Posocco V, Colombo D, Abbruzzese G; DEEP study group. Early DEtection of wEaring off in Parkinson disease: the DEEP study. Parkinsonism Relat Disord. 2014 Feb;20(2):204-11. doi: 10.1016/j.parkreldis.2013.10.027.

57. L, Bonuccelli U, Lopiano L, Pramstaller P, Albanese A, Attar M, Posocco V, Colombo D, Abbruzzese G; DEEP study group. Early DEtection of wEaring off in Parkinson disease: the DEEP study. Parkinsonism Relat Disord. 2014 Feb;20(2):204-11. doi:

58. Sánchez-Rodríguez, R., Munari, F., Angioni, R. *et al.* Targeting monoamine oxidase to dampen NLRP3 inflammasome activation in inflammation. *Cell Mol Immunol* **18**, 1311–1313 (2021).

59. Yan, Jiaxu, Hang Zhang, and Jianwei Zhu. "Recent advances of small molecule fluorescent probes for distinguishing monoamine oxidase-A and monoamine oxidase-B in vitro and in vivo." *Molecular and Cellular Probes* 55 (2021): 101686.

60. Mallajosyula JK, Kaur D, Chinta SJ, Rajagopalan S, Rane A, Nicholls DG, Di Monte DA, Macarthur H, Andersen JK. MAO-B elevation in mouse brain astrocytes results in Parkinson's pathology. PLoS One. 2008 Feb 20;3(2):e1616. doi: 10.1371/journal.pone.0001616. Erratum in: PLoS One. 2012;7(8): doi/10.1371/annotation/3c37bef4-bb5e-4f1e-8551-01afc006df90. PMID: 18286173; PMCID: PMC2229649.

61. O'Sullivan SS, Massey LA, Williams DR, Silveira-Moriyama L, Kempster PA, Holton JL, Revesz T, Lees AJ. Clinical outcomes of progressive supranuclear palsy and multiple system atrophy. Brain. 2008 May;131(Pt 5):1362-72. doi: 10.1093/brain/awn065. Epub 2008 Apr 2. PMID: 18385183.

62. Westlund, K. N., et al. "Distinct monoamine oxidase A and B populations in primate brain." *Science* 230.4722 (1985): 181-183.

63. Af Klinteberg, B., et al. "Personality correlates of platelet monoamine oxidase (MAO) activity in female and male subjects." *Neuropsychobiology* 18.2 (1987): 89-96.

64. Danilova, R.A., Moskvityna, T.A., Obukhova, M.F. *et al.* Pargyline Conjugate-Induced Long-Term Activation of Monoamine Oxidase as an Immunological Model for Depression. *Neurochem Res* 24, 1147–1151 (1999). https://doi.org/10.1023/A:1020764504462ù

65. Grailhe, R., Cardona, A., Even, N., Seif, I., Changeux, J. P., and Cloez-Tayarani, I. (2009). Regional changes in the cholinergic system in mice lacking monoamine oxidase A. Brain Res. Bull. 78, 283–289. doi: 10.1016/j.brainresbull.2008.12.004

66. Van der Schyf, Cornelis J., Werner J. Geldenhuys, and Moussa BH Youdim. "Multifunctional drugs with different CNS targets for neuropsychiatric disorders." *Journal of neurochemistry* 99.4 (2006): 1033-1048.

67. Giacobini G, Marchisio PC, Giacobini E, Koslow SH. Developmental changes of cholinesterases and monoamine oxidase in chick embryo spinal and sympathetic ganglia. J Neurochem. 1970 Aug;17(8):1177-85. doi: 10.1111/j.1471-4159.1970.tb03366.x. PMID: 5457626..

68. Caraci F, Copani A, Nicoletti F, Drago F. Depression and Alzheimer's disease: neurobiological links and common pharmacological targets. Eur J Pharmacol. 2010 Jan 10;626(1):64-71. doi: 10.1016/j.ejphar.2009.10.022. Epub 2009 Oct 18. PMID: 19837057.

69. Cai, Z. (2014). Monoamine oxidase inhibitors: Promising therapeutic agents for Alzheimer's disease (Review). Molecular Medicine Reports, 9, 1533-1541. https://doi.org/10.3892/mmr.2014.2040

70. Adkins DE, Daw JK, McClay JL, van den Oord EJ. The influence of five monoamine genes on trajectories of depressive symptoms across adolescence and young adulthood. Dev Psychopathol. 2012 Feb;24(1):267-85. doi: 10.1017/S0954579411000824. PMID: 22293009; PMCID: PMC3515661.

71. T. Thomas, Monoamine oxidase-B inhibitors in the treatment of Alzheimers disease, Neurobiol. Aging 21 (2000) 343e348, https://doi.org/10.1016/ S0197-4580(00)00100-7.

72. A.J. Cooper, Tyramine and irreversible monoamine oxidase inhibitors in clinical practice, Br. J. Psychiatry 155 (1989) 38e45, https://doi.org/10.1192/ S000712500029747X.

73. G.L. Piccinin, G. Finali, M. Piccirilli, Neuropsychological effects of L-deprenyl in Alzheimer's type dementia, clin, Neuropharmacology 13 (1990) 147e163, https://doi.org/10.1097/00002826-199004000-00004.

74. Streit, Microglial activation and neuroinflammation in Alzheimer's disease: a critical examination of recent history, Front. Aging Neurosci (2010), https:// doi.org/10.3389/fnagi.2010.00022.

75. Mangoni, M.P. Grassi, L. Frattola, R. Piolti, S. Bassi, A. Motta, A. Marcone, S. Smirne, Effects of a MAO-B inhibitor in the treatment of alzheimer disease, Eur, Neurol 31 (1991) 100e107, https://doi.org/10.1159/000116655.

76. M. Sano, C. Ernesto, R.G. Thomas, M.R. Klauber, K. Schafer, M. Grundman, P. Woodbury, J. Growdon, C.W. Cotman, E. Pfeiffer, L.S. Schneider, L.J. Thal, A controlled trial of selegiline, alpha-tocopherol, or both as treatment for alzheimer's disease, N. Engl, J. Med 336 (1997) 1216e1222, https://doi.org/ 10.1056/NEJM199704243361704.

77. G.L. Piccinin, G. Finali, M. Piccirilli, Neuropsychological effects of L-deprenyl in Alzheimer's type dementia, clin, Neuropharmacology 13 (1990) 147e163, https://doi.org/10.1097/00002826-199004000-00004.

78. Muck-Seler, Dorotea, et al. "Platelet serotonin concentration and monoamine oxidase type B activity in female patients in early, middle and late phase of Alzheimer's disease." *Progress in Neuro-Psychopharmacology and Biological Psychiatry* 33.7 (2009): 1226-1231.

79. Parnetti, L., Reboldi, G. P., Santucci, C., Santucci, A., Gaiti, A., Brunetti, M., ... & Senin, U. (1994). Platelet MAO-B activity as a marker of behavioural characteristics in dementia disorders. *Aging Clinical and Experimental Research*, *6*, 201-207.

80. Zhiyou, C., Yong, Y., Shanquan, S., Jun, Z., Liangguo, H., Ling, Y., & Jieying, L. (2009). Upregulation of BACE1 and β-amyloid protein mediated by chronic cerebral hypoperfusion contributes to cognitive impairment and pathogenesis of Alzheimer's disease. *Neurochemical research*, *34*, 1226-1235.

81. Manzoor S, Hoda N. A comprehensive review of monoamine oxidase inhibitors as Anti-Alzheimer's disease agents: A review. Eur J Med Chem. 2020 Nov 15;206:112787. doi: 10.1016/j.ejmech.2020.112787. Epub 2020 Sep 1. PMID: 32942081.

82. Lange, D. J. et al. Selegiline is ineffective in a collaborative double-blind, placebo-controlled trial for treatment of amyotrophic lateral sclerosis. Arch. Neurol. 55, 93–96 (1998).

83. Waibel, S., Reuter, A., Malessa, S., Blaugrund, E. & Ludolph, A. C. Rasagiline alone and in combination with riluzole prolongs survival in an ALS mouse model. J. Neurol. 251, 1080–1084 (2004).

84. Lev N, Melamed E, Offen D. Toxic causes of parkinsonism. vol. 84. 1st ed. Elsevier B.V.; 2007. doi:10.1016/S0072-9752(07)84050-4

85. B. Af Klinteberg, D. Schalling, G. Edman, L. Oreland, M. Åsberg; Personality Correlates of Platelet Monoamine Oxidase (MAO) Activity in Female and Male Subjects. *Neuropsychobiology* 1 February 1987; 18 (2): 89–96. https://doi.org/10.1159/000118399

86. Youdim MB, Edmondson D, Tipton KF. The therapeutic potential of monoamine oxidase inhibitors. Nat Rev Neurosci. 2006 Apr;7(4):295-309. doi: 10.1038/nrn1883. PMID: 16552415.

87. Gareri, P., Falconi, U., De Fazio, P. & De Sarro, G. Conventional and new antidepressant drugs in the elderly. Progr. Neurobiol. 61, 353–396 (2000).

88. Tipton, K. F. What is it that l-deprenyl (selegiline) might do? Clin. Pharmacol. Ther. 56, 781–796 (1994).

89. Knoll J (1989) The pharmacology of selegiline ((-)deprenyl). New aspects. Acta Neurol Scand Suppl 126:83-91.

90. Kalgutkar AS, Dalvie DK, Castagnoli N Jr, Taylor TJ. Interactions of nitrogen-containing xenobiotics with monoamine oxidase (MAO) isozymes A and B: SAR studies on MAO substrates and inhibitors. Chem Res Toxicol. 2001 Sep;14(9):1139-62. doi: 10.1021/tx010073b. PMID: 11559028.

91. Nair NP, Ahmed SK, Kin NM. Biochemistry and pharmacology of reversible inhibitors of MAO-A agents: focus on moclobemide. J Psychiatry Neurosci. 1993 Nov;18(5):214-25. PMID: 7905288; PMCID: PMC1188542

92. Behl T, Kaur D, Sehgal A, Singh S, Sharma N, Zengin G, Andronie-Cioara FL, Toma MM, Bungau S, Bumbu AG (2021) Role of monoamine oxidase activity in Alzheimer's disease: an insight into the therapeutic potential of inhibitors. Molecules 26:3724.

93. M.B.H. Youdim, T. Amit, O. Bar-Am, O. Weinreb, M. Yogev-Falach, Implica tions of co-morbidity for etiology and treatment of neurodegenerative dis eases with multifunctional neuroprotective-neurorescue drugs; ladostigil, Neurotox. Res 10 (2006) 181e192, https://doi.org/10.1007/BF03033355.

94. Binda C, Hubálek F, Li M, et al. Binding of rasagiline-related inhibi tors to human monoamine oxidases: a kinetic and crystallographic analysis. J Med Chem. 2005;48:8148–8154.

95. Dézsi L, Vécsei L. Safinamide for the treatment of Parkinson's disease. Expert Opin Investig Drugs. 2014;23:729–742

96. Ramsay RR. Inhibitor design for monoamine oxidases. Curr Pharm Des. 2013;19:2529–2539.

97. Carradori S, Petzer JP. Novel monoamine oxidase inhibitors: a patent review (2012-2014). Expert Opin Ther Pat. 2015;25:91–110.

98. Alborghetti M, Bianchini E, De Carolis L, Galli S, Pontieri FE, Rinaldi D. Type-B monoamine oxidase inhibitors in neurological diseases: clinical applications based on preclinical findings. Neural Regen Res. 2024 Jan;19(1):16-21. doi: 10.4103/1673-5374.375299. PMID: 37488838; PMCID: PMC10479837.

99. Medvedev, A. E.; Ivanov, A. S.; Kamyshanskaya, N. S.; Kirkel, A. Z.; Moskvitina, T. A.; Gorkin, V. Z.; Li, N. Y.; Marshakov, Vy. Interaction of indole derivatives with monoamine oxidase A and B. Studies on the structure-inhibitory activity relationship. *Biochem Mol Biol Int* **1995**, *36*, 113–122.

100.   Guglielmi, P., Secci, D., Petzer, A., Bagetta, D., Chimenti, P., Rotondi, G., ... & Carradori, S. (2019). Benzo [b] tiophen-3-ol derivatives as effective inhibitors of human monoamine oxidase: design, synthesis, and biological activity. *Journal of Enzyme Inhibition and Medicinal Chemistry*, *34*(1), 1511-1525.

101.   Reis J, Cagide F, Chavarria D, Silva T, Fernandes C, Gaspar A, Uriarte E, Remião F, Alcaro S, Ortuso F, Borges F. Discovery of New Chemical Entities for Old Targets: Insights on the Lead Optimization of Chromone-Based Monoamine Oxidase B (MAO-B) Inhibitors. J Med Chem. 2016 Jun 23;59(12):5879-93. doi: 10.1021/acs.jmedchem.6b00527.

102.   Epub 2016 Jun 10. Erratum in: J Med Chem. 2018 Jun 14;61(11):5054. doi: 10.1021/acs.jmedchem.8b00600. PMID: 27244485.

103.   Trapani, P.; Kvapil, L.; Hradil, P.; Soural, M. Use of Phenacyl Thiosalicylates for the Preparation of 3-Hydroxybenzo[b]thiophene Derivatives. Synlett 2018, 29, 810–814, doi:10.1055/s-0036-1591875.

104.   Pan, B.; Ren, P.; Song, H.; Wang, Z. Facile synthesis of 2-substituted benzo[b]thiophen-3-ols in water. Synth. Commun. 2013, 43, 1337–1344, doi:10.1080/00397911.2011.633203.Chan, S. L. F.; Low, K. H.; Yang, C.; Cheung, S. H. F.; Che, C. M. Iron-ligand coordination in tandem radical cyclizations: Synthesis of benzo[b]thiophenes by a one-pot reaction of iron 1,3-diketone complexes with 2-thiosalicylic acids. Chem. - A Eur. J. 2011, 17, 4709–4714, doi:10.1002/chem.201100377

105.   Mesiti F, Gaspar A, Chavarria D, Maruca A, Rocca R, Gil Martins E, Barreiro S, Silva R, Fernandes C, Gul S, Keminer O, Alcaro S, Borges F. Mapping Chromone-3-Phenylcarboxamide Pharmacophore: Quid Est Veritas? J Med Chem. 2021 Aug 12;64(15):11169-11182. doi: 10.1021/acs.jmedchem.1c00510. Epub 2021 Jul 16. PMID: 34269579.

106.   Chavarria D, Da Silva O, Benfeito S, Barreiro S, Garrido J, Cagide F, Soares P, Remião F, Brazzolotto X, Nachon F, Oliveira PJ, Dias J, Borges F. Fine-Tuning the Biological Profile of Multitarget Mitochondriotropic Antioxidants for Neurodegenerative Diseases. Antioxidants (Basel). 2021 Feb 23;10(2):329. doi: 10.3390/antiox10020329. PMID: 33672269; PMCID: PMC7926627.

107.   Wu, X. A., Ying, P., Liu, J. Y., Shen, H. S., Chen, Y., & He, L. (2009). Lithium Chloride–Assisted Selective Hydrolysis of Methyl Esters Under Microwave Irradiation. Synthetic Communications, 39(19), 3459–3470. https://doi.org/10.1080/00397910902778001

108.   Wang L, Wang N, Zhang W, Cheng X, Yan Z, Shao G, Wang X, Wang R, Fu C. Therapeutic peptides: current applications and future directions. Signal Transduct Target Ther. 2022 Feb 14;7(1):48. doi: 10.1038/s41392-022-00904-4. PMID: 35165272; PMCID: PMC8844085.

109.   Guillemard L, Kaplaneris N, Ackermann L, Johansson MJ. Late-stage C-H functionalization offers new opportunities in drug discovery. Nat Rev Chem. 2021 Aug;5(8):522-545. doi: 10.1038/s41570-021-00300-6. Epub 2021 Jul 13. PMID: 37117588.

110.   Xu L, Kuan SL, Weil T. Contemporary Approaches for Site-Selective Dual Functionalization of Proteins. Angew Chem Int Ed Engl. 2021 Jun 14;60(25):13757-13777. doi: 10.1002/anie.202012034. Epub 2021 Feb 26. PMID: 33258535; PMCID: PMC8248073.

111.   Jbara M, Maity SK, Brik A. Palladium in the Chemical Synthesis and Modification of Proteins. Angew Chem Int Ed Engl. 2017 Aug 28;56(36):10644-10655. doi: 10.1002/anie.201702370. Epub 2017 Aug 7. PMID: 28383786.

112.   Wang W, Lorion MM, Shah J, Kapdi AR, Ackermann L. Late-Stage Peptide Diversification by Position-Selective C-H Activation. Angew Chem Int Ed Engl. 2018 Nov 5;57(45):14700-14717. doi: 10.1002/anie.201806250. Epub 2018 Oct 9. PMID: 29969532.

113.   Ohata J, Martin SC, Ball ZT. Metal-Mediated Functionalization of Natural Peptides and Proteins: Panning for Bioconjugation Gold. Angew Chem Int Ed Engl. 2019 May 6;58(19):6176-6199. doi: 10.1002/anie.201807536. Epub 2019 Mar 4. PMID: 30251344.

114.   H.-R. Tong, B. Li, G. Li, G. He, G. Chen, Postassembly Modifications of Peptides via Metal-Catalyzed C–H Functionalization, CCS Chem. 2021, 3, 1797-1820.

115.   Bottecchia C, Noël T. Photocatalytic Modification of Amino Acids, Peptides, and Proteins. Chemistry. 2019 Jan 2;25(1):26-42. doi: 10.1002/chem.201803074.

116.   J.-Q. Liu, A. Shatskiy, B. S. Matsuura, M. D. Kärkäs, Recent Advances in Photoredox Catalysis Enabled Functionalization of α-Amino Acids and Peptides: Concepts, Strategies and Mechanisms, Synthesis 2019, 51, 2759-2791.

117.   Raynal L, Rose NC, Donald JR, Spicer CD. Photochemical Methods for Peptide Macrocyclisation. Chemistry. 2021 Jan 4;27(1):69-88. doi: 10.1002/chem.202003779. Epub 2020 Oct 27. PMID: 32914455.

118.   Lechner VM, Nappi M, Deneny PJ, Folliet S, Chu JCK, Gaunt MJ. Visible-Light-Mediated Modification and Manipulation of Biomacromolecules. Chem Rev. 2022 Jan 26;122(2):1752-1829. doi: 10.1021/acs.chemrev.1c00357. Epub 2021 Sep 21. PMID: 34546740.

119.   S. Mackay, R. J. Payne, L. R. Malins, J. Am. Chem. Soc. 2022, 144, 23-41.4

120.   Tyson EL, Niemeyer ZL, Yoon TP. Redox mediators in visible light photocatalysis: photocatalytic radical thiol-ene additions. J Org Chem. 2014 Feb 7;79(3):1427-36. doi: 10.1021/jo500031g. Epub 2014 Jan 27. PMID: 24428433; PMCID: PMC3985841.

121.   Wang Y, Wang J, Li GX, He G, Chen G. Halogen-Bond-Promoted Photoactivation of Perfluoroalkyl Iodides: A Photochemical Protocol for Perfluoroalkylation Reactions. Org Lett. 2017 Mar 17;19(6):1442-1445. doi: 10.1021/acs.orglett.7b00375. Epub 2017 Mar 6. PMID: 28263075.

122.   Yu Y, Zhang LK, Buevich AV, Li G, Tang H, Vachal P, Colletti SL, Shi ZC. Chemoselective Peptide Modification via Photocatalytic Tryptophan β-Position Conjugation. J Am Chem Soc. 2018 Jun 6;140(22):6797-6800. doi: 10.1021/jacs.8b03973. Epub 2018 May 23. PMID: 29762027.

123.   B. Ding, Y. Weng, Y. Liu, C. Song, L. Yin, J. Yuan, Y. Ren, A. Lei, C. W. Chiang, Selective Photoredox Trifluoromethylation of TryptophanContaining Peptides, Eur. J. Org. Chem. 2019, 7596-7605.

124.   Tower SJ, Hetcher WJ, Myers TE, Kuehl NJ, Taylor MT. Selective Modification of Tryptophan Residues in Peptides and Proteins Using a Biomimetic Electron Transfer Process. J Am Chem Soc. 2020 May 20;142(20):9112-9118. doi: 10.1021/jacs.0c03039. Epub 2020 May 5. PMID: 32348670; PMCID: PMC7292481.

125.   B. Laroche, X. Tang, G. Archer, R. Di Sanza, P. Melchiorre, Photochemical Chemoselective Alkylation of Tryptophan-Containing Peptides, Org. Lett. 2021, 23, 285-289.

126.   R. N. Lima, J. A. C. Delgado, D. I. Bernardi, R. G. S. Berlinck, N. Kaplaneris, L. Ackermann, M. W. Paixão, Post-synthetic functionalization of tryptophan protected peptide sequences through indole (C-2) photocatalytic alkylation, Chem. Commun. 2021, 57, 5758-5761.

127.   Hoopes, C. R.; Garcia, F. J.; Sarkar, A. M.; Kuehl, N. J.;Barkan, D. T.; Collins, N. L.; Meister, G. E.; Bramhall, T. R.; Hsu, C.-H.; Jones, M. D.; et al. Donor-Acceptor Pyridinium Salts for Photo-Induced Electron-Transfer-Driven Modification of Tryptophan

inPeptides, Proteins, and Proteomes Using Visible Light. J. Am. Chem.Soc. 2022, 144 (14), 6227−6236.

128.   Taylor MT, Nelson JE, Suero MG, Gaunt MJ. A protein functionalization platform based on selective reactions at methionine residues. Nature. 2018 Oct;562(7728):563-568. doi: 10.1038/s41586-018-0608-y. Epub 2018 Oct 15. PMID: 30323287; PMCID: PMC6203954.

129.   Kim J, Li BX, Huang RY, Qiao JX, Ewing WR, MacMillan DWC. Site-Selective Functionalization of Methionine Residues via Photoredox Catalysis. J Am Chem Soc. 2020 Dec 23;142(51):21260-21266. doi: 10.1021/jacs.0c09926. Epub 2020 Dec 8. PMID: 33290649; PMCID: PMC8647115.

130.   Knowles OJ, Johannissen LO, Crisenza GEM, Hay S, Leys D, Procter DJ. A Vitamin B_2 -Photocatalysed Approach to Methionine Analogues. Angew Chem Int Ed Engl. 2022 Dec 12;61(50):e202212158. doi: 10.1002/anie.202212158. Epub 2022 Nov 10. PMID: 36250805; PMCID: PMC10100050.

131.   S. Sato, H. Nakamura, Ligand-Directed Selective Protein Modification Based on Local Single-Electron-Transfer Catalysis, Angew. Chem. Int. Ed. 2013, 52, 8681-8684;

132.   Siodłak D. α,β-Dehydroamino acids in naturally occurring peptides. Amino Acids. 2015 Jan;47(1):1-17. doi: 10.1007/s00726-014-1846-4. Epub 2014 Oct 17. PMID: 25323736; PMCID: PMC4282715.

133.   Dadová J, Galan SR, Davis BG. Synthesis of modified proteins via functionalization of dehydroalanine. Curr Opin Chem Biol. 2018 Oct;46:71-81. doi: 10.1016/j.cbpa.2018.05.022. Epub 2018 Jun 15. PMID: 29913421.

134.   Rossolini T, Leitch JA, Grainger R, Dixon DJ. Photocatalytic Three-Component Umpolung Synthesis of 1,3-Diamines. Org Lett. 2018 Nov 2;20(21):6794-6798. doi: 10.1021/acs.orglett.8b02923. Epub 2018 Oct 15. PMID: 30350662.

135.   Aguilar Troyano FJ, Merkens K, Anwar K, Gómez-Suárez A. Radical-Based Synthesis and Modification of Amino Acids. Angew Chem Int Ed Engl. 2021 Jan 18;60(3):1098-1115. doi: 10.1002/anie.202010157. Epub 2020 Nov 4. PMID: 32841470; PMCID: PMC7820943.

136.   Constantin T, Zanini M, Regni A, Sheikh NS, Juliá F, Leonori D. Aminoalkyl radicals as halogen-atom transfer agents for activation of alkyl and aryl halides. Science. 2020 Feb 28;367(6481):1021-1026. doi: 10.1126/science.aba2419. PMID: 32108109.

137.   Ji P, Zhang Y, Dong Y, Huang H, Wei Y, Wang W. Synthesis of Enantioenriched α-Deuterated α-Amino Acids Enabled by an Organophotocatalytic Radical Approach. Org Lett. 2020 Feb 21;22(4):1557-1562. doi: 10.1021/acs.orglett.0c00154. Epub 2020 Feb 11. PMID: 32045253; PMCID: PMC7936574.

138.   J. A. Leitch, T. Rossolini, T. Rogova, D. J. Dixon, α-Amino Radicals via Photocatalytic Single-Electron Reduction of Imine Derivatives, ACS Catal. 2020, 10, 11430-11437.

139.   Reich D, Trowbridge A, Gaunt MJ. Rapid Syntheses of (-)-FR901483 and (+)-TAN1251C Enabled by Complexity-Generating Photocatalytic Olefin Hydroaminoalkylation. Angew Chem Int Ed Engl. 2020 Feb 3;59(6):2256-2261. doi: 10.1002/anie.201912010. Epub 2019 Dec 30. PMID: 31693285.

140.   van Lier RCW, de Bruijn AD, Roelfes G. A Water-Soluble Iridium Photocatalyst for Chemical Modification of Dehydroalanines in Peptides and Proteins. Chemistry. 2021 Jan 18;27(4):1430-1437. doi: 10.1002/chem.202002599.

141.   B. Josephson, C. Fehl, P. G. Isenegger, S. Nadal, T. H. Wright, A. W. J. Poh, B. J. Bower, A. M. Giltrap, L. Chen, C. Batchelor-Mcauley, G. Roper, O. Arisa, J. B. I. Sap, A. Kawamura, A. J. Baldwin, S. Mohammed, R. G. Compton, V. Gouverneur, B. G. Davis, Light-driven post-translational installation of reactive protein side chains. Nature 2020, 585, 530-537,

142.   X. Wang, Y. Chen, H. Song, Y. Liu, Q. Wang, Nickel/Photo-Cocatalyzed Asymmetric Acyl-Carbamoylation of Alkenes, Org. Lett. 2021, 23, 2199-2204.

143.   Aycock RA, Vogt DB, Jui NT. A practical and scalable system for heteroaryl amino acid synthesis. Chem Sci. 2017 Dec 1;8(12):7998-8003. doi: 10.1039/c7sc03612d. Epub 2017 Oct 2. PMID: 29619169; PMCID: PMC5863445.

144.   Berger F, Plutschack MB, Riegger J, Yu W, Speicher S, Ho M, Frank N, Ritter T. Site-selective and versatile aromatic C-H functionalization by thianthrenation. Nature.

2019 Mar;567(7747):223-228. doi: 10.1038/s41586-019-0982-0. Epub 2019 Mar 13. PMID: 30867606.

145. M. H. Aukland, M. Šiaučiulis, A. West, G. J. P. Perry, D. J. Procter, Metal-Free Photoredox-Catalyzed, Formal C–H/C–H Coupling of Arenes Enabled by Interrupted Pummerer Activation, Nat. Catal. 2020, 3, 163-169.

146. Kafuta K, Korzun A, Böhm M, Golz C, Alcarazo M. Synthesis, Structure, and Reactivity of 5-(Aryl)dibenzothiophenium Triflates. Angew Chem Int Ed Engl. 2020 Jan 27;59(5):1950-1955. doi: 10.1002/anie.201912383. Epub 2019 Nov 26. PMID: 31680351; PMCID: PMC7004049.

147. Meng H, Liu MS, Shu W. Organothianthrenium salts: synthesis and utilization. Chem Sci. 2022 Oct 7;13(46):13690-13707. doi: 10.1039/d2sc04507a. PMID: 36544727; PMCID: PMC9710214.

148. Alvarez EM, Plutschack MB, Berger F, Ritter T. Site-Selective C-H Functionalization-Sulfination Sequence to Access Aryl Sulfonamides. Org Lett. 2020 Jun 19;22(12):4593-4596. doi: 10.1021/acs.orglett.0c00982. Epub 2020 Apr 7. PMID: 32255644; PMCID: PMC7309323.

149. Lansbergen B, Granatino P, Ritter T. Site-Selective C-H alkylation of Complex Arenes by a Two-Step Aryl Thianthrenation-Reductive Alkylation Sequence. J Am Chem Soc. 2021 Jun 2;143(21):7909-7914. doi: 10.1021/jacs.1c03459. Epub 2021 May 24. Erratum in: J Am Chem Soc. 2021 Jul 14;143(27):10477-10478. doi: 10.1021/jacs.1c06057. PMID: 34028272; PMCID: PMC8297726.;

150. Sang R, Korkis SE, Su W, Ye F, Engl PS, Berger F, Ritter T. Site-Selective C-H Oxygenation via Aryl Sulfonium Salts. Angew Chem Int Ed Engl. 2019 Nov 4;58(45):16161-16166. doi: 10.1002/anie.201908718. Epub 2019 Sep 24. PMID: 31475767; PMCID: PMC7754133.

151. Ye F, Berger F, Jia H, Ford J, Wortman A, Börgel J, Genicot C, Ritter T. Aryl Sulfonium Salts for Site-Selective Late-Stage Trifluoromethylation. Angew Chem Int Ed

Engl. 2019 Oct 7;58(41):14615-14619. doi: 10.1002/anie.201906672. Epub 2019 Sep 4. PMID: 31389649; PMCID: PMC7754511.

152.   Juliá F, Yan J, Paulus F, Ritter T. Vinyl Thianthrenium Tetrafluoroborate: A Practical and Versatile Vinylating Reagent Made from Ethylene. J Am Chem Soc. 2021 Aug 25;143(33):12992-12998. doi: 10.1021/jacs.1c06632. Epub 2021 Aug 10. PMID: 34375088; PMCID: PMC8391941.

153.   Buglioni L, Raymenants F, Slattery A, Zondag SDA, Noël T. Technological Innovations in Photochemistry for Organic Synthesis: Flow Chemistry, High-Throughput Experimentation, Scale-up, and Photoelectrochemistry. Chem Rev. 2022 Jan 26;122(2):2752-2906. doi: 10.1021/acs.chemrev.1c00332. Epub 2021 Aug 10. PMID: 34375082; PMCID: PMC8796205.

Publications

- Paciotti, R.; Coletti, C.; Berrino, E.; **Arrighi, F.;** Maccelli, A.; Lasalvia, A.; Crestoni, M.E.; Secci, D.; Carradori, S.; Supuran, C.T.; et al. Carbon Monoxide Release from Aryl-Propargyl Dicobalt(0)Hexacarbonyl Derivatives: A Computational and Experimental Study. *Int. J. Mol. Sci.* **2024**, *25*, 11644. https://doi.org/10.3390/ijms252111644

- Guglielmi, P.; Pulitelli, G.; **Arrighi, F.**; Secci, D.; Pierini, M.; Cirilli, R., "Chiral Hydroxy Metabolite of Mebendazole: Analytical and SemiPreparative High-Performance Liquid Chromatography Resolution and Chiroptical Properties." *Pharmaceuticals* 2024, 17, 696. https://doi.org/ 10.3390/ph17060696

- Kaplaneris N, Akdeniz M, Fillols M, **Arrighi F**, Raymenants F, Sanil G, Gryko DT, Noël T. Photocatalytic Functionalization of Dehydroalanine-Derived Peptides in Batch and Flow. Angew Chem Int Ed Engl. 2024 May 6;63(19):e202403271. doi: 10.1002/anie.202403271. Epub 2024 Apr 8. PMID: 38497510.

- **Arrighi F.**, Granese A., Chimenti P., Guglielmi P. "Novel Therapeutic Opportunities for Toxoplasma gondii, Trichomonas vaginalis and Giardia intestinalis infections", *Expert Opinion in Therapeutic Patents*, 2023

- **Arrighi F.** Berrino E., Secci D. "Angiotensin Converting Enzyme", Metalloenzyme, 239-248, 2023.

Congress and conferences

- XVI Annual Meeting A.It.U.N.: "Università degli Studi di Bari Aldo Moro", 18th october 2024. *"Novel Photocatalytic Method for the Functionalization of Dehydroalanine-Based Peptides in Batch and Flow"*. **Oral Presentation**

- EFMC-YMCS 2024 11th EFMC Young Medicinal Chemists' Symposium,

  "Università di Roma La Sapienza" Roma, Italia, 5-6th September 2024, **Participant**

- EFMC-ISMC 2024, XXVIII EFMC International Symposium on Medicinal Chemistry. "Palazzo Dei Congressi", Roma, Italia, 1-5th September 2024, **Participant**

- SYNC, 2nd Symposium for YouNg Chemists: Innovation and Sustainability, "Sapienza Univsrsità di Roma", Roma Italia, 24-28th June 2024*: "Photocatalytic Functionalization of Dehydroalanine-Derived Peptides in Batch and Flow"*, **Oral Presentation**

- PE MedChem Euro PhD Network 2024, 16-17th June 2024 "Sapienza Università di Roma", Roma, Italia, **Local Commitee**

- PE MedChem Euro PhD Network 2023 Thessaloniki, Greece, 16–18th July 2023., *"Assessment of Safety and Anti-Inflammatory Efficacy of CYS-NAM on Human Keratinocytes: Synthesis and Biological Evaluation"*. **Oral Presentation**

- "12th International conference on Carbonic Anhydrases: emerging advancements in the field" Naples, 5-7th July 2023 | National Research Council > Institute of Biostructures and Bioimaging: **Participant**

- PE MedChem Euro PhD Network 2022, Barcellona, Spagna 14-16th July 2022, *"Design, synthesis and human monoamine oxidase inhibitory activity of 2-aroylbenzofuran-3-ol and 2-aroylbenzofuran derivatives: a new route towards hMAOs inhibition"* **Flash Poster Presentation**

- CIVIS SCHOOL "Drug Design", Atene, Grecia, National and Kapodistrian University of Athens, 4-8th July 2022, *"Design, Synthesis, and Evaluation of Human Monoamine Oxidase Inhibitory Activity of 2-Aroylbenzofuran-3-ol and Its Derivatives: A Novel Approach to hMAO Inhibition"*. **Flash Poster Presentation**